NIST Technical Note
NIST TN 2357

Wind-Driven Fire Spread to a Structure from Composite Fences

Kathryn M. Butler
Erik L. Johnsson
Marco Fernandez
Shonali Nazare
Alex Maranghides

This publication is available free of charge from:
https://doi.org/10.6028/NIST.TN.2357

NIST NATIONAL INSTITUTE OF STANDARDS AND TECHNOLOGY
U.S. DEPARTMENT OF COMMERCE

NIST Technical Note
NIST TN 2357

Wind-Driven Fire Spread to a Structure from Composite Fences

Kathryn M. Butler*
Erik L. Johnsson
Marco Fernandez
Shonali Nazare*
Alex Maranghides*
Fire Research Division
Engineering Laboratory

**Former NIST employees; all work for this publication was done while at NIST.*

This publication is available free of charge from:
https://doi.org/10.6028/NIST.TN.2357

November 2025

U.S. Department of Commerce
Howard Lutnick, Secretary

National Institute of Standards and Technology
Craig Burkhardt, Acting Under Secretary of Commerce for Standards and Technology and Acting NIST Director

NIST TN 2357
November 2025

Certain equipment, instruments, software, or materials, commercial or non-commercial, are identified in this paper in order to specify the experimental procedure adequately. Such identification does not imply recommendation or endorsement of any product or service by NIST, nor does it imply that the materials or equipment identified are necessarily the best available for the purpose.

Publication History
Approved by the NIST Editorial Review Board on 2025-11-18

How to Cite this NIST Technical Series Publication
Butler KM, Johnsson EL, Fernandez M, Nazare S, Maranghides A (2025) Wind-Driven Fire Spread to a Structure from Composite Fences. (National Institute of Standards and Technology, Gaithersburg, MD), NIST Technical Note (TN) 2357. https://doi.org/10.6028/NIST.TN.2357

Author ORCID iDs
Kathryn M. Butler: 0000-0001-7163-4623
Erik L. Johnsson: 0000-0003-1170-7370
Marco Fernandez: 0000-0002-4227-8866
Shonali Nazare: 0000-0002-0407-5849
Alex Maranghides: 0000-0002-3545-2475

Contact Information
erik.johnsson@nist.gov

Abstract

Post-fire field observations show that combustible landscaping features are a common pathway leading fire directly to homes during wildland-urban interface (WUI) fires. NIST is studying how these features near a home burn to better understand their potential roles in spreading WUI fires.

Following up on an earlier NIST study involving a variety of fences and mulch, full-scale fire experiments and cone calorimeter tests were conducted on two types of wood-plastic composite fences and one steel-plastic composite fence available to consumers. Full-scale experiments examined the effects on fire spread toward a structure for each type of composite fence, with and without shredded hardwood mulch placed beneath the fence. A wind machine provided a nominal mean wind speed of 6 m/s (13 mi/h). A small structure was located 1.83 m (6 ft) downwind of the fence as a target for flames and firebrands. The fence and/or mulch bed were ignited by a propane burner on the ground at the end farthest from the structure. A target mulch bed at the base of the structure tested the ability of firebrands or flames produced by the burning fence and mulch bed to ignite spot fires that threatened the structure.

Cone calorimeter tests were performed on samples from all three composite fences and compared to previous results from western red cedar and vinyl privacy fences. Ignitability and flammability measurements were obtained in horizontal and vertical orientations according to standard cone calorimeter protocols described in ASTM E1354.

Full-scale experiments showed that for two of the three investigated composite fences, flames extended above and well downwind of the fence even in the absence of mulch beneath the fence. For one wood-plastic composite fence, the upper frame distorted in the fire, allowing burning vertical boards to fall to each side of the fence and creating a burning zone along the fence path whose width was twice the fence height. The steel-plastic composite fence melted and dripped, resulting in large flames and hanging strands of plastic blown by the wind field. The fire behavior of the second wood-plastic composite fence was less severe, attributed primarily to its horizontal board design. As the fire near the ground consumed each horizontal board in turn, the boards above it slipped downward within the frame. As a result, the flame height stayed below the halfway point on the fence, the burning boards remained close to the centerline of the fence as they fell to the ground, and the fire diminished on its own as it ran low on fuel. In the absence of mulch, this fence burned slowly in a hole near the ignition site, with glowing combustion and occasional small flames.

Findings from the cone calorimeter in a vertical configuration complemented full-scale experiments. Melting and dripping or slipping of the sample surface contributed to large peak heat release rates for the two composite fences with intense full-scale fire behavior. For all three composite fence samples, the effective heat of combustion was much higher than for wood or vinyl.

Recommendations include developing fire test(s) for evaluating fences and fence materials that represent their fire hazard and avoiding composite fences that pose the greatest threat for fire spread.

This study of fire spread over composite fences is part of a series designed to better inform standards and codes regarding placement of landscape features around homes that are at risk of exposure to wildland-urban interface fires.

Keywords

Composite fences; cone calorimeter; fence fires; fences; fence flammability; fire spread; structural ignition; structure vulnerability; wildland-urban interface fires; wind-driven fires; WUI fires.

Table of Contents

List of Figures

List of Tables

Acknowledgments

The Frederick County Fire and Rescue Training Facility in Frederick, Maryland made this work possible by allowing us to perform the experiments on their property. NIST greatly appreciates the cooperation and support from the leadership of Frederick County Fire, including County Fire Chief Tom Coe, Assistant County Fire Chief David Barnes; Battalion Chiefs Lenne Stolberg, Frank Malta, Dan Healy, Jon Newman, and Chris Mullendore; Captains Kathleen Harne, Jeff Shippey, and Michael Webb; Lieutenants Chris Dimopoulos, Mike Moser, and John Arnold; and training coordinator Ben Harris.

Many thanks to Phil Deardorff, Tony Chakalis, Doug Walton, Artur Chernovsky, and Lucy Fox for their expert assistance in instrumenting, setting up, carrying out, and cleaning up after the full-scale experiments. Thank as well to Mike Heck and Helen Catan for conducting many of the cone calorimeter tests.

This report has been strengthened through careful review by NIST colleagues Eric Link, Tom Cleary, and Matt Hoehler and by external reviewer Steve Quarles. Thank you all for your thoughtful comments.

Executive Summary

Wildland-urban interface (WUI) fires threaten communities in many locations around the world. It is important to understand the mechanisms by which combustible landscaping elements can transport fire to a home in order to find ways to address the hazard. Such knowledge helps with proactive design, implementation, and maintenance within the community. It informs homeowners on what they can do to protect themselves and their properties. It also helps fire departments to plan defensive strategies, placing resources and assigning tasks where they will be the most effective. The goal is to enhance the safety of members of the public and first responders and to reduce structural fire losses.

Fences and mulch have been identified as contributors to the spread of WUI fires within communities. Once ignited, these fuels become sources that may ignite nearby objects through direct flame contact, radiation, convection, and firebrands (also referred to as embers). The hazard of wind-driven fire propagation and spread associated with fences varies greatly depending on their design, material composition, configuration with respect to nearby materials and objects, and maintenance.

Composite fences have emerged as an alternative to fences built using more traditional materials such as wood, vinyl, metal, stone, or concrete. Wood-plastic composites combine polyolefins (thermoplastic resins) with wood, or wood-like vegetative, fibers, sometimes recycled materials, to create a material with improved properties over those of plastic alone that can be extruded or injection molded to give a natural look. Steel-plastic composites use steel for structural strength and polyolefins for molding and aesthetic qualities. Flame retardants or other substances may be added to reduce the flammability of these materials. The lack of a standard fire test method that specifically addresses fences makes it difficult to assess the hazard of these materials in this application. Test methods for decks and siding do exist and provide some insight regarding the fire performance of wood and composite decking and siding products, but comparability to fences of similar composition is limited due to substantial differences in thickness, structure, and orientation.

To investigate the spread of fire through direct flame impingement or firebrand generation, resulting in spotting, a limited series of outdoor experiments was performed on three types of composite fences arranged in front of a structure in a generated wind field. This report adds to the knowledge from an earlier study[1] of 187 fence and mulch configurations by presenting the results of six experiments on composite fences, complemented by results from cone calorimeter testing of samples from these fences plus wood and vinyl fences from the earlier report. Full-scale experiments were performed on two types of wood-plastic composite fence and one type of steel-plastic composite fence, each with and without a mulch bed at its base to represent fine combustible materials.

[1] K.M. Butler, E.L. Johnsson, A. Maranghides, S. Nazare, M. Fernandez, M. Zarzecki, W. Tang, E. Auth, R. McIntyre, M. Pryor, W. Saar, and C. McLaughlin (2022) "Wind-Driven Fire Spread to a Structure from Fences and Mulch," NIST Technical Note 2228, National Institute of Standards and Technology, Gaithersburg, MD.

This study of fire spread over composite fences is the fourth in a series of NIST (National Institute of Standards and Technology) experimental studies designed to better inform standards and codes regarding the placement of combustible landscape features around homes that are at risk of exposure to wildland-urban interface fires. In addition to fences and mulch, previous studies covered fire spread from firewood piles,[2] and landscape timbers.[3] The results from this series of studies have informed the recommendations developed by NIST and others on spacings of combustible elements and hardening of structures and parcels published in the WUI Structure/Parcel/Community Fire Hazard Mitigation Methodology (HMM).[4]

CONTRIBUTION OF FENCES TO THE FIRE PROBLEM

WUI fire case studies performed by NIST have identified fences as common contributors to the spread of WUI fires within communities. A combustible fence can act as both a recipient of flames and firebrands from an existing fire and as a source of fire itself. Because of their linear character, fences can contribute to multiple fire pathways, resulting in fire propagation both within and beyond the parcel of origin. This linearity and the resulting extensive spatial fire and ember exposure can potentially increase the hazard to multiple parcels and multiple structures in the vicinity of very high and high fire hazard fences (defined below).

During WUI fires, fires have been observed spreading along fences to structures. Post-fire field observations indicate that wood fences are often totally consumed, leaving behind only the metal hardware (nails and screws) used during their assembly. Conversations with first responders have revealed cases in which fences that burned only partially in high fire and ember exposures may have survived due to defensive actions. In many WUI fires, firefighters have removed fences as part of their defensive strategy aimed at containing the fire or preventing it from reaching a nearby structure. Such activities reduce resources allocated to life safety operations and additional direct structure protection.

In the earlier NIST study exposing fences and mulch to conditions simulating a WUI fire,[1] a variety of fire behaviors were observed. Some fences released little or no energy while others burned vigorously. Four fire spread hazard categories, with examples described for each, were identified for the purpose of these studies: very high, high, medium, and low. The same classification system is used in this report:

- *Very high fire hazard* fence configurations are those that threaten a structure through rapid fire spread and large flames extending above the fence.

[2] E.L. Johnsson, K.M. Butler, M. Fernandez, M. Zarzecki, W. Tang, S. Nazare, D. Barrett, M. Pryor, and A. Maranghides (2023) "Wind-Driven Fire Spread to a Structure from Firewood Piles," NIST Technical Note 2251, National Institute of Standards and Technology, Gaithersburg, MD.

[3] E.L. Johnsson, K.M. Butler, M.G. Fernandez, W. Tang, S. Nazare, P. Deardorff, S. Arana, and A. Maranghides (2025) "Wind-Driven Fire Spread to a Structure from Landscape Timbers," NIST Technical Note 2307, National Institute of Standards and Technology, Gaithersburg, MD.

[4] A. Maranghides, E.D. Link, S. Hawks, J. McDougald, S.L. Quarles, D.J. Gorham and S. Nazare (2022) "WUI Structure/Parcel/Community Fire Hazard Mitigation Methodology," NIST Technical Note 2205, National Institute of Standards and Technology, Gaithersburg, MD.

- *High fire hazard* combinations of fence and mulch release a considerable amount of energy while burning, igniting nearby combustibles through direct flame contact or radiation and convection from the flames. This category also includes fences and mulch that generate firebrands capable of igniting spot fires downwind.
- Fences and mulch are classified as *medium fire hazard* if they are combustible but do not typically ignite nearby combustibles and do not cause significant downwind fire spread.
- Fences made of noncombustible materials such as stone, brick, or steel can be classified as *low fire hazard*. Although these fences do not burn on their own, they can trap and accumulate combustible windblown debris along their length, which can transport fire. Noncombustible fences have not been included in this series of NIST studies.

EXPERIMENTAL DESIGN

This report presents a study of fire spread to a nearby structure in a wind field from three types of composite fences (two wood-plastic and one steel-plastic composite) with and without mulch beneath. The research was conducted to assess the severity of the fire hazard that these fences posed to structures and to gain insight into the mechanisms driving that hazard. The fire behavior of these fuels, including flame spread rate, spotting due to firebrands, and downwind ignition potential, was observed. To see whether the fire behaviors could be readily distinguished using a small-scale fire test, calorimeter testing was performed in both horizontal and vertical orientations for the composite fence materials.

In these field experiments, a fence section or fence/mulch bed combination was arranged perpendicular to the wall of a small structure and separated from it by 1.8 m (6 ft), approximately the length of a fence panel. The configuration is shown in Fig. ES.1. Beyond the fence and/or mulch bed was a large fan that generated a wind field at a speed of 6 m/s (13 mi/h) directed toward the structure. A fire was ignited using a multi-torch propane burner at the end of the fence closest to the fan, and the fire was observed as it spread toward the structure through flame contact and firebrand spotting.

To characterize the ability of flames or firebrands generated by the burning fence or mulch bed to ignite combustible materials near the house, a second mulch bed was placed along the base of the structure as a target. A noncombustible layer was added to the wall, and the structure was considered threatened when the spot fire was observed impinging on the wall. The experiment was terminated using water suppression when fire in the target mulch bed reached the base of the structure, when the fence fire directly impacted the structure, or when the progress of the flame front toward the structure was slow. The eaves and roof of the structure were manually cooled when pyrolysis (smoking) was observed. Factors contributing to structure ignition—including geometry, wall cladding, and construction—were excluded from the scope of this study.

Post processing of the video camera recordings provided data to measure the progress of the fire along the mulch and fence. The time for a firebrand to ignite a spot fire in the target mulch bed was evaluated, along with the time for the spot fire to reach the wall. Ambient wind and

temperature were measured, and bidirectional probes recorded the speed of the wind reaching the test object.

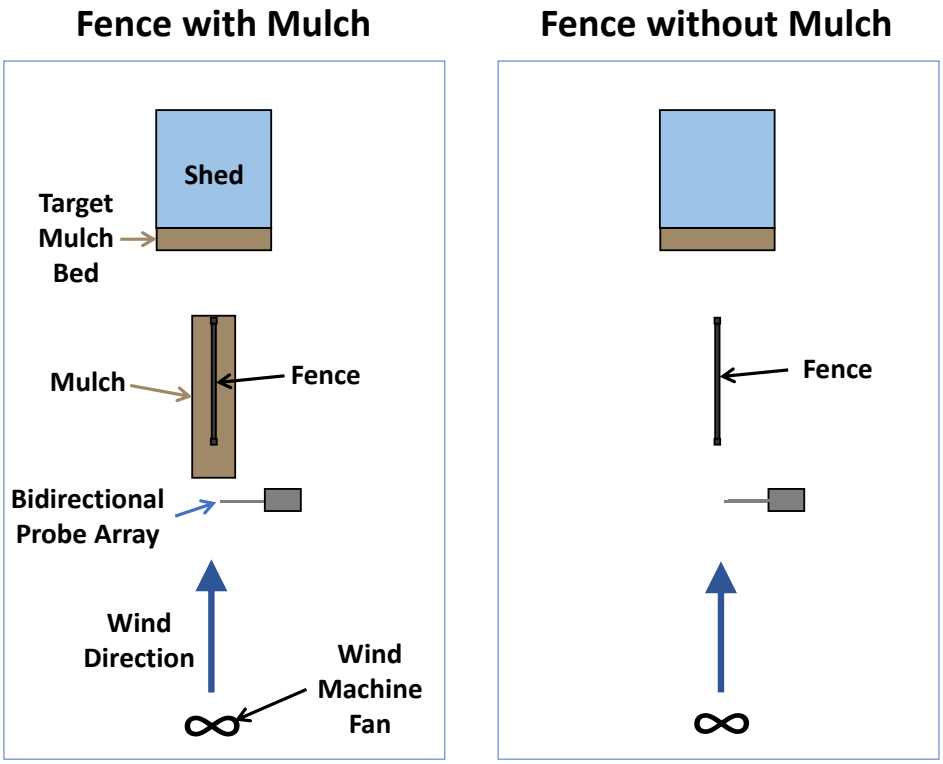

Fig. ES.1. Plan view of fence configurations tested in this study (L) with mulch and (R) without mulch.

In the earlier NIST fence and mulch study,[1] a variety of fence and mulch materials, designs, and combinations were tested at three wind speed levels and four separation distances between the fuel source and the structure. For this limited study, a test condition of 6 m/s (13 mi/h) wind speed (the lowest of the three previously tested) and separation distance of 1.83 m (6 ft) was selected, in agreement with the test conditions used for many earlier experiments. The low-speed wind field resulted in intense fire behavior for certain cases, notably parallel fences, and the separation distance placed the fence outside of the effects of a vortical wind field that was found to form close to the structure.

Cone calorimeter tests were performed on samples from all three composite fences and compared to previous results from western red cedar and vinyl privacy fences. Ignitability and flammability measurements were obtained in horizontal and vertical orientations according to standard cone calorimeter protocols described in ASTM E1354.

LIMITATIONS

This study was a survey of the fire behavior in wind for three types of composite fences near a structure, complemented by a cone calorimeter study of samples derived from these fences. It illuminates the differences in behavior for the materials and designs used for these fences and demonstrates the value of combining insights from full-scale and small-scale testing. Limitations of this research include the following:

- Only three types of composite fences were tested.
- Test replicates for each specimen/condition combination were not conducted.
- Fuels were ignited at a single location on the ground.
- Ignition was by gas burner rather than a natural source.
- The orientation of wind to the structure wall was limited.
- The mulch was preheated by heat conduction through the steel pan.
- Accumulation of windblown debris was not considered in Fence Only experiments.
- Effects of terrain were not studied.
- Smoke toxicity was not included.

KEY FINDINGS

This section lists the key findings from this report, recommendations based on the findings, and recommendations for future work. The conclusions are incorporated into the unified set of conclusions generated from the series of NIST studies on fire hazards associated with various categories of landscape combustibles: fences and mulch, woodpiles, and landscape timbers. The composite fence study reinforces and adds to these findings and recommendations.

The experiments in this study demonstrated a range of fire spread hazards from three types of composite fences, with and without mulch, ignited close to a structure in a wind field. General findings are listed first and followed by findings for configurations classified as very high hazard, high hazard, and medium hazard. The findings are labeled according to the following categories:

FH	Fire Hazard
LS	Life Safety
HR	Hazard Reduction – materials, assemblies, implementation/housekeeping
IC	Improved Characterization – recommended future work to characterize these fuels more fully

General findings

The results from the composite fence full-scale experiments and cone calorimeter tests demonstrated that:

F1. As combustible materials are combined, the hazard increases disproportionately. (FH)

The composite fence study confirmed the previous NIST finding that fuel agglomeration significantly increases energy release and increases fire and ember exposures. The presence of mulch accelerated the progress of flame along two fence types and made the difference between flame spread along the fence and localized burning for a third.

F2. Fences may impede egress. (LS)

In a WUI fire, high and very high hazard fence configurations may result in a line of flames close to egress paths from a house or auxiliary dwelling. For one of the investigated wood-plastic composite fences, the top and bottom frames distorted and allowed vertical burning boards to fall to either side, creating a zone of flames along the fence line that was 3.7 m (12 ft) wide. For a steel-plastic composite fence, the plastic panel distorted, melted, and dripped, resulting in hanging strands of plastic blown by the wind.

F3. Fire spread rates vary with fence materials and design, wind speed, and fuel configuration, including the presence or absence of mulch. (FH)

Two types of composite fences with mulch beneath supported fire spread rates that were faster than all other fence-mulch combinations tested by NIST. Factors that may have contributed to this finding include slippage of surface material to reveal fresh fuel and melting and dripping. Cone calorimeter testing determined that the effective heats of combustion for all three composite fences in this study were considerably higher than for vinyl and wood fences. The physical design of the fences, including vertical versus horizontal boards and distortion of the fence frame with high temperatures, also played an important role in fire spread.

F5. A standard test method is needed to evaluate the burning characteristics of fences. (IC)

A standard test method is needed to assess the fire performance of fences. The method should consider not only materials but also assemblies and be carried out with the fence panels, or sections of them, in a vertical orientation. The method should distinguish the fire behavior of various materials, including wood-plastic composites, wood, and vinyl, and designs, including privacy, lattice, and “good neighbor”.

The significant differences in energy release among the three composite fences tested in this study highlight the need for a fence test method that can be used to assess the hazard of the material/design configuration. The cone calorimeter study in this report demonstrates that a combination of test methods may provide a more comprehensive assessment.

Very High Fire Hazard Configurations

Within the context of this study, very high hazard configurations are defined as those resulting in rapid fire spread and large flames.

F6. Rapid fire growth and large flames were observed for parallel fences a*nd some composite fences*. (FH)

- Limited testing indicates that ignition of certain *wood-plastic and steel-plastic composite fences* can result in very high intensity fire behavior. For two of the three composite fence types in this study, intense fire behavior was observed even in the absence of fine combustible material (mulch) beneath the fence, as shown in Fig. ES.2. Both of these composite fence types burned with flames that extended above the fence. The primary mechanisms for ignitions and rapid fire spread in the target mulch bed next to the

structure were thought to be radiation and direct flame contact rather than firebrands. For one wood-plastic composite fence, the frame distorted in the heat and allowed vertical boards 1.8 m (6 ft) tall to fall to both sides, creating a 3.7 m (12 ft) wide zone of flames that could block egress and threaten property. The steel-plastic composite fence melted and dripped, becoming tattered with hanging strands blown by the wind field.

Cone calorimeter testing in the vertical orientation demonstrated melting and sliding or dripping behaviors for test samples from both composite fences in this category. These material behaviors likely contributed to the very high hazard behavior of these fences even in the absence of mulch beneath them. The cone calorimeter data from these fences displayed peaks in heat release rate that were much higher than for the third composite fence. The distinction was not apparent in horizontal cone testing.

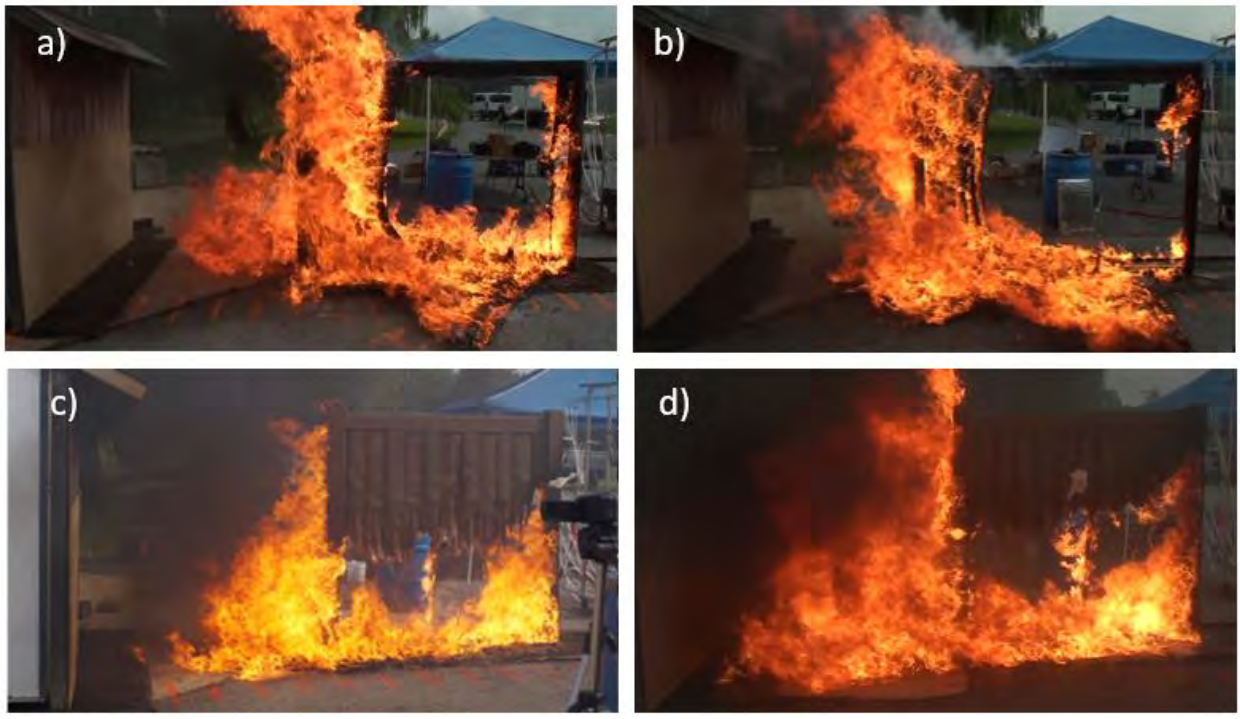

Fig. ES.2. Composite fences exhibiting rapid flame spread and relatively large flames for the investigated specimens: a) wood-plastic composite #1 (WPC1) with and b) without mulch and c) steel-plastic composite (SPC) with and d) without mulch.

High Fire Hazard Configurations

Within the context of this study, landscape fuel configurations that exhibit fire behavior in the high hazard range support fire spread and generate firebrands but do not progress to full involvement with large flames.

F9. A fence with mulch at its base transports fire through the community and provides a steady source of firebrands to ignite combustible material downwind. (FH)

- Because of its physical design, one *wood-plastic composite fence* type in combination with dried mulch beneath displayed high hazard behavior, rather than very high. As

shown in Fig. ES.3, its horizontal boards were held in place by the vertical frame elements on each side of the panel. As the fire consumed each horizontal board in turn, the boards above it slipped downward within the frame. As a result, the flame height stayed below the halfway point on the fence, the burning boards remained close to the centerline of the fence as they fell to the ground, and the fire diminished on its own as it ran low on fuel.

The horizontal boards were observed to burn vigorously, and the cone calorimeter study revealed that the effective heat of combustion of fence samples matched those of the other two composite fences in the study. This raises the question of whether this wood-plastic composite fence would move to the very high hazard category under different conditions, such as multiple ignitions due to firebrands lodging between boards located higher on the fence. Susceptibility to such ignitions was not tested.

Fig. ES.3. Wood-plastic composited fence #2 (WPC2) with mulch exhibiting fire spread but no progression to full involvement with large flames.

Medium Fire Hazard Configurations:

Within the context of this study, landscape fuel configurations whose fire behavior was considered medium hazard demonstrate very slow fire spread without flaming and little or no generation of firebrands.

F12. Without nearby fine combustible materials such as mulch, the fire spread over a single combustible fence is slow and dominated by glowing combustion. (HR)

- In the absence of mulch beneath the fence, one of the three composite fences in this study displayed similar fire behavior to that seen for wood fences in the earlier NIST report.[1] The fire spread in the absence of any fine combustibles was generally slow and dominated by glowing combustion with occasional small flames. This composite fence type was the only one of the three types tested that did not exhibit melting and dripping behavior in cone calorimeter testing.

Fig. ES.4. Wood-plastic composite fence #2 (WPC2) without mulch, exhibiting very slow spread and little or no firebrand generation.

PRIMARY RECOMMENDATIONS

The results of this study add to a comprehensive effort to reduce the vulnerability of structure and parcels to fire and firebrands. A Hazard Mitigation Methodology[4] has been developed with the goal of allowing structures in the WUI to survive fire and firebrand exposures without intervention by first responders. The recommended strategy is to balance a reduction of the exposure with increased hardening of the structure. The exposure may be reduced by removing or reducing the fuels or by relocating the source.

Several of the recommendations from the original NIST fence and mulch report[1] have been reinforced by this study of composite fences and are repeated here. Two recommendations are added to the list from the full series of NIST studies on landscape combustibles: avoid composite fences whose fire behavior presents a very high hazard (as defined within the context of these studies), and avoid framing elements that deform at fire temperatures, leading to obstruction of egress routes. Although the recommendations are intended primarily for moderate to very high hazard WUI locations, they are expected to reduce local fire hazards in any community.

R2. Do not place combustible fences where, if ignited, they could restrict or block egress.

R3. Avoid proximity to other combustible fuels, to reduce fire intensity and limit fire spread. This includes fuels above the fence and fuels across parcel boundaries. Avoid mulch or accumulation of debris along the base of fences. As noted with wood fences, it may be difficult to keep a fence sufficiently clear of fine combustible materials to achieve the slow-growth fire behavior. Windblown debris such as leaves and pine needles may accumulate before or during a WUI fire event.

R4. Avoid proximity of combustible fences to residences, including neighboring residences, to prevent direct ignition. The intense flames from some composite fences

may threaten a nearby residence through radiation and direct flame contact in addition to firebrands.

R5. Replace combustible landscape features with noncombustible or low fire hazard features when possible. Fire spread is more likely with wood and composite fences than with fences made of vinyl or noncombustible materials such as stone, brick, or steel.

R12. Avoid any fence whose fire behavior may present a very high hazard. Two composite fences in this study displayed highly hazardous fire behavior, with relatively large flames (in the context of the investigated systems) that accelerated fire spread and extended into potential egress zones. The fence materials melted and dripped in one case and slid from the surface to reveal fresh fuel in the other. The fire behavior of the third fence was less intense in these experiments, primarily because of its physical design (horizontal rather than vertical boards). However, all three composite fences had a high fuel content as measured by the effective heat of combustion.

R13. Avoid framing elements that deform at fire temperatures. The distortion of the upper frame of one of the composite fences in this study resulted in burning vertical boards falling to each side of the fence, creating a burning zone along its path whose width was twice the fence height.

For more detailed recommendations on spacings of combustible elements and hardening of structures and parcels, refer to the WUI Structure/Parcel/Community Fire Hazard Mitigation Methodology report.[4]

RECOMMENDATIONS FOR FUTURE WORK

This study of composite fences reinforces the need for test methods specific to fences, as stated in the original fence report.[1] The inclusion of a detailed cone calorimeter study in this report shows the benefits of tests at multiple scales and the importance of matching the orientation to the application. This recommendation is repeated and strengthened here:

S5. Develop fire test(s) for evaluating fences and fence materials that represent the actual fire hazard.

A standard test method is needed to assess the fire performance of fences. The method should consider not only materials but assemblies and be carried out in a vertical orientation. It should be able to distinguish the fire behavior of various materials, including wood-plastic composites, wood, and vinyl, and designs, including privacy, lattice, and good neighbor. Both material flammability and physical design contribute to the fire hazard of a fence; this report demonstrates that incorporating complementary tests at different scales into a standard test method may provide a more complete assessment.

A fence test method will inform authorities having jurisdiction (AHJs) and the public about implementation options with fences and allow AHJs not only to assess the performance/hazard of composite fences but to compare and assess all combustible fencing options under identical conditions.

1. Introduction

This report is the fourth in a series of National Institute of Standards and Technology (NIST) experimental studies on fire spread from landscape combustibles to a structure. The studies have looked at fire spread from both flames and firebrands (also called embers). The first report presented a study on fire spread from fences and mulch [1], the second presented fire spread from firewood piles [2], and the third described the fire hazard from burning landscape timbers [3]. This fourth report supplements the fence and mulch study by expanding on fire spread to a structure from three composite fences, accompanied by a detailed cone calorimeter study. All full-scale experiments were performed outdoors at the Frederick County Public Safety Training Facility at the same location as the previous studies with a nearly identical experimental setup, instrumentation, and procedure. For the readers' convenience, the sections of this report describing those common aspects are repeated here, with slight adjustments to account for differences between the experimental series.

The trees, grass, brush, and organic debris that make up wildland vegetation are not the only fuels for wildland-urban interface (WUI) fires. Once such a fire reaches a community, its structures and landscape features can add to and may come to dominate the fire sources, magnifying the hazard. Combustible elements in a neighborhood may transform from being the targets of flames and embers to fire sources themselves that threaten surrounding properties and the people who live there. How and where we build, then, affects the progression of a WUI fire.

NIST has undertaken a long-term project to assess fire hazards in our built environment and to develop a mitigation methodology to harden structures and communities against firebrand and flame exposures [4]. This report on composite fences builds on a growing body of NIST research studying fire behavior and how the materials, designs, and configurations present in a community influence a WUI fire.

1.1. Motivation

The wildland-urban interface refers to areas where dwellings are adjacent to or intermixed with wildland vegetation. A large and growing number of people live in WUI areas in the United States. Residents are attracted to the WUI due to the closeness to natural settings and amenities and to the relative affordability of housing farther from urban centers. The regions where the WUI overlaps with high risk of wildland fires due to fuel, weather, terrain, and sources of ignition are where these wildland fires pose the greatest risk to lives and property. Effective methods are needed in these areas for protecting people, homes, and communities from wildfires.

WUI fires often occur when wildland fires cannot be controlled, typically due to extreme wind and fuel conditions, and spread into communities. Such fires have caused significant losses to life and property in the U.S., Canada, and other parts of the world including Australia and Mediterranean Europe. The costs of damage to the built environment associated with wildfires have increased in time; of the 20 most destructive fires in California history, well over half have occurred since 2017 [5]. At the top of this list is the Camp Fire of November 2018, which

resulted in 85 fatalities and the destruction of over 18 000 structures, including 90 % of the homes in Paradise, CA. The Camp Fire was one of the costliest natural disasters of 2018, with an overall loss of $16.5 billion as estimated by multinational insurance company Munich Re [6]. The Eaton and Palisades Fires in Los Angeles, CA in January 2025 together are expected to significantly exceed these economic losses, with a combined total of 30 fatalities and over 16 000 structures destroyed. Research is urgently needed to better understand WUI fire-structure interactions and to support changes to building and community designs and codes in order to mitigate the increasing losses from the growing number of WUI fire incidents.

NIST has carried out studies on several WUI fires. A multiyear Camp Fire case study is currently ongoing, with published reports on the fire progression timeline [7] and notification, evacuation, and temporary refuge areas (NETTRA) [8]. The final major report will focus on responder actions and structure survivability.

Fences have been identified as common contributors to the spread of WUI fires within communities. Instances of fires spreading to structures along fences were observed in the Witch Creek Fire [9] and the Waldo Canyon Fire [10]. Because of their linear nature, it is possible for fences to spread fire over long distances. In the Waldo Canyon Fire and many others, firefighters removed fences as part of their defensive strategy aimed at containing the fire, reducing resources allocated to direct structure protection.

Combustible landscaping elements can act as both potential ignition sites from existing fires (targets) and sources of fire spread themselves. These materials can be ignited by a fire through direct flame contact, radiation, convection, or firebrands. Firebrands are carried by the wind and may ignite combustible materials in a community far downwind of the fire front. Once ignited, landscape combustibles may ignite nearby objects, including homes, through direct flame contact or firebrands.

The protection of people and property in the WUI depends in part on improvements to building and landscape materials, design, and maintenance practices. Efforts to improve community resistance to fire include: WUI building code organizations, such as the International Code Council (ICC), the National Fire Protection Association (NFPA), and Chapter 7A in the California Building Code; and voluntary fire outreach programs, such as Firewise, Fire Adapted Communities, and the Fire Learning Network. Concepts like defensible space and the home ignition zone educate the public on how to protect their homes. Recently, a fire Hazard Mitigation Methodology (HMM) was developed based on the relationships among fuel layout, fire hazard, and structure hardening [4].

For maximum effectiveness, these efforts require science-based data and guidance. Increased understanding of the vulnerabilities of structures in WUI communities and the potential pathways for flames and firebrands will help to enhance life safety and improve community resilience to these fires. The hazard may be reduced through improvements in materials, building designs, and configurations. Homeowners and community planners can recognize ways in which neighbors can work together to reduce the fire threat. Strategies may be developed for both existing communities and new construction.

The goal of this work is to improve our understanding of the mechanisms by which composite fences, in particular, can transport fire to a home. Better understanding of the role of these features as conduits of fire spread to structures and identification of particularly hazardous configurations promote efforts to protect against ignition and fire spread. Helping fire departments to identify very high hazard situations will enhance first responder safety and effectiveness. The results of this work will be used to improve codes and standards and to provide guidance to homeowners, community designers, and first responders.

1.2. Background

WUI fires ignite the exteriors of structures through flame radiation and convection, direct flame impingement, and firebrands. In contrast to the large body of knowledge on ignition and fire growth within buildings, reflecting decades of fire research, the complexities of the interactions between the built environment and exterior fire exposure are in the early stages of exploration. Our understanding of WUI fire behavior is confounded by the large number of potential fire and firebrand exposure scenarios (with added complexities of local topography such as slope and local weather such as wind and humidity), the wide variety of WUI fuels (vegetative and structural), and the extensive assortment of exterior construction materials and assemblies (with responses affected by particular designs). The research presented in this report joins earlier efforts to better understand structure vulnerabilities to fires from nearby landscape combustibles.

1.2.1. Structure Vulnerabilities

Fire may ignite a structure through numerous pathways. At close range, exposed combustible materials may ignite through radiation/convection or direct flame contact. Ignitions may also occur through firebrands. These burning particles break off from a larger object in a fire and are blown or lofted to a new location, where they can ignite spot fires. Firebrands may ignite susceptible parts of the building exterior and may penetrate into interior spaces through vulnerable openings in the building envelope. An object ignited by flames or firebrands may itself become a fire source of additional firebrands and flame radiation exposures to surrounding fuels (targets).

1.2.2. Composite Fences

Fences are a linear landscaping feature. Fences frequently “link” multiple parcels, as one fence connects to an adjacent fence. If they are combustible, they may provide a linear path for fire from one end of the fence to the other. They may also produce firebrands capable of igniting spot fires downwind.

Several studies have looked at how fences may ignite in a WUI fire and how the fire may behave, including the fire performance of hardwood, treated pine, and sheet steel fences by CSIRO [12]; ignition of fences by grass fire [13]; ignition of wood fencing assemblies by wind-driven firebrand showers by NIST and BRI (Building Research Institute) [14,15] and IBHS

(Insurance Institute for Business & Home Safety) [16,17]; and fire spread along privacy fences in a wind field by NIST [18]. The 2022 NIST report on fence and mulch [1] examined the fire behavior of a variety of materials, designs, and configurations of fences and mulch near a structure under various wind conditions. Full-scale results were presented from two wood-plastic composite fences. The current report includes experiments on a steel-plastic composite fence to expand the discussion on the behavior of composite fences in fire. A detailed cone calorimeter study adds insights to the full-scale fire performance.

Composite fences have emerged as an alternative to fences built using more traditional materials such as wood, vinyl, metal, or stone. Wood-plastic composites combine polyolefins (thermoplastic resins) with wood fibers, typically recycled materials, to create a high stiffness material that can be extruded or injection molded to give a natural look. Steel-plastic composites use steel for structural strength and polyolefins for molding and aesthetic qualities. Other advantages include moisture resistance, low maintenance and durability. A serious issue with these materials is their flammability [19,20]. Flame retardants may be added to address flammability, but at a tradeoff with mechanical properties [21].

In the absence of standard fire tests specifically for fences, some manufacturers have evaluated their products using fire test methods for materials used in building construction. An example is ASTM E84 [22], which is a standard test method for assessing the surface burning characteristics of building materials such as those used for walls, ceilings, and siding. The method mounts a material sample on the ceiling of a tunnel-like chamber, subjects it to a controlled ignition source, and monitors the flame spread along the length. E84 is actually required for testing particular materials in some WUI codes (California's building code Chapter 7A [23] and the International Code Council's IWUIC [24]) and standards (NFPA 1140 [25]). Unfortunately, the E84 test does not account for either the vertical orientation of a fence or its physical design. Also, according to the standard, materials that exhibit significant melting, dripping, and delamination do not provide reliable results. For deck materials, usually thicker than fence boards to provide a weight-bearing function and mostly horizontal in orientation, Fabian found that E84 was a poor predictor of fire performance of actual decks and that the cone calorimeter was better than E84 for material comparisons but not as effective at capturing effects of form [26]. The lack of a standard fire test method that specifically addresses fences makes it difficult to assess the hazard of these materials in this application.

1.3. Approach

NIST staff conducted a series of field experiments on the fire spread behavior of a small number of ignited composite fences with and without mulch. The experimenters examined the spread of fire along composite fences and toward a structure in the presence of wind. They also observed the fire behavior and the ability of flames or firebrands generated by the burning fences to ignite spot fires at the base of the structure.

In each of these experiments, a portable, airboat-style fan was used to direct a wind field with a prescribed speed in the direction of a small shed. A composite fence panel with or without a mulch bed at its base was positioned between the fan and the shed at a prescribed location, aligned with the wind. The fence panel and mulch bed were ignited with a propane burner at

the end near the fan, and the fire spread due to flames, smoldering, and firebrands was observed. Comparing the fire behavior of a fence with and without mulch provided insights into the contribution to WUI fire spread made by fine fuels that accumulate at the base of fences, such as leaves, needles and other debris. The small shed was used as a target structure for flame spread and firebrands, with a target mulch bed placed along the base of the wall to observe spot fire ignitions from firebrands, radiation, or flame impingement.

Two types of wood-plastic composite fences and one steel-plastic composite fence were used in these experiments. The fences were all “privacy” type with panels consisting of either a continuous sheet or an appearance as such with boards having little or no or space between them. Shredded hardwood mulch was spread along and beneath the fence, when required by the experiment, and at the base of the wall.

Full-scale experiments were complemented by results from cone calorimeter tests. Cone tests were performed on samples from all three composite fences and compared to previous results from western red cedar and vinyl privacy fences. Ignitability and flammability measurements were obtained in horizontal and vertical orientations according to standard cone calorimeter protocols described in ASTM E1354.

1.4. Objectives

The overall goal of the work described in this report is to assess the severity of the fire hazard that composite fences pose to structures. This was accomplished by studying the rate and mechanisms of fire spread in the presence of wind, both as the fire progressed along the fence and as it jumped via flames or firebrands to combustible materials at the base of the shed. The main objectives of the experiments were:

- To observe the burning behavior of wind-driven fires along composite fences with and without fine combustibles beneath;
- To understand the rate of fire spread along composite fences as compared to that of other fence types;
- To determine the impact of fence style and fence material type on the fire spread rate;
- To determine whether a fire along a composite fence poses a potential ignition danger to an attached or adjacent structure; and
- To ascertain whether a burning composite fence produces significant firebrands capable of igniting downwind combustibles.

It is anticipated that this work will contribute technical knowledge that will improve building codes, referenced standards test methods, and best practices for home landscape features and will also support efforts to address the WUI fire problem by hardening structures and creating defensible space.

2. Experimental Description

This section provides information on preparation and setup specific to the six experiments on composite fences that are the focus of this report. Some information from the original report on the NIST experimental study of fences and mulch [1] is repeated here. For further details, and to learn about the full range of experiments in the NIST study, please refer to the original report.

Figure 1 shows a schematic of the experimental setup for fences and mulch beds. The wind machine, a large propeller fan mounted on a trailer, was directed toward a small structure. A flow straightener was employed to remove large-scale swirl from the supplied wind and to direct the wind downward slightly toward the ground. The fence section, with or without a mulch bed beneath, was arranged perpendicular to the wall of the structure and parallel to the wind flow. For the composite fence experiments, the nominal applied wind speed was 6 m/s (13 mi/h) which was the lowest of 3 wind speeds explored in the larger fence study [1]. Later references to "low" wind speed will mean this 6 m/s condition. The fence was separated from the wall by a distance of 1.83 m (6 ft). To study the potential for firebrands to ignite the structure, a target pan of hardwood mulch was positioned at the base of the structure wall. This mulch bed served as a surrogate for any combustible material next to a structure.

The fence and mulch bed were ignited with a propane burner to simulate prior ignition via one or more firebrands or firebrand-ignited debris. Cameras were set up to monitor the fire spread behavior for each composite fence with and without mulch. The following sections will detail the experimental setup, equipment, measurements, conditions, and the parameters explored. Many of the uncertainties in the experimental setup and measurements are covered in Appendix B. Generally, unless described otherwise, "±" values used in conjunction with measurements represent the expanded combined uncertainties (2σ).

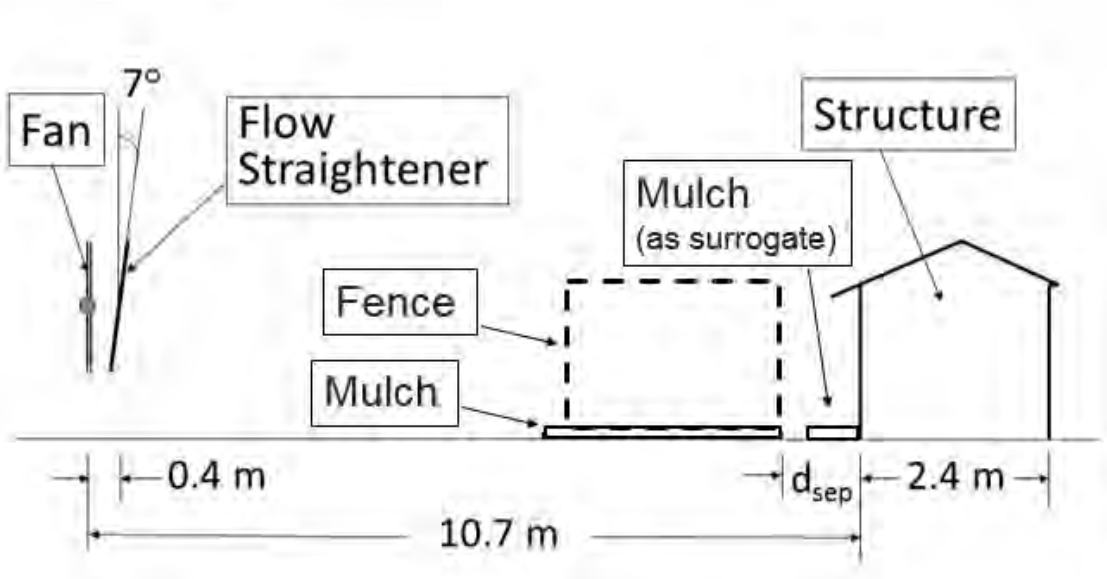

Fig. 1. Major components of the experiment (not to scale).

2.1. Research Location and Site Description

The experiments were conducted in Frederick, MD at the Frederick County Public Safety Training Facility. A large, nearly flat asphalt and concrete area near a water-supply pond was utilized. The pond and its wall provided a noncombustible background downwind of the firebrand-generating experiments. Water for extinguishment was provided through a nearby hydrant and a diesel pump, which provided a high-pressure source of pond water.

An aerial view of the site is shown in Fig. 2, marked up with locations of the target shed, equipment/conditioning building, and wind machine. The wind flow was applied from the wind machine from the SSW direction at an angle of 200.5° ± 1.5°.

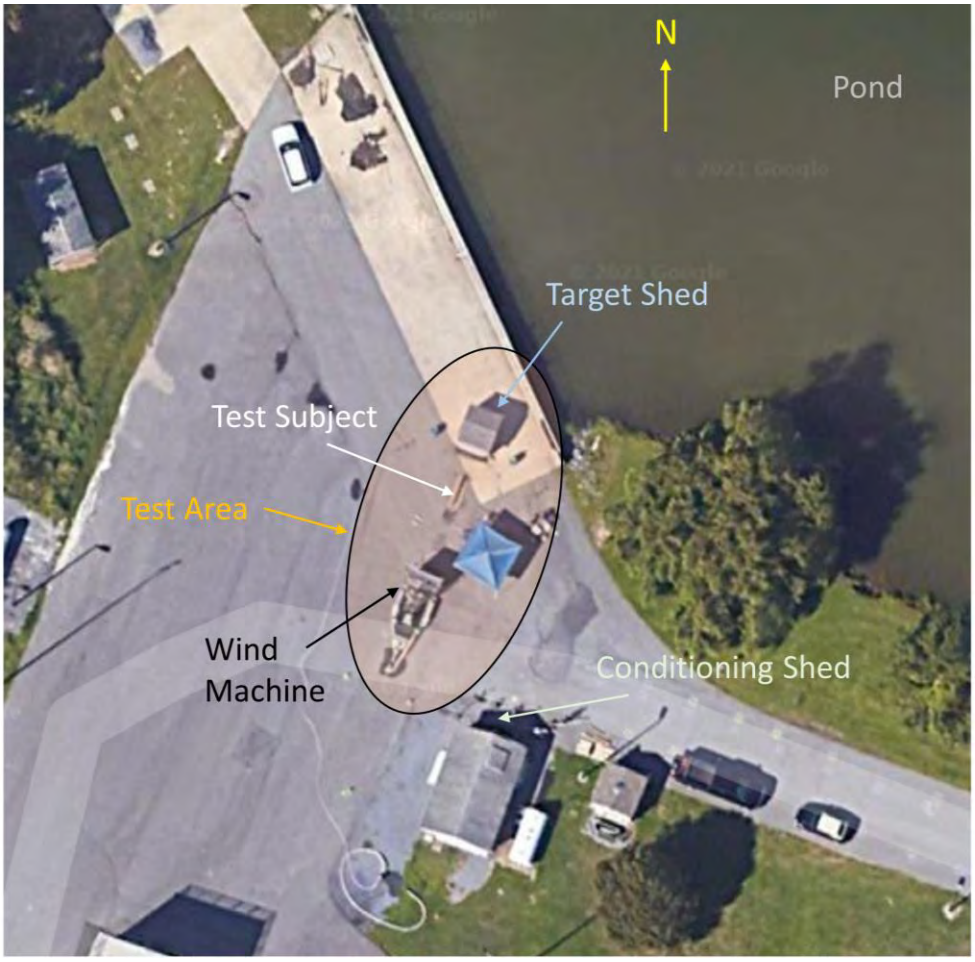

Fig. 2. Aerial view of site used for experiments. Google Earth image with NIST overlay.

2.2. Wind Field Generation

2.2.1. Wind Machine

The wind machine used to impose a wind field on the target structures, shown in the foreground of Fig. 3, was assembled and mounted on a trailer by American Airboat. The power

was provided by a 6.0 L displacement, 336 kW (450 HP) rated marine engine with multi-port fuel injection. The wind machine utilized Whirlwind Propellers model AB300ex-WT79, which had three quiet-design, graphite composite blades with a width of 33 cm (13 in) and a sweep diameter of 2.11 m (83 in). The wind machine incorporated a high-performance positive drive belt with 2.3:1 reduction. A manual "cruise control" mechanism was designed and added to the single lever binnacle-style throttle control in order to maintain selected engine speeds, which were monitored with a built-in tachometer.

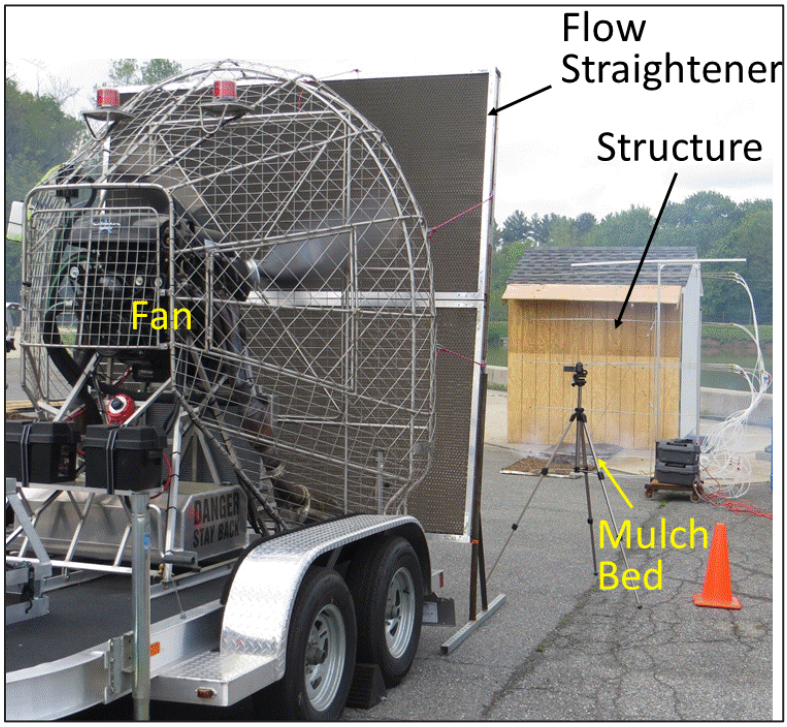

Fig. 3. Photo of test site showing fan, flow straightener and target shed in an experiment on a mulch bed without a fence.

2.2.2. Flow Straightener

A flow straightener was used to remove large-scale swirl from the applied wind and adjust the wind direction. The flow straightener consisted of two framed sections of aluminum honeycomb with cells 19 mm (3/4 in) across and 11 cm (4.4 in) thick. The two framed sections, each measuring 1.2 m × 2.4 m (4 ft × 8 ft), were stacked as shown in Fig. 3, with the front plane of the flow straightener positioned 45 cm (18 in) in front of the fan at the height of the fan center. Since the lowest sweep extent of the wind machine propellers is 1 m above the ground, the column of air moved horizontally by the wind machine by itself would not begin to be felt at the ground for a distance of several meters. To enable the generated wind field to reach the base of the combustible fence and mulch bed with substantial velocity, the flow straightener was angled downward by approximately 7°.

2.2.3. Velocity Profiles

The wind field from the wind machine under the low wind speed test conditions of this composite fence study is characterized in Appendix D of this report. For each experiment, an array of bidirectional probes upwind of the fence monitored the wind field. A discussion of these measurements can be found in Section 2.7.1.

2.3. Target Shed

A shed with a 2.43 m (8 ft) square footprint and a height of 2.43 m (8 ft) along the front and rear faces can be seen in the background of Fig. 3. The shed was positioned 10.67 m (35 ft) away from the plane of the wind machine propellers. An artificial eave was added to the shed on the windward side, extending 45 cm (18 in) outward at the same 30° angle as the roofline. The eave was constructed from standard pressure treated pine 2×4s[5] and 1.5 cm (0.59 in) thick T1-11 weather-resistant southern yellow pine plywood panel siding.

As shown in Fig. 4, a false wall was attached to the shed on the windward side. This allowed replacement of burned wall layers without damaging the original shed wall. The design of the false wall included layers (from the shed outward) of 1.6 cm (5/8 in) gypsum board, standard pressure treated pine 2×4s (the same type used for the eave), 1.6 cm (5/8 in) gypsum board, and 1.5 cm (0.59 in) thick southern yellow pine plywood panel siding.

For the composite fence experiments, a mulch bed at the base of the shed served as a surrogate for combustible materials (such as leaves or pine needles in addition to mulch) that could ignite and carry a fire to the shed wall. In the full NIST fence and mulch study [1], these were classified as Series 2 experiments. To prevent the false wall from getting burned and requiring replacement, James Hardie fiber cement siding was added to the lower half of the false wall, as shown in Fig. 4. The fiber cement siding was 1.22 m (4 ft) tall by 2.44 m (8 ft) wide, with a thickness of 6.4 mm (¼ in).

The false wall and siding layer added approximately 15 cm to the shed depth, for a final shed footprint of 2.43 m wide by 2.58 m deep. The vertical gray strip appearing to the left of the false wall in Fig. 4 is a metal corner bead protecting the edge of the shed.

[5] The term “2×4” is used to refer to dimensional lumber, also known as framing lumber. The cross-sections of lumber are referred to by their nominal size, in this case 2 in by 4 in, but the actual depth and width (the “dressed” size) after cutting and smoothing are 3.8 cm by 8.9 cm (1 ½ in by 3 ½ in) [48]. Similarly, 4×4s measure 8.9 cm by 8.9 cm (3 ½ in by 3 ½ in), and 1×6s measure 1.9 cm by 14.0 cm (¾ in by 5 ½ in).

Fig. 4. Target shed configuration for Series 2 experiments.

2.4. Mulch Preparation

In addition to the target mulch bed at the base of the shed, a mulch bed was placed under the fence in half of the cases to allow testing of the effect of the presence of mulch on flame spread and spot fires. The mulch was considered a surrogate for any fine combustible fuel next to or beneath the composite fence.

2.4.1. Mulch Pans

A set of pans was placed under the fence in each experiment to hold mulch and/or fences and to collect the burned debris.

To accommodate a bed of mulch 5 cm deep, two pans were fabricated from 26 gauge [0.454 mm (0.0179 in) thick] galvanized steel sheets. Each steel sheet pan was 87.6 cm (34.5 in) wide and 1.83 m (6 ft) long with 2.5 cm (1 in) high side walls. The two pans were overlapped and connected at the walls with two small C-clamps, for a total combined length of 3.35 m (11 ft). When mulch was placed in the pan, it was generally spread at a compressed depth of 5 cm ± 1 cm. The mulch depth was tapered over roughly the outermost 20 cm to meet the side walls at a depth of 2.5 cm, and also tapered toward the front of the pan to a depth of 2.5 cm. This slight sloping at the edges was done to decrease the step change from ground to full-depth mulch and reduce the effect of the pan and mulch on the wind field near the ground.

After a fence was placed at the correct location in the pan, the fence panel was raised to the prescribed height above the ground and attached to the end posts. The mulch was checked to make sure that it barely contacted the bottom of the fence and was adjusted where necessary. Downwind edges of the mulch pan and the fence post furthest from the wind machine were both located at the prescribed separation distance from the shed wall. Since the combination of fence panel and posts was typically 2.62 m (8.6 ft) or less in length, the excess pan length extended upwind from the leading fence post and included a 30 cm to 60 cm length of mulch to allow the observation of counterflow flame spread on the mulch upwind of the fence. Approximately 0.17 m^3 (6 ft^3) of uncompressed mulch was required to fill the mulch bed. The shredded hardwood mulch was compressed by stepping on it, with pressure of up to about 34 kPa (5 psi), based on the weight and contact area of the researchers. The resulting density of the mulch measured after compression was 253 kg/m^3 (15.8 lb/ft^3) ± 3 %.

2.4.2. Mulch Type

The mulch used in the composite fence experiments for both the target mulch bed and under the fence was shredded hardwood, shown in Fig. 5. The mulch consistent mostly of “fines” or small and thin pieces of wood, but some larger “chunks” were part of the mix, as shown below.

Fig. 5. Shredded hardwood mulch.

2.4.3. Mulch Conditioning

The shredded hardwood mulch used in these experiments was dried to 6.5 % ± 1 % moisture content. The drying process utilized during the study was placing mesh bags on wire shelving in a wood-drying kiln. A moisture content of 6.5 % was selected because it is on the order of values seen in wood in summertime in the American Southwest [23] – a low value, yet more

realistic than the far lower moisture content that could have been achieved through oven-drying.

Mulch moisture content was measured with an Arizona Instruments Computrac MAX 1000 moisture analyzer (see Fig. 6). After drying, the mulch was placed in plastic bins that could hold between 56.6 L (2 ft^3) and 113.3 L (4 ft^3) for storage and transport. The bins were stored either in a conditioned (30 % RH) indoor space at NIST or in sealed bins in a conditioning shed at the test site. The dehumidifying equipment at the latter site was unable to reduce the water vapor content below 35 % RH; however, with sealed bins, large amounts of mulch, and a small moisture gradient, the moisture content was not expected to change significantly when moved from 30 % to 35 % relative humidity conditions. A chart of equilibrium moisture content (EMC) of wood as a function of relative humidity and temperature shows that EMC ranges from 5.6 % to 6.3 % at 30 % RH and 6.3 % to 7.1 % at 35 % RH, for temperatures from 43.3 °C to -1.1 °C (110 °F to 30 °F) [23,24]. Therefore, a moisture content estimate of 6.5 % ± 1 % encompasses the sets of conditions at both sites, as well as the effects of variations in initial drying.

Fig. 6. Moisture analyzer used for measuring moisture content of mulch.

2.4.4. Target Mulch Bed

To study whether the composite fences were capable of generating firebrands that could threaten a structure through spot fires, the experiments included a target bed of shredded hardwood mulch placed along the base of the shed wall, as shown in Fig. 7. The target mulch bed was 0.46 m (18 in) wide and 2.44 m (8 ft) long. Two steel pans, each 1.37 m (4.5 ft) long,

were overlapped in the middle to create the 2.44 m total length. The pans had 2.5 cm (1 in) walls on the far ends and on the back edge that abutted the shed wall.

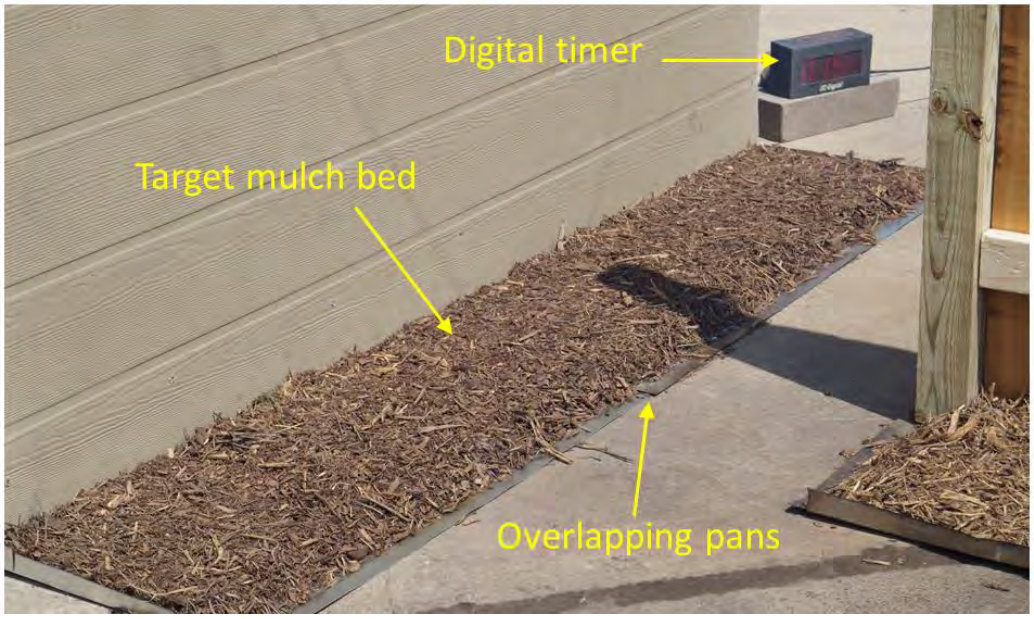

Fig. 7. Target mulch bed and digital timer.

The target mulch bed served as a surrogate for any combustible material next to a structure. Because of its rough texture, any firebrands landing on this surface tended to stay in place. Shredded hardwood mulch was selected as a conservative worst-case for combustibles near the structure: dry, consisting of easily ignited small pieces, and comprised of innumerable crevices in which firebrands could lodge. The mulch was conditioned to 6.5 % ± 1 % moisture content, as described in the previous section.

The mulch bed was prepared by filling the pans with an even layer of mulch and compressing the mulch by foot, as described in Section 2.4.1. The target mulch bed was 2.5 cm thick, with the first 3 cm of the leading edge slightly tapered down to about 1.5 cm thick to decrease the severity of the abrupt change in height from the ground and to reduce the number of sliding firebrands that were caught at the front edge of the bed.

2.5. Composite Fence Types, Materials, and Preparation

The three composite fences tested in this study are shown in Fig. 8. All fences had the same appearance on both sides of the fence so that both neighbors would see the finished, “pretty side” of the fence. Although other styles are available from the manufacturers, the fences used in this study were designed to imitate the look of wood fences.

Fig. 8. Composite fence types: a) wood-plastic composite #1 (WPC1), b) wood-plastic composite #2 (WPC2), c) steel-plastic composite (SPC). White "flags" marked support wires for safety.

2.5.1. Structure and Dimensions

Composite fence material information was collected from product information available from the manufacturers and/or vendors. WPC1 fences, shown in Fig. 8 (a), are made from a UV-resistant composite of approximately 50 % wood fibers and 50 % high-density polyethylene (HDPE) (95 % recycled). The wood-plastic composite boards were extruded individually and designed to interlink, leaving no gaps between boards. The assembly primarily consisted of top and bottom rails holding the interlinked vertical boards. The vertical boards, made of 5.6 mm (7/32 in) thick composite, stood in the slot running along the entire length of the bottom rail made of 2.5 mm (0.1 in) thick aluminum, which was 15 cm (6 in) tall and wrapped with 5.6 mm (7/32 in) thick composite rail covers. At the top, the boards were inserted into the 15 cm (6 in) tall, 13 mm (1/2 in) thick top rail. Both rails were suspended from brackets attached between their ends and the posts. For the experiments, treated 4×4 pine posts were used instead of the sleeves sold with the assembly.

WPC2 fences are an aluminum-framed UV-resistant composite of bamboo fibers and HDPE (35 % recycled) in a ratio of about 1:2 plus some additional additives including calcium carbonate. The boards for the WPC2 fence were arranged horizontally, as shown in Fig. 8 (b). Hollow aluminum posts 10 cm (4 in) wide were mounted on stands at each end of the fence. An aluminum bottom rail 30 mm (1.2 in) high was inserted into slots on the posts, followed by a set of eight fence boards each 21 cm (8.3 in) tall and topped by an aluminum upper rail 30 mm (1.2 in) high. Each board was hollow with braces separating front and back surfaces, for a total board thickness of 17 mm (0.7 in).

The SPC fence is sunlight-stabilized linear low density polyethylene (LLDPE) (25 % recycled) reinforced with galvanized steel (no wood component). For the SPC fences, shown in Fig. 8 (c), the panel was one large piece of molded plastic. The panel was hollow and made from two halves fused together. The plastic thickness varied throughout the panel, but averaged between 3 mm (1/8 in) and 4 mm (5/32 in). Hollow square steel tubing ran through the top and bottom frame sections of the panel. The steel tubing had outside dimensions of 4 cm (1 9/16 in) and the wall thickness was 1 mm (0.04 in). The posts were separate with steel components running lengthwise inside the plastic. End posts were used rather than posts used for joining two panels. The end posts had a U-shaped cross section (unlike the joining posts which had an H-shaped cross section), and for assembly, the panel was inserted into the slots in the posts and two screws connected the panel to each post at the top and bottom.

The masses and dimensions of samples of the composite fences were measured to determine their densities. The densities are listed in Table 1.

Table 1. Composite Fence Densities

Fence	Density (g/cm^3)	Combined Standard Uncertainty, u_c (g/cm^3)	Combined Standard Relative Uncertainty, u_c (%)	Expanded Uncertainty, $2u_c$ (%)
WPC1	1.073	0.004	0.4	0.8
WPC2	1.206	0.007	0.6	1.2
SPC	0.851	0.028	3.3	6.5

Uncertainties for the dimensions of the assembled fence are discussed in Appendix B.1 along with other measurement uncertainties.

2.5.2. Fence Support

Each WPC1 panel was assembled and mounted with wood screws at the top and bottom on two pressure treated pine posts with square cross sections 8.9 cm (3.5 in) on a side (nominal 4×4 lumber). The panel length was 2.31 m (7 ft 7 in). The posts at each end added 17.8 cm (7 in) to the length of a single privacy fence panel, for a total length of 2.62 m (8 ft 2 in). Since experiments were conducted on pavement and holes could not be made for posts, the fence panel and post assemblies were supported by boring a 2.4 cm (0.94 in) diameter hole in the bottom of each post and inserting the 25 cm (10 in) long, 1.91 cm (0.75 in) diameter “leg” of a

steel “foot” in the hole. At the bottom of the vertical leg rod, each foot was made with a cross of 4.8 mm (3/16 in) thick, 2.5 cm (1.0 in) wide steel bars.

WPC2 panel ends were inserted into the vertical slots of the octagonal cross section aluminum posts provided in the kit. The same leg and foot supports used for WPC1 fence posts were inserted into the bottoms of the aluminum posts to provide stability for the fence assembly. For the first WPC2 experiment with mulch under the fence, in order to keep the assembly together while burning and deforming, a 15-gauge (1.45 mm or 0.0571 in diameter) steel wire was wrapped around the whole assembly about 8 cm (3 in) off the ground and twisted to tighten it. For the second WPC2 experiment with no mulch under the fence, an additional wire was wrapped and tightened about 21 cm (8 in) from the top of the assembly to provide even more integrity to the fence based on the first WPC2 fence’s performance while burning. WPC2 fence panels were 1.79 m (70.5 in) long with post spacing of 1.86 m (73 in) and total assembly length of 1.98 m (6 ft 6 in).

SPC fences in these experiments utilized two kinds of manufacturer-provided posts: one for ending a fence line and another for joining two panels together. For these experiments, an end post faced the wind and a joining post faced the shed with the panel between them connected to each. The end post had a U cross section with the panel inserted into the slot opening side of the post. The joining post with an H cross section had slot openings on both sides to accept panels on each. For each experiment, an SPC panel was inserted into the posts and secured with screws at the top and bottom of the posts. The panels were 1.81 m (70.6 in) in length with post spacing of 1.83 m (72 in). Together with the two posts, the total length was 1.96 m (6 ft 5 in).

For all fence types, each end of the fence was connected to two partially filled 208 L (55 gal) barrels of water using 15-gauge (1.45 mm or 0.0571 in diameter) steel wires. The purpose of this was to provide stability and to prevent the wind from blowing the fence over or causing unrealistic vibration or other motion. The wire support system also allowed the fences to be adjusted for verticality. For safety, lengths of thin white paper were tied around the wires to make their positions visible to the experimentalists during setup and teardown. Some ties are visible in Fig. 8 (a) and (c).

2.5.3. Fence Conditioning

Fences and posts, whether wood, plastic, or composite, were stored in the same conditioned spaces as the mulch (30 % RH building on the NIST campus and 35 % RH conditioning shed at the test site). Like the mulch, the moisture content for any wood components was 6.5 % ± 1 %, selected as a value that would provide more realistic conditions for fire spread than the enhanced conditions that would result from using oven- or kiln-dried wood [23]. It was not known how to measure the moisture content of the composite and plastic components, so how it may have changed with the conditioning environment is also not known.

2.6. Ignition Source

Each composite fence was ignited by a propane burner applied near the end farthest from the structure, with the heat applied about 2.5 cm (1 in) from and further downwind of the leading post. The customized burner consisted of eight Venturi-style brass torch heads (Bernzomatic brand Pencil Flame model), arranged with four torch heads on each side of the test object. Two torches of each set pointed 45° upward toward the fence and the other two pointed 45° downward toward the mulch, as can be seen in the overhead view in Fig. 9. The torches were wrapped with Kaowool ceramic fiber blanket and then covered with aluminum foil as shown in Fig. 10 for protection from flames and radiation after ignition of the fence and mulch.

Fig. 9. Propane burner for igniting fence and/or mulch, with torches exposed.

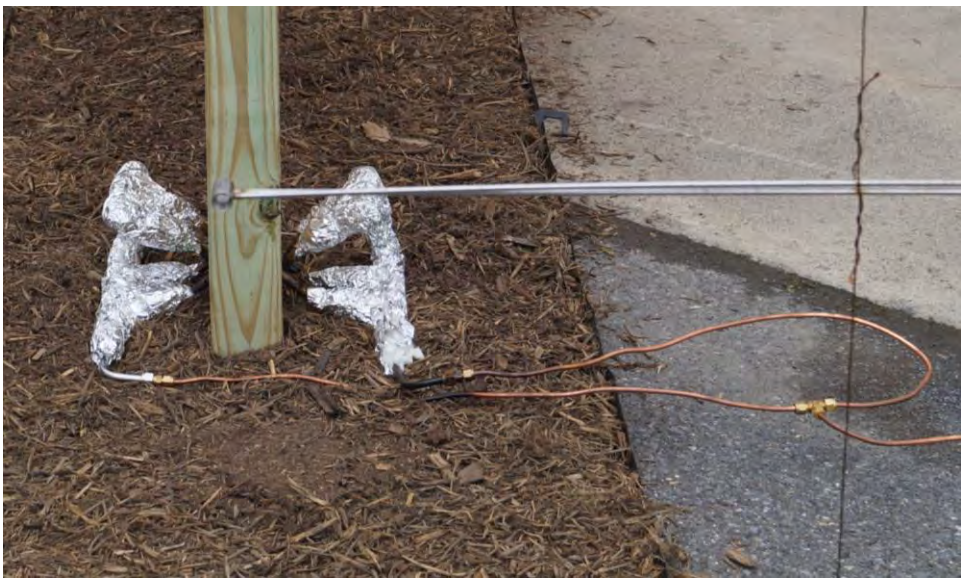

Fig. 10. Propane burner protected by Kaowool blanket and aluminum foil.

2.7. Measurements

2.7.1. Wind Speed Profile

The composite fence experiments were performed under imposed wind speed conditions of 6 m/s in line with the fence. In order to measure the wind velocity field, an array of 13 or 17 bidirectional probes was placed 1.22 m (4 ft) upwind of the fence post closest to the wind machine. This location was selected to capture the wind field close to the fence/mulch that is the focus of the experiment without influencing the upwind measurement. Bidirectional pressure probes measure the difference between the total pressure on the windward side of the probe and the static pressure on the leeward side. The difference is the dynamic pressure caused by the wind, which can be combined with temperature and a probe factor to calculate the wind speed [25]. The leads of the probes were connected to Setra Model 264 bidirectional pressure transducers, which have a pressure range of ±373.6 Pa. Each transducer produced a voltage output from 0 V to 5 V, with 2.5 V output indicating zero pressure differential. Combining the pressure measurement with ambient temperature gave a corresponding velocity range of about ±23 m/s (±52 mi/h). The transducer calibrations were checked periodically with a pressure calibration system, and their sensitivities were found not to drift significantly. Voltage outputs measured during daily pneumatic zeroing (which will be described in Section 2.9.2) were used to account for any voltage offsets.

A photograph of the bidirectional probe array in front of a fence/mulch test combination is shown in Fig. 11, and the diagram in Fig. 12 indicates the locations of the 17 probes used in Tests H-1, H-2, and H-3. The 13-probe array used in Tests E-1, E-2, and F-1 did not include probes 14 through 17. The 13-probe array consisted of five probes arranged vertically on the centerline of the experiment at heights of 0.30 m (1 ft), 0.76 m (2.5 ft), 1.22 m (4 ft), 1.68 m (5.5 ft) and 2.13 m (7 ft) measured from the ground; two sets of two probes each extending out from the centerline in 0.61 m (2 ft) intervals at both the lowest (0.30 m) and highest (2.13 m) positions; and an additional four probes extending out from the centerline in 0.30 m (1 ft) intervals at the middle (1.22 m) position. The 17-probe array added two probes at 0.30 (1 ft) intervals from the centerline at both the 0.76 m (2.5 ft) and 1.68 m (5.5 ft) heights. This allowed for collecting velocity data for a vertical velocity profile at the centerline and a horizontal velocity profile at the center height. It also added several additional velocity measurements to provide a more complete picture of the velocity field generated by the wind machine.

Calculation of the wind speed at a given probe required knowledge of the ambient temperature along with the differential probe pressure. Temperature was measured with a type K thermocouple bead made from 24 AWG wire (0.51 mm diameter). The temperature measurement location was about 2.5 m away from the probe array and shielded from thermal radiation from either the fire or sun.

The wind profile measured by the bidirectional probe array depends primarily on the speed of the applied wind and the distance from the wind machine, with a contribution from the

component of ambient winds in the direction measured by the probes. Because the probe array is 1.22 m (4 ft) upwind from the fence and at least 5 m (16.4 ft) upwind from the shed, the effects of these objects on the measured wind field are minimal.

A study of the wind field measured by the probe array as a function of distance from the wind machine was performed as part of the previous work on fences and mulch and reported in Appendix C.2 of [1]. From this previous study, the average of the velocities of the lower four probes along the centerline was selected as a measure of the characteristic wind velocity for a specific experiment.

Fig. 11. Bidirectional probe array with 17 probes.

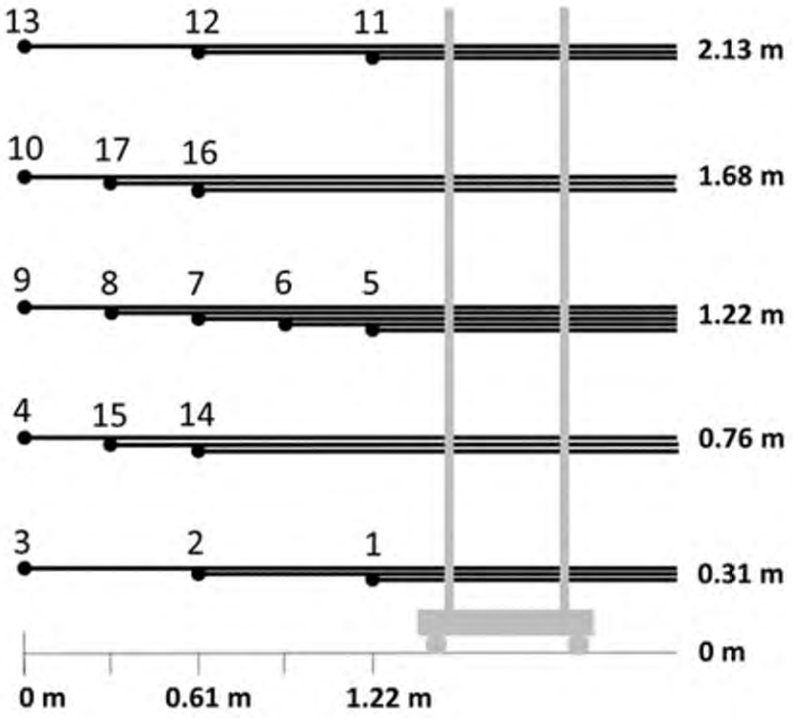

Fig. 12. Diagram of the bidirectional probe array used to measure the velocity field for Tests H-1, H-2, and H-3.

2.7.2. Ambient Wind Speed and Direction

The ambient wind speed and direction were measured by an anemometer mounted on a 3.7 m (12 ft) pole about 7.9 m (26 ft) south-southeast of the wind machine propellers and 17.7 m (58 ft) south-southwest of the target shed. For the final three experiments, a second anemometer was added 6.92 m (22 ft 8 in) left of the centerline (measured perpendicularly) and 4.88 m (16 ft) from the shed toward the wind machine. The instruments were Young model 86000 Ultrasonic Anemometers with 5 V output and 0.25 s response time for both wind speed and wind direction. Wind speed was measured with 0.01 m/s resolution and ± 2 % accuracy as stated by the manufacturer, and the wind direction was measured with 0.1° resolution and ± 2° accuracy. Wind direction accuracy was degraded to about ± 5° due to the estimation of true north during installation and slight positional drift due to high winds, which was periodically corrected. The ambient wind measurement provided an approximate wind environment near but not exactly at the location of the experiments, so some focused wind gusts may have been located at the experiment and not the anemometer or vice versa.

2.8. Data Acquisition

2.8.1. Wind and Temperature Data

A data acquisition system was required to measure from 16 to 22 channels of measurements, depending on the experiment, from the bidirectional probe array located in front of the fence,

an ambient temperature thermocouple, and the local wind speed and direction from the sonic anemometer(s). Voltage and thermocouple data from the sensors were collected using two National Instruments input modules, NI-9205 and NI-9213, respectively inserted in a National Instruments cDAQ-9174 CompactDAQ USB 4-slot chassis. For the earlier experiments, the data were collected at 10 Hz, but for the final three experiments, the data were collected at 10 kHz. For all experiments, the data were averaged over every second for each channel. The program saved the averages and standard deviations of the samples from each channel to the output file, which was stored on a laptop computer and later uploaded to a permanent data storage repository. A LabVIEW program called MIDAS (Modular In situ Data Acquisition System) developed at NIST's National Fire Research Laboratory was used to collect the data and was also used to monitor data quality and spot check for sensor malfunctions.

2.8.2. Digital Video and Photographic Records

A minimum of four high-definition video cameras, Sony model HDR CX-350, were placed around the fence to capture the fire and smoke behavior. Two cameras located on opposite sides of the fence included the fence, shed wall, and shed mulch pan in their fields of view. These cameras captured fire spread and spot fire ignition data. An additional two cameras were located upwind of the fence next to the wind machine flow straightener, including the fence, shed, and shed mulch pans in their views. Figure 13 is a top view schematic of the experimental setup showing the relative positions of the video cameras.

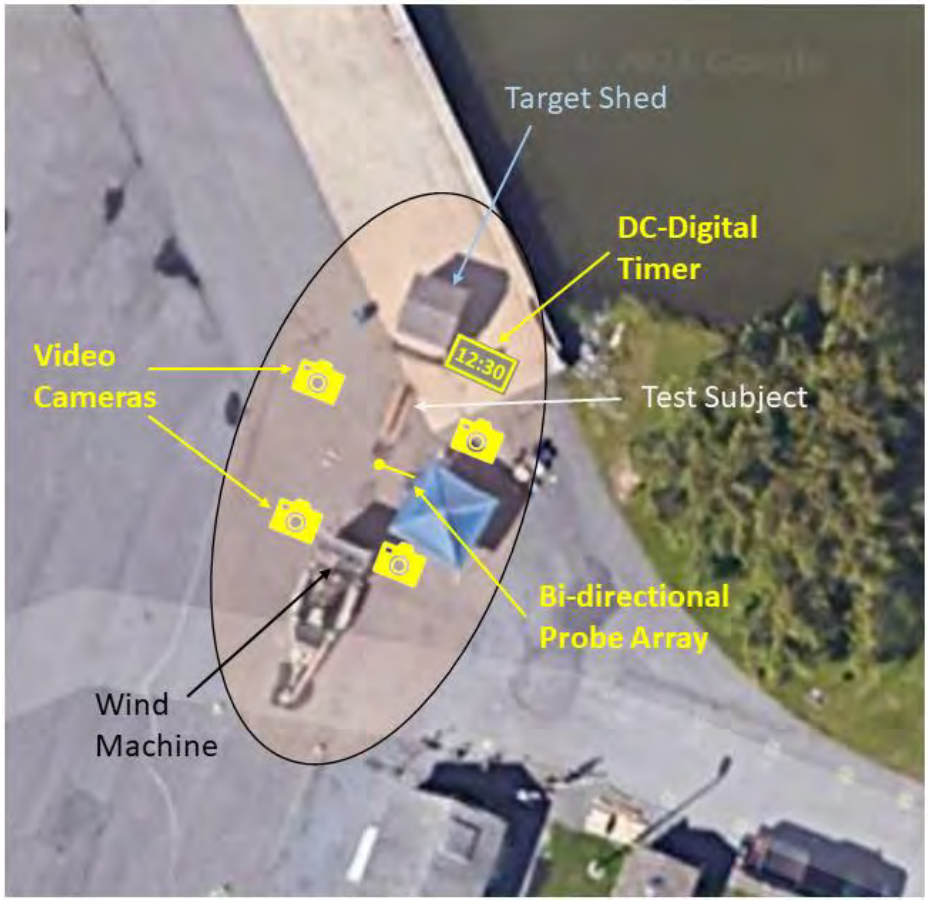

Fig. 13. Top view schematic of experimental setup showing placements of video cameras, timer, and bi-directional probe array. Google Earth image with NIST overlay.

To track experiment time, a DC-Digital timer, model DC-25UT, was placed in view of at least two video cameras. The timer, visible in Fig. 7 and Fig. 11, was started simultaneously with the wind machine. This allowed the video records of the left view and one or two of the front views of the test setup to also record the timer and thus synchronize with the remaining video camera(s), the two stopwatches used, and the wind data, which was referenced to computer time.

Digital still photographs were taken throughout the testing period and afterward. The digital still camera used was Sony model SLT-A58. The handheld camera was used periodically to capture close-up video of interesting phenomena.

2.9. Experimental Procedures

2.9.1. Weather Conditions

The ambient wind speed was required to be less than 33 % of the nominal applied wind speed in order to carry out the experiment. If the ambient wind direction was forecast to be close to perpendicular to the direction of the generated wind, then ambient winds needed to be less

than 25 % of the generated wind. These acceptable limits were supported by simulations of the experimental setup with applied wind and a cross-flow wind using the NIST Fire Dynamic Simulator (FDS) [26]. Under these conditions, the impact of the ambient winds on the wind field generated by the fan was found to be minimal [1].

Winds from the north and northwest were also avoided as they caused smoke and firebrands to overspread the experiment control area.

Testing was usually not scheduled when rain chances were likely during a substantial part of the morning or afternoon. Excessively hot or cold weather conditions also precluded testing. Generally, experiments were not scheduled if the heat index was expected to rise over 32 °C (90 °F) for a large part of the day, in order to avoid heat exhaustion. If temperatures were not expected to surpass 10 °C (50 °F), experiments were precluded by difficulties with handling tools, vaporizing propane, and drying the wet ground after fire extinguishment.

2.9.2. Preparation

Preparation for a typical experiment began with clearing the test area of debris. The mulch pans were connected and located at the prescribed distance from the shed and centered along the shed/wind machine centerline axis. Heavy steel bars were placed in the assembled pan at the leading edge and in the overlap region to weigh it down. If a fence was to be erected, holes were bored into one end of each post and the posts were placed on the post support legs close to their final location. The fence was then positioned for attachment to the posts. Shims were used to raise the fence if a mulch layer was to be laid beneath. The fence and posts were predrilled and then screwed together at each horizontal stringer. After the fence was secured to the posts, the shims were removed, and a mulch layer was laid evenly and compressed by foot throughout the pan. The posts were set perpendicular to the ground and secured with wire to two water-containing barrels located off to the side and also to the shed or shed eaves if located at 0 m or 0.30 m (1 ft) separation distance. After the fence was secured, the support wires were marked for safety with strips of tape or other material to prevent personnel from running into them. Mulch was then laid, spread evenly, and compressed in the target mulch pan at the base of the shed, if prescribed by the test plan.

Preparations for instrumentation included positioning of the four or five video cameras with framing of the appropriate views. The bidirectional probe array was positioned in front of the leading fence post. A burner was connected to the propane gas cylinder and was positioned on both sides of the fence, with its leading torch head located 2.5 cm (1 in) beyond the trailing side of the leading fence post (see Fig. 9 and Fig. 10). Half of the torches on the burner were aimed upward to the face of the fence and the rest aimed downward toward the mulch, if mulch was present. The propane cylinder was opened and the burner line charged to check the burner for leaks, and then the gas was shut off with a valve. Before the first test on a given day, pneumatic zeroing of the pressure transducers was performed by connecting a short length of rubber tubing to each side of the bidirectional probes and recording the data. This also enabled observation of the pressure transducer voltages being read by the data acquisition system for troubleshooting problems. Voltages that were drifting indicated a poor connection, and voltages offset significantly from 2.5 V indicated a plumbing leak.

After a safety check of the surrounding area, the wind machine was warmed up for approximately 5 min prior to each experiment. A garden hose was attached to a fire hose, which was in turn connected to a hydrant. The hydrant was opened to charge the line, and a diesel pump was started up to pressurize the hydrant with water from the nearby pond.

Finally, a safety briefing was conducted to communicate the test procedure, participant roles, and safety reminders. Zeroing tubes were removed from the probe array, and the test description and filename were detailed in the logbook.

2.9.3. Operations

The following procedure was typical, although some minor aspects varied for some tests. The data acquisition system was initiated with the selected filename and description. Between 15 s to 60 s of background data were obtained before two stopwatches were started simultaneously and the program time was recorded. At that time, all video cameras were put into recording mode. After 50 s of stopwatch time, a small propane torch was ignited, and at 55 s the propane cylinder was opened. At 1 min, the ignition torch was held near the burner torches until they were all ignited. The times for initiating and completing burner ignition were recorded. For most experiments, the burner was sustained for 90 s on the fence and/or mulch in order to produce a self-sustaining fire that would not self-extinguish or go out in the wind. Cold conditions (which diminished the propane flow) called for longer burner duration up to 3 min. Photographs of the fence fire were taken shortly after ignition.

A countdown to generating wind was performed, and the digital timer located next to the shed pan and visible in two or three of the video camera views was initiated at the same time as the wind machine was started. The wind level was adjusted by setting the tachometer to 950 rpm (revolutions/min) for the wind [6 m/s (13 mi/h)] conditions used for the composite fence experiments. The times for initiating the wind and completing its adjustment were recorded in the log. As soon as the wind started, the burner was removed to protect it from the fire, and the propane valve was closed.

In addition to the continuous videos recorded on fixed cameras, photographs were taken from many angles and fields of view during the experiment. The photos included the overall views encompassing the entire fence and shed, the linear extent of the fire along the fence/mulch, spot fires in the target mulch bed, and unusual or interesting phenomena. Some interesting phenomena were captured using the video mode of the handheld digital camera. The experiment ended when a spot fire in the target mulch bed at the base of the structure reached the wall and after fire had also reached the end of the fence. Flames at the wall from spot fires were extinguished if the fire had not yet spread over the entire length of the fence/mulch bed in order to capture the fire spread rate over the entire fence. At the end of the test, the fires were extinguished with a water hose and post-fire photographs were obtained.

2.10. Parameter Summary

The six experiments included in this study looked at three types of composite fence: two wood-plastic composites, WPC1 and WPC2, and one steel-plastic composite. Each fence was tested

twice: once with mulch and once without to determine whether fine materials at the base of the fence made a difference to the progress of a fire.

Cone calorimeter testing was performed on the three composite fence materials in both horizontal and vertical orientations. These tests enabled a comparison of flammability of the fence materials themselves. The description of the testing and results for each material are given in Appendix C, and the comparative implications for fire behavior are presented in Section 5.

3. Analytical Tools

The data acquisition systems described in Section 2.8 created a file containing raw sensor data for each experiment. In order to develop an understanding of the fire behavior, the data needed to be analyzed and visualized. This section briefly describes the analysis of the video evidence and wind data collected from each experiment. Full descriptions of the tools and procedures for collecting and displaying the data on flame spread and wind field are discussed in the previous report on fences and mulch [1].

3.1. Video Analysis

The primary data that were collected from each composite fence experiment were flame spread and firebrand spotting. Each experiment employed four video cameras, with views from the left, right, left front, and right front of the object being tested, from the point of view of the fan (facing the shed). The videos recorded the progress of flames and charring and the ignition of spot fires, as well as events such as burner ignition, fan engine startup and shutdown, and the start of suppression. The frame rate was 29.97 frames/s.

Timing, flame spread, and spotting analyses were performed on videos from the left and right side cameras. Commercial software was used for manipulating the experimental videos. The MATLAB computing environment [27] was used to build interactive tools for tracking the flame fronts over the fences and for analyzing the wind field. The graphical user interfaces (GUIs) for selecting points on the video were developed using GUIDE in MATLAB to lay out the GUI components (such as push buttons, pop-up menus, and plots) and to set up the framework for event-driven programming. Several GUI applications were later migrated to MATLAB's App Designer interactive development environment.

3.1.1. Event Timing

All four video cameras monitoring the experiment were turned on shortly before the propane burner was applied to the test subject and turned off as the fire was being extinguished with water from a hose. Each camera view was fixed in place during the experiment after adjustment to capture the field of interest. To compare the views from multiple cameras, usually the right and left views, the timing was synchronized. The five events listed below were selected as the primary timing markers because they were common to all camera views and could be determined within a few video frames. The procedures are explained in more detail in [1].

a) *End of Gas Burner Ignition*
   The End of Gas Burner Ignition event was the last moment that the small propane ignition torch was applied to the gas burner.

b) *Start to Remove Gas Igniters*
   The Start to Remove Gas Igniters event was the moment when the gas igniters/burners began to be moved away from the point of ignition. This typically took place about 1.5 min after the End of Gas Burner Ignition.

c) *Fan On*
The Fan On event marked the time at which the fan reached the initial maximum audio amplitude, as viewed in the audio track display.

d) *Fan Off*
The Fan Off event was the moment at which there was a detectable decrease in the audio amplitude produced by the fan, as viewed in the audio track display.

e) *Water First Applied*
The Water First Applied event marked the first moment when water from the hose was observed to reach the burning object to extinguish the fire.

For the six experiments on composite fences, the digital timer was not needed to resolve timing issues.

The timing of spot fires was measured by observing ignitions in the target mulch bed at the base of the shed. Three simple timing measures were recorded for each experiment: (1) the time at which the first spot fire ignited within the target mulch bed, (2) the time of ignition for the first spot fire to put flames against the wall, and (3) the time at which flames were first observed at the wall. Ignition was detected by the first visible sign of smoke. The right and/or left video recording was used to identify both the first spot fire ignited and the first spot fire resulting in flames on the wall. These two spot fires were then tracked back in time to determine the first time at which a puff of smoke from that location was distinguishable from the surroundings. The time when the first splash of orange was observed at the base of the wall or along its surface was recorded as the time of flames on the wall.

For intense fires such as some of those encountered in this study, the changes in camera exposure settings to adjust to very high light levels caused the target mulch bed to become very dark in the videos. This made it difficult to see incipient smoke. However, the large fires also resulted in spot fire ignitions from radiation and direct flame contact, which created flames much more rapidly than ignitions from firebrands. In these cases, spot fire ignitions were detected by flames rather than smoke.

Uncertainties in the timing of these events are discussed in Appendix B.3.

Timing markers were obtained using VirtualDub [28,29] video processing software or its newer version VirtualDub2 [30] for frame numbers and AVS Video Converter [31] for clock times. Frame numbers or times of events were recorded in an Excel file. Some discrepancies in timing were observed among video handling tools, but markers obtained from these software packages were found to be consistent within ±0.5 s.

3.1.2. Conversion of Videos to Image Sequences

Videos from right and left cameras were used to determine flame spread as a function of time. The tools developed for this analysis required the videos to be converted into sequences of images. Each image needed to be as sharp as possible in order to estimate the location of the flame front in the mulch bed or on the surface of the fence. Other considerations included the digital size of the stored images and the length of time required to create them.

The software selected for this task was VirtualDub [29] or successor VirtualDub2 [30] equipped with Ut Video Codec Suite [32] to provide lossless compression and Smart Deinterlacer Filter [33] to eliminate interlacing artifacts. VirtualDub allowed the extraction of every 30 frames, resulting in a set of images spaced apart by 1.001001 s (corresponding to the video frame rate of 29.97 frames/s). This provided better image quality than other video handling tools that used averaging to create a sequence with one image per second. Ut Video Codec Suite, with fast lossless compression capabilities, was used to first convert the original digital video in .m2ts format to .avi format, using only one out of every 30 frames. For the final image sequence, every frame was then extracted from the .avi video. This procedure reduced the time required to extract images from the original video by more than an order of magnitude. Smart Deinterlacer Filter eliminated lines where there was frame-to-frame motion, such as in areas with flame or smoke, leaving the motionless parts at high resolution.

3.1.3. Fence Flame Front Tracking

A MATLAB GUI tool, fence_test_analysis.m, was developed to track the burned area of the fence as a function of time.

The procedure for defining the geometry for fence experiments is described in detail in Section 3.1.4 of [1]. In brief, the user started by defining four points at the corners of the fence, as shown in Fig. 14.

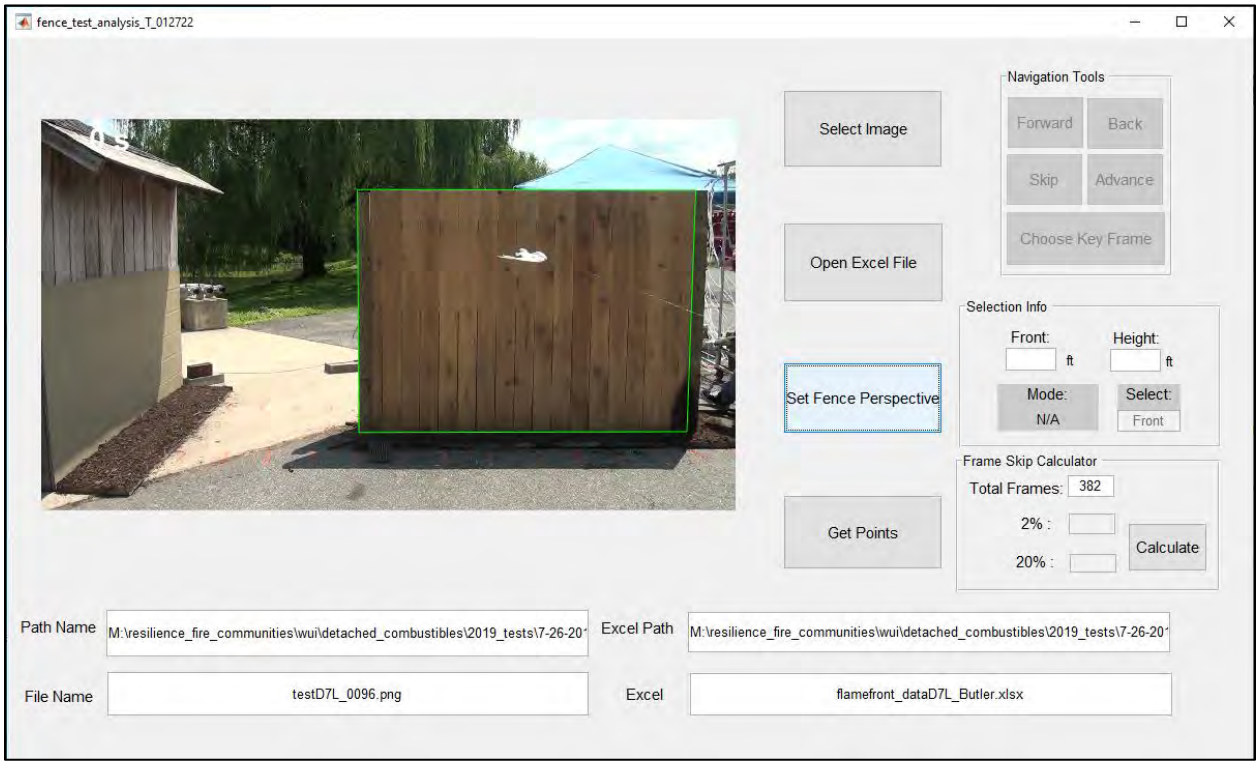

Fig. 14. GUI for selection of location points for fence video.

The GUI then allowed the user to move forward in time by arbitrary intervals. For each displayed frame, the user could identify three points: one to define the progress of the flame front towards the shed, the second to mark the height of fire damage in the area of ignition, and the third to mark the damage height outside of the ignition zone. Damage was defined by darkened material for the two types of wood-plastic composite fences and by wavy distortions for the steel-plastic composite fence. Time and flame front locations were automatically recorded in an Excel file for later plotting.

The MATLAB program also allowed the capture of two-dimensional fire damage profiles on the fence. At five evenly distributed times throughout the experiment, crosshairs could be used to select an arbitrary number of points outlining the damaged region on the fence. For the SPC fences, the profiles were defined by the outline of dripping material (that is, the absence of panel material) rather than the distortion of the plastic panel. A broad outline rather than detailed tracing of the exact profile was considered satisfactory.

Obscuration by flames and smoke, lighting, and placement of the cursor all contributed to the uncertainty in the location of the char front on the fence. Uncertainties in the fence flame front analysis are described in greater detail in Appendix B.4.

3.2. Wind Analysis and Visualization

An interactive graphic user interface (GUI) program, windplots.mlapp, was written to convert the voltage files from the pressure transducers into wind velocities and display the results. This program was based on the MATLAB App Designer tool, and its procedures and outputs are described in detail in Section 3.2 of [1]. A summary is provided here.

As described in Section 2.7, the wind field just upwind of the fence or mulch bed was measured by an array of bidirectional probes, and ambient wind and temperature data were collected from a nearby sonic anemometer and a thermocouple. The data was collected and stored according to the process in Section 2.8.1. At the beginning of each test day, zeroing data was collected for the probes with short lengths of rubber tubing connected to each side, as described in Section 2.9.2. Probe data was later collected during each experiment, along with ambient wind and temperature.

The windplots.mlapp GUI tool enabled analysis and data visualization for both bidirectional probes and ambient measurements. The zeroing data was processed first to obtain the zero voltage level for each probe, which was then used to determine the wind speeds during the experiments. Figure 15 shows the GUI display for a series of fence tests from [1] after carrying out the zeroing analysis. The labeled data columns and plots are as follows:

A. Voltage data as a function of time. Lower and upper time bounds were defined by the user. In the example shown, the data from one probe fluctuated significantly within this range, indicating that there may have been connection issues.

B. The probe array, with a number and radio button for each probe. Probes that were clearly faulty (i.e., with values well outside the expected range or fluctuating wildly, as in this example) could be turned off by clicking on the radio button.

C. Average value for each probe in the array. Black dots at the center of each color square indicate the location of the probe in the array by height and distance from the centerline. Probes that were faulty and had been turned off were assigned the color white.

D. Average values for the five probes plotted along the centerline. Values were not plotted for faulty probes.

E. Average values for the five probes extending horizontally from the centerline to the outer edge of the array at a height of 1.22 m (4 ft) from the ground. Values were not plotted for faulty probes.

F. Table of probe values, showing location, mean, and standard deviation.

G. Ambient temperature as a function of time.

H. Wind rose plot of wind speed and wind direction during the specified time range. The green line indicates the orientation of the experiment, plotting the direction from the fan to the shed. The red line indicates the mean direction of the ambient wind.

I. Ambient wind speed measurements as a function of time.

J. Average values and standard deviations for temperature, wind speed, and wind direction.

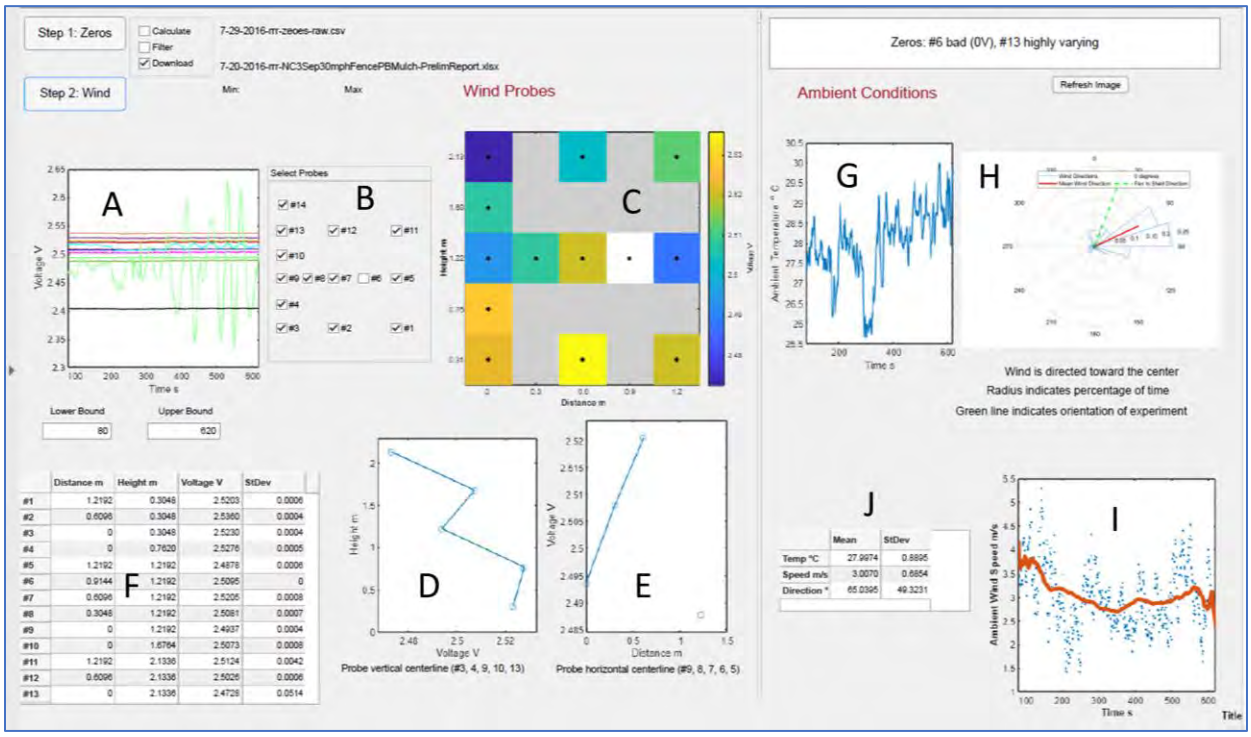

Fig. 15. Visualization of zeroing data for 29 July 2016, used for tests A-57 to A-60 in [1].

The zeroing voltages were then used to calculate wind speeds for each probe during the ensuing experiment(s). Figure 16 shows an example of the data visualization of wind speed

from an experiment that was carried out later the same day. The plots and tables are the same, except that the values from the probes are wind speeds rather than voltage. The lower and upper bounds were selected to encompass only the time range when the fan was on.

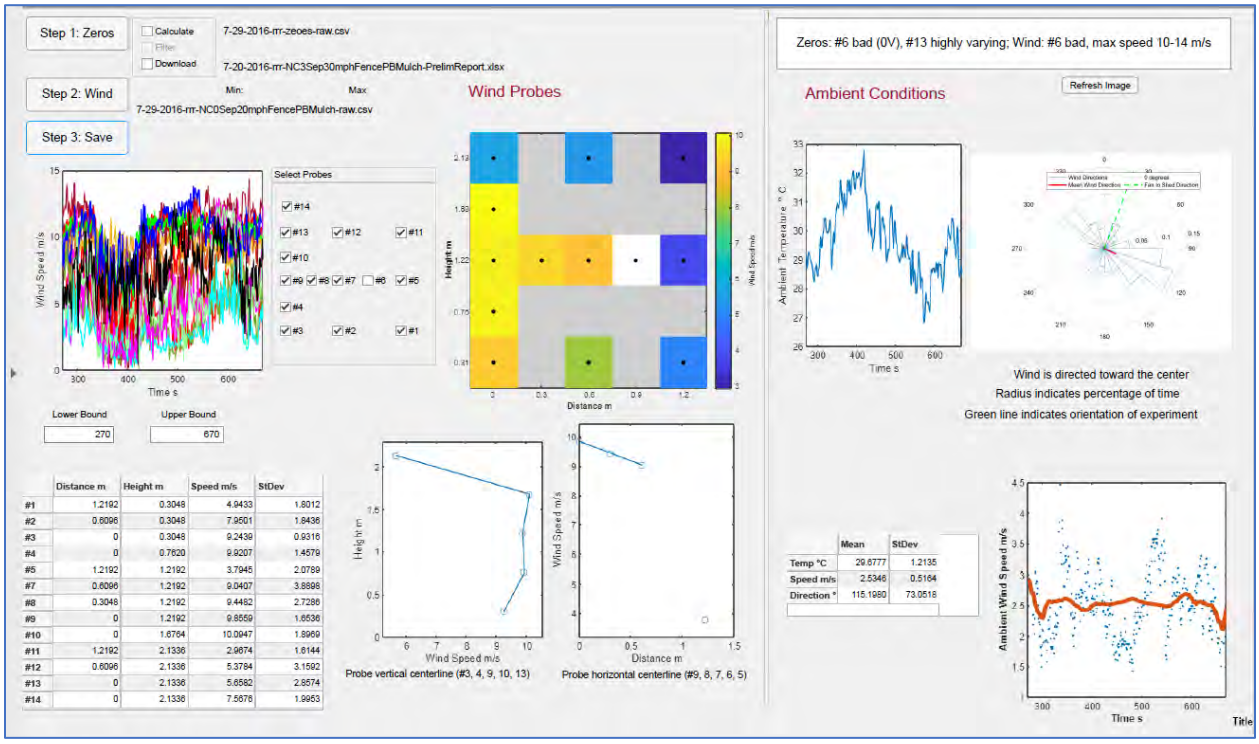

Fig. 16. Visualization of wind speed and ambient data for Test A-57 in [1].

4. Experimental Results

Experiments with and without hardwood mulch were performed on three types of composite fences. As discussed in Section 2.5.1, two were wood-plastic composite fences, mixing different wood and plastic materials and using different board orientations, and the other was a steel-plastic composite fence. The variety was intended to provide some insights into the effects of both fence design and material formulation for composite fences in the market today. All were privacy fences, extending from top to base and side to side with no gaps. All experiments were carried out under low wind speed conditions [6 m/s (13 mi/h)] and with a separation distance of 1.8 m (6 ft) between the downwind end of the fence and the shed.

The resulting fire behavior in each case is presented in this section through photos and flame spread data.

The results are organized by type of fence. For each fence type, the experiment with mulch beneath the fence is presented first, followed by the experiment without mulch. The latter represents the best-case fire scenario for combustible fences, in which the area underneath and along the sides of the fence is completely clear of fine fuels. This is an idealized situation, since a fence is not typically isolated from fine combustible materials. At its base may be grass, mulch, vegetative plantings, or accumulated leaves or needles. Dry leaves and other lightweight materials may be moved around by the wind. Accumulated debris can become compressed by the action of wind and rain, fixing the potential fuel in place as a target for ignition. When a fence is in close contact with the ground, it can be difficult to keep the area near the bottom of the fence clear of combustible materials.

Three experiments (Tests E-1, E-2, and F-1) were first reported in the earlier fence report [1]. The writeups for these experiments are basically repeated here, enabling a full discussion of the differences and similarities of the fire behavior for these three composite fences. Although no experiments were replicated, it is possible to form some conclusions on trends and modes of behavior based on these and the previous work.

More details on the results from each experiment are provided in case writeups in Appendix F. The contents of each case writeup are explained in Appendix E, including a description of the experiment, photographs from before and during the experiment, flame spread plots, critical times, and ambient and applied winds.

4.1. Wood-Plastic Composite Fence #1

Flame spread experiments on the first type of wood-plastic composite fence (WPC1), both with and without mulch, were presented in the earlier fence report [1]. To reiterate from Section 2.5.1, the boards for this fence panel were vertical and interlinked, and their ends fit into slots in the top and bottom rails.

This section reproduces the discussion from the earlier report with minor changes.

4.1.1. With Mulch

Figure 17 shows that a fire ignited at the upwind base of the fence and shredded hardwood mulch bed under low wind conditions in Test E-1 developed into a large fire, with flames extending well above the fence within 6 min after turning on the fan. The fire was expanded by the boards falling out of the top and bottom frames as the composite material softened; boards 1.83 m (6 ft) in length fell to either side of the fence and created a fire zone up to 3.7 m (12 ft) wide. Some softened boards near the post leaned forward as they fell and increased the fire exposure of the shed. The final configuration of the boards after extinguishment is shown in Fig. 18 with the final positions of boards to either side and downwind of the fence panel highlighted with arrows.

Fires ignited in the target mulch bed next to the shed only after the flames had become intense. The first fire in the target mulch bed ignited just before t = 7 min. Because it ignited immediately adjacent to the shed wall, this may have been a spot fire, possibly ignited by a firebrand originating in the mulch bed beneath the fence. The flames then spread laterally along the mulch bed. The set of fires in the target mulch bed just before extinguishment can be seen in the final frame of the sequence in Fig. 17 at t = 7.8 min.

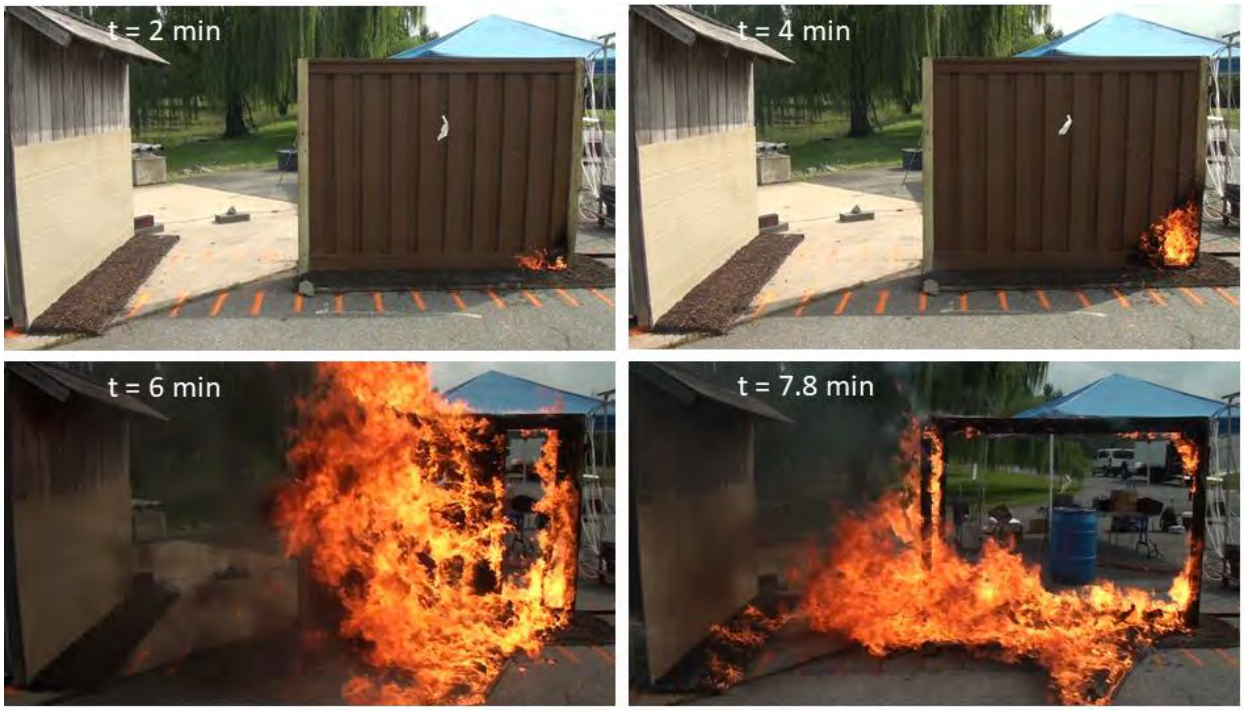

Fig. 17. Time sequence for wood-plastic composite fence #1 at low wind speed and 1.83 m (6 ft) separation distance [Test E-1].

Fig. 18. Final configuration of WPC1 wood-plastic composite boards after Test E-1. Yellow arrows highlight the final positions of fallen fence boards.

4.1.2. Without Mulch

Removing mulch from the base of the composite fence eliminates the contribution of fine fuels to the flame spread along the fence. Nevertheless, the fire behavior for the WPC1 fence without mulch at its base (Test E-2) was similar to that observed in the previous section for the same fence with mulch.

As shown in Fig. 19, a fire ignited at the upwind base of the fence developed into a large fire with flames extending well above the fence and licking the shed from 1.83 m (6 ft) away. As in the previous section, the boards fell to the sides as the top and bottom frames softened and distorted, expanding the fire on both sides and toward the downwind side of the fence and creating a fire zone up to 3.7 m (12 ft) wide. The final configuration of the boards after extinguishment is shown in Fig. 20.

As in the case with mulch (Test E-1), fires ignited in the target mulch bed next to the shed only after the flames had become intense. Fires in the target mulch bed can be seen in the final frame of the sequence in Fig. 19, at t = 14.1 min. Fires ignited along a large part of the front edge of the mulch bed in the final 10 s before the fire was extinguished, likely due to radiation and direct flame contact rather than firebrands.

Fig. 19. Time sequence for Test E-2, wood-plastic composite fence WPC1 alone (without mulch), with low wind speed at 1.83 m (6 ft) separation from shed.

Fig. 20. Final configuration of WPC1 wood-plastic composite boards after Test E-2. Yellow arrows highlight the final positions of fallen fence boards.

As occurred for several other cases in which the fence was fully involved, there was evidence that the shed might have been in danger of igniting if the fire had been allowed to continue. Fig. 21 shows water being applied to the underside of the eaves of the shed as part of the extinguishment of the fire after the experiment. Smoke can be seen rising from the shed roof in this image – water was also applied to cool the roof. It was clear from this and other experiments with large flames that 1.83 m (6 ft) separation distance was insufficient to prevent the structure from ignition.

Fig. 21. Water being applied to the eaves of the shed after Test E-2. Smoke rising from the roof is visible.

4.1.3. Flame Spread

The location of the flame front as a function of time for the WPC1 wood-plastic composite fence with and without mulch is plotted in Fig. 22. Both experiments were performed at low wind speed and at 1.83 m (6 ft) separation distance from the shed. The uncertainties for these plots are described in the uncertainty analysis for fences in Appendix B.4.

Experiments on WPC1 with and without HW mulch (Tests E-1 and E-2, respectively) indicated that the presence of mulch below the fence acted to accelerate the progress of the flame down the fence, approximately halving the time for this single panel test. At 6 min from the point of ignition to the end of the panel, the flame front was found to progress faster over the WPC1 fence/HW mulch combination than for any other fence-mulch combination in the full fence study [1].

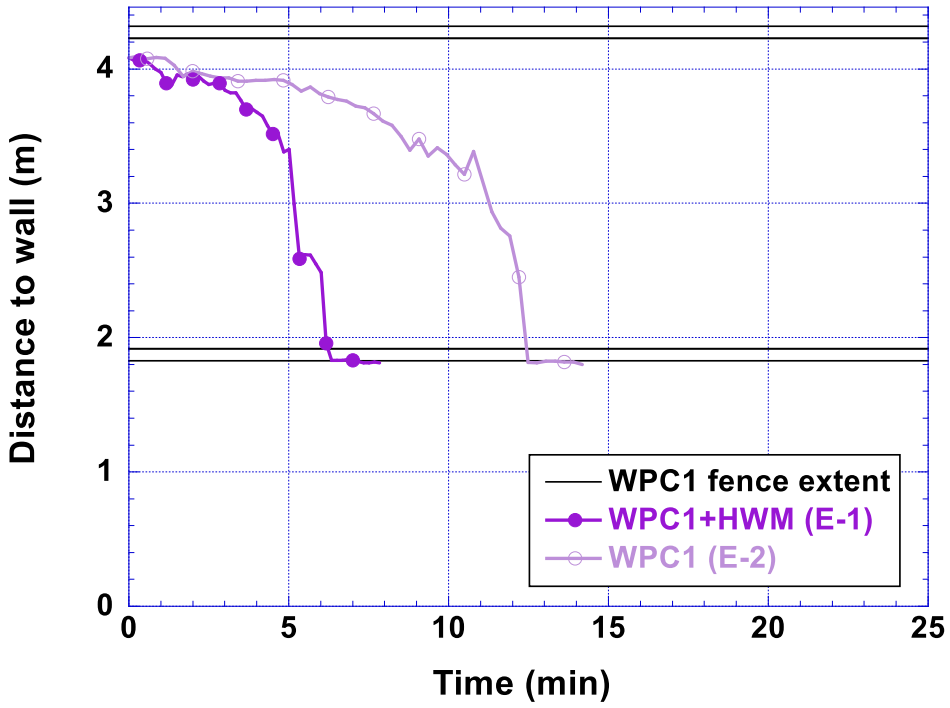

Fig. 22. Flame spread as a function of time for WPC1 fence with and without HW mulch beneath.

4.1.4. Firebrand Spotting

Ignitions occurred in the target mulch bed for WPC1 fence experiments both with and without shredded hardwood mulch at the base of the fence. The times to ignition of the first spot fire, ignition of the first spot fire whose flames reach the wall, and flames reaching the shed wall for these two experiments are presented in Table 2. The ignitions in the target mulch bed occurred near the end of each experiment, when the flaming on the fence panel was intense. In Test E-1, the first spot fire ignited immediately adjacent to the shed wall, with flames reaching the wall 24 s later. This suggests ignition by a firebrand; possibly one that originated in the mulch bed beneath the fence. A piece of burning plastic and other burning firebrands were observed in Test E-2, although the widespread ignition of the target mulch bed in this case was likely due to radiation or direct flame impact. The flames then spread laterally along the mulch bed without reaching the wall.

Table 2. Spot fire timing for WPC1 fences with and without mulch.

Fence w/wo Mulch	Time to Ignition of First Spot Fire	Time to Ignition of First Spot Fire to Reach Wall	Time to Flames on Wall
WPC1 + HWM (Test E-1)	6:44	6:44	7:08
WPC1 (Test E-2)	11:50	N/A	N/A

4.2. Wood-Plastic Composite Fence #2

Unlike the vertical boards for the WPC1 fence, the boards for the WPC2 fence were arranged horizontally. Eight fence boards were inserted into slots on the vertical posts, preceded by the aluminum bottom rail and followed by the aluminum upper rail. A more complete description can be found in Section 2.5.1. An experiment on a WPC2 fence with shredded hardwood mulch (Test F-1) was presented in the earlier fence report [1]. That writeup is repeated here, along with the results from the new experiment without mulch.

4.2.1. With Mulch

This section is borrowed from the full fence report [1] with minor changes.

The fire behavior for the WPC2 fence with shredded hardwood mulch beneath (Test F-1) was quite different from that for the WPC1 fence, as shown in the sequence in Fig. 23. As the fire consumed each horizontal board in turn, the boards above it slipped downward, still confined within the black aluminum frame defining the panel. Figure 24 gives an example of the boards collapsing downward over a period of one second as the support from the bottommost two boards gave way. As the remaining segment of each board fell flat against the ground, it tended to disrupt the flames, slowing the burning process until the flames reestablished themselves on the edges of the board. Although flaming was vigorous, the flame height never reached above the halfway point on the fence, and the fire diminished on its own as it ran low on fuel. With the frame holding the boards in line with the fence during the fire, the fuel stayed within a couple of feet from the centerline. The final configuration of the boards shortly before extinguishment is shown in Fig. 25.

A spot fire ignited at t = 19 min near the wall. It can be seen in the final frame of Fig. 23 as a dark spot with smoke at the far end of the wall near the clock.

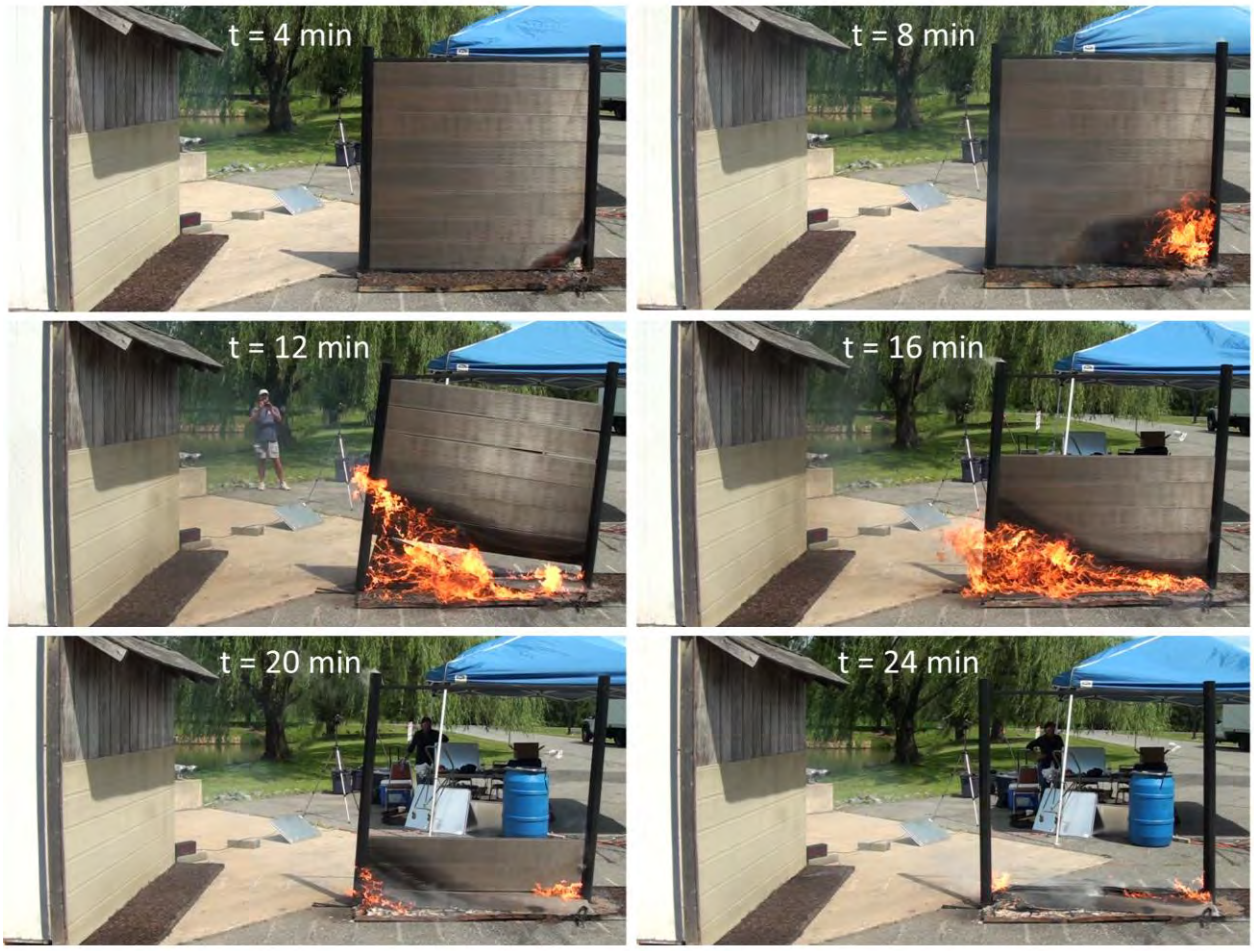

Fig. 23. Time sequence for wood-plastic composite fence #2 at low wind speed and 1.83 m (6 ft) separation distance [Test F-1].

Fig. 24. Collapse of horizontal planks shortly after t = 12 min [Test F-1].

Fig. 25. Final configuration of wood-plastic composite boards after Test F-1.

4.2.2. Without Mulch

Without mulch (Test H-3), the fire behavior of the WPC2 fence remained localized to the area around ignition. The two photos in Fig. 26 show how little the charred area changed over an 11 min period. When the experiment was ended after 20 min, the hole reached slightly higher, but the charred area had not changed significantly. A few pieces broken off from the interior of the board can be seen on the ground at t = 13 min.
The fire behavior of this fence was similar to that of wood and vinyl fences in the absence of mulch. See Section 4.2 in the fence report [1] to compare.

No spot fires were observed for this experiment.

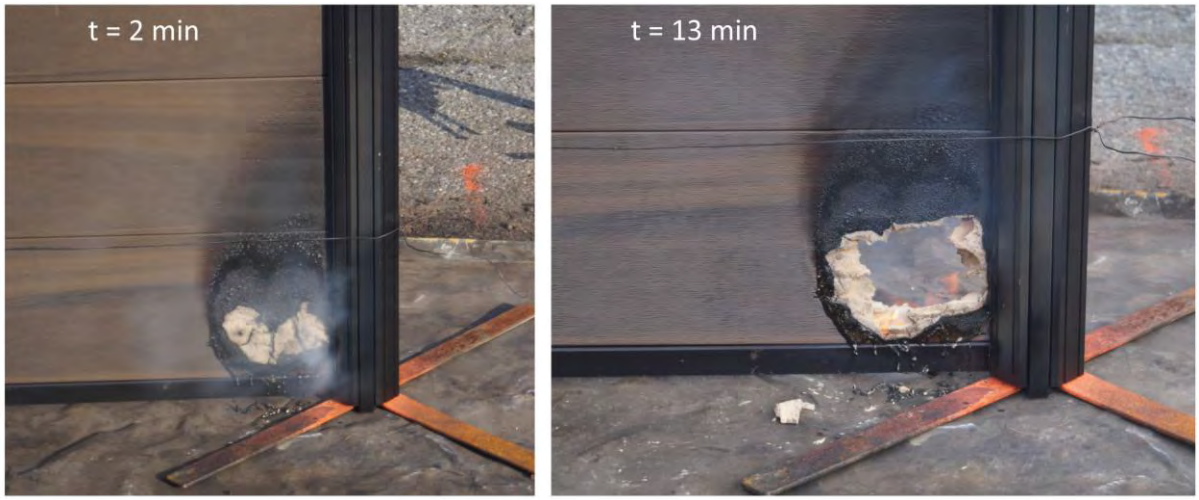

Fig. 26. Area near ignition point for Test H-3 at t = 2 min and t = 13 min, showing slow progress of fire.

4.2.3. Flame Spread

The location of the flame front as a function of time for the WPC2 wood-plastic composite fence with and without mulch is plotted in Fig. 27. Both experiments were performed at low wind speed and at 1.83 m (6 ft) separation distance from the shed. The uncertainties for these plots are described in the uncertainty analysis for fences in Appendix B.4.

Experiments on WPC2 with and without HW mulch (Tests F-1 and H-3, respectively) show that for this fence the presence of fine combustibles beneath the fence was necessary for the flame to progress.

Comparing WPC2 and WPC1 fences with mulch under the same experimental conditions (Tests F-1 and E-1, respectively) in Fig. 28, the flame front for WPC2 is considerably slower, taking almost twice the time to reach the end of the fence. This is despite being ignited closer to the shed due to the shorter length of the WPC2 fence compared to the WPC1 fence. Some insight into this may be provided in the discussion of flammability differences between the two wood-composite materials in Section 5.

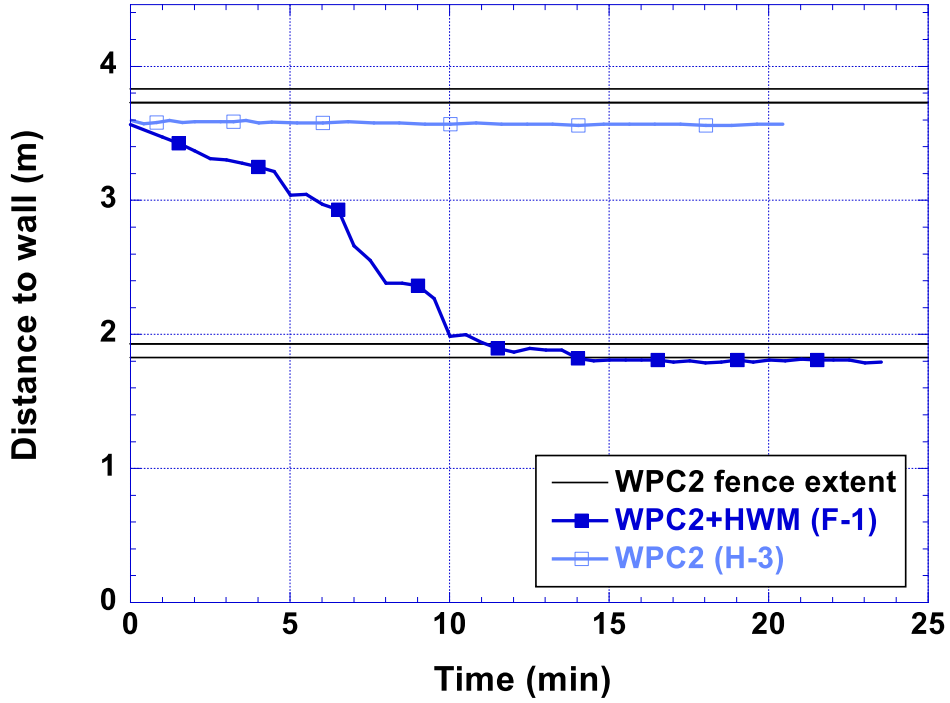

Fig. 27. Flame spread as a function of time for WPC2 fence with and without HW mulch beneath.

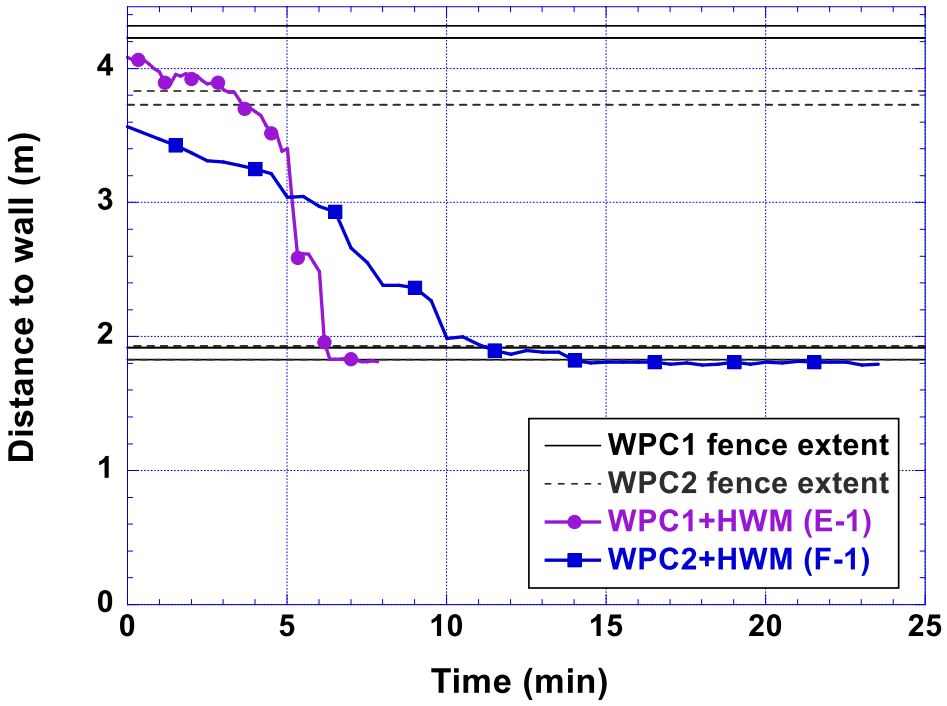

Fig. 28. Flame spread as a function of time for WPC1 and WPC2 fences, both with HW mulch at the base. The solid and dashed black lines show the locations of the posts closest and farthest from the shed for each fence.

4.2.4. Firebrand Spotting

Two ignitions occurred in the target mulch bed for the WPC2 fence experiment with shredded hardwood mulch below the fence. The merged spot fire near the wall of the shed is shown in Fig. 29 at time t = 23 min. This behavior is typical of spot fires observed for firebrand ignitions from wood fences and mulch in the larger study – see Fig. 85 in [1], for example. It is dissimilar from the widespread target mulch bed fires resulting from large fires, such as in Fig. 17 for WPC1.

Fig. 29. Spot fire in target mulch for WPC2 fence with mulch [Test F-1].

In the absence of mulch beneath the WPC2 fence, no visible energetic firebrands were observed – only white ash pieces. No spot fire occurred in this experiment.

The times to ignition of the first spot fire, ignition of the first spot fire whose flames reach the wall, and flames reaching the shed wall for the WPC2 experiments are presented in Table 3. The ignitions in the target mulch bed occurred late in Test F-1, after most of the fence had burned.

Table 3. Spot fire timing for WPC2 fences with and without mulch.

Fence w/wo Mulch	Time to Ignition of First Spot Fire	Time to Ignition of First Spot Fire to Reach Wall	Time to Flames on Wall
WPC2 + HWM (Test F-1)	19:46	20:10	21:08
WPC2 (Test H-3)	N/A	N/A	N/A

4.3. Steel-Plastic Composite Fence

The side posts and top and bottom beams of the steel-plastic composite (SPC) fence were steel bars covered with molded plastic. The panel body was molded as a single piece of plastic, with delineations of each vertical board offset from the opposite side. The design mimicked the look of a wood privacy fence. A more complete description can be found in Section 2.5.1.

4.3.1. With Mulch

The sequence from Test H-1 in Fig. 30 shows that a fire ignited at the upwind base of the SPC fence and shredded hardwood mulch bed under low wind conditions developed into a large fire, with flames extending above and well beyond the fence between 6 min and 8 min after turning on the fan. The plastic panel distorted and dripped, as shown in the close-ups in Fig. 31. The panel became tattered, with hanging strands of plastic blown by the wind field. The final appearance of the panel after extinguishment is shown in Fig. 32, with close-ups of the dripping material and residue on the ground in Fig. 33.

The target mulch bed next to the shed was ignited only after the flames had become intense, just before t = 7 min. Fires in the target mulch bed can be seen in the final frame of the sequence in Fig. 30, at t = 8 min. The flames then spread laterally along the mulch bed, likely due to radiation and direct flame contact rather than firebrands.

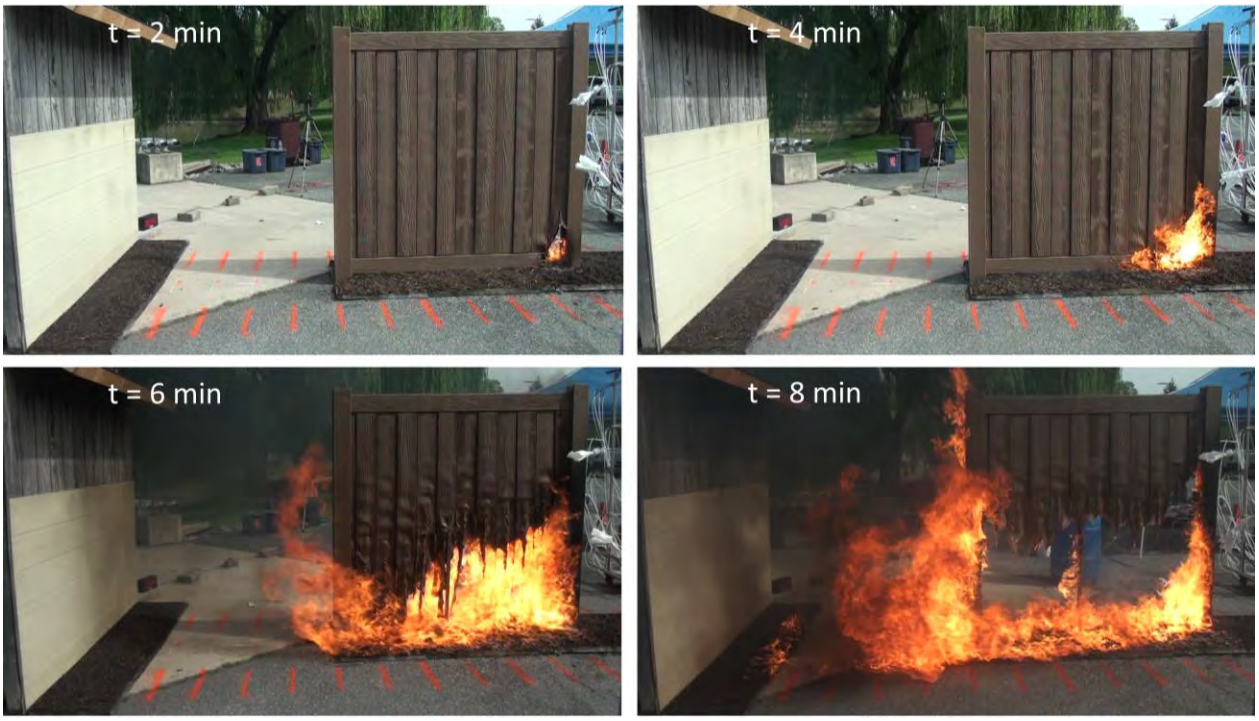

Fig. 30. Time sequence for SPC fence with WRC mulch in low wind speed [Test H-1].

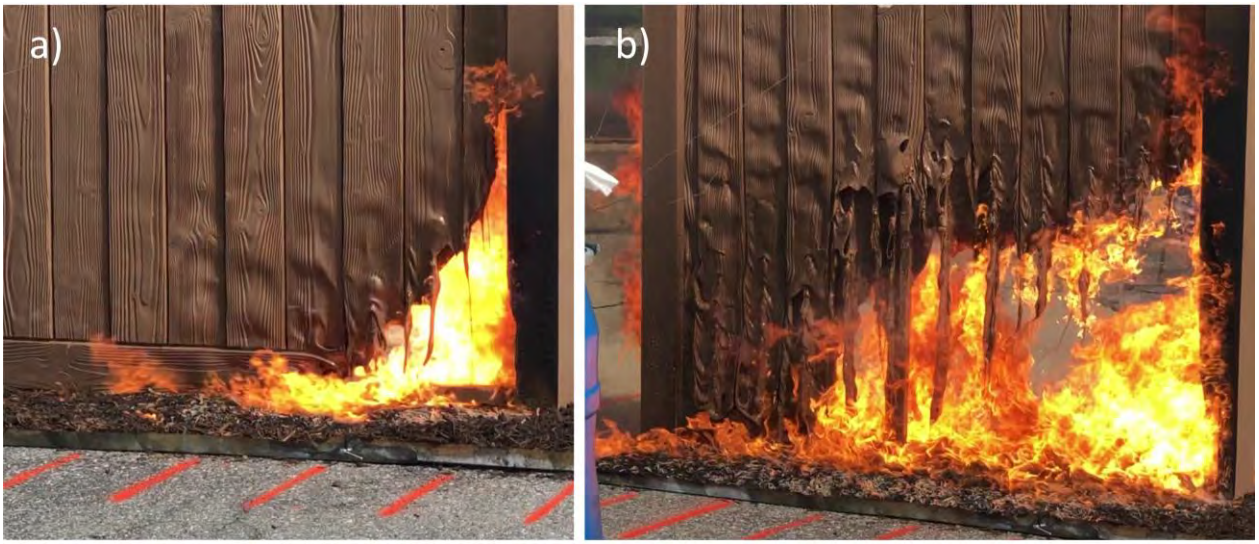

Fig. 31. Close-ups of SPC fence distortion and dripping a) shortly after t = 4 min and b) around t = 6 min during Test H-1.

Fig. 32. Remains of SPC fence with WRC mulch after extinguishment [Test H-1]. Wind was applied from left.

Fig. 33. Close-up of dripping material and residue from SPC fence after extinguishment [Test H-1].

4.3.2. Without Mulch

Removing mulch from the base of the composite fence eliminates the contribution of fine fuels to the flame spread along the fence. Nevertheless, the fire behavior for the SPC fence without mulch at its base (Test H-2) was similar to that observed in the previous section for the same fence with mulch.

The sequence in Fig. 34 shows that a fire ignited at the upwind base of the SPC fence developed into a large fire with flames extending beyond and above the fence and licking the shed from 1.83 m (6 ft) away by t = 7.5 min. The plastic panel distorted and dripped, as shown in the close-ups in Fig. 35. The final appearance of the panel after extinguishment is shown in Fig. 36, with a close-up residue on the ground in Fig. 37.

As in the case of a SPC fence with mulch (Test H-1), fires ignited in the target mulch bed next to the shed only after the flames had become intense. Fires in the target mulch bed can be seen in the final frame of the sequence in Fig. 34, at t = 7.5 min. Fires ignited along a large part of the front edge of the mulch bed, likely due to radiation and direct flame contact rather than firebrands.

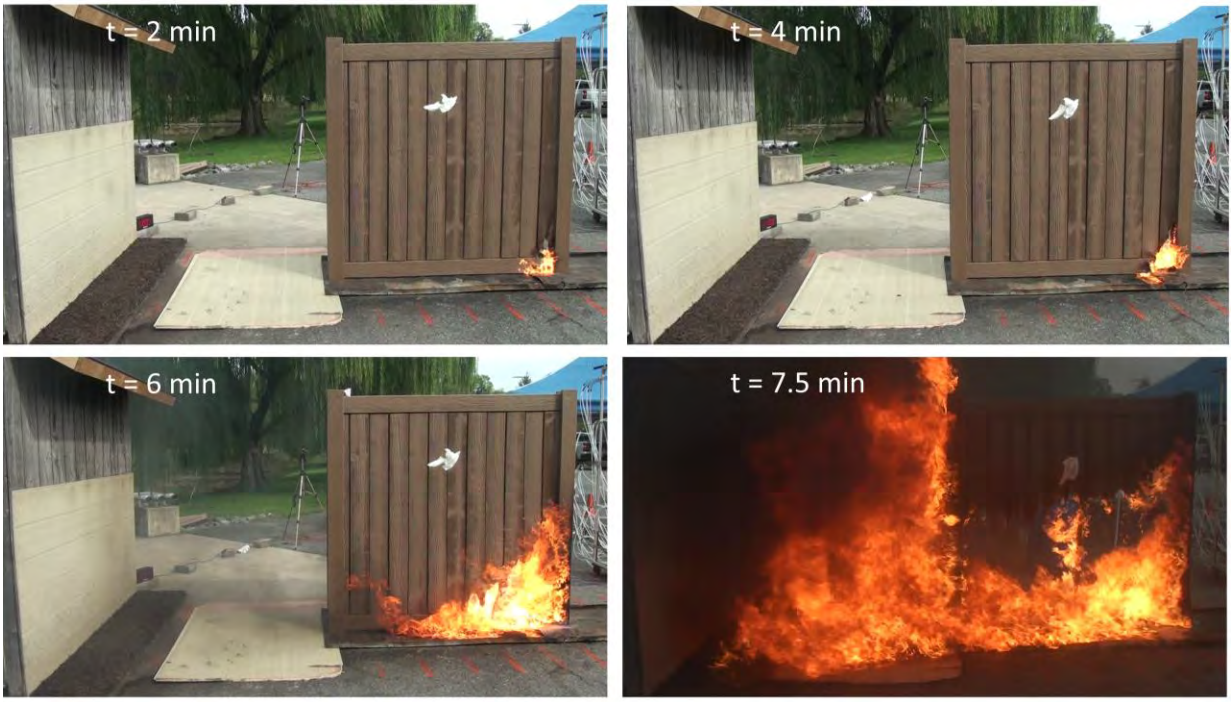

Fig. 34. Time sequence for SPC fence without mulch in low wind speed [Test H-2].

Fig. 35. Close-ups of SPC fence distortion and dripping a) shortly after removal of the gas burner and b) around t = 6 min during Test H-2.

Fig. 36. Remains of SPC fence without mulch after extinguishment [Test H-2]. Wind was applied from left.

Fig. 37. Close-up of residue from SPC fence without mulch after extinguishment [Test H-2].

4.3.3. Flame Spread

The location of the flame front as a function of time for the SPC steel-plastic composite fence with and without mulch is plotted in Fig. 38. Both experiments were performed at low wind speed and at 1.83 m (6 ft) separation distance from the shed. The uncertainties for these plots are described in the uncertainty analysis for fences in Appendix B.4.

The plots for the SPC experiments with and without HW mulch (Tests H-1 and H-2, respectively) indicate that the presence of mulch below the fence acted to accelerate the progress of the flame down the fence, although the difference was not as great as for the two WPC1 experiments presented in Section 4.1.3. At about 6 min from the point of ignition to the end of the panel, the SPC/HWM and WPC1/HW fence/mulch combinations both support the fastest fire spread compared to other fence-mulch combinations in the full fence study [1].

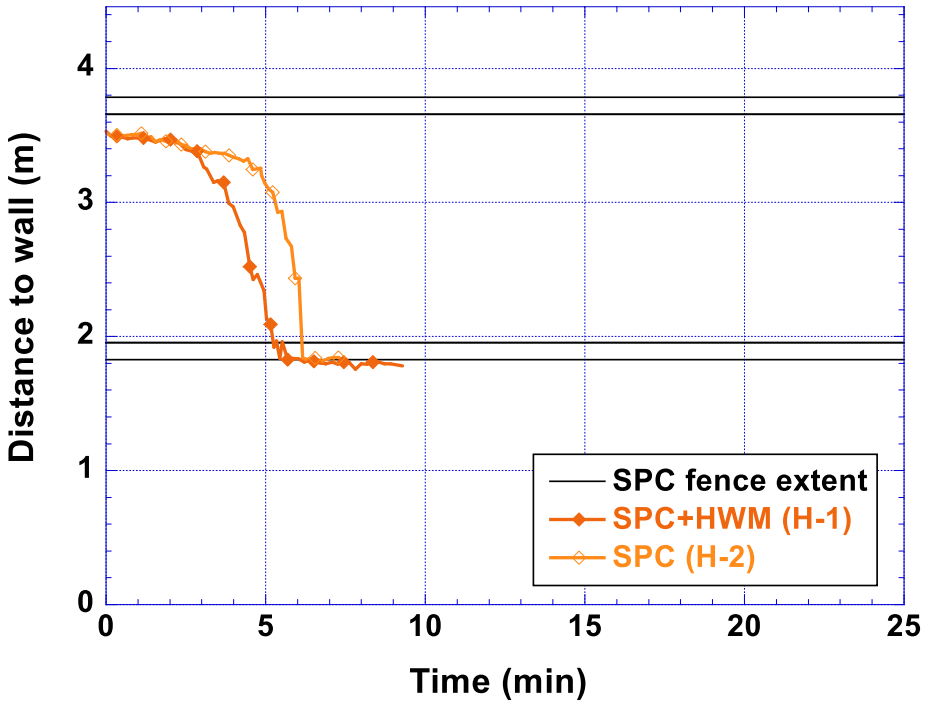

Fig. 38. Flame spread as a function of time for SPC fence with and without HW mulch beneath.

4.3.4. Firebrand Spotting

Ignitions occurred in the target mulch bed for SPC fence experiments both with and without shredded hardwood mulch at the base of the fence. The times to ignition of the first spot fire, ignition of the first spot fire whose flames reach the wall, and flames reaching the shed wall for these two experiments are presented in Table 4. The ignitions in the target mulch bed occurred near the end of each experiment, when the flaming on the fence panel was intense. The flames then spread laterally along the mulch bed, reaching the wall in the case with mulch but not in the case without. Ignitions and rapid fire spread over the front of the target mulch bed were likely due to radiation or direct flame impact, although a firebrand ignition source could not be ruled out when mulch was present.

Table 4. Spot fire timing for SPC fences with and without mulch.

Fence w/wo Mulch	Time to Ignition of First Spot Fire	Time to Ignition of First Spot Fire to Reach Wall	Time to Flames on Wall
SPC + HWM (Test H-1)	6:55	6:55	9:19
SPC (Test H-2)	7:06	N/A	N/A

4.4. Summary

This section compares the fire behavior for the three types of composite fences studied here. It also connects the six composite fence experiments to the fire behavior of fences in the large previous fence and mulch study [1].

The flame front locations as a function of time for the two wood-plastic and one steel-plastic composite fence experiments in this study are plotted in Fig. 39. This combines the flame front vs. time plots for all three composite fence types, as presented earlier in Section 4 in Fig. 22, Fig. 27, and Fig. 38. Note that the lines denoting the fence posts are in different locations because the fence types differ in length. All experiments were performed at low wind speed and at 1.83 m (6 ft) separation distance from the shed. The uncertainties for these plots are described in the uncertainty analysis for fences in Appendix B.4.

Figure 39 demonstrates that the presence of mulch beneath the fence is a strong factor in accelerating the progress of the flame down the fence. This is consistent with findings in the previous fence study [1]. It is important to note that only three fence experiments were found to result in rapid flame spread and large flames in the absence of mulch: the WPC1 and SPC composite fences shown here and a double redwood lattice fence in low wind speed that was discussed in Section 4.4.4 of [1].

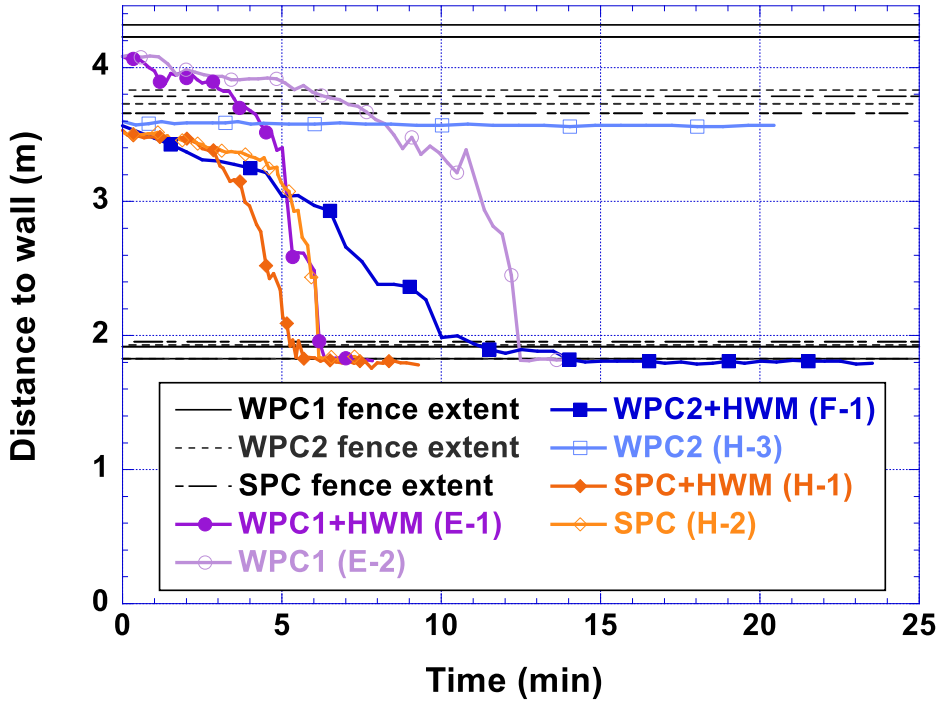

Fig. 39. Flame spread as a function of time for all six composite fence experiments. The solid and dashed black lines show the locations of the posts closest and farthest from the shed for each fence.

With and without mulch, the flame front spread rates for the WPC1 and SPC composite fences were found to be among the fastest for transporting fire when compared to the fences studied under the same test conditions (low wind speed and 1.83 m (6 ft) separation distance) in

Ref. [1]. The development of large flames over these two composite fence types revealed a serious fire hazard. The only comparable fire behavior was observed for parallel wood fences, where the radiative and convective heat transfer between adjacent fences contributed to very large fires. (See Section 4.4 of [1].)

Although significant flames developed over the WPC2 fence boards with mulch beneath, as seen in Fig. 23, the dropping of each board as the ones below it collapsed limited the height of the fire and kept the burned debris within the footprint of the mulch pan. The progress of the flame front was therefore comparable to those for the wood fences with mulch under the same test conditions described in Section 4.3 of [1]. In the absence of mulch, the WPC2 fence behaved like the majority of the wood fences in Section 4.2 of [1], for which the fire remained in the vicinity of the ignition site.

The following key findings for composite fence experiments in Sections 4.4.1 and 4.4.2 are intended to supplement the summaries for fence/mulch and fence only experiments in Sections 4.3.6 and 4.2.5, respectively, of the previous fence report [1].

4.4.1. With Mulch

A fence with mulch at its base is generally more hazardous than either the fence or the mulch bed separately. The mulch and fence interact to promote rapid flame spread downwind plus the generation of firebrands that can ignite other fuels in the vicinity. The fire behavior depends on fuel, geometry, and wind. More specifically, in these experiments the fire behavior depends on the types of fence and mulch, wind speed, and distance from the structure.

Fence experiments that include mulch are also informative for a fence with vegetation planted close by or for a fence with windblown leaves, needles, and other debris at its base. Any fine fuels adjacent to a fence are likely to interact with it during a fire.

Key findings from the three experiments that combine composite fences with shredded hardwood mulch are listed below. The list follows the format in Section 4.3.6 of [1], replacing the original list of findings on Wood-Plastic Composite Fences with this revised list on Composite Fences. Other findings in the previous fence report remain unchanged.

Composite fences. Ignition of certain wood-plastic or steel-plastic composite fences were found to result in high intensity fire behavior.

- For the WPC1 fence:
    - The entire fence became engulfed in flames.
    - The top and bottom frames distorted and released burning boards, which fell and extended the flaming region a distance equal to the fence height of 1.83 m (6 ft) to each side of the fence. Some softened boards fell forward in the wind, extending the flaming region beyond the fence as well. This is a life safety hazard for people attempting to egress near the fence.
    - Fires ignited in the target mulch bed only after the flames had become intense. Spot fires close to the shed wall were apparently ignited by firebrands, possibly

from the mulch. Many fires in the target mulch bed were ignited by radiation and direct flame contact.

- Smoke coming from the roof of the shed after the experiment indicated that a separation distance of 1.83 m (6 ft) between a fence and a structure was inadequate to prevent ignition from this burning fence.

- For the WPC2 fence:
  - Horizontal boards slipped downward through the frame and burned in line with the fence, within a couple of feet from the centerline.
  - Although flaming was vigorous, the fire remained below the halfway point of the fence height.
  - The fire diminished on its own as fuel ran low.
  - Two ignitions were observed in the target mulch bed late in the experiment (19 min after ignition).
- For the SPC fence:
  - The entire fence became engulfed in flames.
  - The fence panel, which was molded as a single piece, became distorted, dripped, and developed long streamers.
  - Fires ignited in the target mulch bed only after the flames had become intense. Ignition and lateral spread appeared to be primarily through radiation and direct flame contact rather than by firebrands.
  - Smoke coming from the roof of the shed after the experiment indicated that a separation distance of 1.83 m (6 ft) between a fence and a structure was inadequate to prevent ignition from this burning fence.
- A long fence will increase the fire exposure by adding to the available fuel and linear extent, and other factors such as sloping terrain will also add to the hazard.
- Both material selection and physical arrangement, including orientation of the boards (vertical vs. horizontal) and design of molded parts, appear to have a strong influence on fire behavior. The limited experiments performed in this study were not sufficient to uncover the detailed mechanisms behind their contributions.
- The significant differences in energy release among the three composite fences tested in this study highlight the need for a fence test method that can be used to assess the hazard of the material/design configuration.

4.4.2. Without Mulch

For most of the wood and vinyl fence experiments discussed in the previous fence report [1], the absence of mulch beneath the fence was found to slow the spread of fire considerably. It is recognized that fence experiments without mulch represent an ideal condition, since even with

careful maintenance wind may allow fine combustibles such as leaves and pine needles to accumulate during a WUI event. Experiments without mulch explore the lower limits of fire behavior for a fence under specified test conditions. Related to this, experiments reported in Section 4.3.2.4 of [1] for wood fences raised up as much as 15.4 cm above the mulch to provide a gap between the fence and ground combustibles showed that physical distancing of the fence above the combustibles can slow fire spread significantly although not as much as complete removal of the combustibles.

Key findings from the three experiments that combine composite fences with shredded hardwood mulch are listed below. The list follows the format in Section 4.2.5 of [1], replacing the original list of findings on Wood-Plastic Composite Fences with this revised list on Composite Fences. Other findings in the previous fence report remain unchanged.

Composite fences. Even in the absence of fine combustibles, ignition of composite fences may result in high intensity fire behavior.

- For the WPC1 fence:
    - The fire behavior without mulch was similar to that with mulch, with flame spread slowed by about a factor of two.
    - The entire fence became engulfed in flames.
    - The top and bottom frames distorted and released burning boards, which fell and extended the flaming region a distance equal to the fence height of 1.83 m (6 ft) to each side of the fence. Some softened boards fell forward in the wind, extending the flaming region beyond the fence as well. This is a life safety hazard for people attempting to egress near the fence.
    - Fires ignited in the target mulch bed only after the flames had become intense. Ignition and lateral spread appeared to be primarily through radiation and direct flame contact rather than by firebrands.
    - Smoke coming from the roof of the shed after the experiment indicated that a separation distance of 1.83 m (6 ft) between a fence and a structure was inadequate to prevent ignition from this burning fence.
- For the WPC2 fence:
    - Fire behavior was similar to that of wood and vinyl fences in the absence of mulch [1].
    - The fire remained localized to the area around ignition, causing charring and a slowly-growing hole in the fence. Little to no firebrand generation was observed.
    - No spot fires were observed.
- For the SPC fence:
    - The fire behavior without mulch was similar to that with mulch, with flame spread slowed only slightly.

  - The entire fence became engulfed in flames.
  - The fence panel, which was molded as a single piece, became distorted, dripped, and developed long streamers. Falling fragments of dripping plastic, too heavy to become wind-borne, were created rather than firebrands.
  - Fires ignited in the target mulch bed only after the flames had become intense. Fires then spread laterally, likely due to radiation and direct flame contact.
  - Smoke coming from the roof of the shed after the experiment indicated that a separation distance of 1.83 m (6 ft) between a fence and a structure was inadequate to prevent ignition from this burning fence.
- A long fence will increase the fire exposure by adding to the available fuel and linear extent, and other factors such as sloping terrain will also add to the hazard.
- Both material selection and physical arrangement, including orientation of the boards (vertical vs. horizontal) and design of molded parts, appear to have a strong influence on fire behavior. The limited experiments performed in this study were not sufficient to uncover the detailed mechanisms behind their contributions.
- The significant differences in energy release among the three composite fences tested in this study highlight the need for a fence test method that can be used to assess the hazard of the material/design configuration.

5. Fence Material Flammability

Flammability measurements to compare the composite fence materials (WPC1, WPC2, and SPC) were obtained using the cone calorimeter in both horizontal and vertical configurations. This study had two goals: (1) to improve our understanding of the differences in fire behavior among the three composite fence types by separating material properties from fence design and (2) to compare the validity of horizontal and vertical cone tests for assessing the flammability of fences.

Insights into flammability for composite fence materials were supplemented by cone calorimeter results for rigid polyvinyl chloride (PVC) and western redcedar (WRC) fence samples previously reported in Appendix B of the comprehensive fence report [1]. A subset of test results from wood-plastic composite #1 (WPC1) fence samples were also presented previously.

This section compares the results of the cone calorimeter tests to provide insights on the effects of material properties on the composite fence experiments and on the validity of flammability testing in a horizontal configuration for vertical fences. Cone calorimeter testing is described in detail in Appendix C, including results from individual tests.

5.1. Cone Calorimeter Experiments

Specimens with nominal dimensions of 100 mm × 100 mm were cut from PVC, WRC, WPC1, WPC2, and SPC fence panels. Cross-sectional and top views of all sample types are shown in Fig. 40. Nominal masses for PVC, WRC, WPC1, WPC2, and SPC samples were measured as 44.4 g, 66.7 g, 60.0 g, 139.8 g, and 30.9 g, respectively.

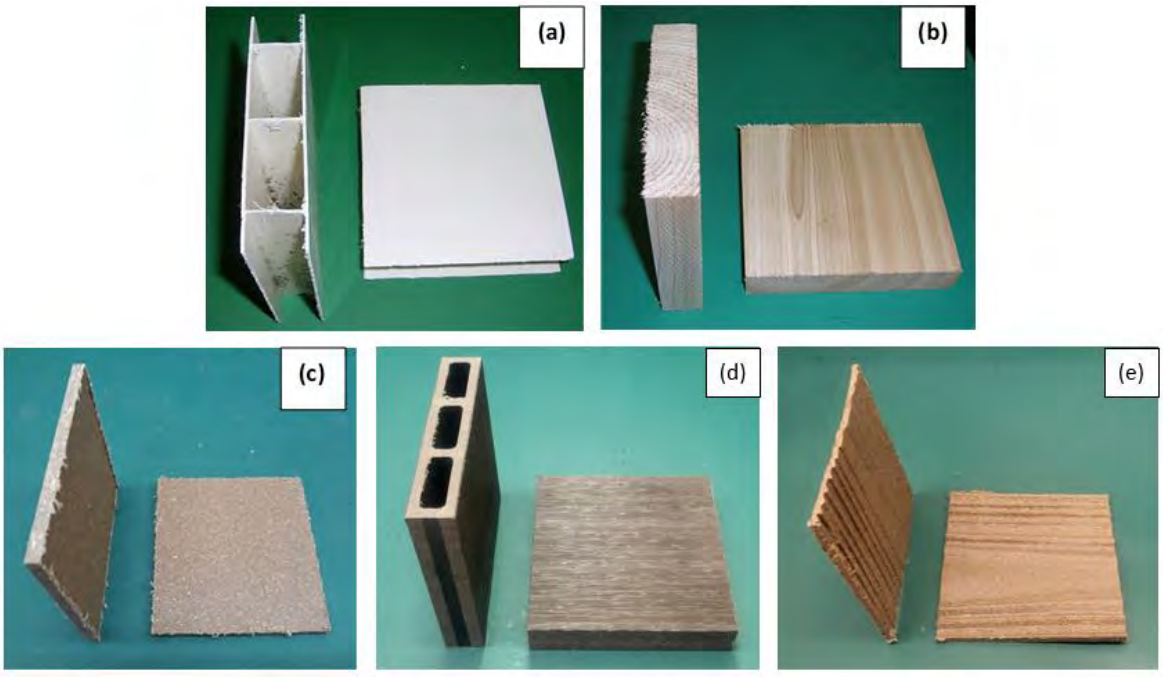

Fig. 40. Specimens of a) PVC, b) WRC, c) WPC1, d) WPC2, and e) SPC fence boards showing cross-sectional and top views.

Figures 40 and 41 show how the cone samples from composite fences relate to the fence boards from which they were cut. The thin solid WPC1 specimens in Fig. 40 (c) were cut from a fence such as that in Fig. 41 (a), whose boards interlock as shown in (b). The hollow WPC2 specimens in Fig. 40 (d), with flat outer faces separated by braces, were cut from a board from the fence type shown in Fig. 41 (c), for which the braces are oriented horizontally as shown in (d). The thin solid SPC samples in Fig. 40 (e) were cut from a flat segment of the fence type in Fig. 41 (e), molded to mimic the appearance of a wood privacy fence as shown in (f).

Fig. 41. Structures of composite fences: a) WPC1 fence and b) interlocking solid boards; c) WPC2 fence and d) boards showing braces oriented horizontally; and e) SPC molded panel and f) cross-section showing molding of front and back board faces.

Further details of specimen dimensions, preparation, and experimental procedures are given in Appendices C.1 and C.2.

5.2. Test Results

The cone calorimeter enables comparisons of the flammability properties of materials at a small scale. The analysis produces several measures that relate to ignitability and fire behavior under real world conditions, including times to ignition and flame out, heat release rate, total heat release, and effective heat of combustion.

Ignitability describes the tendency of a material to ignite and burn. The cone calorimeter characterizes ignitability by measuring the time to ignition (TTI) under conditions of piloted ignition under a radiant heat flux. The time to flame out (FO), marking the end of combustion, measures how quickly the material extinguishes after the ignition source is removed. Materials with a higher fire hazard related to ignitability have a short TTI and a long flaming duration (FO minus TTI).

Heat release rate (HRR) is a key flammability property measured using the cone calorimeter, since the fire hazard is dominated by the rate of heat released as the material is consumed in a fire. Heat release rate is largely influenced by the chemical stability of a material. A burning material will spread fire to nearby products only if it emits enough heat to ignite them. Several parameters are derived from heat release rate data, including the peak heat release rate, the average heat release rate over a specified time period, the total heat release, and the effective heat of combustion. These parameters provide measures for comparing the burning intensities of samples.

The peak heat release rate (PHRR) is the peak value in the HRR curve. For multiple peaks, PHRR states the highest value. Many studies use PHRR obtained in the horizontal configuration for screening materials. The end use application of the product being tested determines whether PHRR measured in this way is an appropriate indicator of fire hazard.

The total heat release (THR), which is obtained by integrating HRR over the duration of flaming combustion, is related to the total amount of fuel present and the fraction consumed. Thus, the THR is an indicator of the fire load and fire hazard associated with the material, as is the average HRR over the first 600 s.

The effective heat of combustion (EHOC) is the instantaneous HRR divided by the instantaneous mass loss rate. The EHOC is used to provide time-resolved insights into the materials undergoing combustion, including burning intensity and the completeness of the combustion process. Values shown here were calculated at the time of flame out.

This section combines plots from the results of individual cone calorimeter tests detailed in Appendix C.4 for each of the four test conditions (horizontal and vertical orientations and two incident heat fluxes) in Section 5.2.2 and for each of the five fence materials in Section 5.2.1. This highlights the effects of the fence material and of the test condition, respectively. Bar charts that compare cone calorimeter test data for each summary parameters are presented in

Section 5.2.3, and firebrand generation and char residue are discussed in Section **Error! Reference source not found.**.

The data presented in this section will be summarized in Section 5.3 and compared to the results from full-scale fence experiments in Section 5.4.

5.2.1. Heat Release Rate Curves: Effects of Fence Material

In this section, the cone calorimeter heat release rate curves for PVC, WRC, WPC1, WPC2, and SPC fence samples from Appendix C.4 are plotted together according to test condition (horizontal or vertical orientation and one of two incident heat fluxes). All fence materials tested under that test condition are included in each plot, enabling a direct comparison of their time-dependent flammability behavior.

Figure 42 shows the temporal profiles of HRR for PVC, WRC, WPC1, WPC2, and SPC samples in a horizontal orientation with an incident heat flux of 50 kW/m^2. The first thing to note is that the peak HRR for each of the three composite fence materials is more than double that for either PVC or wood (WRC). This suggests that fences made from these composite materials may generate more heat to ignite combustible objects nearby than either PVC or WRC fences. Among the composite fence materials, SPC shows the highest peak HRR, but the value decreases quickly with time as the sample is consumed. WPC1 and WPC2 have similar PHRR, but the shape of the curves indicates that WPC1 maintains a high HRR over the first 600 s while WPC2 samples release heat at a lower level over a far longer time period (see Fig. C.14). Regarding ignitability, the rapid rise in HRR that corresponds with time to ignition (TTI) is fastest for WPC1 and wood.

Figure 43 shows HRR plots for a vertical orientation under the same incident heat flux of 50 kW/m^2. The fence samples that were tested in the cone calorimeter under this test condition were PVC, WPC1, WPC2, and SPC. Comparing the vertical scale and HRR peaks for this set of plots with those for Fig. 42, it is instantly apparent that (with one exception discussed in Appendix C.4.3) the WPC1 fence samples are exhibiting a considerably higher HRR in the vertical orientation than in the horizontal. While the HRR for the first peak is nearly identical for horizontal and vertical cone tests of WPC1 samples, the second peak soars to a value two to three times the first peak. For those vertical cone tests, the outer layer of the WPC1 sample was observed to fall off as it burned, exposing fresh fuel that burned with a very high heat release rate. With vertical mounting, the single peak for HRR from SPC fence samples is generally higher than for the horizontal orientation. Ignition still occurs fastest for WPC1, although the ordering of ignition times for WPC2 and SPC samples has reversed.

HRR plots for the three composite fence samples in horizontal and vertical configurations with an incident heat flux of 35 kW/m^2 are shown in Fig. 44 and Fig. 45, respectively. The results are similar to those observed for the horizontal configuration at 50 kW/m^2 in Fig. 42. The highest PHRR is seen for SPC, whose heat release rate decreases rapidly after the single peak. The HRR for WPC1 remains elevated for the first 600s, while WPC2 samples release heat at a lower level over a longer time period. The WPC1 sample ignites earliest under every test condition.

As discussed in Appendix C.4.3, neither WPC1 cone calorimeter test performed in the vertical orientation in 2024 exhibited a large second HRR peak. The reason for this is unknown.

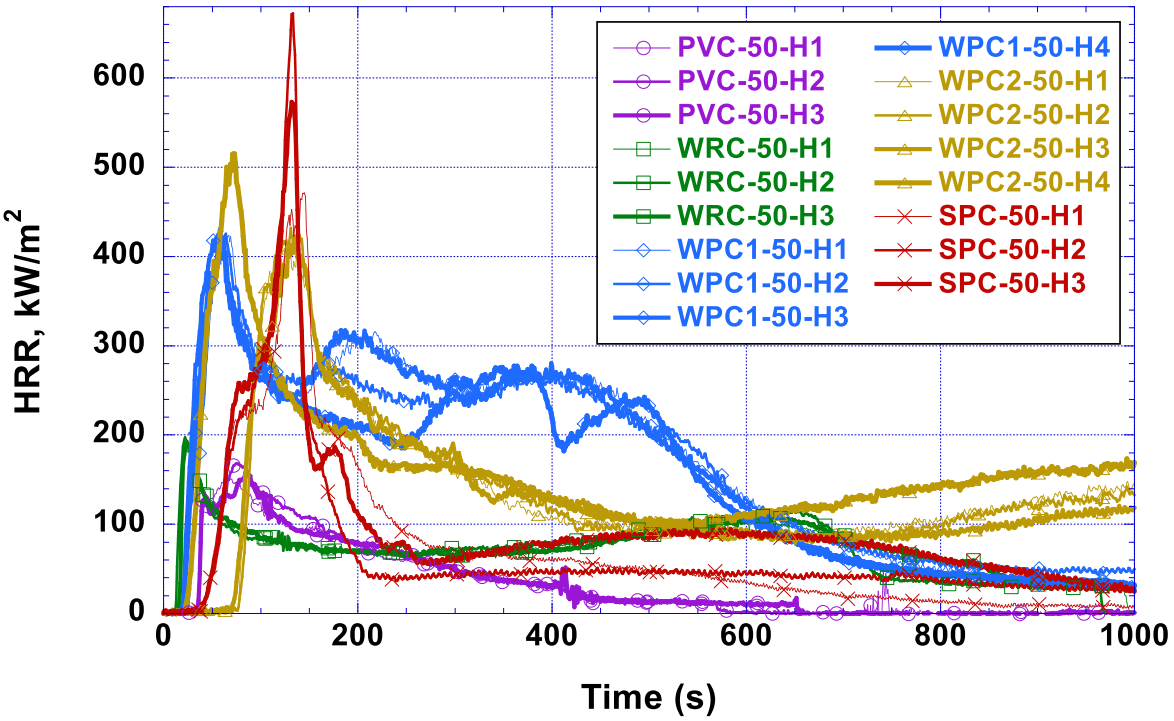

Fig. 42. Heat release data for PVC, WRC, and composite fence materials: Horizontal orientation at 50 kW/m^2 incident heat flux.

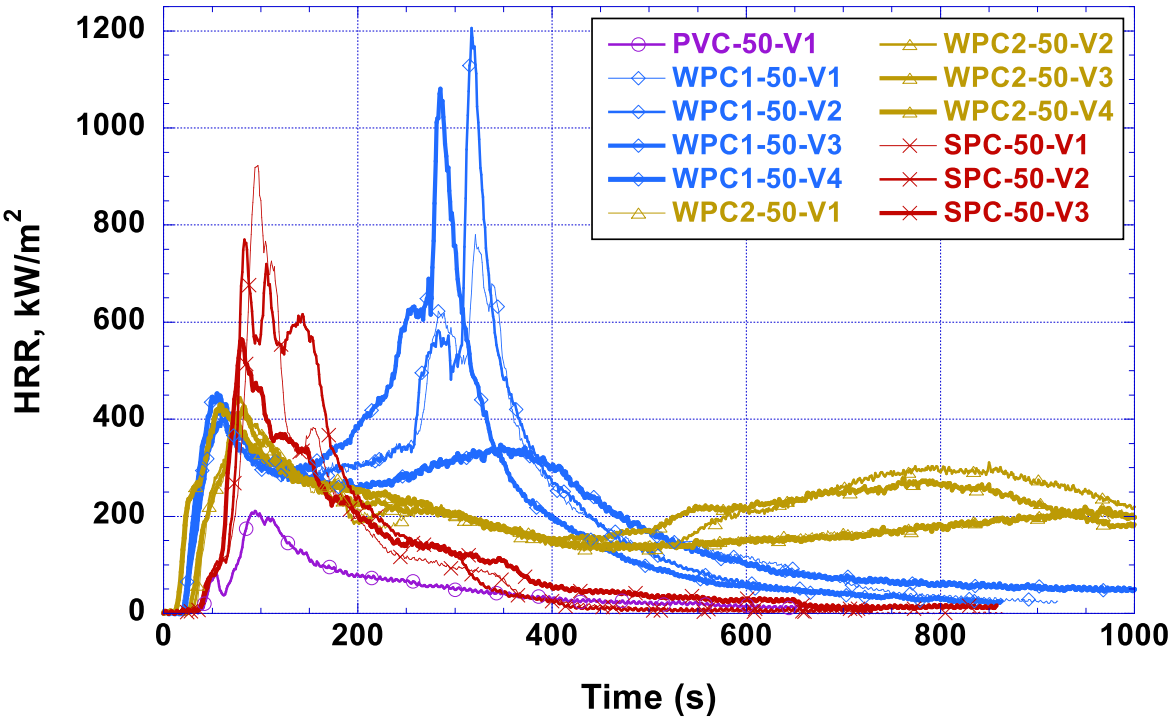

Fig. 43. Heat release data for PVC and composite fence materials: Vertical orientation at 50 kW/m^2 incident heat flux.

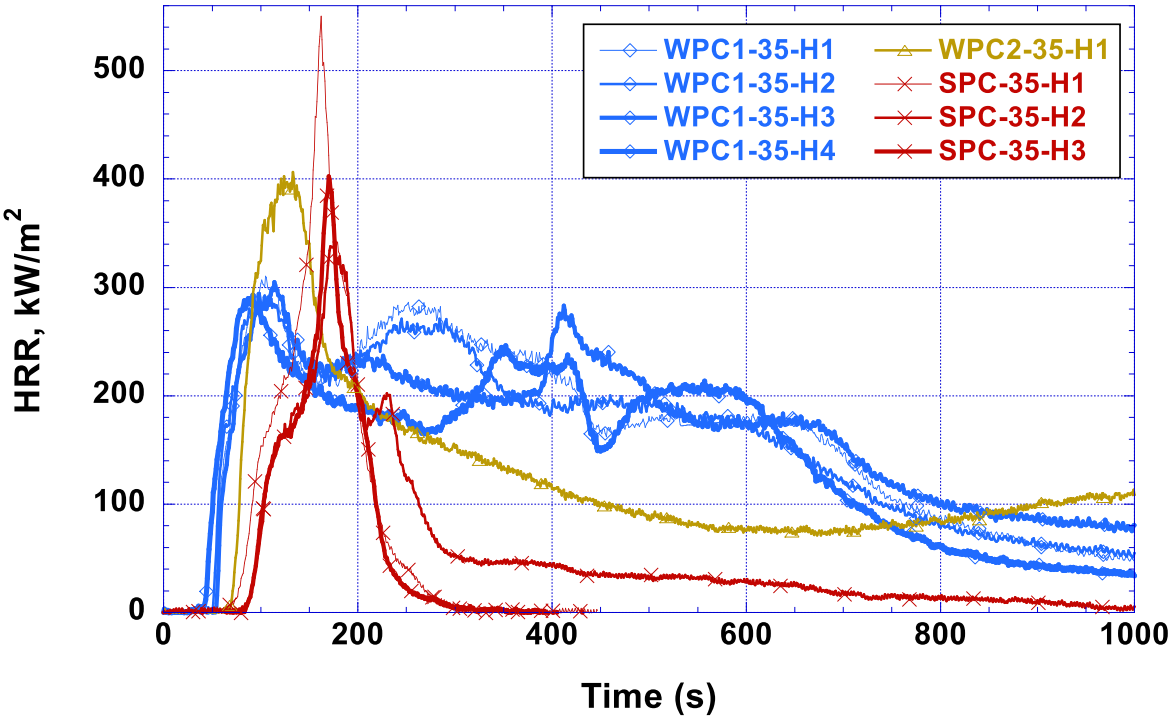

Fig. 44. Heat release data for composite fence materials: Horizontal orientation at 35 kW/m^2 incident heat flux.

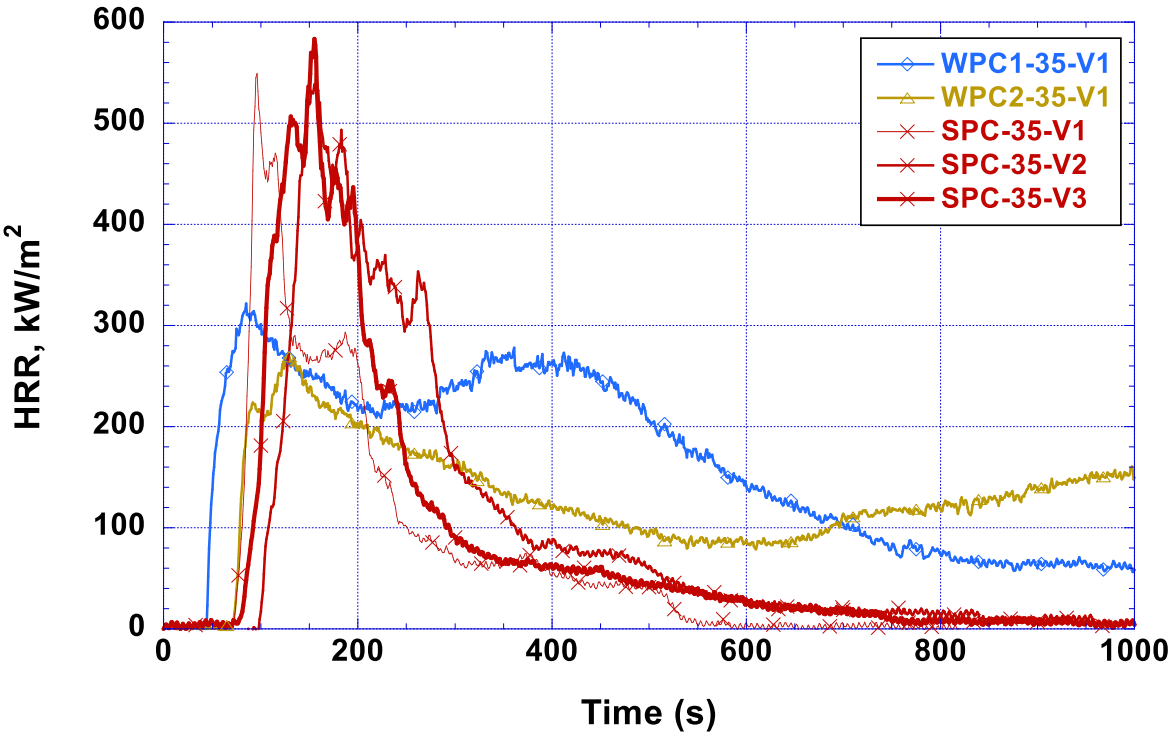

Fig. 45. Heat release data for composite fence materials: Vertical orientation at 35 kW/m^2 incident heat flux.

5.2.2. Heat Release Rate Curves: Effects of Orientation and Incident Heat Flux

In this section, the cone calorimeter heat release rate curves for PVC, WRC, WPC1, WPC2, and SPC fence samples from Appendix C.4 are plotted together according to fence material. All test conditions are included in each plot. This enables a direct comparison of the time-dependent flammability behavior under horizontal and vertical orientations of the cone calorimeter and at two levels of incident heat flux.

PVC: Figure 46 compares HRR as a function of time for PVC fence samples in the vertical cone calorimeter orientation to that in the horizontal orientation. The plot shapes are similar, with a single peak that reflects a single burning stage with no charring. The ignition time is approximately the same for horizontal and vertical orientations. In agreement with Tsai [34], the peak heat release rate is higher for the vertical orientation and the total heat release appears to be approximately the same.

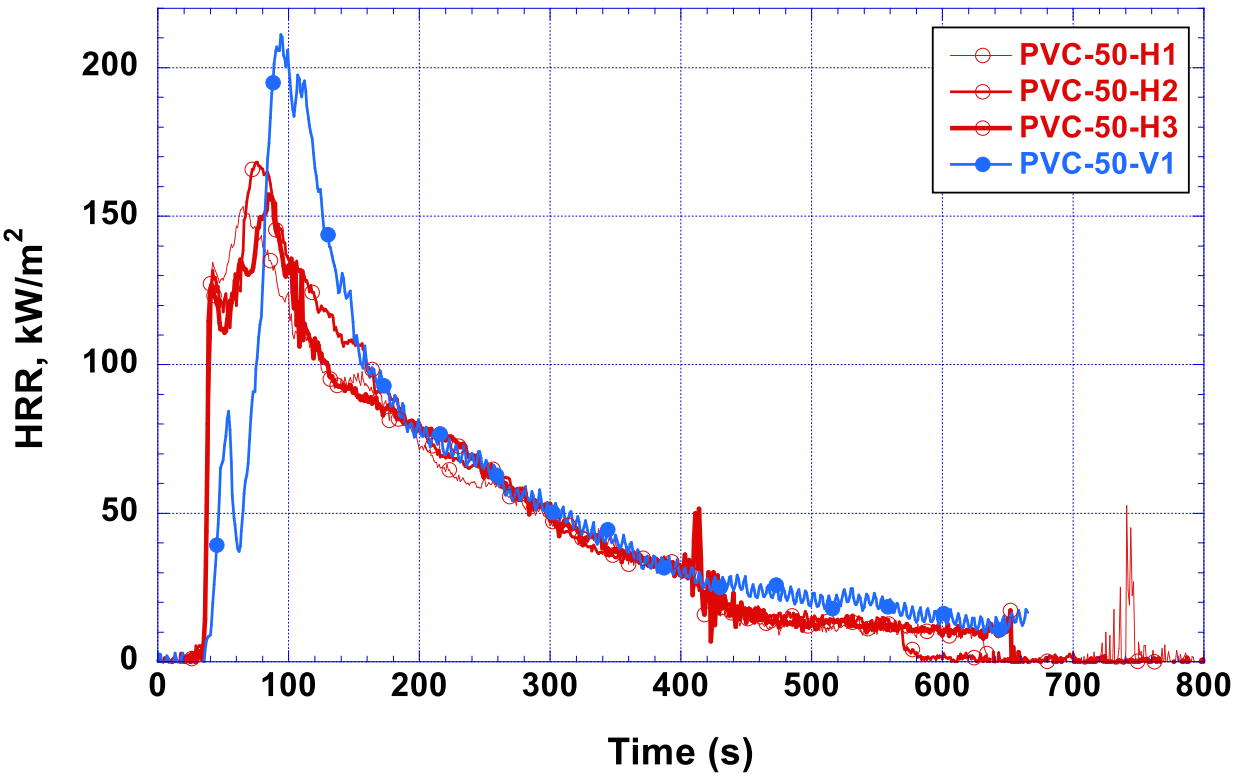

Fig. 46. *PVC:* Heat release rate as a function of time for all PVC cone calorimeter tests, comparing horizontal (red) and vertical (blue) tests at an incident heat flux of 50 kW/m^2.

WRC: As shown in Fig. 47, the WRC fence samples were tested only in a horizontal configuration with an incident heat flux of 50 kW/m2. The HRR plots exhibit the characteristic two peaks of burning wood, with the second peak due to charring [20,35,36]. The effects of orientation and incident heat flux can be found from the literature on cone calorimeter testing of wood samples [37,34].

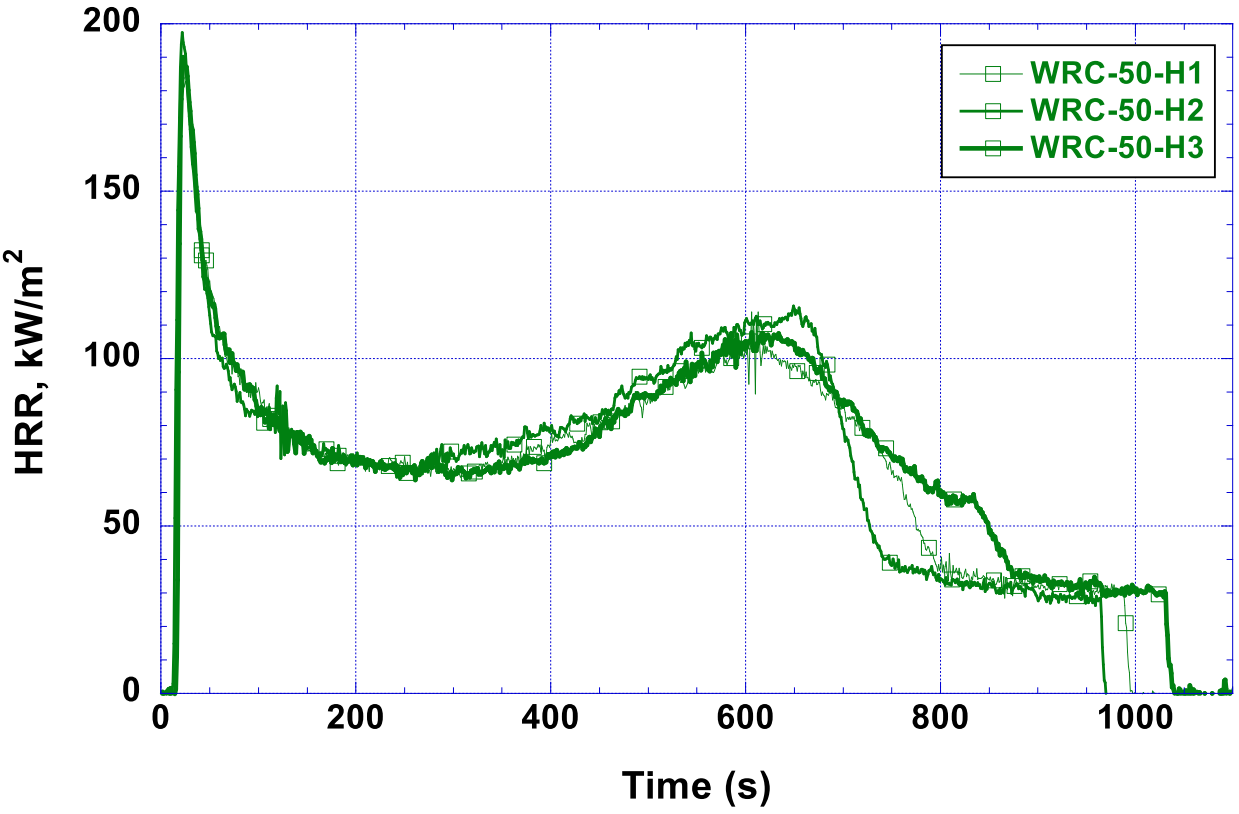

Fig. 47. *WRC:* Heat release rate as a function of time for all WRC cone calorimeter tests, all of which were performed in a horizontal configuration at an incident heat flux of 50 kW/m^2.

Compared to a vertical orientation, horizontal testing has been found to result in shorter time to ignition, lower PHRR, nearly identical total heat release, and longer burning times. The shorter ignition time for horizontal testing may be attributed to lower convective cooling in this orientation [37,34].

As the incident heat flux increases, the time to ignition shortens, PHRR increases, and total heat release and burning times are generally unaffected [37,34].

WPC1: HRR plots for WPC1 fence samples are plotted in Fig. 48. The most significant difference between horizontal and vertical cone tests was in the PHRR of the highest peak for three of the four vertical tests. During these vertical cone calorimeter tests, the outer layer was observed to burn and fall off, exposing more fuel that burned with a very high heat release rate. This resulted in a very high second peak of HRR at about t = 300 s, at between two and three times the size of the first peak. The HRR in these cases decreased rapidly after the peak, as compared to WPC1 fence samples mounted horizontally, which maintained HRR at a relatively high level for the first 600 s. (As discussed in Appendix C.4.3, neither WPC1 cone calorimeter test performed in the vertical orientation in 2024 exhibited a large second HRR peak, for unknown reasons.) Neither the time to ignition nor the PHRR for the first peak differed significantly for horizontal and vertical orientations.

For higher incident heat flux, the time to ignition was shorter and the PHRR for the first peak was higher.

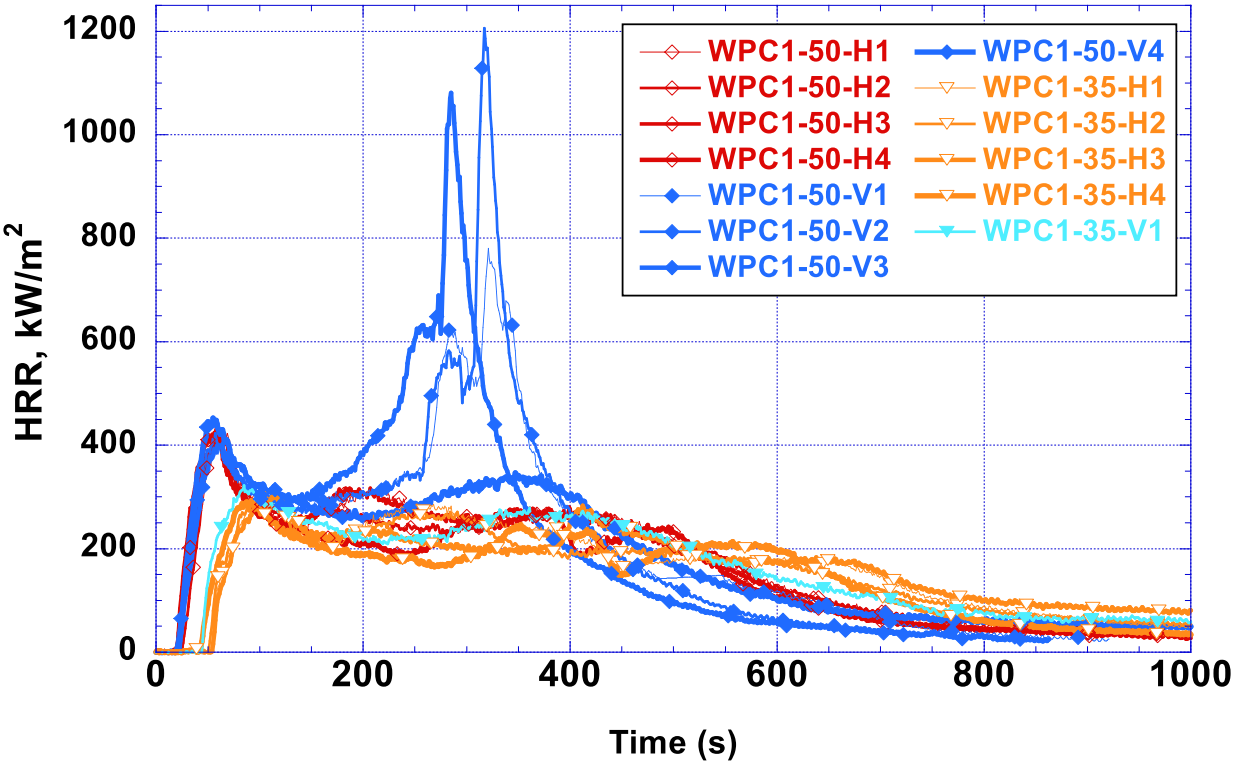

Fig. 48. *WPC1:* Heat release rate as a function of time for all WPC1 cone calorimeter tests, comparing horizontal (red, orange) and vertical (blue, teal) tests at incident heat fluxes of 50 kW/m^2 and 35 kW/m^2, respectively.

WPC2: The HRR plots for WPC2 fence samples in Fig. 49 show the double peak characteristic of wood and other charring materials. Unlike WPC1 cone tests, the fire behavior of WPC2 samples did not differ dramatically between horizontal and vertical orientations, and the second peak in HRR was found to be shorter than the first peak in all cases. For vertical cone tests, the second peak was higher and earlier than for horizontal tests with both incident heat flux levels. With one exception, as discussed in Appendix C.4.4, the time to ignition was approximately the same for horizontal and vertical tests.

Higher incident heat flux resulted in a shorter time to ignition (with one exception), higher peak HRR values for both peaks, and a more rapid onset of the second peak.

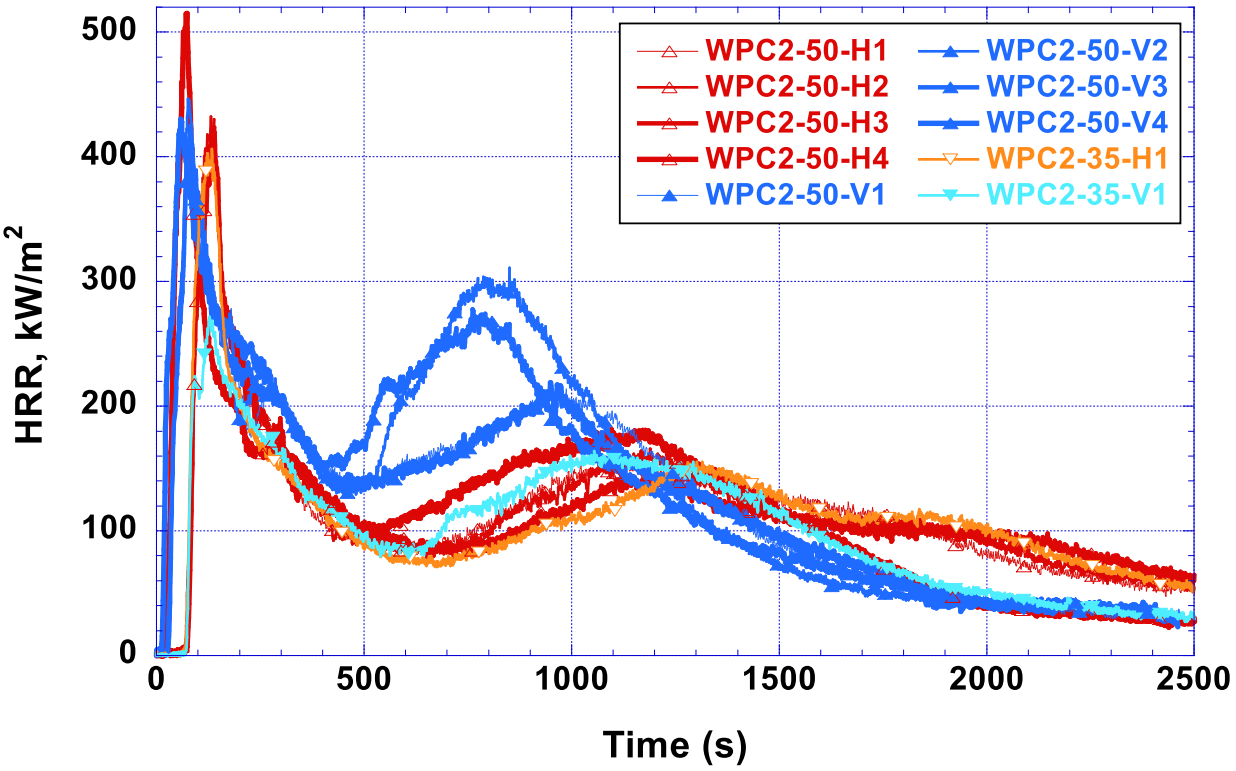

Fig. 49. *WPC2:* Heat release rate as a function of time for all WPC2 cone calorimeter tests, comparing horizontal (red, orange) and vertical (blue, teal) tests at incident heat fluxes of 50 kW/m^2 and 35 kW/m^2, respectively.

SPC: HRR plots for WPC1 fence samples are plotted in Fig. 50. Like the PVC fence samples, and SPC samples produce single peak plots in cone calorimeter testing, reflecting a single burning stage with no charring. There is significant variability in the HRR plots for each test condition in comparison with the other fence types. This is likely related to the dripping of fragments from the burning sample, some of which continue to burn and some of which fall onto nearby surfaces and extinguish.

Compared to cone tests in a horizontal orientation, the HRR for WPC1 samples mounted vertically reached the peak earlier and with a higher PHRR. The time to ignition was approximately the same for horizontal and vertical orientations.

Higher incident heat flux resulted in a shorter time to ignition and a peak that occurred earlier and had a higher PHRR.

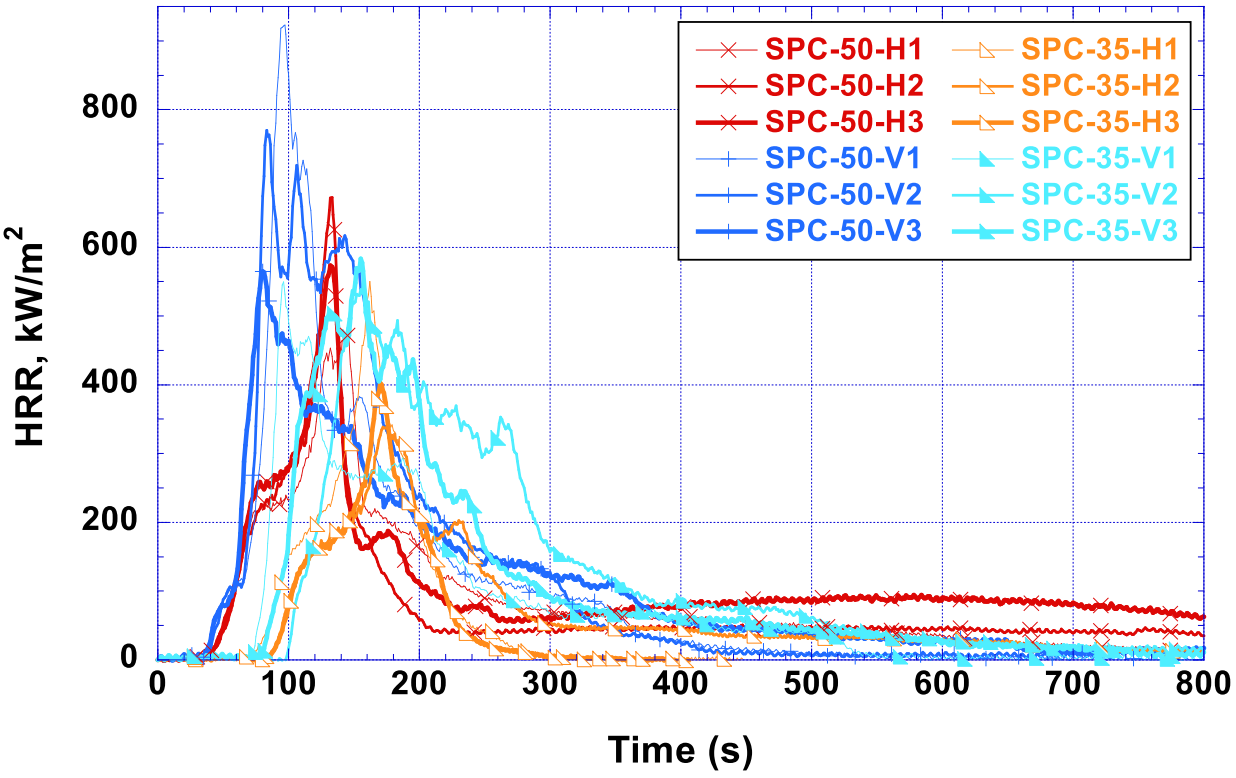

Fig. 50. *SPC:* Heat release rate as a function of time for all SPC cone calorimeter tests, comparing horizontal (red, orange) and vertical (blue, teal) tests at incident heat fluxes of 50 kW/m^2 and 35 kW/m^2, respectively.

5.2.3. Flammability Measures

The bar charts in this section display the cone calorimeter test data in Appendix C.4 in Table C.2 through Table C.16. Charts for each summary variable present the value obtained for each test condition by fence material. This enables visual comparison of values and complements the HRR plots discussed in Sections 5.2.1 and 5.2.2.

The bar charts include error bars for test conditions in which multiple cone tests have been performed. The error bars indicate the standard deviation of the sample for these cases, taken from the data tables, which expresses only the variability of the cone test results. The uncertainties of the measurements themselves are not included. Large error bars indicate an outlier within the set of tests, which are discussed in the relevant section in Appendix C.4. The absence of an error bar indicates that there was only a single test performed under those conditions. The values from those single tests lack statistical validity and are used here to strengthen conclusions reached over multiple fence materials.

Mass Loss: Mean values are provided in Fig. 51 for initial sample mass and percentage of mass lost at the time of flame out for each fence material under each set of test conditions.

As expected, the variability of initial sample mass for each fence material is small, and the statistics may be combined. In increasing order, the initial masses of the fence samples, along with their corresponding standard deviations of the sample are SPC (30.9 g ± 2.0 g) < PVC (44.4 g ± 0.2 g) < WPC1 (60.0 g ± 1.0 g) < WRC (66.7 g ± 2.0 g) < WPC2 (139.8 g ± 0.9 g).

Over 70 % of the initial sample mass was lost for every type of fence material tested. Note that the mass lost from SPC fence samples was set to 100 % to reflect the observation that no material remained in the sample holder after any test. The material from SPC samples that dripped out of the holder and extinguished, as discussed in Appendix C.4.5, was neglected in this chart. The lowest percentage of mass loss was from WPC2, followed in order by PVC, WRC, WPC1, and SPC. For PVC and WPC1, fence samples mounted vertically lost more mass than those mounted horizontally, with WPC2 showing no significant difference with orientation.

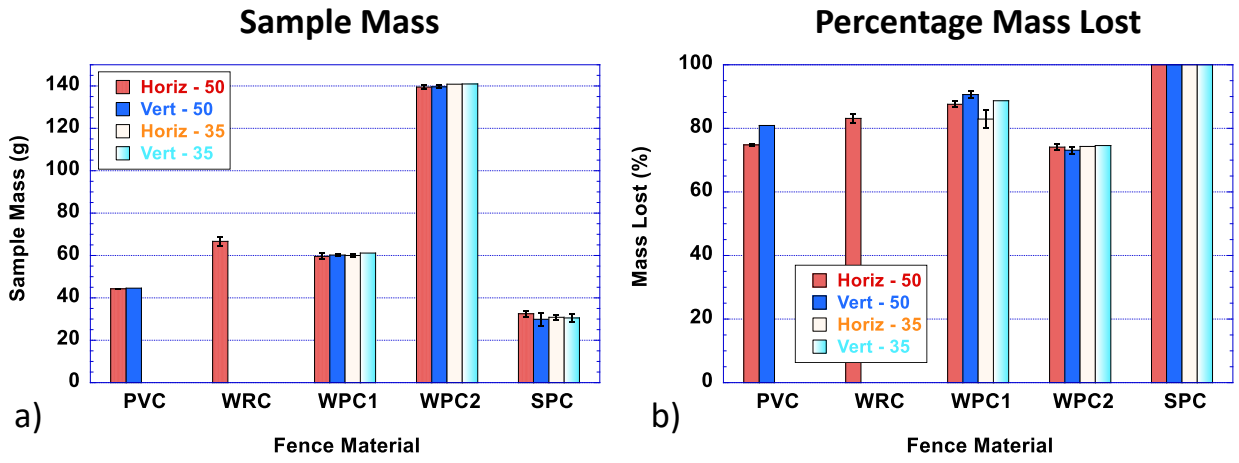

Fig. 51. Mean values of a) sample mass and b) percentage of mass lost from the five fence materials in horizontal and vertical orientations at 50 kW/m^2 and 35 kW/m^2.

Ignitability: Ignitability of materials is associated with the initiation and subsequent growth of fire under real world conditions. The time to ignition (TTI) provides a proxy for ignitability, measuring how long it takes to ignite a sample under conditions of piloted ignition under a radiant heat flux. The time to flame out (FO) marks the end of combustion and measures how quickly the material extinguishes after the ignition source is removed.

TTI values for the fence materials in this study are displayed in Fig. 52 (a). The data for horizontal orientation with an incident heat flux of 50 kW/m^2 (red bars) indicate that WRC is the quickest to ignite, followed in order by WPC1, PVC and SPC, and WPC2. The large error bar for WPC2 reflects the existence of an outlier under these conditions. All other test conditions indicate that the ordering of TTI values among the three composite fence samples is WPC1 < WPC2 < SPC. This chart clearly shows the sensitivity of TTI to incident heat flux – decreasing the incident heat flux from 50 kW/m^2 to 35 kW/m^2 roughly doubles the TTI in all but one case.

Figure 52 (b) illustrates the data for FO. The WPC2 fence sample takes considerably longer to extinguish (up to nearly 55 min) compared to all other fence materials under every test condition. SPC and PVC have the shortest FO, with one exception, and the FO for WPC1 is similar to that for WRC (wood). At an incident heat flux of 50 kW/m^2, FO is significantly shorter in the vertical configuration than horizontal.

Materials with a higher fire hazard related to ignitability have a short TTI and a long flaming duration (FO minus TTI). Generalizing from this data, SPC and PVC rank lowest in ignitability. Both the TTI and FO for WPC1 are comparable to those of WRC, resulting in similarly high ignitability. Although the TTI for WPC2 is longer than WPC1, the FO is considerably longer. Once ignited, therefore, WPC2 fence samples burn for a long time.

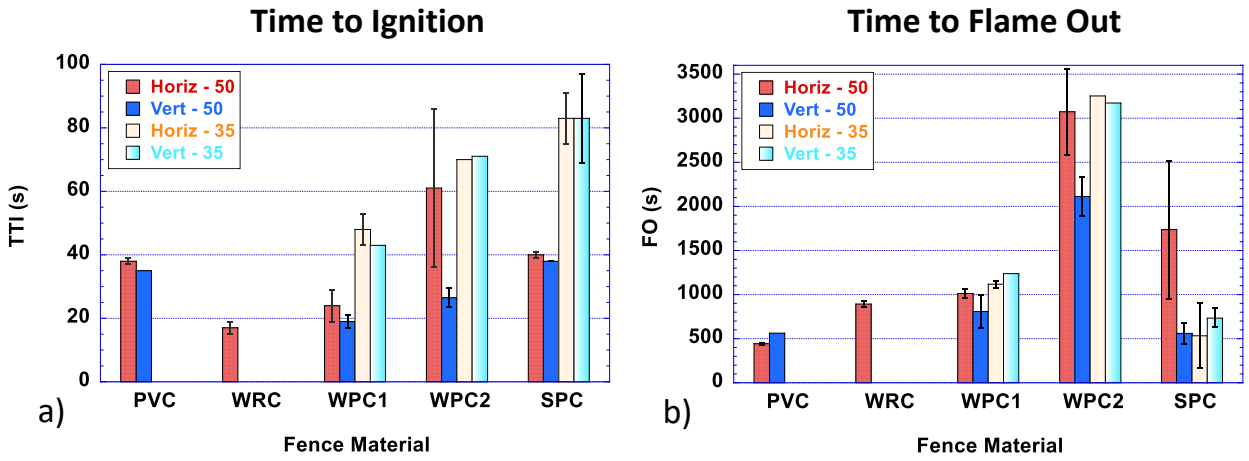

Fig. 52. Mean values of a) time to ignition and b) time to flame out from the five fence materials in horizontal and vertical orientations at 50 kW/m^2 and 35 kW/m^2.

Heat Release Rate: Many key flammability properties measured by the cone calorimeter are based on heat release rate (HRR). Figure 53 provides bar charts comparing peak heat release rate (PHRR), total heat release (THR), average HRR over the first 600 s, and effective heat of combustion (EHOC). The significance of each measure is discussed at the beginning of Section 5.2.

Figure 53 (a) shows that the PHRR for all three of the composite fences is much higher (at least double) that for either PVC or WRC under the same conditions. The PHRR is highest for the WPC1 fence sample mounted vertically with an incident heat flux of 50 kW/m^2 (blue bar for WPC1). This is due to the falling of the outer layer from this set of samples, which exposed a fresh surface of combustible material unprotected by char. The large error bar for this case indicates an outlier that did not undergo this behavior, as discussed in Appendix C.4.3. Under the same test condition, the PHRR is also very high for SPC and lower for WPC2. The ordering of PHRR values differs for fence samples mounted horizontally; in this configuration, SPC has the largest PHRR, followed in decreasing order by WPC2 and WPC1.

The total heat release (THR), shown in Fig. 53 (b), is the total amount of heat released during combustion of the cone calorimeter samples, which provides an indicator of fire load and fire hazard. The data displayed in the bar chart is consistent with THR as a function of the type of material and its mass, with little variation as a function of test condition (with the exception of one case for SPC). THR is the highest for WPC2 fence samples, followed by WPC1, then SPC and WRC with roughly the same value, and PVC as the smallest. The differences are large, with each value of THR nearly halving the previous value in the ordering.

The average value of HRR over the first 600 s, shown in Fig. 53 (c), differentiates among fire load and fire hazard for the various cone calorimeter samples by comparing heat release rates during early combustion. The ordering of cone samples from highest to lowest is WPC1 > WPC2 > SPC > WRC > PVC. The lower ranking of WPC2 for this measure compared to THR is due to the long tail of these samples, which burn much longer than the other samples before extinguishing. The value of HRR for WPC1 samples remains high over the first 600 s, dropping to the much lower levels for the other fence samples after the initial peak, as observed in Fig. 42 through Fig. 45. With one exception, the average HRR over the first 600 s is higher for samples mounted vertically rather than horizontally.

The effective heat of combustion (EHOC) for all fence samples at the time of flame out are shown in Fig. 53 (d). This variable measures the amount of heat energy released per unit mass loss when a fuel burns, providing insight into burning intensity and the completeness of the combustion process. All three composite fence sample types show high EHOC relative to WRC and PVC fences. EHOC values for PVC and western red cedar are in good agreement with literature values of 9.3 MJ/kg (rigid PVC) and 13.1 MJ/kg, respectively, compiled by Janssen and Ostman [38], who incorporated data for plastics from Table 3.11 of Lyon [39]. From the same sources, EHOC values for the three composite fences are comparable to those of flammable plastics such as polystyrene at 27.9 MJ/kg and nylon at 29.8 MJ/kg.

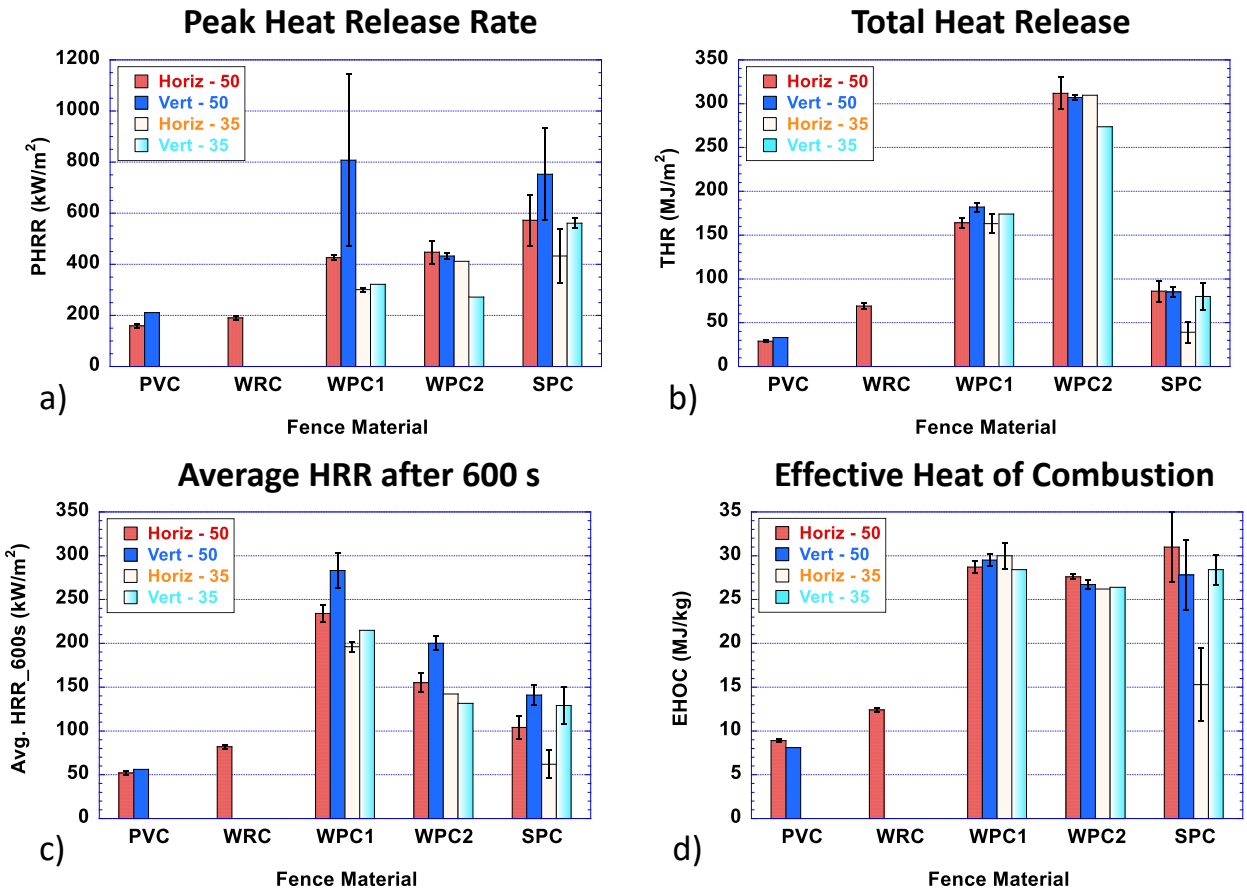

Fig. 53. Mean values of a) peak heat release rate (PHRR), b) total heat release (THR). C) average value over HRR over the first 600 s, and d) effective heat of combustion (EHOC) from the five fence materials in horizontal and vertical orientations at 50 kW/m² and 35 kW/m².

5.2.4. Firebrand Generation and Char Residue

The characteristic burning behavior of each of the cone calorimeter fence sample types is indicated in Fig. 54. These photos demonstrate the tendency of each fence material to char, drip, or fragment into small particles that may become airborne as firebrands. Each sample in was mounted horizontally and exposed to the same conditions of 50 kW/m² heat flux for a time period exceeding 800 s. The fire behavior seen in vertical cone testing agrees qualitatively with the horizontal results.

The final form of the PVC fence sample, shown in Fig. 54 (a), is a dome-shape hard carbonaceous residue with a layer of white particles. The white particles are understood to be the residue of metal elements incorporated to improve the flame retardancy and smoke suppression of the polymer [40].

Formation of firebrands in the WRC sample is clearly shown in Fig. 54 (b) and (c). As is typical for wood, charring and deep cracks formed during sustained flaming combustion. Small glowing firebrands were observed to separate from the test specimen and fly away from the sample

holder, potentially generating secondary ignition sources. Image (c) shows that flaky ash residue remained after glowing combustion ceased.

The WPC1 sample burned intensely, leaving the flaky char layer shown in Fig. 54 (d). However, no evidence of firebrand generation was observed. The residue of the WPC1 sample resembled caked fine sawdust and exhibited no glowing combustion after the flaming combustion ceased.

WPC2 cone samples left a crumbling residue that burned for a long time under all test conditions. The sample in Fig. 54 (e) was still smoldering 30 min after flameout.

SPC samples dripped heavily in both horizontal and vertical configurations. No residue remained in the sample holders at the end of the cone calorimeter tests. Figure 54 (f) shows the empty holder from a horizontal test next to unburned sample pieces that were collected from the floor and other nearby surfaces after the test.

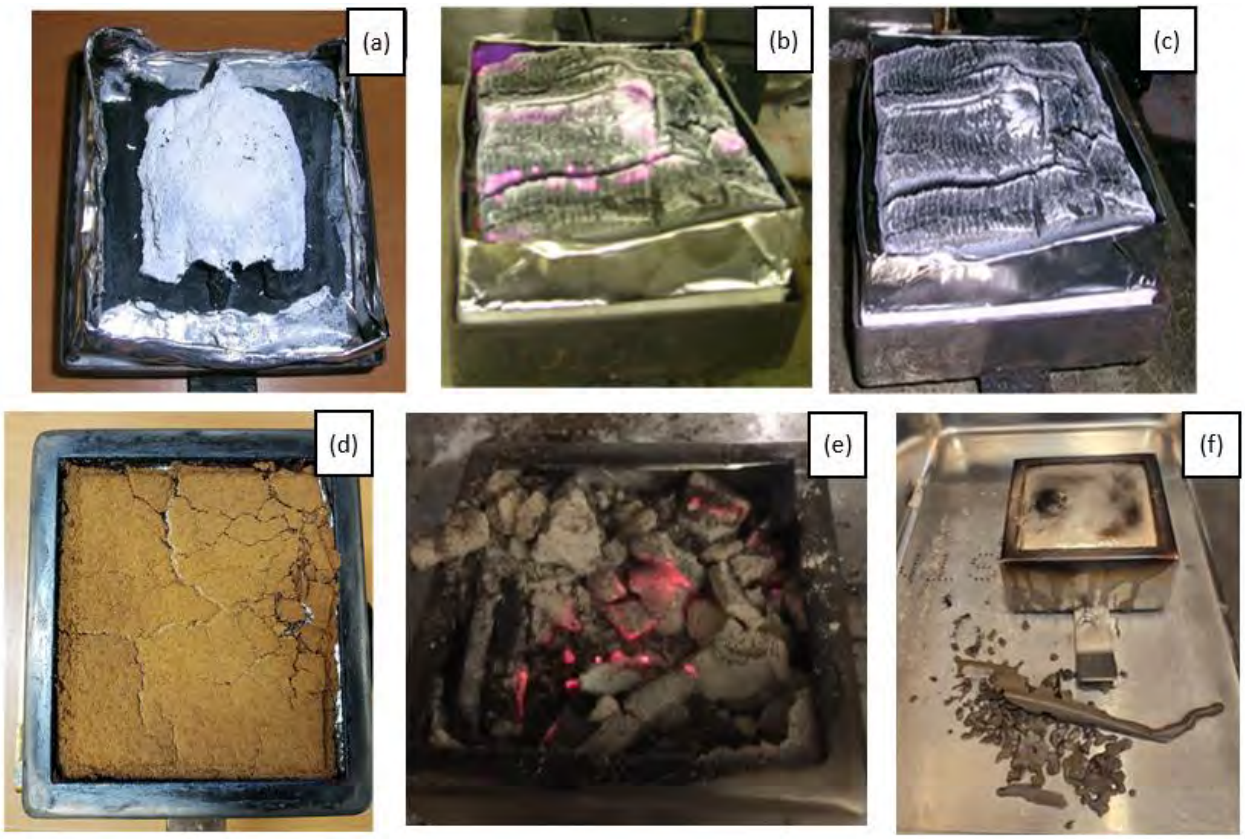

Fig. 54. Photos of (a) hard char residue of PVC sample, (b) firebrand formation after flame extinction and c) flaky, ash residue of WRC wood sample, (d) flaky residue of WPC1 sample, (e) crumbling, smoldering residue of WPC2 sample, and (f) no residue for SPC sample except for material that dripped away from the heat source and extinguished. All samples were mounted horizontally and exposed to 50 kW/m^2 heat flux for over 800 s.

5.3. Summary for Cone Calorimeter Tests

Flammability measurements were made using the cone calorimeter to compare the composite fence materials (WPC1, WPC2, and SPC) with each other and with western redcedar (WRC) and rigid polyvinyl chloride (PVC) fence samples. Test results were obtained in both horizontal and vertical configurations. The goals of this study were: (1) to improve our understanding of the differences in fire behavior among the three composite fence types by separating material properties from fence design and (2) to compare the validity of horizontal and vertical cone tests for assessing the flammability of fences.

Flammability measures included ignitability measures and properties based on heat release rate. Ignitability is associated with the initiation and subsequent growth of fire under real world conditions and heat release rate relates to fire hazard during combustion.

Key findings from the cone calorimeter tests on samples from WPC1, WPC2, SPC, WRC, and PVC fences are listed below.

Material flammability properties. Cone calorimeter tests consistently showed that composite fence materials are considerably more flammable than western red cedar and vinyl. However, the flammability characteristics of the three composite fence materials did not enable a clear ranking among them.

- Ignitability:
    - The time to ignition (TTI) measures how long it takes to ignite a sample using piloted ignition under a radiant heat flux. Wood (WRC) fence samples were the quickest to ignite, followed generally by WPC1, WPC2, and both SPC and PVC with timings approximately the same. TTI was considerably slower with lower incident heat flux and insensitive to orientation (horizontal vs. vertical).
    - The time to flameout (FO) marks the end of combustion and measures how quickly the material extinguishes after removal of the ignition source. WPC2 took considerably longer (on the order of twice the time) to extinguish than all other fence samples. FO was similar for WPC1 and WRC, and SPC and PVC generally extinguished the fastest. For SPC, FO occurred because all the sample material was consumed.
    - Although more difficult to ignite than the other fence samples, once ignited the WPC2 samples burned about twice as long as the other materials. On the other hand, PVC samples exhibited longer ignition times and shorter flaming durations. This suggests that from an ignitability perspective, the risk of contributing to the fire hazard is highest for WPC2 and lowest for PVC relative to the other fence types.
- Heat Release Rate Measures:
    - High peak heat release rate (PHRR) suggests that the fire more readily ignites nearby objects. Orientation of the cone sample significantly affected the ranking

of composite fence materials based on this measure. For horizontal cone tests, SPC displayed the highest value, followed by WPC2 and WPC1. For vertical cone tests at a high incident heat flux of 50 kW/m^2, WPC1 showed the highest value by far, due to the outer layer falling and exposing a new layer of fuel for three of the four cone tests. Dripping SPC came next, followed by WPC2, which was relatively unaffected by orientation. The fire hazard for PVC and WRC fence materials was much lower than for any of the three composite fence materials.

- The total heat release (THR) is an indicator of fire load. Because of its long flaming duration and much higher initial sample mass, WPC2 showed the highest value, almost double that of WPC1. The values for SPC and WRC were comparable, and PVC showed the lowest fire load.
- The average HRR after 600 s was highest for WPC1, followed by WPC2, SPC, and WRC. Changing the orientation from horizontal to vertical for composite fence samples resulted in higher values but did not affect the ranking. PVC displayed the lowest fire hazard based on this measure.
- The values of the effective heat of combustion (EHOC), measuring the amount of heat energy released by the fuel per unit mass loss and thus burning intensity, were comparable to literature values for several flammable plastics for the three composite fences. The EHOC was much lower for WRC and lowest for PVC.
- In summary, PVC consistently ranked as the lowest fire hazard using heat release rate measures, followed by WRC, yet both materials are still combustible and can present an appreciable fire hazard, especially in certain configurations (see the detailed hazard evaluations in [1]). The fire hazards for the composite fence samples were considerably higher than those of PVC and WRC. Depending on the measure and orientation, either WPC1, WPC2, or SPC could be ranked as having the highest fire hazard of all fence samples in this study.

5.4. Applicability of Cone Calorimeter Results to Full-Scale Fence Study

The detailed cone calorimeter study presented in this section (Section 5) and in Appendix C may be used to address the question of whether small-scale cone calorimeter testing is capable of serving as an adequate replacement for full-scale testing of fence panels. Cone tests were performed on samples taken from the three types of composite fences studied in this report and from wood and vinyl fences that are in common use. In this section, small-scale cone calorimeter results are compared to the results from full-scale fence experiments to determine in what sense and how well they agree. Results from vinyl (PVC) and wood (WRC) fence experiments have been derived from the 2022 fence report [1].

5.4.1. Full-scale Fence Fire Behavior

The full-scale fence panel experiments described in Section 4 showed that each composite fence behaved differently under the test conditions. In several cases, the fire behavior matched or exceeded the flaming intensity of fences studied previously and presented in Ref. [1].

Figure 55 presents representative images from fire experiments on each of the five fence types (PVC, WRC, WPC1, WPC2, and SPC) whose samples were tested in the cone calorimeter. These fence experiments were all performed with hardwood mulch beneath the fence, and all but the PVC fence were tested under conditions of low wind speed and 1.83 m (6 ft) separation from the shed. The PVC fence was tested at medium wind speed [10 m/s (22 mi/h)] and adjacent to the shed, considered to be a more challenging test condition. Fig. 56 adds data from WRC fence test A-102 [1] to plots from Fig. 39 to compare flame spreads over all but the PVC fence.

Fire progressed the slowest along the PVC fence in Fig. 55 (a), with flames remaining close to the mulch on the ground. The fire along the WRC fence in Fig. 55 (b) remained below the center stringer. The flame heights on both WPC1 (c) and SPC (e) composite fences exceeded the height of the fence, and the fire spreads were among the fastest of all fences tested in this effort. Of all fences studied, only parallel wood fences displayed similarly severe fire behavior [1]. In the case of the WPC1 fences, the flames were also carried by falling vertical boards, extending the width of the fire on the ground to up to 3.7 m (12 ft). For WPC2 fences in Fig. 55 (d), on the other hand, each horizontal board dropped to the ground, in turn, within the same footprint, gradually lowering the height of the fence. Because of this, the flames never extended much above the halfway point of the fence, and the fire behavior was closer to that of the wood fence than to the other composite fences. In fact, the fire spread over the WPC2 fence was even slower than over the WRC fence, as shown in Fig. 56.

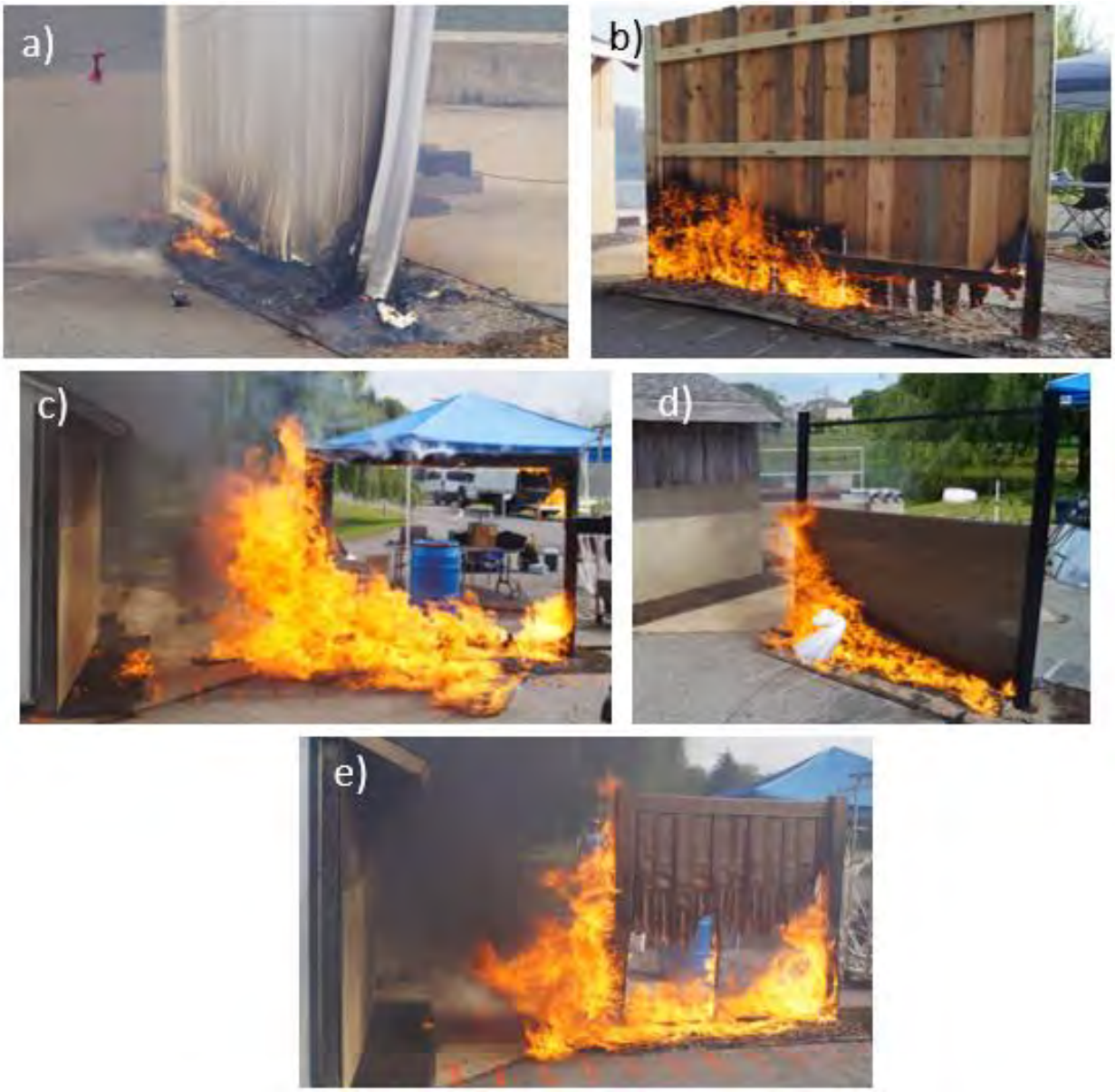

Fig. 55. Comparison of flames from fence experiments with mulch beneath: a) PVC [Test A-35], b) WRC [Test A-102], c) WPC1 [Test E-1], d) WPC2 [Test F-1], and e) SPC [Test H-1].

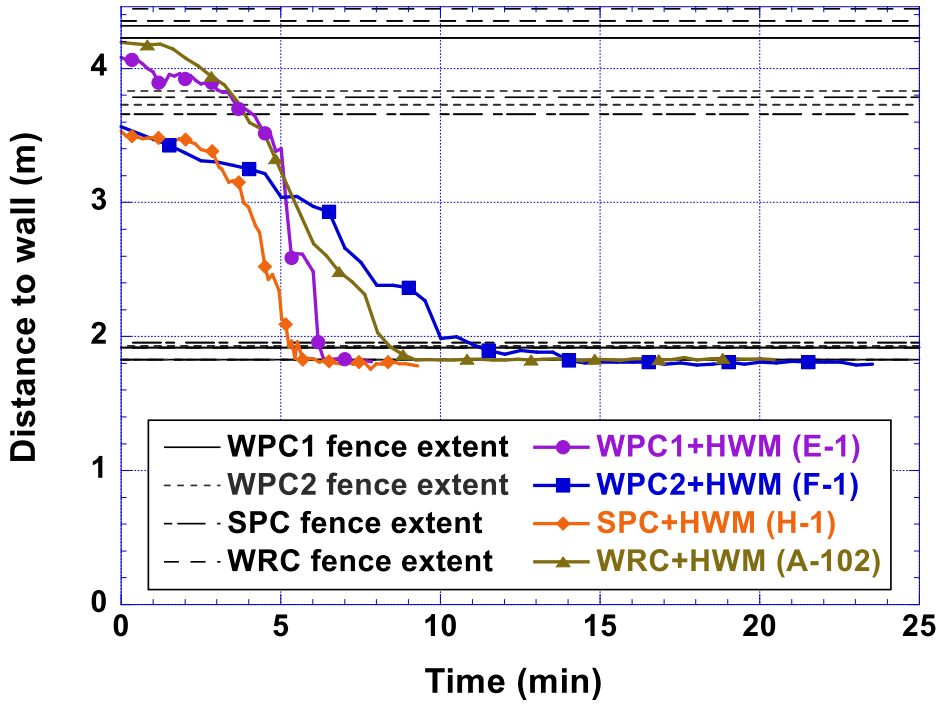

Fig. 56. Flame spread as a function of time for three composite fence experiments with hardwood mulch beneath plus a western red cedar fence experiment under the same test conditions [1]. Solid and dashed black lines show the locations of the posts closest and farthest from the shed for each fence.

Figure 57 and Fig. 58 present corresponding images and flame spread plots, respectively, for fence experiments in the absence of mulch. Experiments on the three composite fences were all performed at low wind speed and 1.83 m (6 ft) separation from the shed. The WRC fence [1] was tested under medium wind speed [10 m/s (22 mi/h)] and 1.83 m (6 ft) separation. The PVC fence [1] was tested at high wind speed [14 m/s (31 mi/h)] and adjacent to the shed, considered to be a more challenging test condition.

In the absence of fine fuels beneath vinyl or wood fences, the fire spread from a single point of ignition was found to be exceptionally slow, characterized by glowing combustion and occasional small flames [1]. The attempt to ignite the PVC fence resulted in a char pattern limited to the region of exposure to the propane burner, as shown in Fig. 57 (a). The progression of fire along the WRC fence without mulch in Fig. 57 (b) was caused by the transitioning of the lower stringer to flaming combustion for an extended time, with boards breaking off one-by-one and continuing to burn through glowing combustion. However, fire progression was slow, taking more than an hour to reach a point halfway down the length of the fence. The plot of flame spread from this experiment is included in Fig. 58. In another WRC fence case under the same conditions, the absence of flaming resulted in even slower progression.

The absence of mulch made little difference to the fire behavior of WPC1 and SPC composite fences, as shown in Fig. 57 (c) and (e), respectively, other than a brief delay in timing. For both WPC1 and SPC fences, the flame heights exceeded fence height, and fire spreads were among

the fastest of all fences tested in this effort. As in the case with mulch, the flames on the WPC1 fence were carried by falling vertical boards, potentially extending the width of the fire on the ground to up to 3.7 m (12 ft). The other composite fence type, WPC2, showed very different behavior in Fig. 57 (d). Like vinyl and wood fences, the fire effects remained localized to the area around the ignition point. Plots showing fire spread as a function of time over each of the three composite fences are included in Fig. 58.

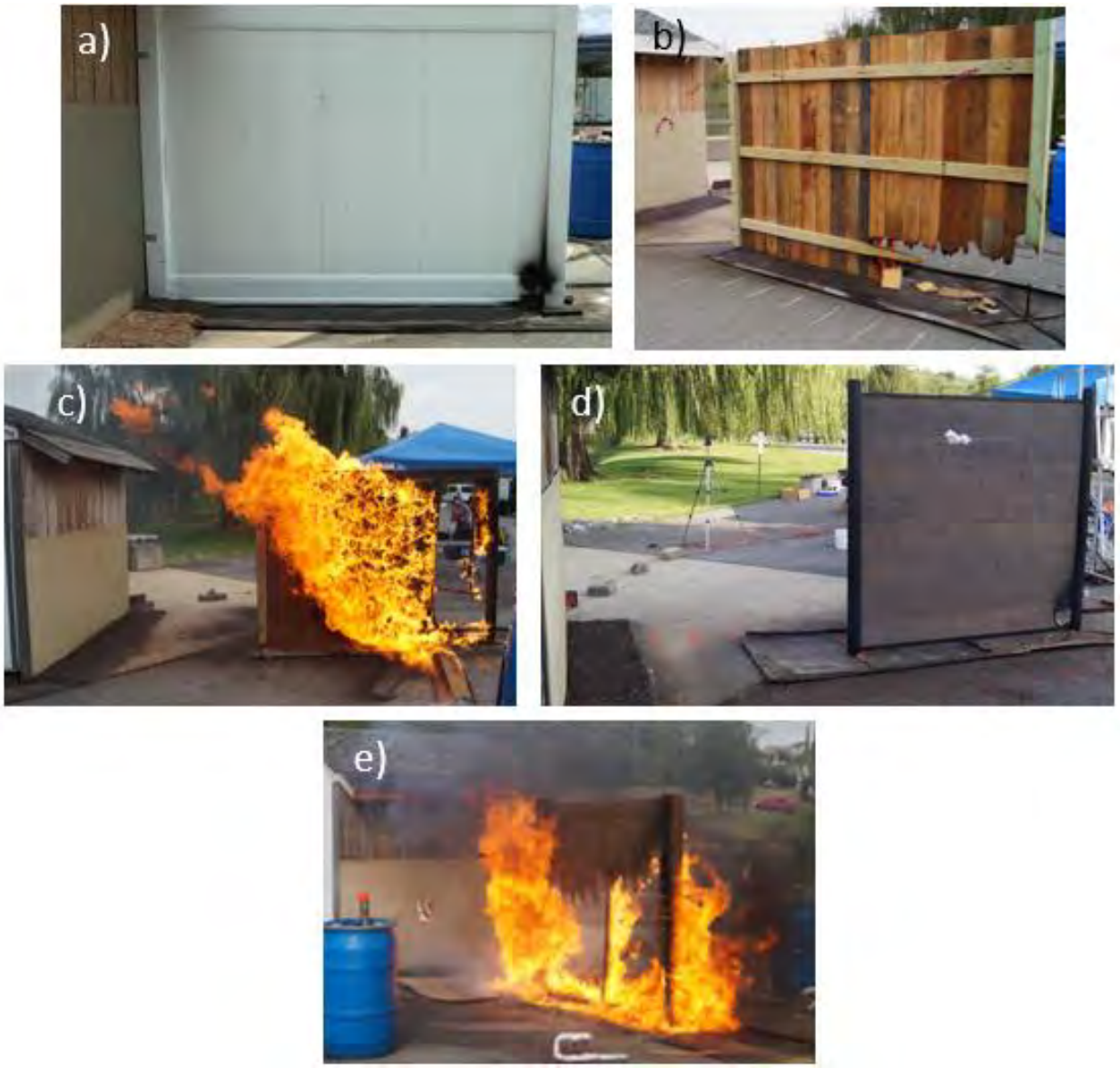

Fig. 57. Comparison of flames from fence experiments without mulch: a) PVC [Test A-34], b) WRC [Test A-101], c) WPC1 [Test E-2], d) WPC2 [Test H-3], and e) SPC [Test H-2].

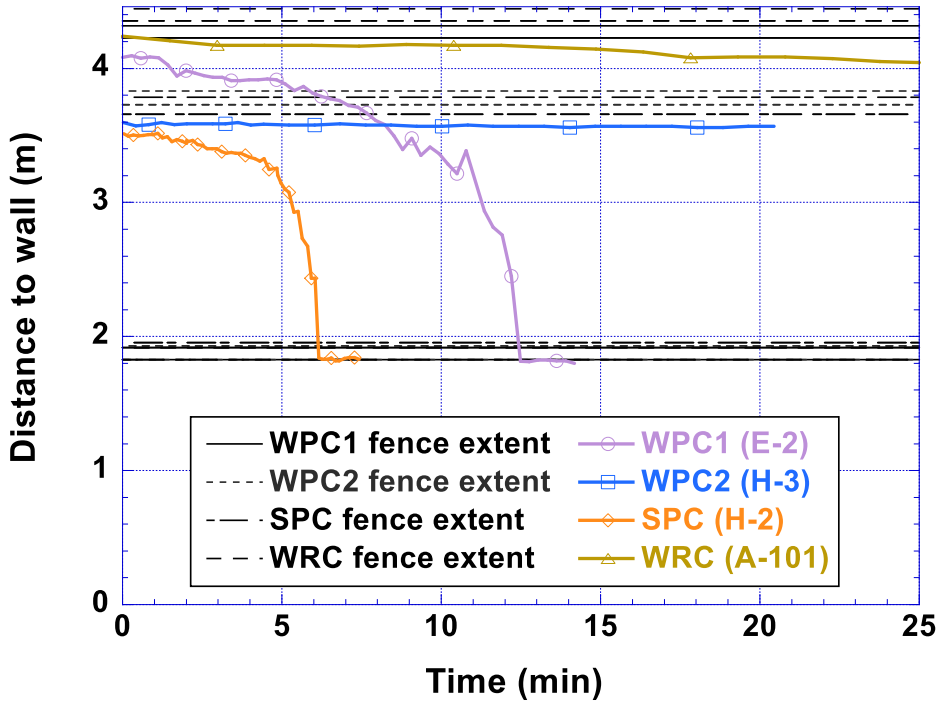

Fig. 58. Flame spread as a function of time for three composite fence experiments plus a western red cedar fence experiment [1] in the absence of hardwood mulch. Solid and dashed black lines show the locations of the posts closest and farthest from the shed for each fence.

5.4.2. Comparison with Cone Test Results

In some ways, the ignitability and flammability results from cone calorimeter testing supported the results of the full-scale study on composite fences. In other ways, cone results differed from full-scale findings. In combination, the small-scale cone calorimeter tests and full-scale fence experiments provide a more complete interpretation of the results and give us insights into the differences in fire behavior among five fence types.

Before discussing the specific factors on which small-scale and full-scale tests agreed and disagreed, here is a list of the key results from cone calorimeter testing and full-scale fence experiments:

- Full-scale experiments showed severe fire behavior from two of the three composite fences (WPC1 and SPC), with flames extending above and well beyond the fence even in the absence of mulch beneath the fence. The fire behavior of the other composite fence, WPC2, appeared significantly less severe. Although vigorous, flames remained below the middle of the fence when mulch was placed below the fence. This result was attributed to the slippage of horizontal fence boards along the vertical sides of the panel frame. If for some reason due to age, installation factors, damage, or higher ignition location, the boards did not slip downward, a different fire behavior could occur. In the absence of mulch, fire growth over the WPC2 fence was limited to a hole in the ignition region that expanded slowly.

- Small-scale cone calorimeter tests did not readily identify WPC2 fence samples as less hazardous than WPC1 and SPC fence samples. Instead, the ranking of the three composite fence samples was dependent on the specific measure of ignitability or flammability.
- Cone calorimeter tests and full-scale fence experiments agreed that PVC represents the lowest fire hazard of the fences in this study. They also agreed that the fire hazard from wood fences lies between that of PVC fences and any of the three composite fences.

Several factors demonstrated agreement between full-scale experiments and cone calorimeter testing, including the following:

- *Melting and dripping*: Melting and dripping contributed to both small-scale and full-scale results for WPC1 and SPC fences. In three of four vertical cone calorimeter tests, the outer layer of the WPC1 fence sample slipped off, exposing a fresh fuel surface and resulting in a large peak of heat release rate that was two or three times the value of the first peak. This was consistent with the rapid fire spread and intense flaming over the entire surface of the WPC1 fence in full-scale experiments both with and without mulch. In the cone calorimeter, SPC fence samples melted and dripped from sample containers in both horizontal and vertical configurations. In full-scale experiments, the dripping SPC fences resulted in large flames along the fence and on the ground even when mulch was absent. The burning fence turned into dripping streamers blown (but not transported) by the wind field.
- *Vertical cone test results*: Vertical cone calorimeter tests showed a large difference in fire behavior among the three composite fence samples. For WPC1 in the vertical orientation, the large second peak of heat release rate (PHRR) resulted from the outer layer of material sliding down and exposing fresh fuel. This phenomenon was missed completely by the horizontal cone test. For vertical SPC cone tests in which attempts were made to contain the material within the apparatus, the dripping of the fence sample considerably increased the PHRR of the single peak over that in the horizontal orientation. The PHRR of the WPC2 fence samples, on the other hand, displayed only minor changes between horizontal and vertical tests. This finding of more severe fire behavior of WPC1 and SPC over WPC2 fence samples was indicated only by the vertical cone calorimeter tests and agreed with the findings for full-scale experiments of these fence types.

  A fence is inherently vertical in orientation. It follows that the recommendation of Tsai 2009 [34] that cone calorimeter tests in the vertical orientation be used to evaluate material fire performance is particularly appropriate for this application. Standardized fire testing on materials to be used for decking would not necessarily apply to materials to be used for fences.
- *Effective heat of combustion (EHOC):* Cone calorimeter tests and full-scale fence experiments agreed that PVC represents the lowest fire hazard of the fences studied here. They also agreed that the fire hazard from wood fences lies between that of PVC fences and any of the three composite fences. The effective heat of combustion (EHOC)

was the clearest measure of this, with values for the three composite fence samples that were close to each other and comparable to literature values for flammable plastics, and with much lower values for WRC and PVC.

Note that its high EHOC raises the question of whether WPC2 materials in a different fence design (e.g. vertical rather than horizontal boards) or under different environmental conditions could display more hazardous fire behavior.

Several factors could not be reconciled between full-scale experiments and cone calorimeter testing, including the following:

- *Physical design of fence – Board orientation*: The horizontal board design of the full-scale WPC2 fences studied here has been identified as a major reason for the reduction in fire hazard relative to that of the vertical boards of the WPC1 fence. While the horizontal boards slid down into the footprint of the WPC2 fence as they were consumed, limiting the height and width of flaming, the vertical boards fell out of the top railing of the WPC1 fence and widened the flaming range to up to 3.7 m (12 ft). This type of physical effect cannot be reproduced with the cone calorimeter. Since WPC1 was not tested with horizontal boards and WPC2 was not tested with vertical boards, the level of impact of board orientation on the full-scale burning behavior and hazard of each material is not known.
- *Physical design of fence – Chimney effect*: The SPC fence panel was molded as a single piece, hollow in the middle. Because of this narrow gap, holes opened in the fence panel as it burns could lead to a chimney effect that would intensify the fire. Although WPC2 fence boards were hollow on a small scale, the horizontal orientation of the boards precluded any chimney effect on the burning fence. The chimney effect could contribute to the more intense fire behavior for the SPC fence. The thin SPC samples that were cut from one face of the fence were not capable of introducing this effect into cone calorimeter testing
- *Cone sample vs. fence board*: Samples from WPC2, wood, and vinyl fence boards were fully representative of board geometry, but samples cut from WPC1 and SPC fences were not. As shown in Appendix C.1, cone calorimeter samples were cut from flat areas of the WPC1 and SPC fences. They omitted interlocking portions of the WPC1 boards and the opposite side of the SPC fence. The cone samples therefore contained less material than they would have had if the fences had contained the same fuel load and been of uniform thickness. Neither the fuel load nor the complex geometry of these two fences was fully represented in cone calorimeter testing. Fabian [26] also noted the disconnect between fire performance of cone samples of deck board materials and full-scale fire performance of deck boards in realistic installations likely due to the cone test not capturing differences related to board structures.
- *Horizontal cone tests*: Cone calorimeter testing in the horizontal orientation did not capture the differences in full-scale fire behavior among WPC1, WPC2 and SPC fences. No ignitability or flammability measure indicated a lower fire hazard for WPC2 fence samples relative to the other two composite fence materials. The peak heat release

rates (PHRR) were identical within uncertainty limits. The flaming duration of the WPC2 fence sample was over three times as long as for the WPC1 sample and twice as long as for the SPC sample. The total heat release (THR) was larger for WPC2, although the average HRR over the first 600 s was larger for WPC1 due to the long flaming duration of WPC2.

- *Presence of continuous incident heat flux*: Cone calorimeter testing involves continuous application of an incident heat flux to the object being tested. For full-scale experiments on WPC2 fences, removal of the mulch that provided incident heat flux completely changed the fire behavior. For the other two composite fences, fire growth was sufficiently rapid – and accompanied by dripping behavior – that little difference was observed between full-scale experiments with and without mulch.
- *Ignition on both sides of the sample:* In full-scale testing the fence was ignited from both sides of the fence, whereas cone calorimeter ignition is one-sided. Note that one-sided ignition is a reasonable choice for fire testing of decks.

The cone calorimeter testing on samples taken from the three composite fence types plus wood and vinyl fences has enhanced the understanding of the fire hazard posed by these fences. Neither the cone calorimeter test nor the full-scale fence experiments provide a comprehensive picture of the fire behavior of fences in WUI fires. However, they do complement each other, helping to separate the effects of the fence material from those of the physical design.

Vertical cone calorimeter tests are far more informative than horizontal cone tests for studying the fire hazards of fences. Cone calorimeter tests are not adequate for assessment, however, since small-scale tests are unable to represent many effects of the physical design of the fence and of the complexities of molded fence boards and panels. Conversely, full-scale experiments mask the potential of the composite material to behave differently if the physical design is modified.

For this study, the combination of small-scale tests and full-scale experiments leads to the conclusion that, while one fence design behaved better under the full-scale test conditions, the fire hazard of all composite fences could potentially be very high.

This comparison between small-scale and full-scale results has provided some insights into the fire behavior of composite fences and the need for better fire tests specific to the application. With only three material types and fence designs in this study, it is recognized that the conclusions are not definitive and may be revised with future testing. However, the hazard of these fences is clear, and caution is advised in their use.

As a final thought, it is important to note that this study did not consider the quantity or content of the smoke emitted in fence fires. A broader look would weigh smoke toxicity effects when combustible fences contribute to a WUI fire.

6. Discussion

The findings for composite fences in this study can inform building codes, referenced standards test methods, and best practices for communities. This section presents a review of hazardous scenarios involving composite fences and fences in general, recommendations for addressing these hazards, and limitations to the study.

6.1. Hazardous Scenarios

Fences are widely used in the WUI for various purposes. They can be found in all WUI structure density settings, from high density neighborhoods to low density rural settings. Combustible fences can impact fire spread and life safety in three distinct ways:

Fences as linear fire spread enhancers.

Fences can act as "wicks" carrying fire along fence lines within and across parcels. This can negatively impact one or more parcels (residential or commercial lots), as fences are frequently connected or adjacent to one another. Rapidly spreading burning fences can bring fire to one or more parcels in a matter of minutes. This can challenge the available suppression resources, particularly during a large incident where hundreds or even thousands of structures are exposed to fire and embers in minutes or hours. Under these conditions, even relatively small fire spread rates can bring the fire to the structure and/or other combustibles before defensive actions by first responders can stop structure ignitions.

Fences can act as a ladder fuel, over which a fire burning low to the ground can climb to ignite combustible items at higher levels, such as the under-eaves area, edge of roof, or tree branches. Multiple ignition points along the fence and the presence of nearby vegetation will worsen the hazard.

Fences as fire spread enhancers.

All combustible fences are susceptible to fire. The energy that can be released from a particular fence is a function of the fence construction material, the fence design and local fire and ember exposures. Fuels agglomeration, in scenarios where fuels are near one another, can have significant impact on how fences behave. In the study of fences performed by NIST [1], these differences in energy release have been observed in two documented scenarios:

- Fence versus fence plus mulch,
- Single versus parallel fences.

Fuels agglomeration can therefore have significant impact on the energy released from a burning fence. The issue of fuels agglomeration is not unique to fences, however. Because of their design and use, fences are frequently in close proximity to other fuels (e.g.: other fences, mulch and other ground covers, and auxiliary fuels near the property line like wood piles or sheds).

The amount of energy release from a burning fence can also impact adjacent fuels that may not have otherwise ignited. This is particularly true for fences that fall out and away from the fence line. Such a fence can result in direct flaming exposures to other fuels 1.83 m (6 ft) or more from the fence line.

Melting and dripping can pose an additional fire spread hazard, particularly with topography. The resulting liquid can readily flow downhill, enhancing fire spread within and potentially across parcels. Other parcel level combustibles have been identified as melting and dripping fire spread hazards, including certain sheds that resulted in pooling of burning liquid in fire experiments [41].

Fences as egress restrictors.

In certain scenarios fences can also potentially directly impact life safety. The use of high heat of combustion materials for fence construction in a backyard that contains one or more Auxiliary Dwelling Units (ADUs) can impede egress from these occupied structures. Burning high energy release fences can entrap residents and hinder access. Two particularly dangerous scenarios are demonstrated in this report:

- In the process of burning, the fence collapses outward, resulting in large areas of burning materials [as wide as 3.66 m (12 ft) for a 1.83 m (6 ft) tall fence]. This event would be particularly hazardous if it occurs near the gate that provides access to the street.
- Melting and dripping results in long burning streamers that flap in the wind and can potentially burn residents on contact or by emitting airborne molten droplets.

6.2. Addressing the Fire Hazard of Fences

The fence experiments conducted at NIST provide insight in the fire spread potential of selected commercially available material/design configurations. The results show the complexities of experimental design on characterizing the fire hazard provided by fences. The small-scale cone calorimeter experiments provide additional insight on how the effects of heat of combustion can impact the understanding of the full-scale experiments.

There are no fence fire testing standards currently available. To reduce fire spread and enhance life safety, authorities having jurisdiction may want to review the use of high energy release fence materials for use in WUI fire prone areas.

A more detailed discussion on implementing guidance based on the relationships among fuel layout, fire hazard, and structure hardening can be found in the recently published NIST report entitled *WUI Parcel/Structure/Community Fire Hazard Mitigation Methodology* (HMM) [4]. Some ignition pathways over which combustible fences and mulch beds could transport fire to multiple residences in a moderate- to high-density WUI residential communities were described under Hazardous Scenarios in the Discussion in [1]. These scenarios illustrate the critical role combustible fences can play in carrying fire between and within parcels.

It should be noted that noncombustible fences, such as those composed of masonry, concrete or metal, will not generate firebrands or spread fire between and within parcels. However, maintenance is necessary to keep all fences free of leaf litter and other combustible debris that can accumulate next to any obstacle and itself create a fire hazard.

Field observations from NIST WUI case studies and the NIST experiments have identified the need to restrict the presence of high fire hazard fences in high-density WUI, to spatially segregate fuels to prevent direct flame propagation, and to limit the nonlinear effects of multiple fuels in contact with each other. The connectivity of fences to residential structures is explicitly addressed in some building codes and WUI hazard mitigation best practices; however, the issue of fuels agglomeration on the hazards presented from fences near other fuels is not in current guidance. Solutions to reduce the structure ignition hazards posed by high fire hazard fences include but are not limited to:

- Best practices guidance for homeowners
- Homeowners Association (HOA) requirements on placement of high fire hazard fences
- County or State regulations on the placement of high fire hazard fences
- National or international codes and standards

More information on these approaches is in the HMM report [4].

6.3. Limitations

This study was a survey of the fire behavior in wind of three combustible fences near a structure, as a supplement to a report published in 2022 on a variety of fences and mulch [1]. The limitations of the current work are similar. Understanding them will help to direct application of the results and to plan additional research to improve our knowledge. To focus on simple fire spread rather than ignition, the full-scale scenario studied in this report did not include multiple ignition points along the fence or mulch bed, the presence of nearby vegetation, sloping terrain, or other factors that can increase the ignition propensity, complicate and enhance the rate of fire spread, and amplify fire intensity. These experiments may therefore underpredict the fire hazard associated with fences in actual WUI fires.

Some limitations of this research include:

- *Only three types of composite fences were included in this study.* New information has been added to the previous larger study [1], which considered a small number of common fence types and mulches. In communities, there are innumerable combinations of fences, mulches, landscape designs, orientations, proximity to other fuel sources, and ambient conditions. Continuing attention to fire pathways observed in WUI fires and development of a standard fire test focused on fences will help to identify other situations that should be addressed.
- *No experiments were repeated*: The ability to quantify the effects of the parameters in this study was severely limited by the lack of replications, the stochastic nature of fire phenomena, and the variables that could not be well-controlled, such as ambient

conditions. The analysis of these data was therefore focused on uncovering trends and on discovering different modes of behavior, rather than on quantitative results.

- *Fuels were ignited at a single location on the ground*: The test protocol provided repeatable conditions to characterize fire performance and identify both dangerous and potentially desirable attributes of landscape features. In WUI fires, however, firebrands can ignite fences, mulch, and leaf or needle debris at multiple locations on the ground and at higher locations. The WPC2 fence in particular, with its horizontal boards that provide many elevated locations for firebrands to land, would be markedly more vulnerable to multiple ignitions. It is likely that this would result in a faster spreading fire. Burning vegetation can also ignite fences at locations above the ground.
- *Ignition was by gas burner rather than a natural source:* In these experiments, the fence and/or mulch bed were ignited at a single point at ground level by a propane gas burner. The method differs from natural ignition in WUI fires in multiple ways. A gas burner is a severe ignition source, igniting by continuous flame contact and differing in heating rate and geometric extent from most natural ignition sources in a WUI fire. The burner was used to provide a consistent ignition condition since flame spread rather than ignition was the focus of the study.
- *The orientation of wind was limited*: The full-scale fence experiments were conducted with the shed wall perpendicular to the fence and mulch bed and with the wind aligned with the fence. This resulted in a wind field with certain features, including a recirculation zone, that influenced flame behavior and firebrand trajectories. In an actual WUI fire, the wind may come from any direction and fluctuate considerably in both direction and amplitude.
- *The mulch was preheated by heat conduction through the steel pan:* The use of steel pans to hold the fence and/or mulch being tested introduced a heat transfer mechanism that does not contribute to fire spread under real conditions. The thermally conductive metal pans evaporated water and preheated the mulch ahead of the fire front. Soil has a much lower thermal conductivity, for which preheating is negligible.
- *Accumulation of windblown debris was not considered in Fence Only experiments*: This study considered the fire behavior of composite fences free of fine combustible mulch at their base, as an ideal. These fence experiments likely underestimate the hazard. Catastrophic WUI events most frequently occur during windy conditions. During such an event, a fence that extends to the ground, even if kept clear and well-maintained, can accumulate windblown debris at its base. If this occurs, the combination of fence and combustible materials at its base may ignite and generate significant flame and firebrand exposures.
- *Effects of terrain were not studied*: The experiments documented in this report were conducted on level ground. Terrain may significantly impact fire development. In general, fire spreads upslope faster than downslope. Melting may send burning liquids downhill. The interaction of terrain with wind can greatly affect fire spread, flame lengths and ember generation, transport, and ignitions.

- *Smoke toxicity was not included:* This study was focused on fire behavior and did not include smoke toxicity as a factor in the total hazard from burning fences or mulch. Composite fences include plastic, which releases toxic chemicals and fumes while burning.

7. Conclusions

Combustible fences and mulch provide pathways by which wildland-urban interface (WUI) fires may reach and potentially ignite structures in a community. Once ignited, these fuels become sources that may ignite nearby objects through radiation, direct flame contact, and generation of firebrands. It is important to understand the mechanisms by which these combustible landscaping elements can transport fire to a home in order to find ways to address the risk. Such knowledge helps with proactive design within the community. It informs homeowners on what they can do to protect themselves and their properties. It also helps fire departments to plan defensive strategies, placing resources and assigning tasks where they will be the most effective. The goal is to enhance the safety of members of the public and first responders.

This section lists the key findings from this report, practical recommendations based on the findings, and recommendations for future work. The conclusions are incorporated into the unified set of conclusions generated from the series of NIST studies on fire hazards associated with various categories of landscape combustibles: fences and mulch [1], woodpiles [2], and landscape timbers [3]. The composite fence study reinforces and adds to findings and recommendations from the unified set of conclusions.

7.1. Key Findings

The six experiments in the composite fence study demonstrated a range of fire spread hazards that were influenced by fence material, physical design and the proximity of fine combustibles. The full-scale experiments were complemented by small-scale cone calorimeter tests that informed the results. In this section, general findings are listed first and followed by very high, high, and medium configurations[6]. The findings are labeled according to the following categories:

FH	Fire Hazard
LS	Life Safety
HR	Hazard Reduction – materials, assemblies, implementation/housekeeping
IC	Improved Characterization – recommended future work to characterize these fuels more fully

7.1.1. General Findings

The results from the composite fence full-scale experiments and cone calorimeter tests demonstrated that:

F1. As combustible materials are combined, the hazard increases disproportionately. (FH)

The original fence and mulch study [1] and landscape timber study [3] demonstrated that fuel agglomeration significantly increases energy release and increases fire and ember exposures. The composite fence study confirmed this finding, showing that the presence of mulch

[6] Relative terms used in the context of the NIST fence studies and defined in the first fence report [1].

accelerated the progress of flame along two fence types and made the difference between flame spread along the fence and localized burning for a third.

F2. Fences may impede egress. (LS)

In a WUI fire, high and very high hazard[6] fence configurations may result in a line of flames close to egress paths from a house or auxiliary dwelling. Additional life safety hazards were revealed in the composite fence experiments. In experiments on one of the wood-plastic composite fences tested, the top and bottom frames distorted and allowed burning boards to fall to either side. This created a zone of flames along the fence line that was 3.7 m (12 ft) wide. In a set of experiments on a steel-plastic composite fence, the plastic panel distorted, melted, and dripped, resulting in hanging strands of plastic blown by the wind.

F3. Fire spread rates vary with fence materials and design, wind speed, and fuel configuration, including the presence or absence of mulch. (FH)

The original fence and mulch study [1] compared fire spread data in a specific wind-driven scenario for a variety of fence and mulch materials, designs, and configurations. This study found that two types of composite fences in combination with mulch supported fire spread rates that were faster than all other fence-mulch combinations tested. Factors that may have contributed to this finding include melting and dripping and slippage of surface material. Cone calorimeter testing determined that the effective heats of combustion of all composite fences in this study were considerably higher than for vinyl and wood fences. The physical design of the fences, including vertical vs horizontal boards and distortion of the fence frame with high temperatures, also played a role in how the fires spread.

F5. A standard test method is needed to evaluate the burning characteristics of fences. (IC)

A standard test method is needed to assess the fire performance of fences. The method should consider not only materials but assemblies and be carried out in a vertical orientation. It should be able to distinguish the fire behavior of various materials, including wood-plastic composites, wood, and vinyl, and designs, including privacy (continuous or nearly continuous panel of boards), lattice (woven, crisscrossing strips of wood), and good neighbor (similarly appearing, alternating boards and spaces on each side and no visibility through).

The significant differences in energy release among the three composite fences tested in this study highlight the need for a fence test method that can be used to assess the hazard of the material/design configuration. The cone calorimeter study in this report demonstrates that a combination of test methods may provide a more comprehensive assessment.

7.1.2. Very High Hazard Configurations

Within the context of this study, very high hazard[6] configurations are defined as those resulting in rapid fire spread and large flames.

F6. Rapid fire growth and large flames were observed for parallel fences *and some composite fences*. (FH)

- Limited testing indicates that ignition of certain *wood-plastic and steel-plastic composite fences* can result in very high intensity fire behavior. For two of the three composite fence types in this study, intense fire behavior was observed even in the absence of fine combustible material (mulch) beneath the fence. Both of these composite fence types burned with large flames that extended above the fence. The primary mechanisms for ignitions and rapid fire spread in the target mulch bed next to the structure were thought to be radiation and direct flame contact rather than firebrands. For one wood-plastic composite fence, the frame distorted in the heat and allowed vertical boards 1.8 m (6 ft) tall to fall to both sides, creating a 3.7 m (12 ft) wide zone of flames that could block egress and threaten property. A steel-plastic composite fence melted and dripped, becoming tattered with hanging strands blown by the wind field.

  Cone calorimeter testing demonstrated melting and sliding or dripping behaviors for both composite fences in this category. This may have contributed to the very high hazard behavior of these fences alone, in the absence of mulch beneath them.

7.1.3. High Hazard Configurations

Within the context of these studies, landscape fuel configurations that exhibit fire behavior in the high hazard[6] range support fire spread and generate firebrands but do not progress to full involvement with large flames.

F9. A fence with mulch at its base transports fire through the community and provides a steady source of firebrands to ignite combustible material downwind. (FH)

- Because of its physical design, one *wood-plastic composite fence* type in combination with dried mulch beneath displayed high hazard behavior. Its horizontal boards were held in place by the vertical frame elements on each side of the panel. As the fire consumed each horizontal board in turn, the boards above it slipped downward within the frame. As a result, the flame height stayed below the halfway point on the fence, the burning boards remained close to the centerline of the fence as they fell to the ground, and the fire diminished on its own as it ran low on fuel. The horizontal boards were observed to burn vigorously, and the cone calorimeter study revealed that the effective heat of combustion matched that of the other two composite fences in the study.

7.1.4. Medium Hazard Configurations

Within the context of these studies, landscape fuel configurations whose fire behavior was considered medium hazard[6] demonstrate very slow fire spread without flaming and little or no generation of firebrands.

F12. Without nearby fine combustible materials, the fire spread over a single combustible fence is slow and dominated by glowing combustion. (HR)

- In the absence of mulch beneath the fence, one of the three composite fences in this study displayed similar fire behavior to that seen for wood fences in the earlier

report [1]. The fire spread in the absence of fine combustibles was generally slow and dominated by glowing combustion with occasional small flames. It may be relevant that this composite fence type was the only one of the three types tested that did not exhibit melting and dripping behavior in cone calorimeter testing.

As noted with wood fences, it may be difficult to keep a fence sufficiently clear of fine combustible materials to achieve the slow-growth fire behavior [1]. Windblown debris such as leaves and pine needles may accumulate before or during a WUI fire event.

7.2. Primary Recommendations

The results of this study add to a comprehensive effort to reduce the vulnerability of structure and parcels to fire and firebrands. A Hazard Mitigation Methodology [4] has been developed with the goal of allowing structures in the WUI to survive fire and firebrand exposures without intervention by first responders. The recommended strategy is to balance a reduction of the exposure with increased hardening of the structure. The exposure may be reduced by removing or reducing the fuels or by relocating the source.

Several of the recommendations from the original fence and mulch report [1] have been reinforced by this study of composite fences and are repeated here. Two recommendations are added to the comprehensive list from the full series of NIST studies on landscape combustibles: avoid composite fences whose fire behavior presents a very high hazard, and avoid framing elements that deform at fire temperatures.

R2. **To protect life safety, do not place combustible fences where, if ignited, they could restrict or block egress.**

R3. **Avoid proximity to other combustible fuels, to reduce fire intensity and limit fire spread.** This includes fuels above the fence and fuels across parcel boundaries. Avoid mulch along the base of fences.

R4. **Avoid proximity of combustible fences to residences, including neighboring residences, to prevent direct ignition.** The intense flames from some composite fences may threaten a nearby residence through radiation and direct flame contact in addition to firebrands.

R5. **Replace combustible landscape features with noncombustible or low fire hazard features when possible.** Fire spread is more likely with wood and composite fences than with fences made of vinyl or noncombustible materials such as stone, brick, or steel.

R12. **Avoid any fence whose fire behavior may present a very high hazard.** Two composite fences in this study displayed highly hazardous fire behavior, with large flames that accelerated fire spread and extended into potential egress zones. The fence materials melted and dripped in one case and slid from the surface to reveal fresh fuel in the other. The fire behavior of the third fence was less intense in these experiments, primarily because of its physical design. However, all three composite fences had a high fuel content as measured by the effective heat of combustion.

R13. Avoid framing elements that deform at fire temperatures. The distortion of the upper frame of one of the composite fences in this study resulted in burning vertical boards falling to each side of the fence, creating a burning zone along its path whose width was twice the fence height.

These recommendations agree with requirements in the IBHS Wildfire Prepared Home Base Designation [42] and recently enacted California legislation AB-3074 [43], both of which call for not allowing attached combustible fencing in the 0 m to 1.5 m (0 ft to 5 ft) zone next to a house. For more detailed recommendations on spacings of combustible elements and hardening of structures and parcels, refer to the WUI Structure/Parcel/Community Fire Hazard Mitigation Methodology report [4].

7.3. Recommendation for Future Work

This study of composite fences reinforces the need for test methods specific to fences, as stated in the original fence report [1]. The inclusion of a detailed cone calorimeter study in this report shows the benefits of tests at multiple scales and the importance of matching the orientation to the application. This recommendation is repeated and strengthened here:

S5. Develop fire test(s) for evaluating fences and fence materials that represent the actual fire hazard.

A standard test method is needed to assess the fire performance of fences. The method should consider not only materials but assemblies and be carried out in a vertical orientation. It should be able to distinguish the fire behavior of various materials, including wood-plastic composites, wood, and vinyl, and designs, including privacy, lattice, and good neighbor. Both material flammability and physical design contribute to the fire hazard of a fence; this report demonstrates that incorporating complementary tests at different scales into a standard test method may provide a more complete assessment.

A code-adopted fence test method with established results interpretation and acceptance criteria will inform authorities having jurisdiction (AHJs) and the public about implementation options with fences and allow AHJs not only to assess the performance/hazard of composite fences but to compare and assess all combustible fencing options under identical conditions.

References

[1] Butler KM, Johnsson EL, Maranghides A, Nazare S, Fernandez M, Zarzecki M, Tang W, Auth E, McIntyre R, Pryor M, Saar W, and McLaughlin C (2022) Wind-Driven Fire Spread to a Structure from Fences and Mulch NIST Technical Note 2228. Gaithersburg, MD. https://doi.org/10.6028/NIST.TN.2228-upd1.

[2] Johnsson E, Butler K, Fernandez M, Zarzecki M, Tang W, Nazare S, Barrett D, Pryor M, and Maranghides A (2023) Wind-Driven Fire Spread to a Structure from Firewood Piles NIST Technical Note 2251. Gaithersburg, MD. https://doi.org/10.6028/NIST.TN.2251.

[3] Johnsson EL, Butler KM, Fernandez MG, Tang W, Nazare S, Deardorff P, Arana S, and Maranghides A (2024) Wind-Driven Fire Spread to a Structure from Landscape Timbers Technical Note 2307. Gaithersburg. https://doi.org/10.6028/NIST.TN.2307.

[4] Maranghides A, Link E, Hawks S, McDougald J, Quarles S, Gorham D, and Nazare S (2022) WUI Structure/Parcel/Community Fire Hazard Mitigation Methodology. (National Institute of Standards and Technology, Gaithersburg, MD) NIST Technical Note 2205. https://doi.org/0.6028/NIST.TN.2205.

[5] CAL FIRE (3 Apr 2025) Statistics; California Wildfires; Top 20 Most Destructive Wildfires. Available at https://www.fire.ca.gov/our-impact/statistics.

[6] Münchener Rückversicherungs-Gesellschaf, NatCatSERVICE (January 2019) Munich Re NatCatSERVICE, Natural catastrophes in 2018. Available at https://www.munichre.com/content/dam/munichre/contentlounge/website-pieces/documents/munichre-natural-catastrophes-in-2018.pdf.

[7] Maranghides A, Link E, Mell W, Hawks S, Wilson M, Brewer W, Brown C, Vihnaneck B, and Walton WD (2021) A Case Study of the Camp Fire - Fire Progression Timeline. (National Institute of Standards and Technology, Gaithersburg, MD) NIST Technical Note 2135. https://doi.org/10.6028/NIST.TN.2135.

[8] Maranghides A, Link ED, Mell W, Hawks S, Brown C, and Walton WD (2023) A Case Study of the Camp Fire - Notification, Evacuation, Traffic, and Temporary Refuge Areas (NETTRA). (National Institute of Standards and Technology, Gaithersburg, MD) NIST Technical Note 2252. https://doi.org/10.6028/NIST.TN.2252.

[9] Maranghides A, McNamara D, Mell W, Trook J, and Toman B (2013) A case study of a community affected by the Witch and Guejito Fires: Report #2 - Evaluating the effects of hazard mitigation actions on structure ignitions. (National Institute of Standards and Technology, Gaithersburg, MD) NIST Technical Note 1796. https://doi.org/10.6028/NIST.TN.1796.

[10] Maranghides A, McNamara D, Vihnanek R, Restaino J, and Leland C (2015) A case study of a community affected by the Waldo Fire - Event timeline and defensive actions. (National Institute of Standards and Technology, Gaithersburg, MD) NIST Technical Note 1910. https://doi.org/10.6028/NIST.TN.1910.

[11] Leonard J E, Blanchi R, White N, Bicknell A, Sargeant A, Reisen F, and Cheng M (2006) Research and investigation into the performance of residential boundary fencing systems

in bushfires. (CSIRO Manufacturing & Infrastructure Technology, Clayton South, Victoria, Australia).

[12] Grishin AM, Filkov AI, Loboda EL, Reyno VV, Kozlov AV, Kuznetsov VT, Kasymov DP, Andreyuk SM, Ivanov AI, and Stolyarchuk ND (2014) A field experiment on grass fire effects on wooden constructions and peat layer ignition. *International Journal of Wildland Fire* 23(2):445-449.

[13] Suzuki S, Johnsson E, Maranghides A, and Manzello SL (2016) Ignition of wood fencing assemblies exposed to continuous wind-driven firebrand showers. *Fire Technology* 52:1051-1067.

[14] Suzuki S and Manzello SL (2019) Understanding structure ignition vulnerabilities using mock-up sections of attached wood fencing assemblies. *Fire and Materials* TBA:1-10. https://doi.org/10.1002/fam.2716.

[15] Insurance Institute for Business & Home Safety (2020) IBHS Wildfire Fence Research. Available at https://vimeo.com/433770802. [Accessed on June 9, 2022.]

[16] Insurance Institute for Business & Home Safety and National Fire Protection Association (2017) Wildfire Research Fact Sheet: Fencing. Available at https://www.nfpa.org/-/media/Files/Firewise/Fact-sheets/FirewiseFactSheetsFencing.ashx. [Accessed on June 9, 2022.]

[17] Johnsson EL and Maranghides A (2016) Effects of wind speed and angle on fire spread along privacy fences. (National Institute of Standards and Technology, Gaithersburg, MD) NIST Technical Note 1894. https://doi.org/10.6028/NIST.TN.1894.

[18] Renner JS, Mensah RA, Jiang L, Xu Q, Das O, and Berto F (2021) Fire Behavior of Wood-Based Composite Materials. *Polymers* 13:4352-4384. https://doi.org/10.3390/polym13244352.

[19] Seefeldt H and Braun U (2011) Burning behaviour of wood-plastic composite decking boards in end-use conditions: The effects of geometry, material composition, and moisture. *Journal of Fire Sciences* 30(1):41-54.

[20] Mokhena TC, Sadiku ER, Mochane MJ, and Ray SS (2021) Mechanical properties of fire retardant wood-plastic composites: A review. *eXPRESS Polymer Letters* 15(8):744-780. https://doi.org/10.3144/expresspolymlett.2021.61.

[21] ASTM International (2023) ASTM E84 - 23d: Standard Test Method for Surface Burning Characteristics of Building Materials. West Conshohocken, PA. Available at https://compass.astm.org/document/?contentCode=ASTM%7CE0084-23D%7Cen-US.

[22] California Building Standards Commission (2024) Chapter 7A: Materials and Construction Methods for Exterior Wildfire Exposure (Cal. Code Regs., Title 24, Part 2). Available at https://codes.iccsafe.org/content/CABC2022P4#CABC2022P4_Ch07A_Sec706A.

[23] International Code Council (2024) International Wildland-Urban Interface Code (IWUIC). Available at https://codes.iccsafe.org/content/IWUIC2024V2.0.

[24] National Fire Protection Association (2022) NFPA 1140 Standard for Wildland Fire Protection. Available at https://www.nfpa.org/codes-and-standards/nfpa-1140-standarddevelopment/1140.

[25] Fabian T (January 2014) Fire Performance Properties of Solid Wood and Lignocellulose-Plastic Composite Deck Boards. *Fire Technology* 50. https://doi.org/10.1007/s10694-012-0307-4.

[26] Simpson WT (1998) Equilibrium moisture content of wood in outdoor locations in the United States and worldwide. Madison, WI.

[27] Glass SV and Zelinka SL (2010) Chapter 4: Moisture Relations and Physical Properties of Wood. *Wood Handbook, Wood as an Engineering Material, General Technical Report FPL-GTR-190* (U.S. Department of Agriculture, Forest Service, Forest Products Laboratory, Madison, WI), 4-1 to 4-19.

[28] McCaffrey BJ and Heskestad G (1976) A robust didirectional low-velocity probe for flame and fire application. *Combustion and Flame* 26:125-127.

[29] McGrattan KB, McDermott RJ, and Weinschenk CG (2013) Fire Dynamics Simulator Users Guide. (National Institute of Standards and Technology, Gaithersburg, MD) NIST Special Publication 1019, 6th ed. https://doi.org/10.6028/NIST.SP.1019.

[30] The MathWorks, Inc (2023) MATLAB: The Language of Technical Computing. Available at https://www.mathworks.com/help/matlab/.

[31] Diamantopoulos G, Salehi S, and Buechler J (2005) *Learning VirtualDub: The complete guide to capturing, processing, and encoding digital video* (Packt Publishing, Birmingham, UK).

[32] Lee A (2013) virtualdub.org: Proof that I had too much free time in college. Available at https://www.virtualdub.org/.

[33] shekh (2017) VirtualDub2; An enhanced version of the original VirtualDub. Available at http://virtualdub2.com/.

[34] AVS4YOU.com (2020) AVS Video Converter; Free Video Converter for Windows. Available at https://www.avs4you.com/avs-free-video-converter.aspx.

[35] Umezawa T (2023) Ut Video Codec Suite 23.1. Available at https://www.free-codecs.com/download/ut_video_codec_suite.htm.

[36] Graft D (2020) Smart Deinterlacer Filter. Available at http://rationalqm.us/smart/smart.html.

[37] Tsai K-C (2009) Orientation effect on cone calorimeter test results to assess fire hazard of materials. *Journal of Hazardous Materials* 172:763-772.

[38] Sanned E, Mensah RA, Forsth M, and Das O (2023) The curious case of the second/end peak in the heat release rate of wood: A cone calorimeter investigation. *Fire and Materials* 47:498-513.

[39] Lowden LA and Hull TR (2013) Flammability behaviour of wood and a review of the methods for its reduction. *Fire Science Reviews* 2:4.

[40] Babrauskas V and Parker WJ (1987) Ignitability measurements with the cone calorimeter. *Fire and Materials* 11(1):31-43.

[41] Janssens M and Ostman B (2022) Chapter 5: Reaction to fire performance. *Fire Safe Use of Wood in Buildings* (CRC Press), 153-192. https://doi.org/10.1201/9781003190318-5.

[42] Lyon RE (2004) Chapter 3: Plastics and Rubber. *Handbook of Builoding Materials for Fire Protection* (McGraw-Hill), 3.1 - 3.51. https://doi.org/10.1036/0071433309.

[43] Cheng L, Wu W, Meng W, Xu S, Han H, Yu Y, Qu H, and Xu J (2018) Application of metallic phytates to poly(vinyl chloride) as efficient biobased phosphorous flame retardants. *Journal of Applied Polymer Science* 135(33):46601-46610. https://doi.org/10.1002/app.46601.

[44] Maranghides, Alexander; Nazare, Shonali; Hedayati, Faraz; Gorham, Daniel; Link, Eric; Hoehler, Matthew; Bundy, Matthew; Monroy, Xareni; Morrison, Murray; Mell, William; Bova, Anthony; McNamara, Derek; Milac, Thomas; Hawks, S; Hawks, Steven; Bigelow, Frank; Raymer, Bob; Frievalt, Frank; Walton, William; (2022) Structure Separation Experiments: Shed Burns without Wind Technical Note 2235. Gaithersburg, MD. https://doi.org/10.6028/NIST.TN.2235a.

[45] Insurance Institute for Business and Home Safety (2025) Wildfire Prepared. Available at https://wildfireprepared.org/wp-content/uploads/WFPH-Technical-Standard.pdf.

[46] State of California (2020) AB-3074 Fire prevention: wildfire risk: defensible space: ember-resistant zones. Available at https://leginfo.legislature.ca.gov/faces/billNavClient.xhtml?bill_id=201920200AB3074.

[47] Taylor BN and Kuyatt CE (1994) Guidelines for evaluating and expressing the uncertainty of NIST measurement results. Gaithersburg, MD.

[48] Bryant RA (2009) A comparison of gas velocity measurements in a full-scale enclosure fire. *Fire Safety Journal* 44:793-800.

[49] Twilley WH and Babrauskas V (1988) User's guide for the Cone Calorimeter. Gaithersburg, MD.

[50] ASTM International (2023) E1354 - 23: Standard Test Method for Heat and Visible Smoke Release Rates for Materials and Products Using an Oxygen Comsumption Calorimeter. West Conshohocken, PA. Available at https://compass.astm.org/document/?contentCode=ASTM%7CE1354-23%7Cen-US.

[51] Enright PA and Fleischmann CM (1999) Uncertainty of heat release rate calculation of the ISO5660-1 cone calorimeter standard test method. *Fire Technology* 35(2):152-169.

[52] Lukosius A and Vekteris V (2003) Precision of heat release rate measurement results. *Measurement Science Review* 3(3):13-16.

[53] (2021) American Softwood Lumber Standard, Voluntary Product Standard PS 20-20, Revision 1. Gaithersburg, MD.

Appendix A. List of Symbols, Abbreviations, and Acronyms

AHJ
Authority Having Jurisdiction

BRI
Building Research Institute

EHOC
Effective heat of combustion (MJ/m^2)

FDS
Fire Dynamics Simulator

FO
Flame out time (s)

GUI
Graphic User Interface

HMM
Hazard Mitigation Methodology

HOA
Homeowners Association

HRR
Heat release rate (kW/m^2)

HWM or **HW**
Shredded hardwood mulch

IBHS
Insurance Institute for Business & Home Safety

NFPA
National Fire Protection Association

NIST
National Institute of Standards and Technology

PHRR
Peak heat release rate (kW/m^2)

PVC
Polyvinyl chloride, commonly referred to as vinyl

RH
Relative humidity

RSS
Root sum square

SPC
Steel-plastic composite

THR
Total heat release, obtained by integrating HRR over duration of flaming combustion (MJ/m^2)

TTI
Time to ignition (s)

WPC
Wood-plastic composite

WRC
Western redcedar

WUI
Wildland-urban interface

Appendix B. Uncertainties

Each measurement of wind speed, distance, time, or other variable discussed in this report is associated with an uncertainty. Uncertainties generally consist of several components that are grouped into two categories according to the method used to estimate their value [42]. Type A uncertainties are quantified by statistical methods, including the calculation of standard deviation, curve fitting using the method of least squares, or analysis of variance (ANOVA). Type B uncertainties are evaluated by other means, usually using scientific judgment based on all available relevant information. This may include previous measurement data, experience with relevant materials and instruments, manufacturer's specifications, or data from literature sources and handbooks.

For an output quantity Y that is not measured directly but is determined from N input quantities $X_1, X_2, \dots, X_N$ through a functional relation f:

$$Y = f(X_1, X_2, \dots, X_N)\ , \tag{B-1}$$

the estimate y of the output quantity is given by applying the same function to estimates $x_1, x, \dots, x_N$ of the input quantities:

$$y = f(x_1, x_2, \dots, x_N)\ . \tag{B-2}$$

For Type A evaluation of uncertainties, in which n repeated independent observations are made under the same conditions, the input quantity x_i can be estimated by the sample mean,

$$x_i = \bar{X}_i = \frac{1}{n}\sum_{k=1}^{n} X_{i,k} \tag{B-3}$$

and the standard uncertainty $u(x_i)$ associated with x_i is the estimated standard deviation of the mean,

$$u(x_i) = s(\bar{X}_i) = \left(\frac{1}{n(n-1)}\sum_{k=1}^{n}\left(X_{i,k} - \bar{X}_i\right)^2\right)^{1/2} \tag{B-4}$$

This is equivalent to the estimated standard deviation of the input quantity s_i divided by the square root of the size of the sample:

$$s(\bar{X}_i) = \frac{s_i}{\sqrt{n}} \tag{B-5}$$

For Type B evaluations, estimates of the input quantity x_i and standard uncertainty $u(x_i)$ depend on the assumed form of the probability distribution and the range of values. If the quantity is modeled by a normal distribution with essentially all (approximately 99.73 %) of its values contained within a lower limit a_- and an upper limit a_+, and with a mean value

$$x_i = \frac{(a_+ + a_-)}{2} \tag{B-6}$$

then the standard uncertainty is given by

$$u(x_i) = \frac{a}{3} \tag{B-7}$$

where $a = (a_+ - a_-)/2$. In this case, a is equivalent to the 3σ value.

Another alternative is to assume a rectangular probability distribution., with a lower limit a_- and upper limit a_+ and a value that is equally probable to lie anywhere within the interval. In this case, the input quantity can be estimated by Equation (A-6) and the standard uncertainty is

$$u(x_i) = \frac{a}{\sqrt{3}} \tag{B-8}$$

The combined standard uncertainty of the measurement result y, representing its estimated standard deviation, is the positive square root of the variance obtained from the law of propagation of uncertainty:

$$u_c^2(y) = \sum_{i=1}^{N} \left(\frac{\partial f}{\partial x_i}\right)^2 u^2(x_i) + 2\sum_{i=1}^{N-1}\sum_{j=i+1}^{N} \frac{\partial f}{\partial x_i}\frac{\partial f}{\partial x_j} u(x_i, x_j) \tag{B-9}$$

where $u(x_i)$ is the standard uncertainty associated with the estimate of input quantity x_i and $u(x_i, x_j)$ is the estimated covariance associated with x_i and x_j. When the input quantities are uncorrelated, the equation reduces to the RSS (root sum square) method of combining uncertainties,

$$u_c(y) = \sqrt{\sum_{i=1}^{N} [c_i u(x_i)]^2} \tag{B-10}$$

where $c_i = \partial f / \partial x_i$.

Finally, an expanded uncertainty U is determined by multiplying the combined standard uncertainty u_c by a coverage factor k,

$$U = k u_c \, . \tag{B-11}$$

This provides an interval $y - U$ to $y + U$ within which the value of Y can be asserted to lie with a high level of confidence. A coverage factor of $k = 2$ defines a level of confidence of approximately 95 %.

Relative standard uncertainty $u_r(x_i)$, relative combined standard uncertainty $u_{c,r}(y)$, and relative expanded uncertainty U_r are calculated by dividing the uncertainty measure by the absolute value of the associated quantity, as in:

$$u_r(x_i) = \frac{u(x_i)}{|x_i|} \qquad u_{c,r}(y) = \frac{u_c(y)}{|y|} \qquad U_r = \frac{U}{|y|}$$

Equation (B-10) can be written in terms of relative standard uncertainties as

$$\frac{u_c(y)}{y} = \sqrt{\sum_{i=1}^{N} s_i^2 \left(\frac{u(x_i)}{x_i}\right)^2} \tag{B-12}$$

where s_i is the nondimensional sensitivity coefficient for input quantity x_i,

$$s_i = \frac{\partial y}{\partial x_i}\frac{x_i}{y} \tag{B-13}$$

This appendix does not address the matter of reproducibility of the measurement results in this study; that is, the closeness of the agreement of measurements under different conditions. All experiments in this study of composite fences were unique.

The uncertainties examined in this section are associated with four categories of variables. Section B.1 looks at the uncertainties for the experimental setup, including dimensions of test objects, setup distances, and material preparation. Section B.2 discusses the Type A uncertainties in the wind data measured by bidirectional probes and the Type B uncertainties for ambient measurements. Section B.3 looks at the uncertainties inherent in assessing the timing of events, and Section B.4 considers the uncertainties in the flame spread analysis.

B.1. Experimental Setup

Setting up the experiments included preparing the materials for testing, assembling the mulch beds and fences, and arranging the test setup. The setup and procedures were described in Section 2 of this report. The uncertainties associated with the experimental setup are Type B, either estimated through scientific judgment or obtained from source literature.

The uncertainties for fence panel and mulch pan dimensions and the locations relative to the shed and centerline of mulch pan, bidirectional probe array, and wind machine are presented in Table B.1. All uncertainties listed in this table are Type B, determined by scientific judgment.

In addition to the uncertainties due to the dimensions of the mold, molded parts are subject to shrinkage and warpage during cooling. Definitive information was not available on the dimensional uncertainties of the components of the composite fence panels; in its absence, an estimated value of ±1 mm is assumed for the standard uncertainty. Variations during assembly are estimated as ±3 mm along the length and ±2 mm in height for the assembled fence panel.

The mulch pan is described in Section 2.4.1 and the target mulch bed at the base of the shed is described in Section 2.4.4. The mulch pans were 87.6 cm (34.5 in) wide with 2.5 cm (1 in) high side walls, and two pans were overlapped and clamped for a total length of 3.35 m (11 ft). The expanded uncertainties for both pan width and length are estimated as ±1 cm. The target mulch pans along the shed were 46 cm (18 in) wide and 1.37 m (4.5 ft) long, with two pans overlapped to give a total length matching the shed wall dimension at 2.44 m (8 ft) long. The target mulch bed was not confined by a lip on the outside edge facing the fence, which allowed firebrands to land on the target mulch without needing to clear a height. The width of the target mulch bed thus varied over its length, by an expanded uncertainty of ±2.0 cm.

The mulch to be ignited was prepared by spreading it over the mulch pans and compressing it by foot to a depth of 5 cm, double the height of the walls of the mulch pan, as discussed in Sections 2.4.1 and 2.9.2. The mulch was tapered at the edges of the pan to a depth of 2.5 cm. For cases with a fence, the depth was designed to cover the gap between the pan top surface and the bottom of the fence, which was set (with a pair of measured shims) at 5 cm. The mulch bed thickness varied over its surface due to the nature of the mulch as overlapping particles whose individual thicknesses are an appreciable fraction of the thickness of the mulch layer. The mulch bed thickness also depended on the evenness of the spreading over the mulch bed and the uniformity of the compaction. The expanded uncertainty of the mulch bed depth was ±1 cm. The same uncertainty was estimated for the depth of the mulch at half thickness and for the target mulch bed, both of which were compressed at a nominal height of 2.5 cm.

After the shed and wind machine were placed into position, a tape measure extending longer than the nominal distance of 10.7 m (35 ft) was used to adjust the equipment to the desired position. This procedure was estimated to result in an expanded uncertainty (95 % confidence level) of ±3 cm. In the transverse direction, the center of the fan hub was within ±1 cm of the centerline of the experiment.

The separation distance, from the shed to the mulch pan, was measured by tape measure for each experiment. The expanded uncertainty for a confidence level of 95 % was estimated as ±1 cm.

The bidirectional probe array was placed 4 ft from the end of the fence. The expanded uncertainty was estimated for the distance of the array from the shed as ±2 cm and for the distance of the centerline probes to the actual centerline as ±1 cm. There was an additional uncertainty for the position of each probe within the array, which was estimated as ±1 cm in the vertical direction and ±0.5 cm perpendicular to the plane of the probe array.

Table B.1. Uncertainty in dimensions for experimental setup

Measurement	Component Standard Uncertainty u_i	Combined Standard Uncertainty u_c	Expanded Uncertainty $2u_c$
Fence panel length (1.96 m to 2.31 m)		3.2 mm	6.4 mm
Components	1 mm		
Assembly	3 mm		
Fence height (1.74 m to 1.83 m)		2.2 mm	4.4 mm
Components	1 mm		
Assembly	2 mm		
Mulch bed width (0.88 m)	5 mm	5 mm	10 mm
Mulch bed length (3.35 m)	5 mm	5 mm	10 mm
Target mulch bed width (0.46 m)	10 mm	10 mm	20 mm
Mulch thickness (50 mm or 25 mm)	5 mm	5 mm	10 mm
Wind machine to shed (10.67 m)	15 mm	15 mm	30 mm
Wind machine to centerline	5 mm	5 mm	10 mm
Mulch pan to shed:			
Separation distance (1.83 m)	5 mm	5 mm	10 mm
Bidirectional probe array to shed	10 mm	10 mm	20 mm
Bidirectional probe array to centerline	5 mm	5 mm	10 mm
Probe position, x (toward shed)		10.3 mm	20.6 mm
Probe array	10 mm		
Position within array	2.5 mm		
Probe position, y (toward center)			
Probe array	5 mm	5 mm	10 mm
Probe position, z (vertical)			
Position within array	5 mm	5 mm	10 mm

B.2. Wind and Ambient Data

Wind speed uncertainties involve the bidirectional probe design and the measurement statistics from the wind field. Bidirectional probes are simple tubular devices that calculate velocities from the pressure differential between front and back openings. They are similar to pitot static tubes, with added advantages of robustness in a fire environment and insensitivity to flow angle. Velocity is calculated using the equation:

$$V = \frac{1}{C}\sqrt{\frac{2R_u}{P_s M_{air}}\Delta P\, T} \tag{A-14}$$

where C is the probe constant, R_u is the universal gas constant, P_s is standard atmospheric pressure, M_{air} is the molecular mass of dry air, ΔP is dynamic pressure, and T is absolute temperature.

McCaffrey and Heskestad [25] measured the probe constant for the bidirectional probe as C = 1.08 for Reynolds numbers greater than 1000. A study of the angular sensitivity showed the value remaining within ±10 % for flow directions within 50° of the probe axis. For flows generally parallel to the probe axis and a probe Reynolds number above 500, a relative standard uncertainty of 0.07 can be used for the probe constant [43]. For the fence and mulch study, the Reynolds number was above this limit for all wind velocities.

The dynamic pressure in Equation (A-14) was the difference in pressure between windward and leeward sides of the bidirectional probe. As described in Section 2.7.1, the probe signals were converted to a pressure differential through transducers, which the manufacturer rated with an accuracy of 1 %. Because the probe array was located upwind of the fire and not exposed to its heat, the ambient temperature measurement was used to calculate velocity. The standard limit of error for the Type K thermocouples used in this study was 0.75 % or 2.2 °C, whichever is greater.

Table B.2 lists the relative standard uncertainty for each variable and uses Equation (B-12) to determine the contribution of each variable to the relative standard uncertainty of the wind speed calculated from the bidirectional probe $u_{r,BP} = 0.0703$. This Type B uncertainty of the calculated wind speed from the probe could then be combined with the Type A evaluation of the uncertainty of unsteady wind speed measurements (the standard error of the mean) to determine a total uncertainty of the mean wind speed for each probe.

In Appendix C.2 of [1], the Type A relative standard uncertainty for weighted mean wind speeds over each probe was found to have a maximum value of 0.0067. Since this was an order of magnitude smaller, than the type B uncertainty of 0.0703, the Type B uncertainty was found to dominate the total uncertainty in the bidirectional probe measurement.

Table B.2. Uncertainty budget for point velocity measurements

Measurement Component	Value x_i	Relative standard uncertainty $u_{r,i} = u(x_i)/x_i$	Nondimensional sensitivity coefficient s_i	Percent contribution, %
Probe constant, C	1.08	0.07	-1.0	99.2 %
Probe differential pressure, ΔP (Pa)	56	0.01	0.5	0.5 %
Ambient temperature, T (K)	293	0.0075 (not less than 2.2 °C)	0.5	0.3 %
Standard atmospheric pressure, P_s (Pa)	101325	0.0003	-0.5	0 %
Molecular weight of dry air, M_{air} (kg/kmol)	28.97	0.0001	-0.5	0 %
Velocity, V	8.93	0.0703 [a] (0.1406 [b])		

[a] Total relative standard uncertainty

[b] Total relative expanded uncertainty (coverage factor $k = 2$ for a confidence level of about 95 %)

Uncertainties inherent to the temperature and ambient wind measurements are listed in Table B.3. These are Type B uncertainties that were obtained from the manufacturer.

As previously mentioned in this section, the standard limit of error for temperature measurements using Type K thermocouples was 0.75 % or 2.2 °C, whichever is greater.

As stated by the manufacturer, wind speed was measured with ± 2 % ± 0.1 m/s accuracy and wind direction was measured with ± 2° accuracy. However, as previously stated in Section 2.7.2, the wind direction accuracy was degraded to about ± 5° due to the estimation of true north during installation and slight positional drift due to high winds, which was periodically corrected.

To complete the calculation of uncertainty for each ambient measurement, the Type B uncertainties in Table B.3 were combined with Type A statistical measurements using the RSS method in Equation B-10 or Equation B-12 before calculating the expanded uncertainty.

Table B.3. Type B uncertainties for ambient measurements

Measurement	Relative Standard Uncertainty $u_{r,i} = u(x_i)/x_i$	Standard Uncertainty u_j
Temperature – Type K thermocouple	0.0075 (not less than 2.2 °C)	
Ambient Wind Speed – Anemometer	± 0.02	± 0.1 m/s
Ambient Wind Direction – Anemometer		± 5°

B.3. Timing Data

A common system of timing was required in order to synchronize multiple videos recorded during each experiment and relate the experiments to each other. As explained in Section 3.1.1, five events that could be easily identified in the test videos were selected: End of Gas Burner Ignition, Start to Remove Gas Igniters, Fan On, Fan Off, and Water First Applied. Time t = 0 for each experiment was defined as the Fan On event, when the engine of the wind machine engaged after turning over, and the end of the experiment was defined as Fan Off, when the engine was turned off and the audio signal (including the sound pitch and amplitude) started to change.

In addition to the above key events, three times were identified to evaluate how fast spot fires occurred in the target mulch bed and how quickly they threatened the structure. The first was the time at which the first spot fire ignited. Even if this spot fire did not reach the shed wall, it could threaten other combustible objects, such as vegetation, near the structure. The second event was ignition of the first spot fire to result in flames against the wall, and the third was the first time at which flames were observed on the wall.

The estimations of uncertainties for these timing events, which were all Type B (determined by scientific judgment), were described in Appendix A.3 of [1]. Table B.4 summarizes these uncertainty values.

Table B.4. Uncertainty in timing data

Measurement	Component Standard Uncertainty u_j	Combined Standard Uncertainty u_c	Expanded Uncertainty $2u_c$
End of Gas Burner Ignition (s)	1.0	1.0	2.0
Start to Remove Gas Igniters (s)	0.5	0.5	1.0
Fan On (s)	0.5	0.5	1.0
Fan Off (s)	1.0	1.0	2.0
Water First Applied (s)	1.0	1.0	2.0
Test duration (s)		1.1	2.2
Fan on	0.5		
Fan off	1		
Time to spotting (s)		10	20
Fan on	0.5		
Smoke detected	10		
Time to flames on wall (s)		3.0	6.1
Fan on	0.5		
Flame detected	3		

B.4. Fence Flame Spread Analysis

The measurement of the flame front location, described in Section 3.1.3, was subject to uncertainty from multiple sources. These included the physical uncertainties of the experimental setup as described in Appendix B.1, the process of determining the perspective lines, the uncertainty in setting the physical scale, and the determination of the leading edge of the flame front. Uncertainties in timing, covered in Appendix B.3, also contributed to the uncertainty of the plotting of flame front location as a function of time, but the contribution was small relative to the uncertainties in the location of the flame front.

Sources of uncertainty were Type B, with standard uncertainty based on scientific judgment. An estimate of the component standard uncertainty is given for each source.

For fence experiments, the location of the flame front was expressed in two dimensions extending over the surface of the fence and including the posts at both ends. Section 3.1.3 describes the analysis of video images to track the progress of the flame front over time. The horizontal location of the flame front was considered to be the furthest point the fire damage had reached downwind, and the vertical location was the highest point reached by the fire damage. The height of the damage was measured both in the ignition region and in the area downwind from ignition. In addition to flame front location as a function of time, 2-D profiles of the damaged region were captured at specific times.

Sources of uncertainty in defining the boundaries of the char front in horizontal and vertical directions included the dimensions and setup of the fence, the selection of points identifying fence corners, and the ability to locate the flame front visually.

Uncertainties for the lengths and heights of the composite fences were estimated in Appendix B.1. The maximum standard uncertainty values for these measures are repeated in Table B.5.

Identification of the corners of the fence in the video images was subject to some imprecision. For the two lower corners, the mulch may obscure the exact location, introducing an uncertainty estimated as ±5 mm in both directions. For the upper corners, the height of the post sometimes differed slightly from that of the fence panel, introducing an uncertainty of ±3 mm in the vertical direction. The uncertainty of the position of each upper point in the horizontal direction was also estimated as ±3 mm. Combining these values separately in vertical and horizontal directions resulted in a standard uncertainty of ±8 mm for this factor.

The selection of each point using the mouse was dependent on the accuracy of the pointer and the patience and care of the analyst. An uncertainty of ±2 cm was included for this factor.

Camera lens distortions were neglected in the assessment of uncertainty.

The visual determination of the fire damage boundary provided some challenges. Dark spots in the boards and shadows sometimes masked the location of the char front, as did the presence of flames and smoke. The char front was not sharp – the color changed from light to dark over a distance of a few millimeters. Error was also introduced when selecting points on the rough surfaces of the composite panel because they were not all in the same plane. This source of uncertainty was estimated as ±1 cm.

The combined standard uncertainty for the flame front location for fence experiments, calculated as the square root of the sum of squares from all of these sources, was 2.4 cm in both horizontal and vertical directions, as listed in Table B.5. Fence experiments: Uncertainty in flame spread analysis. The expanded uncertainty with coverage factor $k = 2$, for a confidence level of 95 %, was ±4.8 cm (±1.9 in).

Table B.5. Fence experiments: Uncertainty in flame spread analysis

Measurement	Component Standard Uncertainty u_j	Combined Standard Uncertainty u_c	Expanded Uncertainty $2u_c$
Horizontal flame front		24 mm	48 mm
Fence length (from App. B.1)	3.2 mm		
Four corner points	8 mm		
Point selection	20 mm		
Visual char boundary	10 mm		
Vertical flame front		24 mm	48 mm
Fence height (from App. B.1)	2.2 mm		
Four corner points	8 mm		
Point selection	20 mm		
Visual char boundary	10 mm		
Timing		0.5 s	1.0 s
Fan On (from App. B.3)	0.5 s		

In the experiments with intense flames, smoke sometimes emerged from under the fence ahead of the char, making it difficult to decide on the flame front location. Fortunately, the fire spread in these experiments was rapid, making the precision of each point less important.

Appendix C. Cone Calorimeter Testing

Flammability measurements to compare composite fence materials were obtained using the cone calorimeter [44] in both horizontal and vertical configurations. Samples cut from the two wood-plastic (WPC1 and WPC2) and steel-plastic (SPC) composite fences were tested. The first purpose of this study was to improve our understanding of the differences in fire behavior among the three composite fence types, by separating material properties from fence design. The second purpose was to compare the validity of horizontal and vertical cone tests for assessing the flammability of fences.

In Appendix B of the previous fence report [1], cone calorimeter results were reported in a horizontal configuration for rigid polyvinyl chloride (PVC), western redcedar (WRC) wood, and wood-plastic composite #1 (WPC1) fence samples. These results are repeated in this report for comparison.

Cone calorimeter measurements were performed using a Dual Cone Calorimeter from Fire Testing Technology Ltd. The flammability performance of all fence materials was tested using standard cone calorimetry protocols as described in the ASTM E1354 standard [45], with an incident heat flux of either 50 kW/m² or 35 kW/m². According to ASTM E1354, the normal specimen testing orientation is horizontal, regardless of whether the end-use orientation is horizontal or vertical. However, the apparatus can be configured for vertical use for exploratory or diagnostic studies. Since fences are inherently vertical, composite fence samples were tested in both horizontal and vertical orientations to see whether and in what way the results differ.

The cone calorimeter test results reported here include ignitability, heat release rate, and mass loss of samples. The study did not include measures of smoke toxicity.

This appendix contains data and plots from each of the 42 cone calorimeter tests performed on fence materials. See Section 5 for comparisons of test results from the perspective of the fence experiments, including how material properties relate to fence experiment results and the difference between vertical and horizontal cone calorimeter configurations.

C.1. Test Samples

Specimens with nominal dimensions of 100 mm × 100 mm were cut from PVC, WRC, WPC1, WPC2, and SPC fence panels. Cross-sectional and top views of all specimens are shown in Fig. C.1. The PVC samples in Fig. C.1 (a) consisted of two sheets 1.23 mm (0.048 in) thick separated by a gap of 18 mm that was supported by three 1.23 mm thick braces. The WRC and WPC1 samples in (b) and (c) were solid, with nominal thicknesses of 20 mm and 6 mm respectively. The construction of the WPC2 samples in (d) was similar to that of the PVC samples, with two flat faces connected evenly by braces. Both the outer board faces and internal connections for these samples were 5 mm thick, and the hollow space between the faces was 1 cm thick, resulting in a total board thickness of 20 mm. The SPC samples in (e) were solid but ranged in thickness from 1.5 mm to 5 mm due to the peaks and valleys of the simulated wood grain on the outer surface. The average thickness of these samples was about 3 mm.

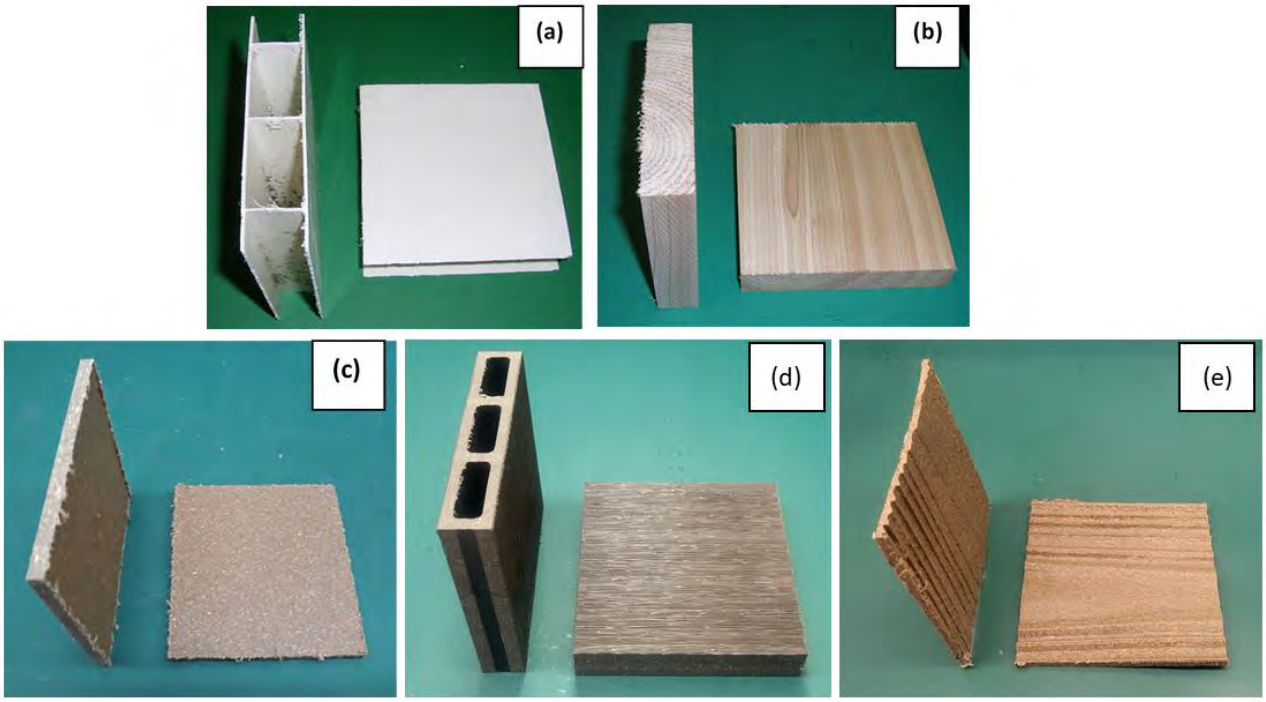

Fig. C.1. Specimens from a) PVC, b) WRC, c) WPC1, d) WPC2, and e) SPC fence boards showing cross-sectional and top views.

Nominal masses for PVC, WRC, WPC1, WPC2, and SPC samples were 44.4 g ± 0.2 g, 66.7 g ± 2.0 g, 60.0 g ± 1.0 g, 139.8 g ± 0.9 g, and 30.9 g ± 2.0 g, respectively. Uncertainties given for each material are Type A, with a level of confidence of approximately 95 %. Mass data can be found in the summary tables for each material in Appendix C.4.

Although PVC, WRC, and WPC2 cone samples were approximately the same total thickness, the geometry was very different. The PVC samples can be characterized as hollow structures with thin elements separated by large gaps and braces, as seen in Fig. C.1 (a). A similar hollow geometry with thicker elements is seen for WPC2 samples in Fig. C.1 (d). A study of wood-plastic composite decking boards [20] showed that the geometry of the sample specimen (solid or hollow) has a strong effect on combustion behavior; hollow-shaped geometries remove combustible material and reduce the fire load, but they also increase fire propagation through thermal feedback within the cavities.

Cone calorimeter samples from PVC, WRC, and WPC2 fences were also alike in that they were cut through the full thickness of the fence. Unlike these three samples, those from WPC1 and SPC fences, shown in Fig. C.1 (c) and (e), respectively, were not fully representative of the fences from which they were taken. The selection of cone calorimeter samples from each of the three composite fences is illustrated in Fig. C.2. End views of a) WPC1 and b) WPC2 fences and c) cross-section of SPC fence with 10 cm widths of cone calorimeter samples superimposed. The full WPC1 fences were constructed with 19 interlinking vertical boards, with alternating boards facing opposite directions. The end view of one board is shown in Fig. C.2. End views of a) WPC1 and b) WPC2 fences and c) cross-section of SPC fence with 10 cm widths of cone calorimeter samples superimposed. As indicated in the image, the 10 cm square cone calorimeter samples

were cut from the area of uniform thickness between the parts of the molded board that overlap the adjacent board. For WPC2 fences, cone calorimeter samples were cut through the full thickness of a WPC2 board, as shown in Fig. C.2 (b). The hollow structure of the board design was therefore retained. A photo of the bottom part of an SPC fence panel cut just above the base in Fig. C.2 (c) shows the cross-section of the SPC panel molded to mimic the vertical boards of a wood privacy fence on both sides. As outlined in the image, the cone calorimeter samples from the SPC fence were cut from areas of uniform thickness between molded details that are further explained below.

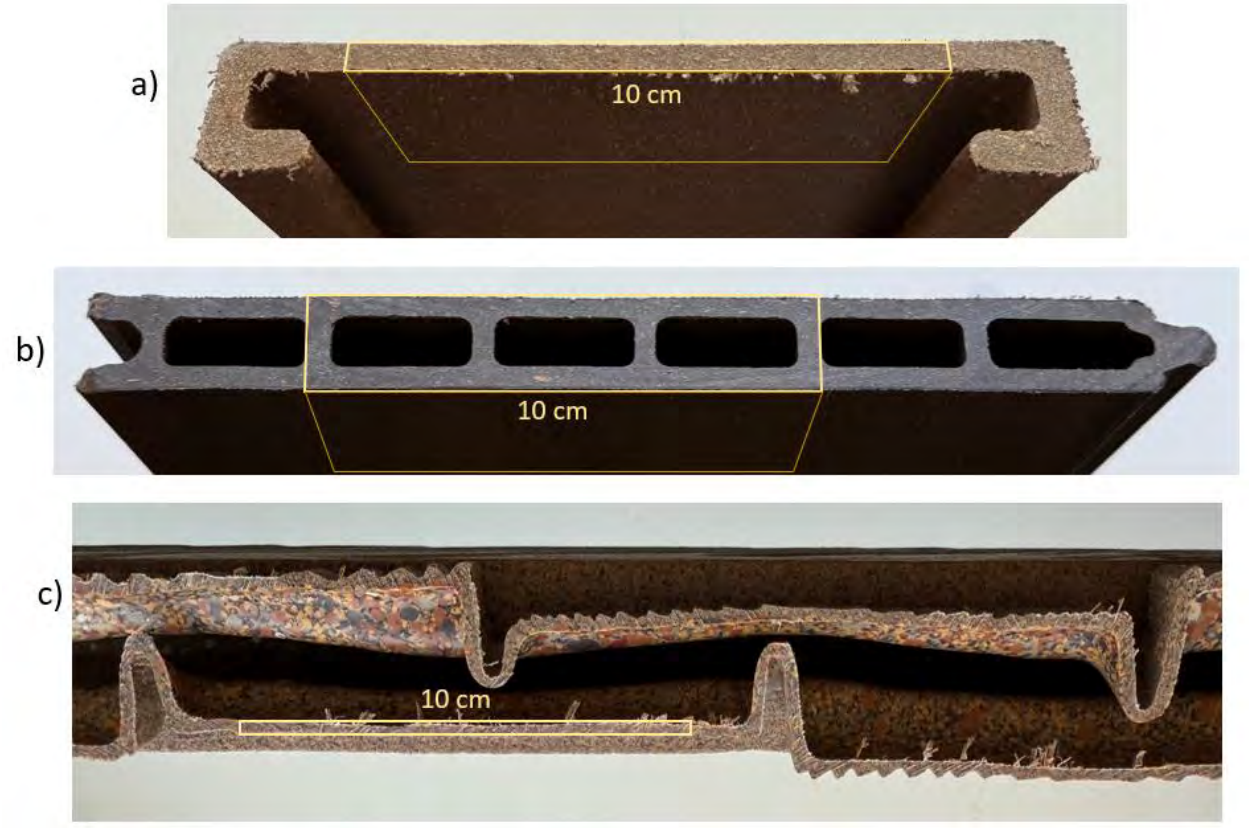

Fig. C.2. End views of a) WPC1 and b) WPC2 fences and c) cross-section of SPC fence with 10 cm widths of cone calorimeter samples superimposed.

A wider view of the molded SPC fence panel is shown in Fig. C.3. The SPC fence panels were molded as a single piece to give the appearance of wooden boards on both sides. This was accomplished by offsetting the vertical board divisions on one face with the vertical divisions on the other face, as shown by the cross-section in Fig. C.3 (b). On a large scale, therefore, the boards for SPC fences are hollow. The thickness of the entire SPC fence panel averaged about 47 mm, with a 40 mm wide hollow space between faces. As depicted in Fig. C.2 (c), the SPC cone samples shown in Fig. C.1 (e) were cut from a single face. As a caution, then, the flammability properties of the solid SPC samples may not be fully representative of the fire behavior of the SPC fences.

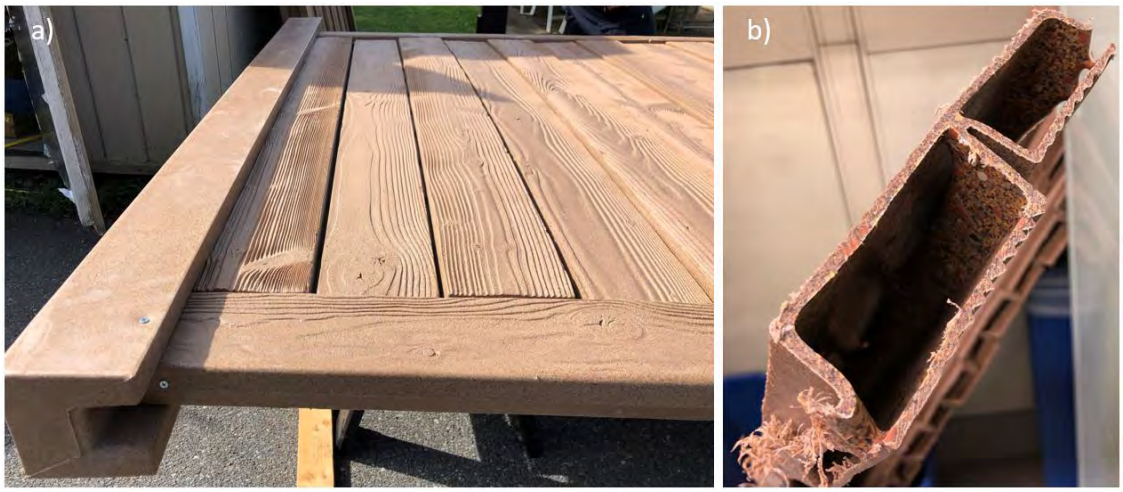

Fig. C.3. Structure of steel-plastic composite (SPC) fence: a) view of the molded panel and b) cross-section showing molding of front and back board faces.

C.2. Experimental Procedure

The protocols described in ASTM E1354 [45] were followed in operating the equipment and analyzing the results. Preparation of the fence samples for cone calorimeter testing started with placing the samples in an aluminum foil pan with nominal thickness of 0.035 mm ± 0.01 mm (specified by ASTM E1474), as shown in Fig. C.4. The fence samples in this figure can be compared with the corresponding samples in Fig. C.1.

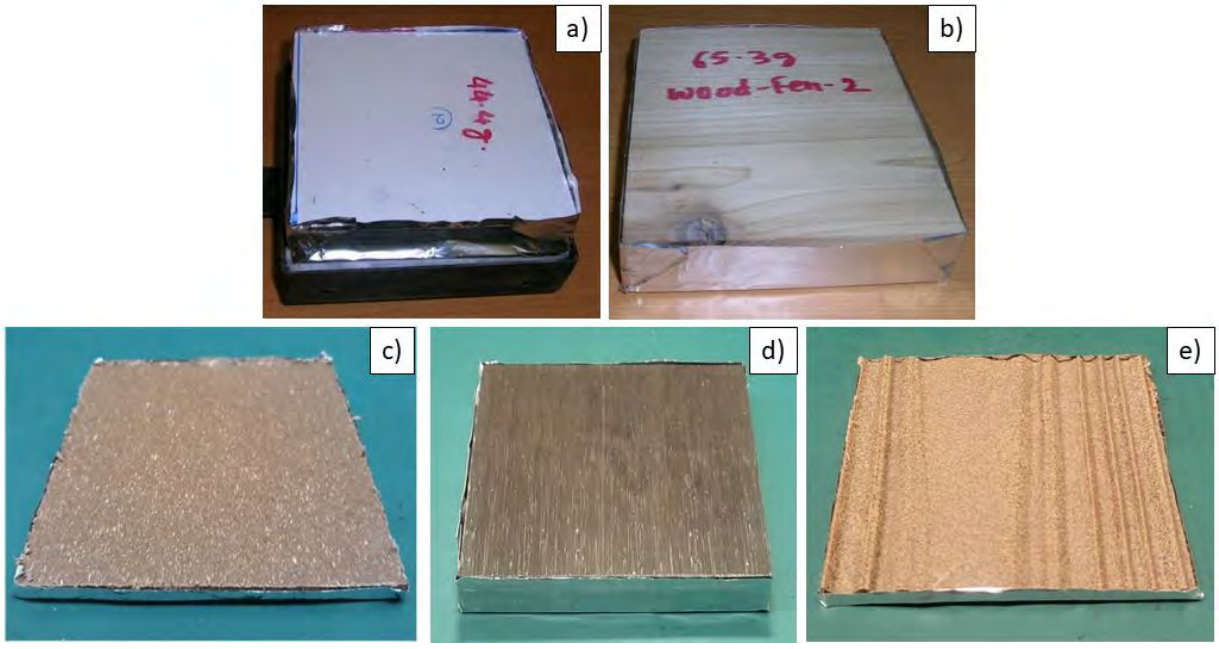

Fig. C.4. Preparing fence material samples of a) PVC, b) WRC, c) WPC1, d) WPC2, and e) SPC for cone calorimeter testing by placing them in an aluminum foil pan.

The full assembly for fence samples for the cone calorimeter is shown in Fig. C.5. Components for a horizontal cone test, shown in (a), include the fence sample with a sheet of aluminum foil, Kaowool blankets to hold the sample against the holder surface, and top and bottom pieces of the sample holder. The fence sample was wrapped with the aluminum foil on all sides but one, as in Fig. C.4, and placed on top of the bottom holder piece containing a sufficient number of Kaowool blankets to hold the sample tightly against the top surface of the holder after assembly. The top holder was then placed over the bottom and attached to create the assembly in Fig. C.5 (b), ready for use in the horizontal configuration as shown in Fig. C.6 (a).

The sample assembly for the vertical configuration includes the same components placed in a different holder. The front view of the assembly is shown in Fig. C.5 (c), and the rear view in (d) shows prongs holding the Kaowool blankets in place. The installed assembly is visible in the vertical cone calorimeter setup of Fig. C.6 (b).

In all tests, the holder included a retainer frame to hold the fence sample in place.

For fence samples with a tendency to melt and drip, aluminum drip pans were positioned below the sample in both horizontal and vertical configurations to catch drips and make cleanup easier, as seen in Fig. C.6.

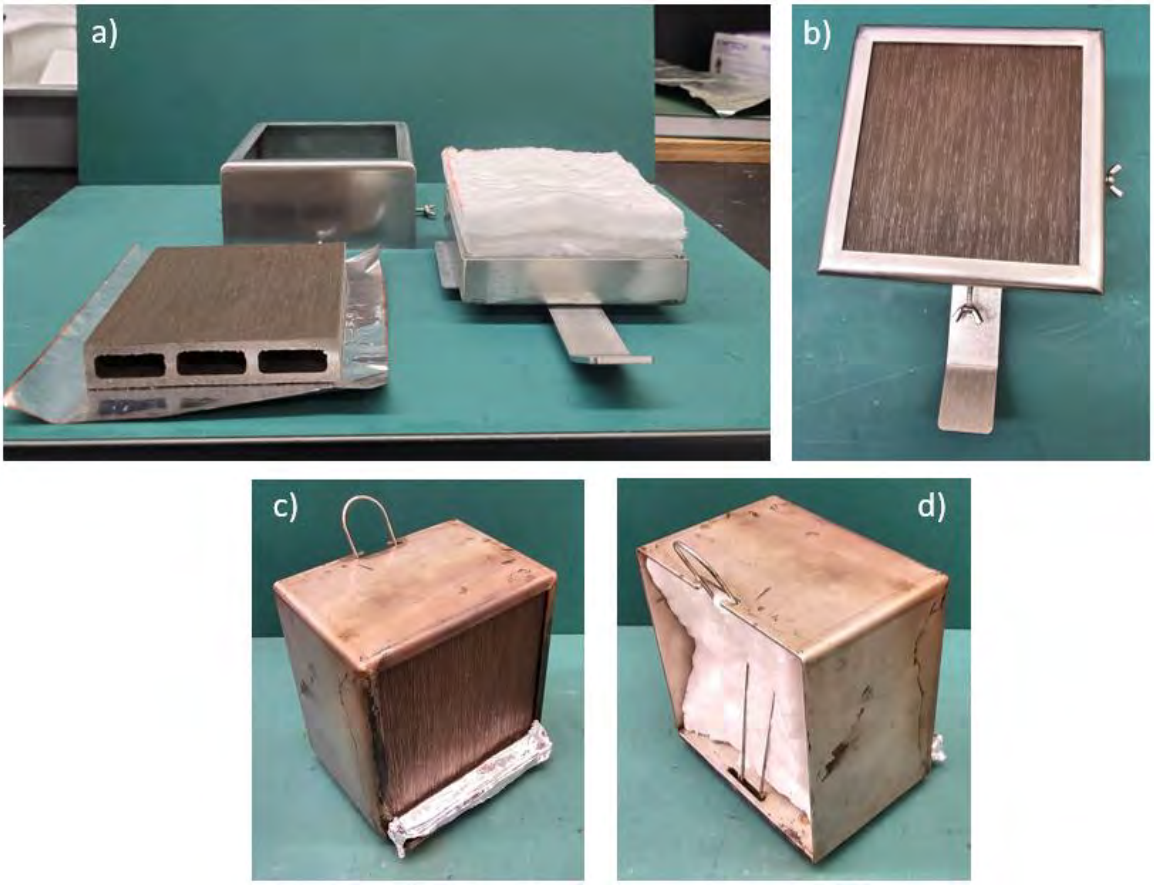

Fig. C.5. Assembly for cone calorimeter tests: a) components to be assembled, b) completed assembly for horizontal test, c) sample side for vertical test, and c) back side for vertical test.

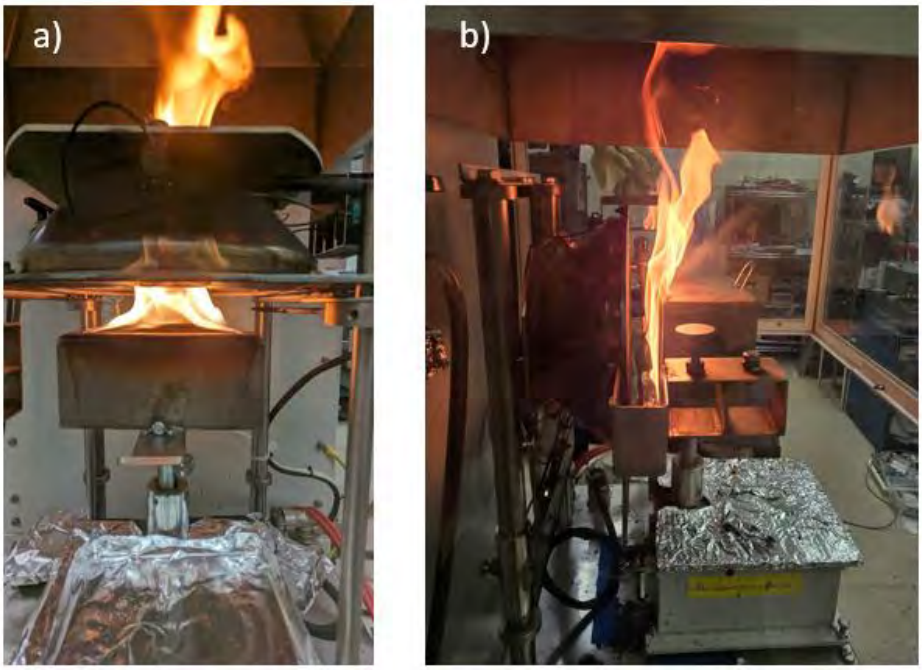

Fig. C.6. Sample burning in cone calorimeter in a) horizontal and b) vertical configurations.

In the horizontal configuration, the sample surface was placed at a distance of 25 mm from the cone heater base. In the vertical configuration, the distance between sample holder and cone was 28 mm. A spark igniter was used to ignite pyrolysis gases generated by heating the sample. During tests, digital still images were taken from various locations to provide additional visual characterization of test samples.

C.3. Test Matrix

A total of 42 cone calorimeter tests were performed on five fence materials tested at NIST. Table C.1 provides a list of the number of tests performed for each material under each of the four test conditions: horizontal or vertical configuration at an incident heat flux of either 50 kW/m^2 or 35 kW/m^2.

Table C.1. Number of cone calorimeter tests performed for each fence material type, by configuration (horizontal and vertical) and incident heat flux (50 kW/m^2 and 35 kW/m^2).

Fence Material	Horizontal, 50 kW/m^2	Vertical, 50 kW/m^2	Horizontal, 35 kW/m^2	Vertical, 35 kW/m^2
PVC	3	1	0	0
WRC	3	0	0	0
WPC1	3 + ***1****	3 + ***1****	3 + ***1****	***1****
WPC2	3 + ***1****	3 + ***1****	***1****	***1****
SPC	***3****	***3****	***3****	***3****

*Tests performed in 2024.

Cone tests for the fence study were carried out over multiple years. Horizontal tests on PVC and WRC fence samples were performed in 2019; horizontal tests on WPC1 and WPC2 were performed in 2020; and vertical tests on PVC, WPC1, and WPC2 were performed in 2021. All cone tests on SPC fence samples (three tests under each of the four test conditions) were performed in 2024, along with a single cone test under each condition for WPC1 and WPC2 to compare with previous tests. The tests performed in 2024 were carried out under somewhat different conditions than the earlier tests. Some differences were observed in the test results, which will be discussed for each of the fence materials in the following section.

For the cone calorimeter tests performed in 2019, 2020, and 2021, samples were conditioned for 48 hours in the laboratory, with nominal temperatures of 20 °C and variable relative humidity not exceeding 50 %. The samples were allowed to come to equilibrium under laboratory conditions. For the cone tests performed in 2024, samples were conditioned for one week at room temperature and 55 % ± 2 % relative humidity.

C.4. Test Results

This section presents cone calorimetry data for PVC, WRC, WPC1, WPC2, and SPC fence materials. Results are presented separately for each fence material and include photos, heat release rate plots, and summary tables of results. All data were calculated using the same methodology. Some of these cone tests were previously discussed in the comprehensive fence report published in 2022 [1].

The plots and tables are organized by test condition, namely orientation (horizontal or vertical) and incidental heat flux (50 kW/m^2 or 35 kW/m^2). The number of tests performed for each material under each of the four test conditions were listed in Table C.1. Tests are numbered sequentially according to date and time; comparison tests performed in 2024 for WPC1 and WPC2 appear last under each test condition.

Heat release rate (HRR), the rate at which heat is released in a burning material, is a fitting way to characterize its fire hazard. The cone calorimeter enables measurement of HRR as a function of time for the cone sample under the test conditions [45]. HRR plots presented for each fence material indicate the intensity and time evolution of the fire in each cone test. Uncertainties in heat release rate measurements have been found to lie typically within 5 % and 10 % for HRR larger than 50 kW/m² [46,47]. Times to ignition and flame out are indicated by dashed vertical lines in each plot.

Data reported in the summary tables for each material include the original sample mass, times to ignition (TTI) and to flame out (FO), peak heat release rate (PHRR), average HRR integrated over the first 600 s of the test, total heat release (THR), effective heat of combustion (EHOC), and percentage of original sample mass lost during the test. The THR is the total amount of heat released by the sample during the cone test, calculated by integrating HRR over the duration of flaming combustion. It relates to the total amount of fuel present and the fraction consumed, and is therefore an indicator of the fire load and fire hazard associated with the material. The EHOC is the amount of heat released during the test per unit mass, calculated by dividing THR by total mass loss. It provides time-resolved insights into the materials undergoing

combustion, including burning intensity and the completeness of the combustion process. The values of THR, EHOC, and the percentage of sample mass lost that appear in the summary table were calculated at the time of flame out.

Where multiple cone tests have been performed under a given test condition, summary tables include mean values and the standard deviation of the sample (in parenthesis) for each variable. Note that conclusions from single tests are only suggestive and lack statistical validity.

C.4.1. Polyvinyl Chloride (PVC)

Cone calorimeter results for PVC fence samples in a horizontal orientation were reported and discussed in Appendix B of the comprehensive fence report [1], where descriptions of this fence type and results of full-scale fire testing may also be found. This section includes these three tests and adds data from a single test performed on a PVC fence sample in a vertical orientation. All cone tests on PVC fence samples were performed with an incident heat flux of 50 kW/m^2.

The photos in Fig. C.7 show specimens cut from the PVC fence studied in the previous fence report, a sample under preparation for cone calorimeter testing, and the remains of a sample after a horizontal cone test. The remains shown in Fig. C.7 (c) illustrate that the PVC sample has formed a dome-shaped hard carbonaceous residue with a layer of white particles. The white particles are understood to be the residue of metal elements incorporated to improve the flame retardancy and smoke suppression of the polymer [40].

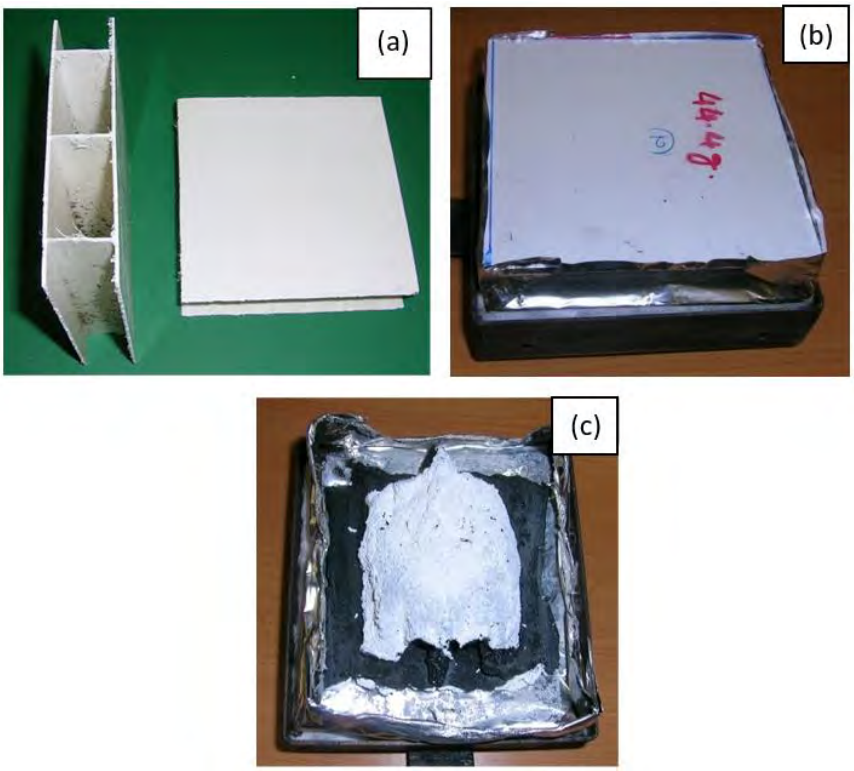

Fig. C.7. PVC cone calorimetry sample: a) specimen cut from fence, b) preparing sample for test, and c) remains of sample after testing.

The plots in Fig. C.8 show heat release rates as a function of time for PVC cone calorimeter tests at 50 kW/m^2 in horizontal and vertical configurations. Times at which ignition (TTI) and flame out (FO) occur for each test are indicated by corresponding dashed vertical lines. Table C.2 and

Table C.3 list the summary data from the horizontal tests and single vertical test, respectively. The ordering of cone tests is the same in plots and tables.

The curves for the three horizontal tests in Fig. C.8 (a) are in good agreement. Each exhibits a single peak, indicating that there is a single stage of burning, with no significant char creation.

The peak heat release rate (PHRR) is significantly higher for the PVC sample burning in a vertical configuration than horizontally, while the total heat release (THR) is similar. This agrees with a study on cone calorimeter configuration effects by Tsai [34].

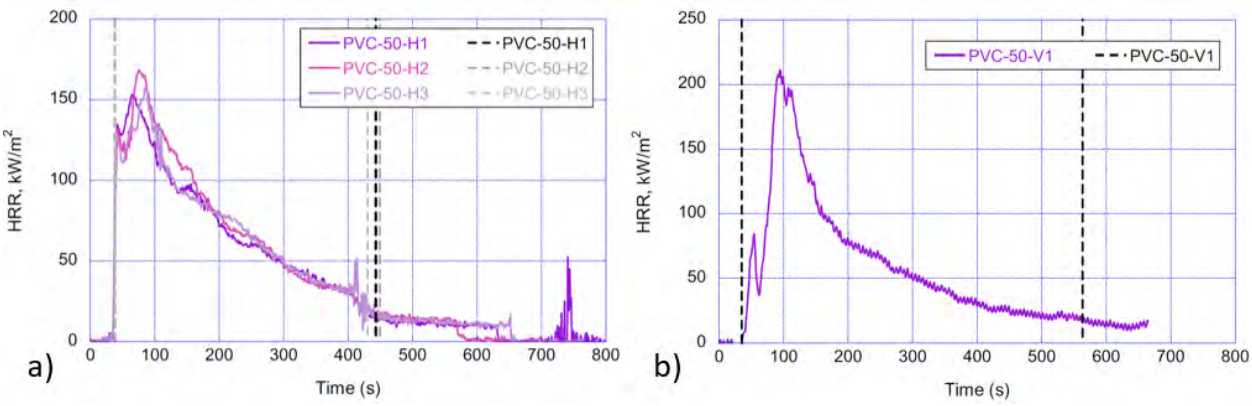

Fig. C.8. Heat release rate as a function of time for PVC cone calorimeter tests in a) horizontal and b) vertical configurations at 50 kW/m^2. Dashed lines in each plot show time to ignition (left) and time to flame out (right) for each test.

Table C.2. Cone calorimetry data for PVC fence material at 50 kW/m^2 in Horizontal configuration.

Test #	Mass, g	TTI, s	FO, s	PHRR, kW/m^2	Avg. HRR_600s, kW/m^2	THR, MJ/m^2	EHOC, MJ/kg	Mass lost, %
50-H1	44.2	37	443	153	51	29	8.7	74.9
50-H2	44.4	37	449	157	54	29	8.9	74.5
50-H3	44.2	39	430	168	52	30	9.1	75.1
Mean (SD)	**44.3 (0.1)**	**38 (1)**	**441 (10)**	**159 (8)**	**52 (2)**	**29 (1)**	**8.9 (0.2)**	**74.8 (0.3)**

Table C.3. Cone calorimetry data for PVC fence material at 50 kW/m^2 in Vertical configuration.

Test #	Mass, g	TTI, s	FO, s	PHRR, kW/m^2	Avg. HRR_600s, kW/m^2	THR, MJ/m^2	EHOC, MJ/kg	Mass lost, %
50-V1	44.6	35*	563	211.1	56.0	33.1	8.1	80.9

*Estimated from HRR plot, based on start of rapid growth.

C.4.2. Western Red Cedar (WRC)

Cone calorimeter results for western red cedar (WRC) fence samples were reported and discussed in Appendix B of the comprehensive fence report [1], where descriptions of this fence type and results of full-scale fire testing may also be found. This section presents plots and data from the three tests on WRC fence samples, all of which were performed in a horizontal orientation with an incident heat flux of 50 kW/m^2.

The photos in Fig. C.9 show specimens cut from the WRC fence studied in the previous fence report, a sample under preparation for cone calorimeter testing, and the remains of a sample after a horizontal cone test. As is typical for wood, Fig. C.9 (c) and (d) show that the sample charred and developed deep cracks during combustion.

During these cone tests, firebrands were observed in the wood specimen following sustained flaming combustion. Small glowing firebrands separated from the test specimen and flew away from the sample holder, suggesting generation of potential secondary ignition sources. The photo of sample remains in Fig. C.9 (c) clearly shows formation of these firebrands. Image (d) shows the flaky ash residue that remained after glowing combustion ceased.

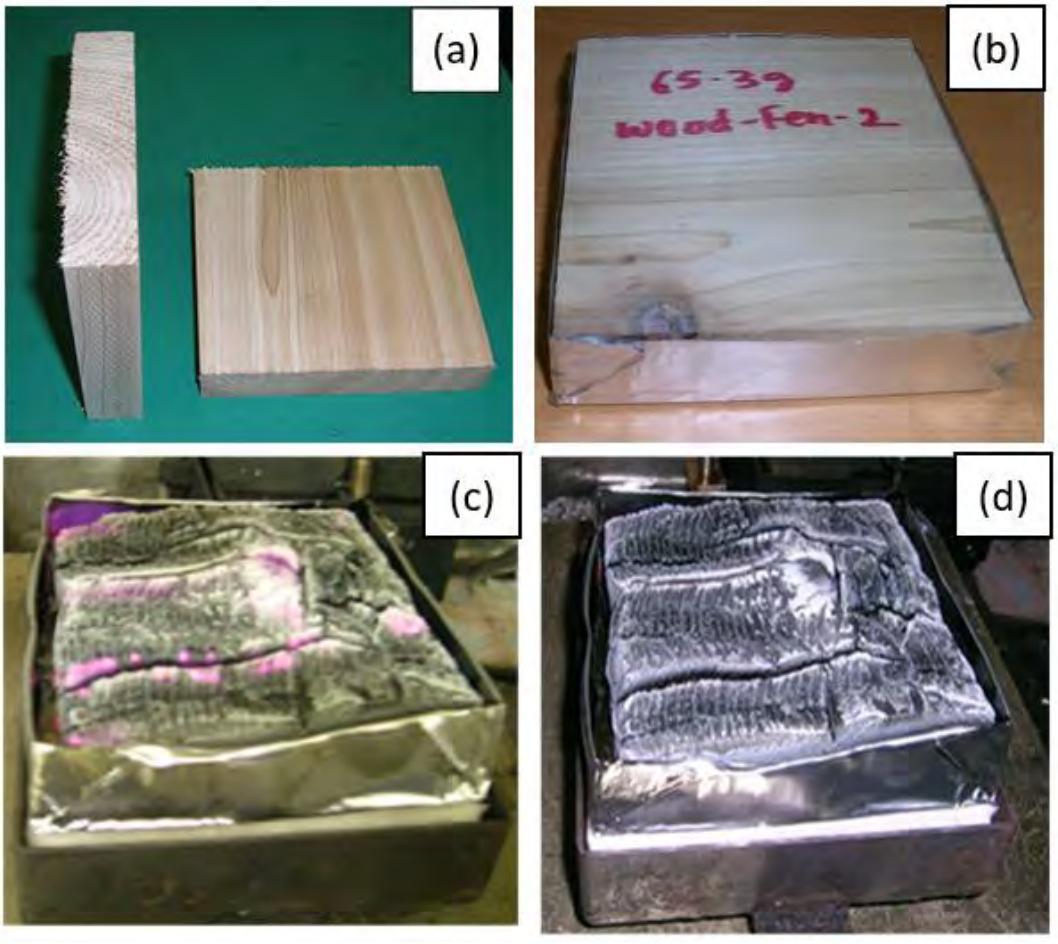

Fig. C.9. Western red cedar (WRC) cone calorimetry sample: a) specimen cut from fence, b) preparing sample for test, and c) and d) remains of sample after testing.

Heat release rates as a function of time for the horizontal WRC cone calorimeter tests at 50 kW/m^2 are plotted in Fig. C.10. Dashed vertical lines indicate the times at which ignition (TTI) and flame out (FO) occur for each test. Table C.4 lists the summary data from the cone tests. The ordering of tests is the same in the plot and table.

The curves for the three horizontal tests in Fig. C.10 are in good agreement. Each exhibits the characteristic two peaks of burning wood, with the second peak due to charring [20,35,36]. Char is insulating; as it progresses through the wood, it slows down pyrolysis and impedes the transport of heat and volatiles, decreasing HRR. When the pyrolysis zone reaches the opposite side of an insulated sample, both temperature and HRR increase. The height and timing of the second peak are affected by several factors, including cracks in the char and moisture transport [35].

The WRC results are included in the discussion of cone calorimeter results for fence materials in Section 5 of this report in order to compare the flammability characteristics of composite fence materials to those of wood.

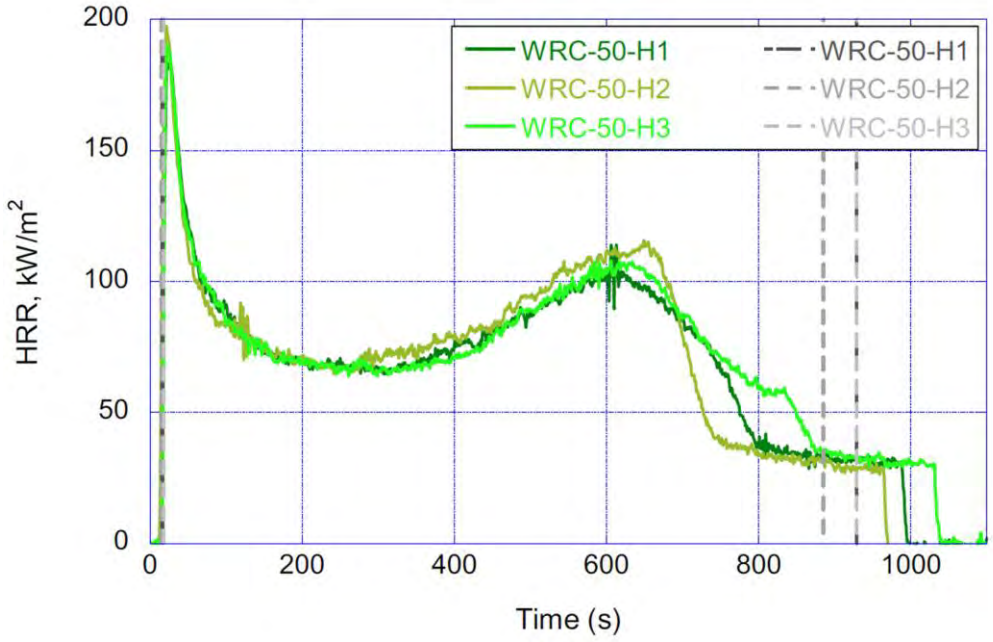

Fig. C.10. Heat release rate as a function of time for WRC cone calorimeter tests in horizontal configuration at an incident heat flux of 50 kW/m^2. Dashed lines show time to ignition (left) and time to flame out (right) for each test.

Table C.4. Cone calorimetry data for WRC fence material at 50 kW/m^2 in Horizontal configuration.

Test #	Mass, g	TTI, s	FO, s	PHRR, kW/m^2	Avg. HRR_600s, kW/m^2	THR, MJ/m^2	EHOC, MJ/kg	Mass lost, %
50-H1	65.8	18	864	184	81	67	12.3	82.5
50-H2	65.3	15	885	197	84	69	12.4	84.6
50-H3	69.0	18	929	190	81	72	12.6	82.2
Mean (SD)	**66.7 (2.0)**	**17 (2)**	**893 (33)**	**190 (7)**	**82 (2)**	**69 (3)**	**12.4 (0.2)**	**83.1 (1.3)**

C.4.3. Wood-Plastic Composite 1 (WPC1)

Results of three cone calorimeter tests for WPC1 fence samples were reported and discussed in Appendix B of the comprehensive fence report [1]. These three tests, performed in a horizontal orientation with an incident heat flux of 50 kW/m^2, are included in this section, along with data from cone tests performed on WPC1 fence samples in a vertical orientation and at an incident heat flux of 35 kW/m^2. These tests include a set of four cone tests that was carried out in the 2024 cone calorimeter study to compare with previous results, with one test performed under each of the four test conditions.

Descriptions of WPC1 fences and results of full-scale fire testing are presented in Section 2.5 and Section 4.1 of this report, respectively.

The photos in Fig. C.11 show (a) specimens cut from the WPC1 fence, (b) a sample under preparation for cone calorimeter testing, near-peak burning in the cone calorimeter in (c) horizontal and (d) vertical configurations, and the remains of a sample after (e) horizontal and (f) vertical cone tests. The WPC1 fence samples were found to burn intensely in both configurations, without evident firebrand generation. The flaky, woody residues remaining after each cone test exhibited no glowing combustion after flaming combustion ceased. The formation of char after the horizontal test, shown in Fig. C.11 (e), is consistent with the cone calorimeter study on wood-plastic composite materials for use in decking boards by Seefeldt and Braun [20].

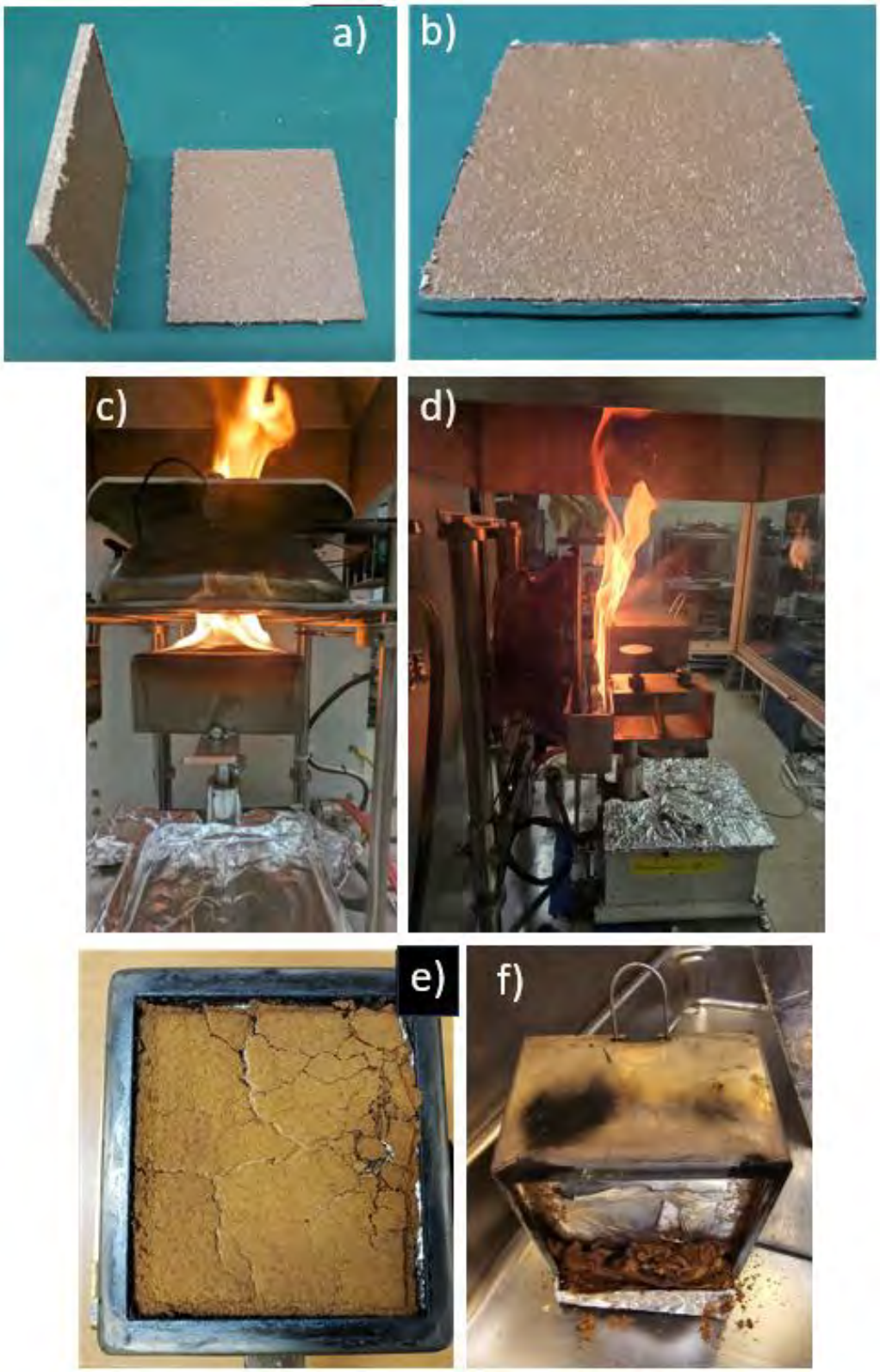

Fig. C.11. Wood-plastic composite #1 (WPC1) cone calorimetry sample: a) specimen cut from fence, b) preparing sample for test, near-peak burning of samples in c) horizontal and d) vertical orientation, and remains of sample after e) horizontal and f) vertical testing.

Heat release rates as a function of time for WPC1 cone calorimeter tests in horizontal and vertical configurations at incident heat fluxes of 50 kW/m^2 and 35 kW/m^2 are plotted in Fig. C.12. Times at which ignition (TTI) and flame out (FO) occur for each test are indicated by corresponding dashed vertical lines. Table C.5 through Table C.8 list the summary data from each of the four test conditions. The ordering of cone tests under each condition is the same in corresponding plots and tables.

For horizontal tests in Fig. C.12 (a) and (c), the HRR plots display two or three distinct peaks, with the initial peak the strongest at both levels of incident heat flux. Like wood, the first peak results from ignition at the surface [36], followed by reduction of HRR due to the insulating char layer. The second and third peaks indicate multiple burning stages, including char cracking and heat build-up when the pyrolysis zone reaches the rear side of the sample.

The first three horizontal cone tests for each incident heat flux are in reasonably good agreement. However, the second and third peaks are delayed for the fourth cone test in each case. As discussed in Section C.3, the final test under each test condition was carried out in 2024 under somewhat different conditions, including higher humidity during conditioning. Although the exact reasons for the differences in the HRR plots are unknown, slowing of the rate of pyrolysis is consistent with a higher moisture content [35].

For WPC1 cone calorimeter tests in the vertical configuration, only two peaks appear in the plots of HRR vs. time in Fig. C.12 (b) and (d). Comparing the scale of the plot in Fig. C.12 (b) with that in (a), it is instantly apparent that, for an incident heat flux of 50 kW/m^2, three of the four WPC1 samples exhibited a considerably higher HRR in the vertical cone calorimeter orientation than in the horizontal. For these tests, the first peak HRR is nearly identical in plots (a) and (b), but the second peak in (b) soars to a value two to three times the first peak. This is attributed to the observed loss of the outer layer of the WPC1 sample as it burned, which slipped off and exposed fresh fuel that burned with a very high heat release rate. This phenomenon could only occur with a sample mounted vertically.

The fourth cone calorimeter test in Fig. C.12 (b), performed in 2024, does not display the same large second peak as the three earlier tests; neither does the single cone test in Fig. C.12 (d) that was carried out vertically at the lower incident heat flux, also in 2024. The reason for this large difference in fire behavior is unclear; further testing would be needed to resolve the conditions in cone calorimeter testing that determine whether or not the outer layer of the WPC1 sample slips off.

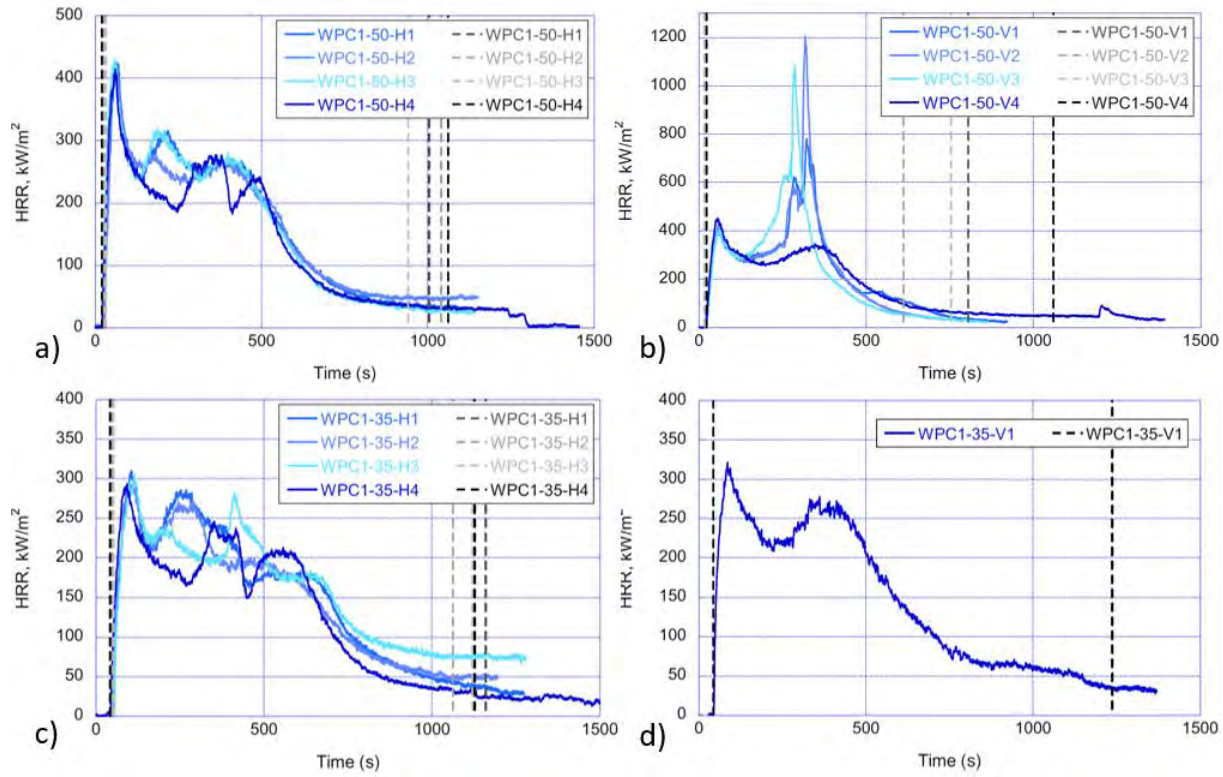

Fig. C.12. Heat release rate as a function of time for WPC1 cone calorimeter tests in a) horizontal and b) vertical configurations at 50 kW/m² and c) horizontal and d) vertical configurations at 35 kW/m². Dashed lines in each plot show time to ignition (left) and time to flame out (right) for each test.

Table C.5. Cone calorimetry data for WPC1 fence material at 50 kW/m² in Horizontal configuration.

Test #	Mass, g	TTI, s	FO, s	PHRR, kW/m²	Avg. HRR_600s, kW/m²	THR, MJ/m²	EHOC, MJ/kg	Mass lost, %
50-H1	59.8	24	1004	423.6	240.7	168.3	28.5	87.1
50-H2	57.7	23	1040	425.5	233.1	168.1	29.6	87.1
50-H3	59.7	31	941	440.6	241.0	164.4	28.0	87.0
50-H4	61.34	19	1061	414.1	219.4	154.7	28.7	89.1
Mean (SD)	**59.6 (1.5)**	**24 (5)**	**1012 (53)**	**426 (11)**	**234 (10)**	**164 (6)**	**28.7 (0.7)**	**87.6 (1.0)**

Table C.6. Cone calorimetry data for WPC1 fence material at 50 kW/m² in Vertical configuration.

Test #	Mass, g	TTI, s	FO, s	PHRR, kW/m²	Avg. HRR_600s, kW/m²	THR, MJ/m²	EHOC, MJ/kg	Mass lost, %
50-V1	59.9	17	805	780	292.1	189.0	30.6	91.2
50-V2	60	17	611	1205	297.7	179.3	29.2	90.4
50-V3	60	18	754	1081	288.4	179.8	28.9	91.6
50-V4	60.91	22	1060	452.4	253.1	180.4	29.4	89.1
Mean (SD)	**60.2 (0.5)**	**19 (2)**	**808 (187)**	**880 (336)**	**283 (20)**	**182 (5)**	**29.5 (0.7)**	**90.6 (1.1)**

Table C.7. Cone calorimetry data for WPC1 fence material at 35 kW/m^2 in Horizontal configuration.

Test #	Mass, g	TTI, s	FO, s	PHRR, kW/m^2	Avg. HRR_600s, kW/m^2	THR, MJ/m^2	EHOC, MJ/kg	Mass lost, %
35-H1	59.6	48	1160	310.3	201.8	168.4	30.2	82.6
35-H2	59.4	50	1062	294.6	197.4	159.1	29.3	80.9
35-H3	59.7	52	1121	305.0	195.8	173.5	31.7	81.1
35-H4	61.16	41	1127	293.0	188.5	149.3	28.2	86.9
Mean (SD)	**60.0 (0.8)**	**48 (5)**	**1118 (41)**	**301 (8)**	**196 (6)**	**163 (11)**	**30.0 (1.5)**	**82.9 (2.8)**

Table C.8. Cone calorimetry data for WPC1 fence material at 35 kW/m^2 in Vertical configuration.

Test #	Mass, g	TTI, s	FO, s	PHRR, kW/m^2	Avg. HRR_600s, kW/m^2	THR, MJ/m^2	EHOC, MJ/kg	Mass lost, %
35-V1	61.1	43	1237	321.6	214.8	174.1	28.4	88.7

C.4.4. Wood-Plastic Composite 2 (WPC2)

Six cone calorimeter tests on WPC2 fence samples were carried out in 2020 and 2021 but not published previously. Three of these tests were in a horizontal orientation and three were vertical, all with an incident heat flux of 50 kW/m^2. The results from these six tests are included in this section, along with data from four cone tests performed on WPC2 fence samples in the 2024 study under each of the four test conditions, including horizontal and vertical orientations at an incident heat flux of 35 kW/m^2.

Descriptions of WPC2 fences and results of full-scale fire testing are presented in Section 2.5 and Section 4.2 of this report, respectively.

The photos in Fig. C.13 show (a) specimens cut from the WPC2 fence, (b) a sample under preparation for cone calorimeter testing, near-peak burning in the cone calorimeter in (c) horizontal and (d) vertical configurations, and the remains of a sample after (e) horizontal and (f) vertical cone tests. The WPC2 fence samples burned for a long time under all test conditions. The WPC2 sample in Fig. C.13 (e) left a crumbling residue that was still smoldering 30 min after flameout.

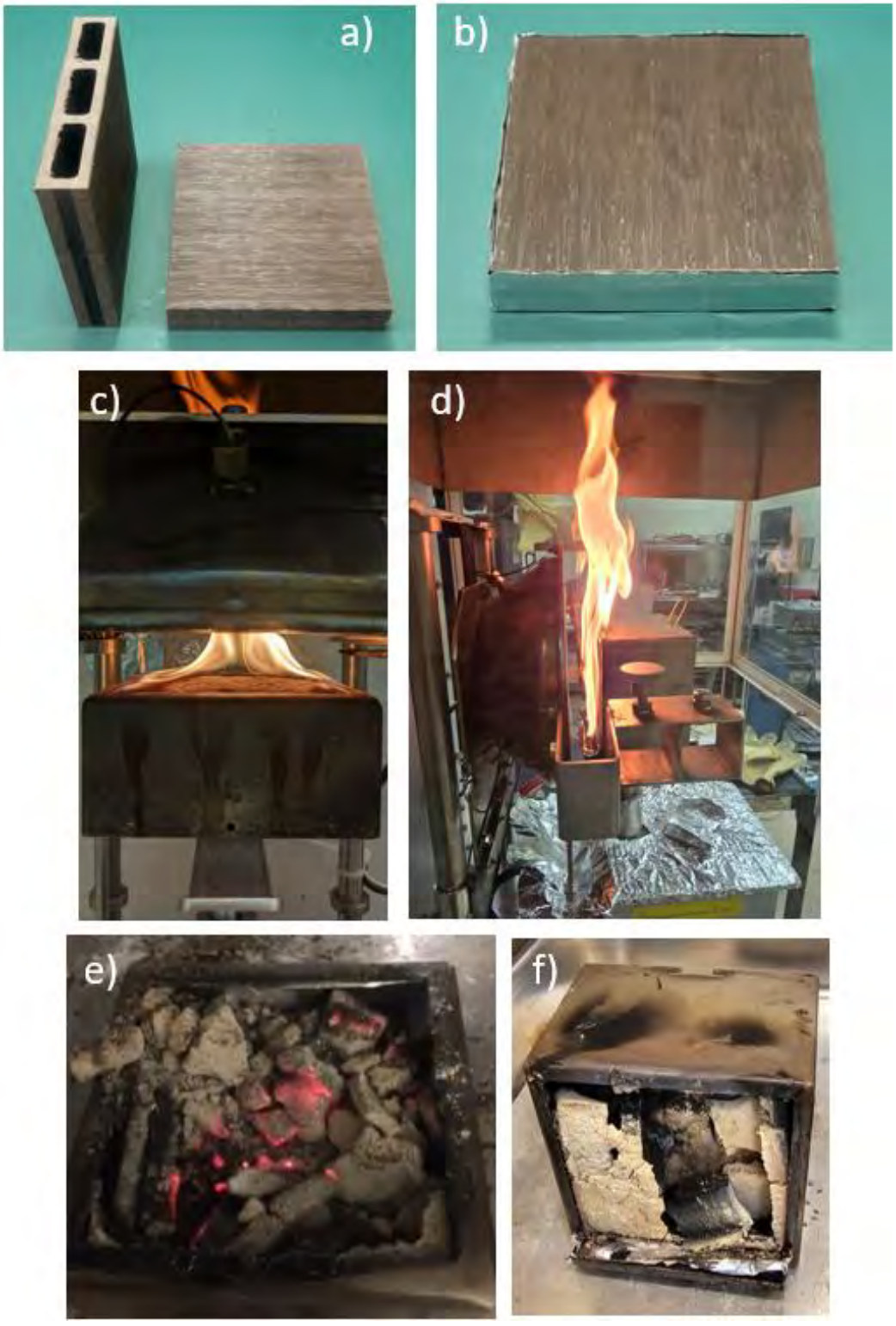

Fig. C.13. Wood-plastic composite #2 (WPC2) cone calorimetry sample: a) specimen cut from fence, b) preparing sample for test, near-peak burning of samples in c) horizontal and d) vertical orientation, and remains of sample after e) horizontal and f) vertical testing.

Heat release rates as a function of time for WPC2 cone calorimeter tests in horizontal and vertical configurations at incident heat fluxes of 50 kW/m^2 and 35 kW/m^2 are plotted in Fig. C.14. Times at which ignition (TTI) and flame out (FO) occur for each test are indicated by corresponding dashed vertical lines. Table C.9 through Table C.12 list the summary data from each of the four test conditions. The ordering of cone tests under each condition is the same in corresponding plots and tables.

Each HRR plot in Fig. C.14 exhibits two peaks, matching the pattern for burning wood discussed in Section C.4.2. The presence of char, which accounts for the second peak, is clear from the sample remains in Fig. C.13 (e) and (f). As was observed for WRC, the second peak is lower than the first in all cases.

In a study of wood-polypropylene decking boards by Seefeldt and Braun [20], hollow geometries resulted in a third peak in the HRR plot due to the pyrolysis front crossing the air gap. For the WPC2 samples, the hollow geometry is apparent in Fig. C.13 (a). However, evidence of the air gap between top and bottom board faces was not readily observed in these HRR plots. it is uncertain how long the initial hollow geometry held up during pyrolysis before crumbling as shown in Fig. C.13 (e).

Although the first three curves in Fig. C.14 (a) are in good agreement, the fourth curve differs significantly in timing for both TTI and FO and in heat release rate measures, including peak HRR for both the first and second peaks. The fourth cone test, WPC2-50-H4, was performed in 2024, separately from the first three. In Fig. C.14 (b), differences are observed for the timing and height of the second peak. In this case, however, the HRR plot for Test WPC2-50-V4, performed in 2024, matches that of one of the previous tests. The reason for these differences is unknown.

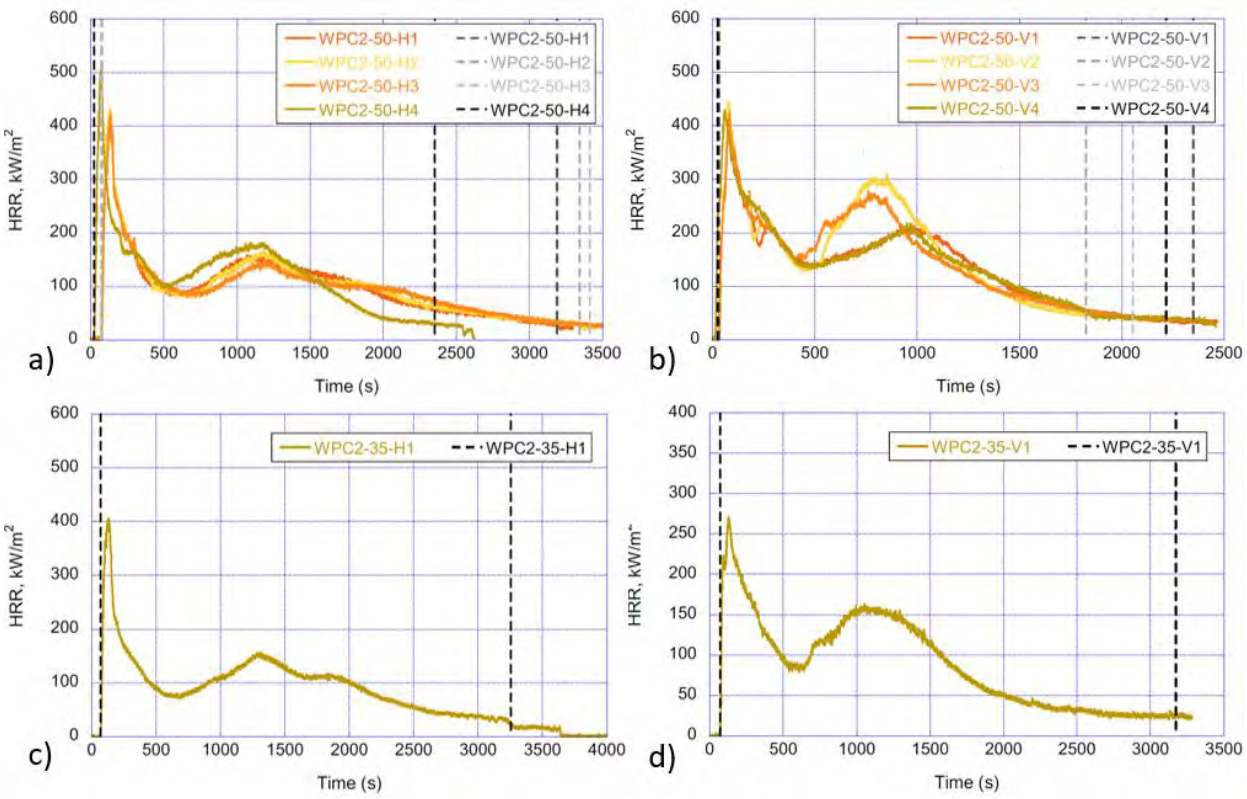

Fig. C.14. Heat release rate as a function of time for WPC2 cone calorimeter tests in a) horizontal and b) vertical configurations at 50 kW/m² and c) horizontal and d) vertical configurations at 35 kW/m². Dashed lines in each plot show time to ignition (left) and time to flame out (right) for each test.

Table C.9. Cone calorimetry data for WPC2 fence material at 50 kW/m² in Horizontal configuration.

Test #	Mass, g	TTI, s	FO, s	PHRR, kW/m²	Avg. HRR_600s, kW/m²	THR, MJ/m²	EHOC, MJ/kg	Mass lost, %
50-H1	139	75	3188	418.9	146.6	315.7	27.3	73.4
50-H2	139	76	3343	432.1	151.4	324.7	27.9	73.9
50-H3	139.3	70	3411	422.3	151.5	321.8	27.6	74.0
50-H4	140.75	23	2353	515.0	170.8	286.2	27.4	75.2
Mean (SD)	**139.5 (0.8)**	**61 (25)**	**3074 (489)**	**447 (46)**	**155 (11)**	**312 (18)**	**27.6 (0.3)**	**74.1 (0.8)**

Table C.10. Cone calorimetry data for WPC2 fence material at 50 kW/m² in Vertical configuration.

Test #	Mass, g	TTI, s	FO, s	PHRR, kW/m²	Avg. HRR_600s, kW/m²	THR, MJ/m²	EHOC, MJ/kg	Mass lost, %
50-V1	139.4	31	2350	424.9	189.9	304.0	27.0	71.3
50-V2	138.7	27	1825	446.7	197.6	308.7	26.9	73.1
50-V3	139.4	24	2055	425.2	206.4	311.1	26.7	73.9
50-V4	140.73	24	2218	429.9	204.7	305.9	26.0	73.9
Mean (SD)	**139.6 (0.8)**	**26.5 (3)**	**2112 (226)**	**432 (10)**	**200 (8)**	**307 (3)**	**26.7 (0.5)**	**73.1 (1)**

Table C.11. Cone calorimetry data for WPC2 fence material at 35 kW/m^2 in Horizontal configuration.

Test #	Mass, g	TTI, s	FO, s	PHRR, kW/m^2	Avg. HRR_600s, kW/m^2	THR, MJ/m^2	EHOC, MJ/kg	Mass lost, %
35-H1	140.81	70	3254	411.8	142.1	309.7	26.2	74.3

Table C.12. Cone calorimetry data for WPC2 fence material at 35 kW/m^2 in Vertical configuration.

Test #	Mass, g	TTI, s	FO, s	PHRR, kW/m^2	Avg. HRR_600s, kW/m^2	THR, MJ/m^2	EHOC, MJ/kg	Mass lost, %
35-V1	141.01	71	3173	271.5	131.6	273.7	26.4	74.6

C.4.5. Steel-Plastic Composite (SPC)

All twelve cone calorimeter tests on SPC fence samples were carried out in the recent (2024) study. Three tests were performed under each of the four test conditions, with horizontal or vertical orientation and an incident heat flux of 50 kW/m^2 or 35 kW/m^2.

Descriptions of SPC fences and results of full-scale fire testing are presented in the main body of this report.

The photos in Fig. C.15 show (a) specimens cut from the SPC fence, (b) a sample under preparation for cone calorimeter testing, near-peak burning in the cone calorimeter in (c) horizontal and (d) vertical configurations, and the remains of a sample after (e) horizontal and (f) vertical cone tests. SPC was found to drip heavily. This can be observed in Fig. C.15 (c), with material from the sample dripping over the retainer frame in a horizontal orientation, and in Fig. C.15 (d), with flames extending upward from drippings caught by the aluminum foil pan in a vertical orientation. The bare holders in Fig. C.15 (e) and (f) show that the SPC fence material in the holders burned completely and left no visible residue. However, some drippings from the sample fell onto the floor and other nearby surfaces, extinguished, and hardened. In Fig. C.15 (e), unburned pieces that were collected after the cone calorimeter test have been placed next to the empty holder.

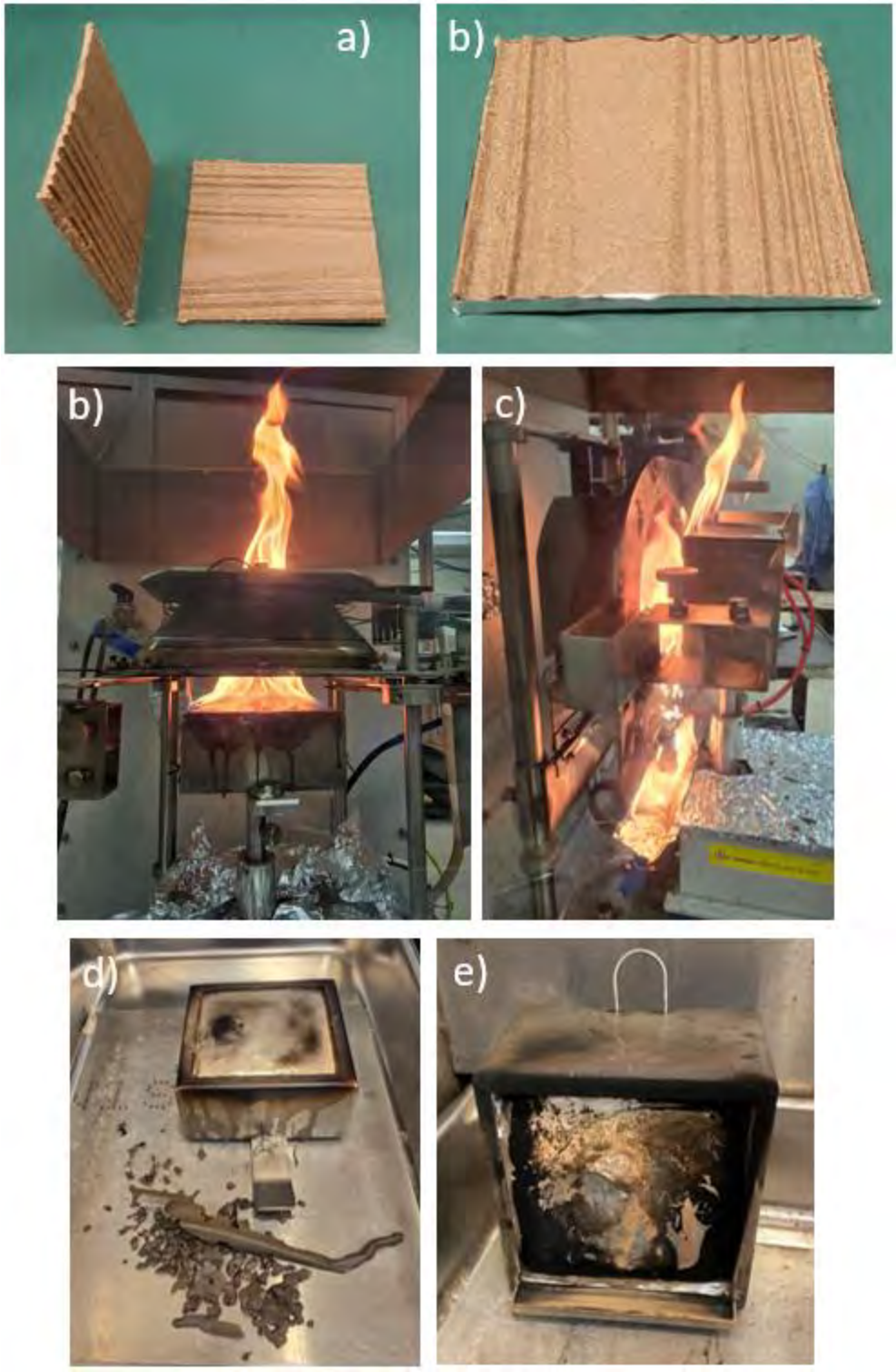

Fig. C.15. Steel-plastic composite (SPC) cone calorimetry sample: a) specimen cut from fence, b) preparing sample for test, near-peak burning of samples in c) horizontal and d) vertical orientation, and remains of sample after e) horizontal and f) vertical testing.

Heat release rates as a function of time for SPC cone calorimeter tests in horizontal and vertical configurations at incident heat fluxes of 50 kW/m^2 and 35 kW/m^2 are plotted in Fig. C.16. Times at which ignition (TTI) and flame out (FO) occur for each test are indicated by corresponding dashed vertical lines. Table C.13 through Table C.16 list the summary data from each of the four test conditions. The ordering of cone tests under each condition is the same in corresponding plots and tables.

The curves of HRR vs. time for horizontal cone tests Fig. C.16 (a) and (c) are in reasonable agreement with each other. More variability in is seen among the curves for vertical cone tests in (b) and (d). The dripping of fragments from the burning sample, some of which continue to burn and some of which fall onto nearby surfaces and extinguish, likely contribute to the variation. Under all conditions, the HRR plots consistently show a strong first peak and weak or nonexistent second peak, which is consistent with little or no char formation.

In Table C.13 through Table C.16, a column was added for the mass of dripped material that was recovered from the floor and other nearby surfaces. However, as indicated in these columns, this data was not consistently measured for every test. The cone calorimeter tests on SPC were messier than the tests for other fence materials, possibly accounting for some of the higher variability in results. Much of the material that fell but remained under the cone continued to burn, so the correspondence between mass measured by the load cell and HRR was lost. The comparisons of cone calorimeter results for studied fence materials in Section 5.2 assume that the mass loss for SPC at flame out is 100 %.

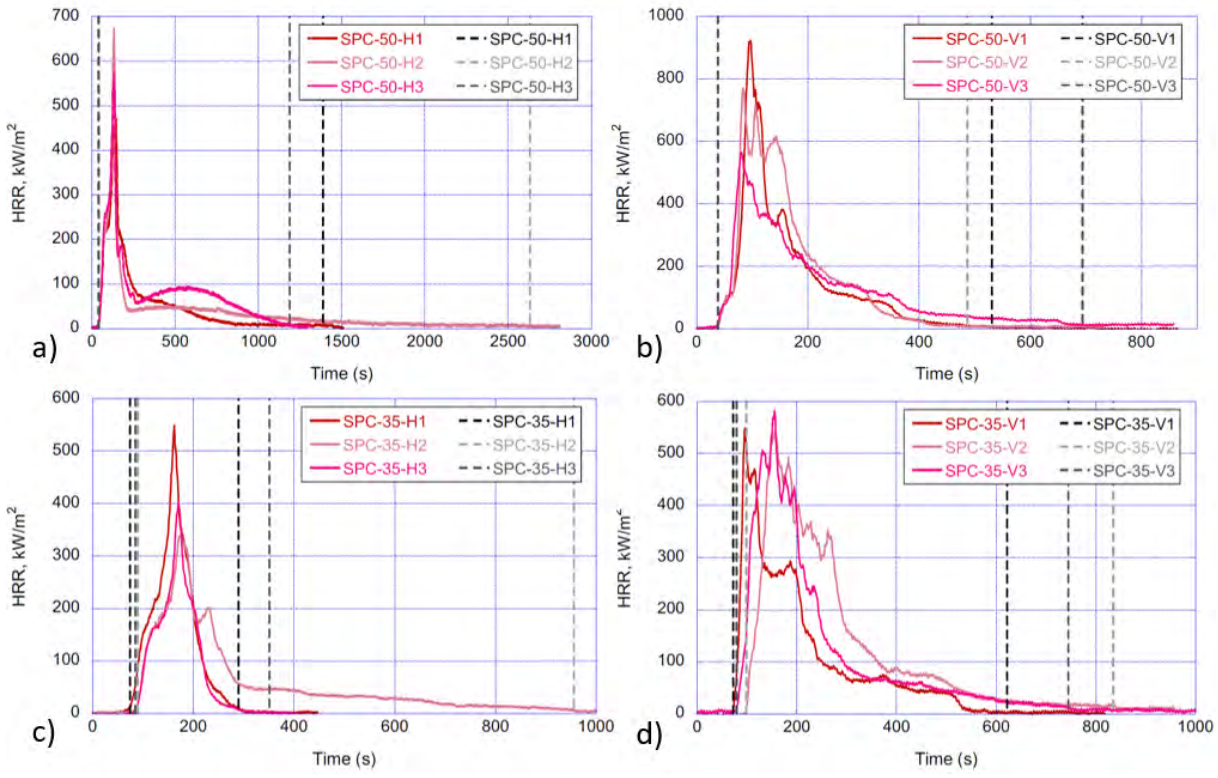

Fig. C.16. Heat release rate as a function of time for SPC cone calorimeter tests in a) horizontal and b) vertical configurations at 50 kW/m^2 and c) horizontal and d) vertical configurations at 35 kW/m^2. Dashed lines in each plot show time to ignition (left) and time to flame out (right) for each test.

Table C.13. Cone calorimetry data for SPC fence material at 50 kW/m² in Horizontal configuration.

Test #	Mass, g	TTI, s	FO, s	PHRR, kW/m²	Avg. HRR_600s, kW/m²	THR, MJ/m²	EHOC, MJ/kg	Dripped Mass (g)	Mass lost, %
50-H1	33.55	41	1389	471.3	106.8	73.3	26.1	11.10	84.2
50-H2	32.82	40	2631	672.5	90.5	88.1	32.4	7.42	83.2
50-H3	31.08	40	1187	573.2	116.0	97.0	34.4	5.75	91.1
Mean (SD)	**32.5 (1.3)**	**40 (1)**	**1736 (782)**	**572 (101)**	**104 (13)**	**86.1 (12)**	**31.0 (4)**		**86.2 (4.3)**

Table C.14. Cone calorimetry data for SPC fence material at 50 kW/m² in Vertical configuration.

Test #	Mass, g	TTI, s	FO, s	PHRR, kW/m²	Avg. HRR_600s, kW/m²	THR, MJ/m²	EHOC, MJ/kg	Dripped Mass (g)	Mass lost, %
50-V1	32.98	38	531	923.2	132.5	79.2	22.7	8.79	93.7
50-V2*	29.99	38	454	770.0	153.1	90.6	30.5	~8 after both tests	87.6
50-V3	26.83	38	694	564.8	136.1	83.7	30.3		91.0
Mean (SD)	**29.9 (3)**	**38 (0)**	**560 (123)**	**753 (180)**	**141 (11)**	**85 (6)**	**27.8 (4)**		**90.8 (3)**

***Timing was adjusted for this test. TTI was set to the average value of Tests 1 and 3.

Table C.15. Cone calorimetry data for SPC fence material at 35 kW/m² in Horizontal configuration.

Test #	Mass, g	TTI, s	FO, s	PHRR, kW/m²	Avg. HRR_600s, kW/m²	THR, MJ/m²	EHOC, MJ/kg	Dripped Mass (g)	Mass lost, %
35-H1	29.36	74	290	550.1	62.3	37.1	15.1	13.08	73.8
35-H2	31.27	89	956	344.4	78.0	52.2	19.6	13.39	85.1
35-H3	31.84	85	351	402.3	45.7	27.8	11.2	18.92	78.3
Mean (SD)	**30.8 (1.3)**	**83 (8)**	**532 (368)**	**432 (106)**	**62 (16)**	**39.0 (12)**	**15.3 (4.2)**		**79.1 (6)**

Table C.16. Cone calorimetry data for SPC fence material at 35 kW/m² in Vertical configuration.

Test #	Mass, g	TTI, s	FO, s	PHRR, kW/m²	Avg. HRR_600s, kW/m²	THR, MJ/m²	EHOC, MJ/kg	Dripped Mass (g)	Mass lost, %
35-V1	31.63	72	622	549.3	106.0	63.8	26.5	7.48 - 8.48	67.1
35-V2	31.63	99	835	549.4	148.1	93.9	29.7	~6	88.4
35-V3	28.29	79	745	583.4	134.0	83.1	28.9	NM*	89.9
Mean (SD)	**30.5 (1.9)**	**83 (14)**	**734 (107)**	**561 (20)**	**129 (21)**	**80 (15)**	**28.4 (1.7)**		**81.8 (13)**

***Not measured.

Appendix D. Wind Characterization

A characterization of the wind profiles for the experimental setup used in this study is described in Appendix C of the full fence and mulch report [1]. It was obtained from measurements from the bidirectional probe array collected during 179 experiments, with the data separated into twelve categories according to wind speed level (low, medium, or high), and separation distance between the fence and/or mulch bed and the shed.

This appendix provides context for the composite fence study by summarizing the wind fields from the low wind speed experiments that are directly applicable to the current work. The wind characterization suggests how uniform the wind field may be over the fence. The wind field plots and horizontal and vertical plots from each of the six composite fence experiments (displayed in Appendix F) may be compared to the plots reproduced here from [1].

The measure of wind speed used to characterize each experiment is described in Appendix D.3.

Further details can be found in Appendix C of [1].

D.1. Measurement Distance from Wind Machine

The wind field generated by the fan depends on how far downstream it's measured. A calculation of the distance from the fan to the bidirectional probe array is based on the experimental setup shown in Fig. D.1. The horizontal distance d_{wp} from the wind machine to the bidirectional probe array is equal to the distance d_{ws} from the wind machine to the shed minus the distance d_{ps} from the probe array to the shed, $d_{wp} = d_{ws} - d_{ps}$. The distance of the probe array from the target shed is equal to the distance d_{pf} of the probe array from the fence plus the total length d_{fence} of a privacy fence plus the separation distance d_{sep} of the fence from the target shed, or $d_{ps} = d_{pf} + d_{fence} + d_{sep}$. Combining these equations results in d_{wp} as a function of separation distance, $d_{wp} = [d_{ws} - (d_{pf} + d_{fence})] - d_{sep}$.

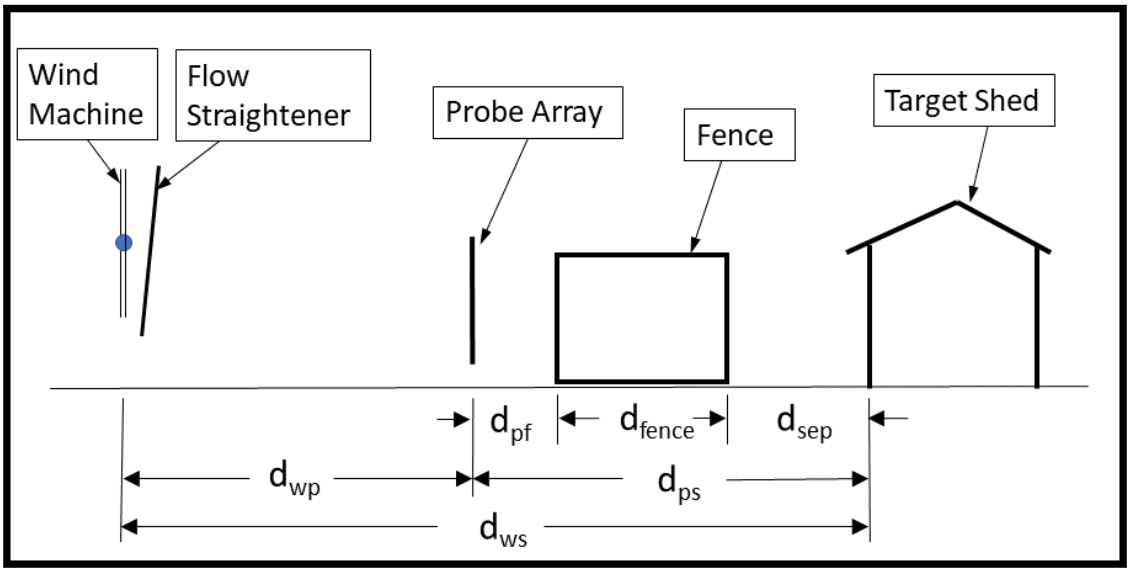

Fig. D.1. Distances between experimental elements. Distances to scale.

For all experiments, d_{ws} = 10.67 m (35 ft) and d_{pf} = 1.22 m (4 ft). The characterization of the wind field in Ref. [1] assumed that the fence length equaled the panel length of western red cedar (WRC) privacy fences plus the width of the two posts at each end of the panel, for a total length of 2.62 m (8 ft 7 in). The distance from the wind machine to the probe array as a function of separation distance was therefore $d_{wp} = 6.83\ \mathrm{m} - d_{sep}$, with all measurements in meters.

In Fig. D.2, the locations of the probe array are highlighted for the four separation distances between fence/mulch and target shed that were used in the previous study [1]. The position of the WRC privacy fence that corresponds to the longest separation distance, $d_{sep,A}$ = 1.83 m (6 ft), is shown in gray. For cases at this separation distance, the fence and/or mulch bed overlaps probe array locations C and D. The velocity profiles at these locations therefore directly relate to the flow field over the test object in these cases. As the location moves closer to the target shed, the flow field may be expected to be more diffuse, lower to the ground, and increasingly affected by the target shed.

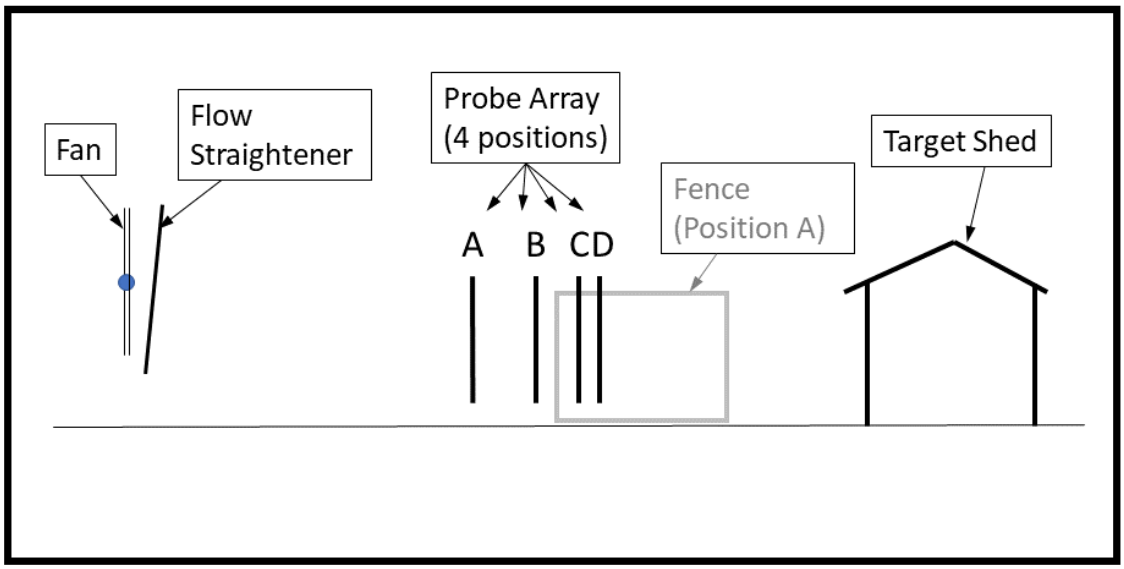

Fig. D.2. Locations of bidirectional probe array for separation distances of (A) 1.83 m, (B) 0.91 m, (C) 0.30 m, and (D) 0 m. Distances to scale.

Because the fence panel lengths for each of the three composite fence types are shorter from that of the wood privacy fence panel, and because the upstream position of the bidirectional probe array from the fence is always 1.22 m (4 ft), the location of the probe array for these experiments will be between positions A and B. Table D.1 includes the locations of the probe array for each type of composite fence in order among positions A through D.

Table D.1. Distances from fan for bidirectional probe array at various separation distances.

Probe array location	Separation distance d_{sep} (m)	Length of fence: d_{fence} (m)	Distance from probe array to shed: d_{ps} (m)	Distance from fan to probe array: d_{wp} (m)
A	1.83	2.62	5.67	5.00
for WPC1	1.83	2.49	5.54	5.13
for WPC2	1.83	1.98	5.03	5.64
for SPC	1.83	1.96	5.01	5.66
B	0.91	2.62	4.75	5.92
C	0.30	2.62	4.14	6.53
D	0	2.62	3.84	6.83

To better understand the wind field seen by the fence, the position of the farthest end of the fence from the shed may be compared with the probe array locations. In Table D.2, the fence length is added to the separation distance of 1.83 m to show the farthest upstream location of each fence. Comparing to d_{ps} in Table D.1 indicates that the WPC1 fence sees a wind field that is at least as uniform as that characterized for probe array location C, and the WPC2 and SPC fences see a wind field as uniform or better than that seen for location D.

Table D.2. Location of the farthest end of the fence from the shed for separation distance of 1.83 m (6 ft).

Fence Type	Length of fence (m)	Distance from upstream end of fence to shed (m)
WRC (wood privacy)	2.62	4.45
WPC1	2.49	4.12
WPC2	1.98	3.81
SPC	1.96	3.79

D.2. Wind Profiles

In the previous fence and mulch study, the wind data from the full set of experiments was organized to study velocity patterns at multiple wind speeds and increasing distances from the fan. The calculation of weighted mean wind speed and uncertainty for each bidirectional probe in each category of wind speed and probe array location can be found in Appendix C.2 of [1]. The resulting data are replotted in Fig. D.3 for the low wind speed condition under which all composite fence experiments were carried out.

In Fig. D.3 (a), the data are displayed in pseudocolor plots, in which a matrix of colored cells on a gray background represents the wind speed value at each probe. The dimensions in horizontal and vertical directions are to scale on these plots, and velocity scales are identical. Dots indicate the location of bidirectional probes.

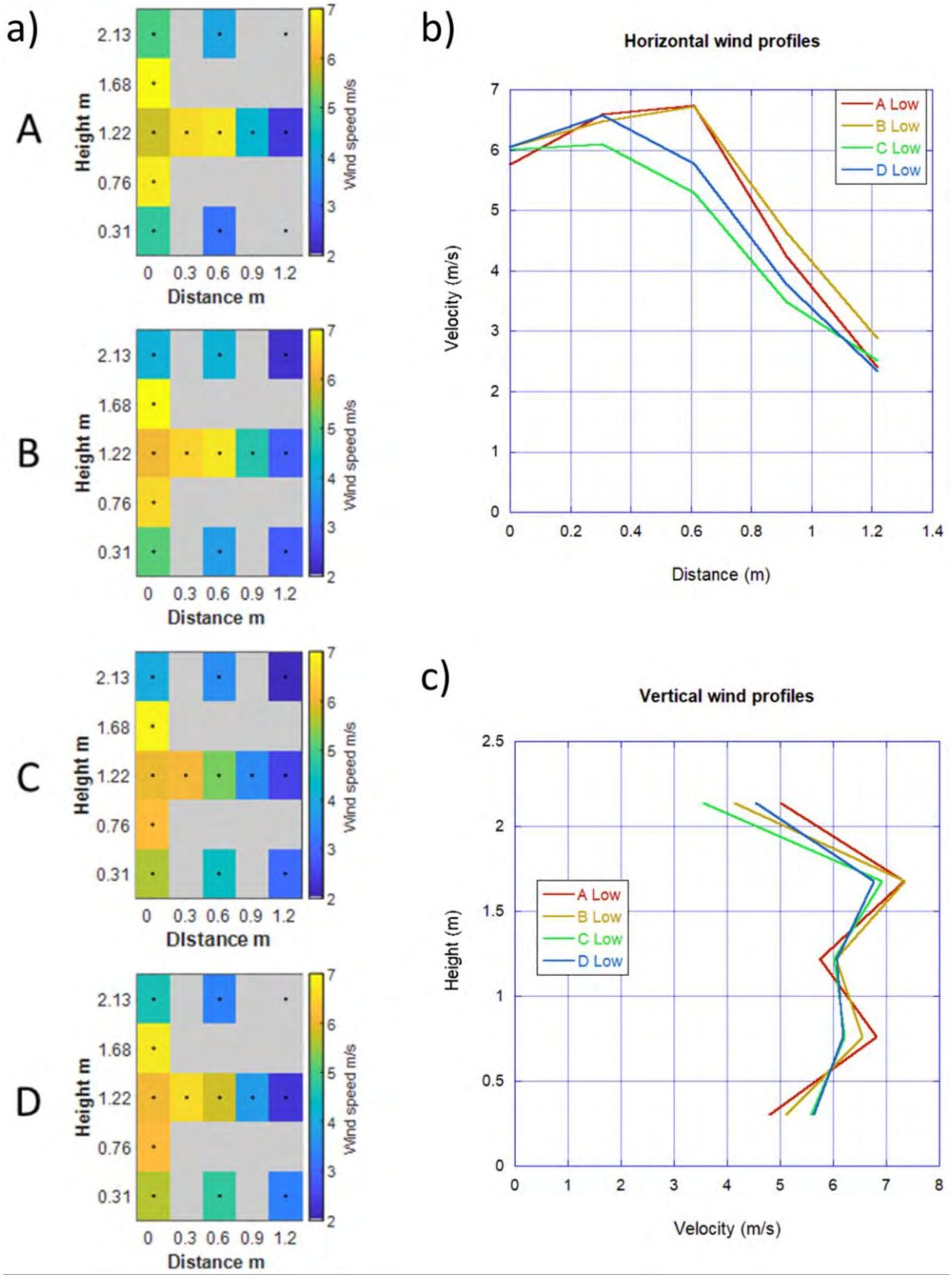

Fig. D.3. Wind field characterization at low wind speeds: a) Mean wind speed pseudocolor plots by probe array location, over all experiments (Dimensions to scale), b) horizontal weighted mean wind speed profiles 1.22 m (4 ft) above the ground, c) vertical weighted mean wind speed profiles along the centerline. Replotted from Fig. C.4, Fig. C.5 and Fig. C.6 of [1].

The plots in Fig. D.3 (a) show that the winds from the fan were felt over a region with a diameter of about 1.2 m (4 ft) approximately centered on probe 9, at 1.2 m (4 ft) above the ground. With the probe array at position A, at a distance of 5 m (16.4 ft) from the fan, there was a strong minimum at the center that corresponded to the hub of the fan. As the distance from the fan increased, this minimum washed out, until the velocity profile became reasonably uniform over this entire region at positions C and D. As discussed in the previous section, the wind field seen by the composite fences is this uniform or better. The uniform region extended from the ground to over 1.7 m (5.5 ft) above the ground, spanning both the mulch bed and the fence along essentially its full height.

The plots in Fig. D.3 (a) also illustrate the tendency of the wind speed at the centerline point at ground level (at probe #3) to increase with increasing distance from the fan. This is in accordance with the angled flow straightener that tilts the flow field toward the ground.

To get a clearer look at the variation of the mean wind speeds across the flow field, weighted mean values of probes along the horizontal line 1.22 m (4 ft) above the ground and along the vertical centerline are plotted in Fig. D.3 (b) and Fig. D.3 (c), respectively. Both plots demonstrate the trend toward a more uniform flow field with increasing distance downwind from the fan, from position A (red) to position D (blue). The profiles in Fig. D.3 (c) support the selection of the average of the velocities of the lower four probes along the centerline as a measure of the average wind velocity for a given experiment.

D.3. Measure of Wind Speed for Each Experiment

As discussed in Appendix C.3 of the previous fence report [1], the measure that was chosen to represent the wind field for each experiment was the mean wind speed for the lower four bidirectional probe values along the centerline. Using the probe numbers from Fig. 12, the characteristic wind speed for a specified experiment k is given by

$$\bar{V}_k = \frac{\left(V_{3,k} + V_{4,k} + V_{9,k} + V_{10,k}\right)}{4} \tag{C-8}$$

This measure uses data from probes that extend from 0.30 m (1 ft) to 1.68 m (5.5 ft) in the vertical direction along the centerline. It measures wind speeds starting a short distance above the mulch bed and encompassing nearly the full height of a fence.

The standard uncertainty for this wind speed measure for experiment k is given by

$$u_{c,k} = \frac{1}{4}\sqrt{u_c^2\left(V_{3,k}\right) + u_c^2\left(V_{4,k}\right) + u_c^2\left(V_{9,k}\right) + u_c^2\left(V_{10,k}\right)} \tag{C-9}$$

Both calculations account for bad probes by dropping their wind speed or uncertainty values from the equation and averaging over the number of good probes.

The case details in Appendix F provide this wind speed measure in the table at the lower left, as described in Appendix E.4.

Appendix E. Reading the Case Descriptions

This appendix explains how to read the data from the experimental cases listed in Appendix F. The data for each experiment includes a brief description, photographs from before and during the experiment, flame spread plots, summary data, and plots showing applied winds and ambient weather conditions. An example of the data provided for each experiment is shown in Fig. E.1, and explanations of data boxes A through F follow.

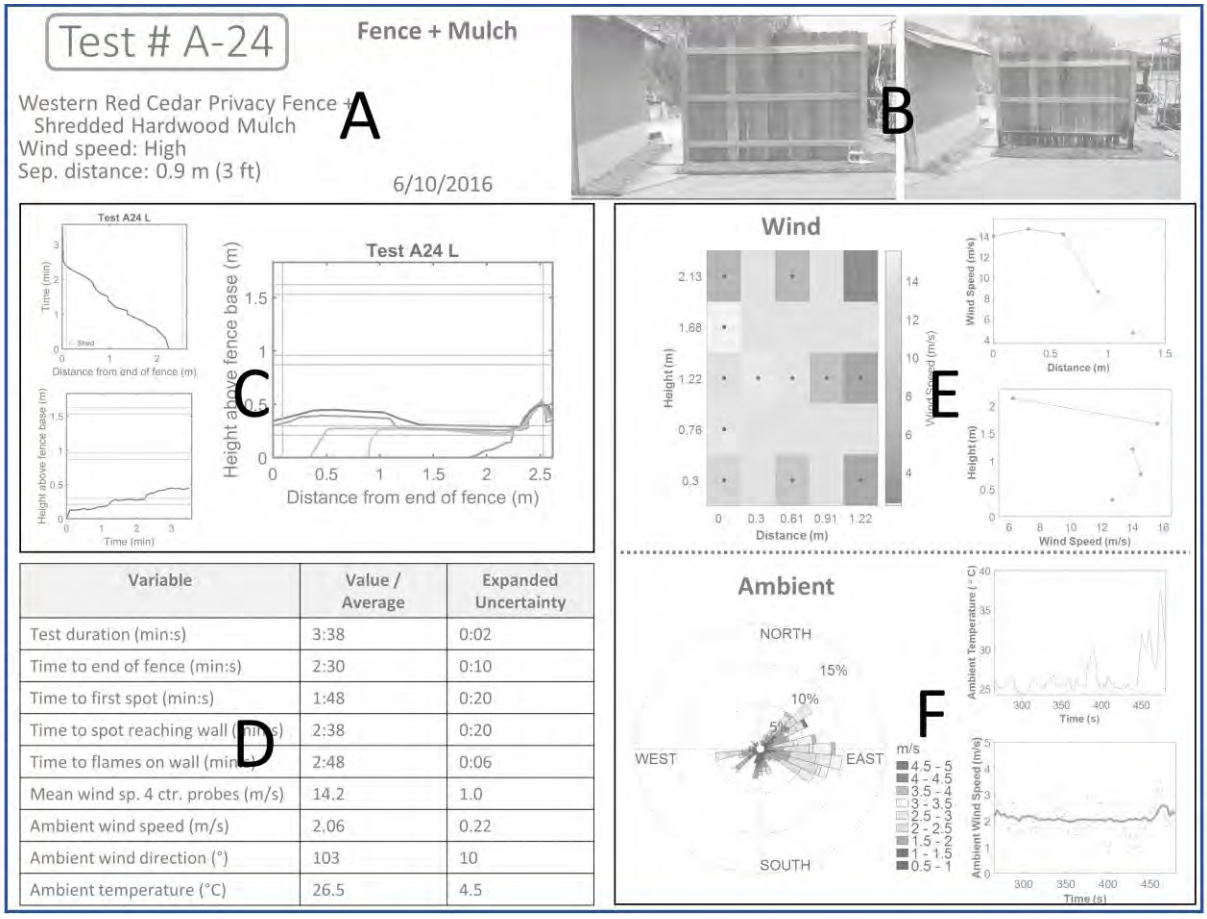

Variable	Value / Average	Expanded Uncertainty
Test duration (min:s)	3:38	0:02
Time to end of fence (min:s)	2:30	0:10
Time to first spot (min:s)	1:48	0:20
Time to spot reaching wall (min:s)	2:38	0:20
Time to flames on wall (min:s)	2:48	0:06
Mean wind sp. 4 ctr. probes (m/s)	14.2	1.0
Ambient wind speed (m/s)	2.06	0.22
Ambient wind direction (°)	103	10
Ambient temperature (°C)	26.5	4.5

Fig. E.1. Experimental case description.

E.1. Data Box A: Experimental Configuration

The top left corner of each experimental case description, shown in Fig. E.2 , provides the basic configuration for the experiment. This includes the test number, the category of the experiment (Fence Only, Mulch Only, Fence + Mulch, Parallel Fence with/without Mulch, or No Shed), and the date on which the experiment was performed. The material and type of fence and/or mulch, the applied wind speed level (Low, Medium, or High), and the separation distance of the end of the fence or mulch bed from the wall of the structure are also listed. All of the composite fence experiments in this study were performed at low applied wind speeds which fall into a range of 5 m/s to 9 m/s as measured by the bidirectional probes near the centerline of the flow.

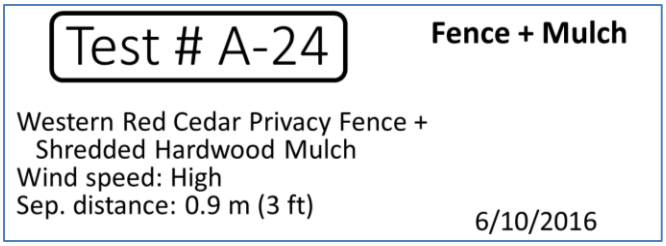

Fig. E.2. Data Box A – Experimental configuration.

E.2. Data Box B: Photographs Taken Before and During the Experiment

In the top right corner of each case description are two photos, as shown in Fig. E.3. The photo on the left is the initial setup of the experiment as observed by the camera on the left side as viewed from the fan. In this photo, the shed appears to the left of the fence or mulch bed. For cases with single fences, the fence was typically mounted with the stringers facing this side.

The photo on the right was taken during the experiment and may show the testbed from any angle. This photo was selected to show an interesting feature of this experiment. In some cases, this photo shows the pattern of fire damage near the end of the experiment; in other cases, flames are shown from a period when the fence was burning strongly.

Fig. E.3. Data Box B – Photographs taken before and during the experiment.

E.3. Data Box C: Flame Spread as a Function of Time - Fences

The center left box in the case description contains plots that illustrate the progress of the flame spread over the fence. The plots used data from the fence analysis procedures described in Section 3.1.3.

For fence experiments, three flame spread plots are shown, as in Fig. E.4. Distance from the shed is always plotted along the horizontal axis and height is plotted along the vertical axis. For plots as a function of time, therefore, the axis representing time will vary.

The upper left plot shows the distance of the char front from the end of the fence nearest the shed as a function of time. Time is plotted on the vertical axis, and the locations of the end posts are marked with vertical lines as a visual aid. The char front begins at t = 0 s close to the

outer end post at the lower right of the plot. With time, the front advances toward the end of the fence closest to the shed at the upper left.

The lower left plot shows the maximum height of the char front downwind of the ignition zone as a function of time. To look at the flame spread characteristics independent of the ignition zone, this plot tracks the maximum char height at least two board widths downwind from the ignition zone. In this plot, time is along the horizontal axis, and the locations of the stringers are marked with horizontal lines.

On the right is a plot showing the contours of the burned area of the fence over time. Contours have been obtained at five points in time spaced evenly between the initial and final times. The order of the sequence is displayed using color, with blue indicating the earliest contour and red the contour at the end of the experiment.

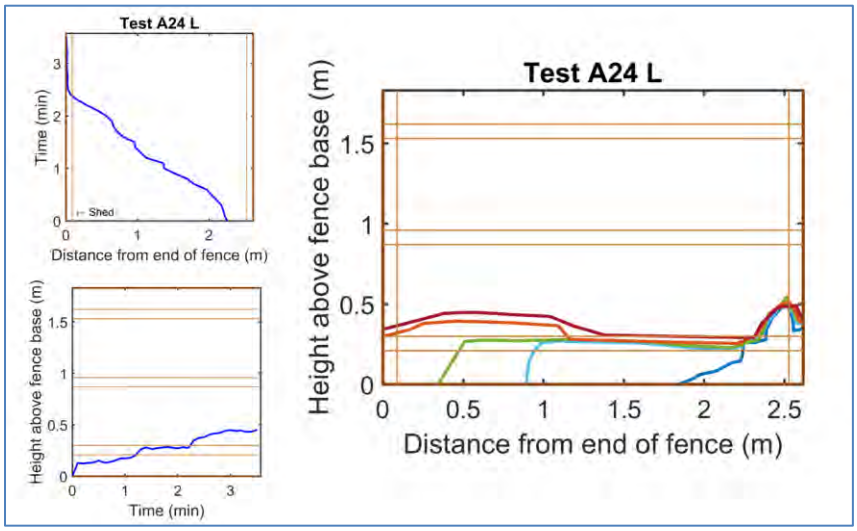

Fig. E.4. Data Box C – Flame spread as a function of time for fence experiments.

E.4. Data Box D: Table of Timing Values and Environmental Factors

At the lower left of the case description is a table containing average values and standard deviation for timing and environmental variables, as shown in Fig. E.5.

The test duration was obtained from subtraction of the time at which the fan was turned on from the time at which the fan was turned off, as determined from videos recorded from cameras mounted to the right and left of the fence. Other times listed in this table include the time for the flame front to reach the end of the fence or mulch bed, the time for the first firebrand ignition to occur in the target mulch bed, the time for ignition of the spot fire that puts flames on the wall of the shed, and the time for those flames to reach the wall. Expanded uncertainties (at the 95 % confidence level) for these values are estimated from the Type B uncertainties of determining the time from the videos, as explained in Appendix B.3.

Environmental variables include the average values and expanded uncertainties of applied wind speed, ambient wind speed and direction, and ambient temperature. The value used to characterize the applied wind speed is an average of the mean values for the lower four

bidirectional probes along the centerline of the probe array, as discussed in Appendix D.3. These probes measure the wind field that strikes the edge of the fence facing the fan. Ambient data were collected from probes mounted on a 3.7 m (12 ft) pole about 7.9 m (26 ft) south-southeast of the wind machine propellers and 17.7 m (58 ft) south-southwest of the target shed, as described in Section 2.7.2. Expanded uncertainties were calculated as described in Appendix B.2.

Variable	Value / Average	Expanded Uncertainty
Test duration (min:s)	3:38	0:02
Time to end of fence (min:s)	2:30	0:10
Time to first spot (min:s)	1:48	0:20
Time to spot reaching wall (min:s)	2:38	0:20
Time to flames on wall (min:s)	2:48	0:06
Mean wind sp. 4 ctr. probes (m/s)	14.2	1.0
Ambient wind speed (m/s)	2.06	0.22
Ambient wind direction (°)	103	10
Ambient temperature (°C)	26.5	4.5

Fig. E.5. Data Box D – Table of timing values and environmental factors.

E.5. Data Box E: Applied Wind

Wind speeds averaged over the duration of the experiment (the time during which the fan is on) are displayed in the three plots in data box E, as shown in Fig. E.6. The wind speeds were measured by either 13 or 17 bidirectional probes in the probe array described in Section 2.7.1.

The pseudocolor plot on the left displays the mean wind speed value for each probe as a colored cell in a rectangular array. The array represents the probe locations in Fig. 12. (In this example, the array has 13 rather than 17 probes.) The scale along the right of the plot relates color to wind speed. If any of the probes are not operational during the experiment, they appear as white.

The plot at the top right of data box E shows the mean wind speeds for probes #9, #8, #7, #6, and #5, which extend horizontally out from the centerline at a height of 1.22 m (4 ft) above the ground. The probe distance is plotted along the horizontal axis, and the wind speed is along the vertical axis. The plot typically indicates a minimum at the centerline, which is a flow field artifact from the hub region of the wind machine propellers. The wind speed decreases rapidly away from the central flow field.

The plot at the bottom right shows the mean wind speeds for probes #3, #4, #9, #10, and #13, which are arrayed along the centerline of the wind field. For this plot, the height of each probe is plotted along the vertical axis, and the wind speed is along the horizontal axis. The wind speeds are typically highest in the central region and lower at the position of the top probe. The tilt of the wind straightener, described in Section 2.2.2, helped to extend higher wind speeds toward the ground.

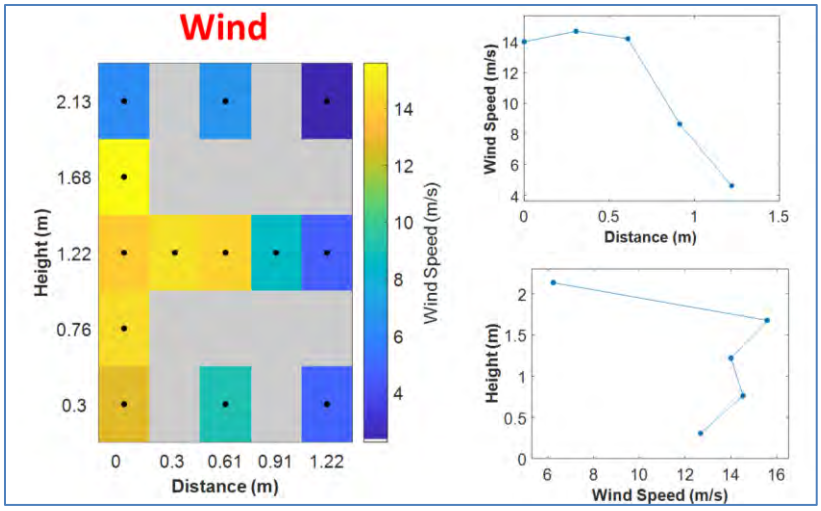

Fig. E.6. Data Box E – Applied wind.

E.6. Data Box F: Ambient Wind

Data box F, located at the lower right of the case description, displays a wind rose and time plots of temperature and wind speed based on data taken over the duration of the experiment, as shown in Fig. E.7. The instruments used to measure ambient temperature and winds have been described in Sections 2.7.1 and 2.7.2, respectively.

In the wind rose plot on the left, the wind speed and direction of the ambient winds are binned. The length of each spoke indicates the percentage of time that the wind blew from that direction during the experiment. The concentric rings are labeled to show the frequency. The colored bins within each spoke indicate wind speed ranges, which are listed in the scale to the right of this diagram.

On the upper right of data box F is a plot of ambient temperature as function of time. The time begins when the fan is turned on and ends when it is turned off, which defines the timing for the experiment.

On the lower right is a plot of ambient wind speed as a function of time. The red line applies a moving average filter with a 300 s span to the data, indicating the value and trend of the ambient wind speed over the experiment.

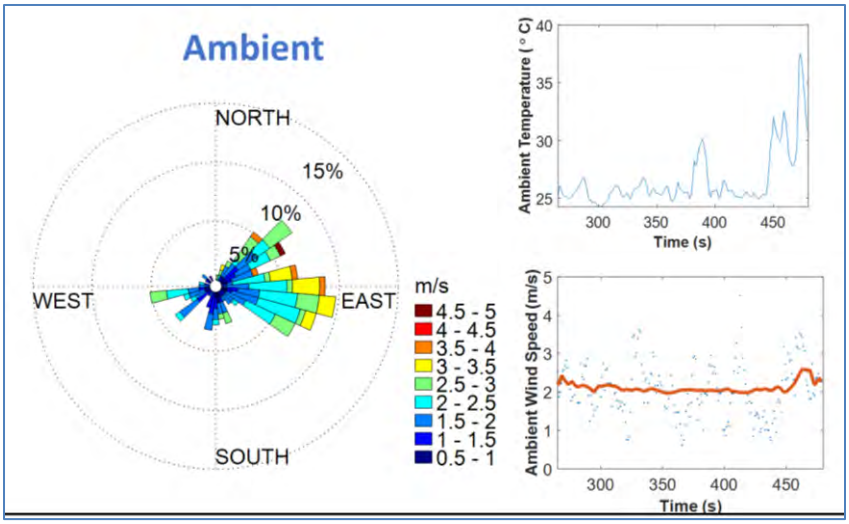

Fig. E.7. Data Box F – Ambient wind.

Appendix F. Case Details: Composite Fences

This appendix provides the data from the six composite fence cases: three fence types, each with and without mulch. The data are presented in the same format as used for the full fence and mulch study in [1]. Each case includes a description of the experiment, photographs from before and during, flame spread plots, critical times, and ambient and applied winds. The data for each experiment can be read as described in Appendix E.

Test # E-1

Fence + Mulch

Wood-Plastic Composite (WPC1) Fence + Shredded Hardwood Mulch
Wind speed: Low
Sep. distance: 1.8 m (6 ft)
9/25/2020

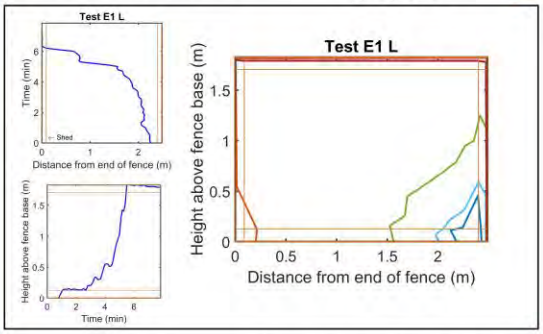

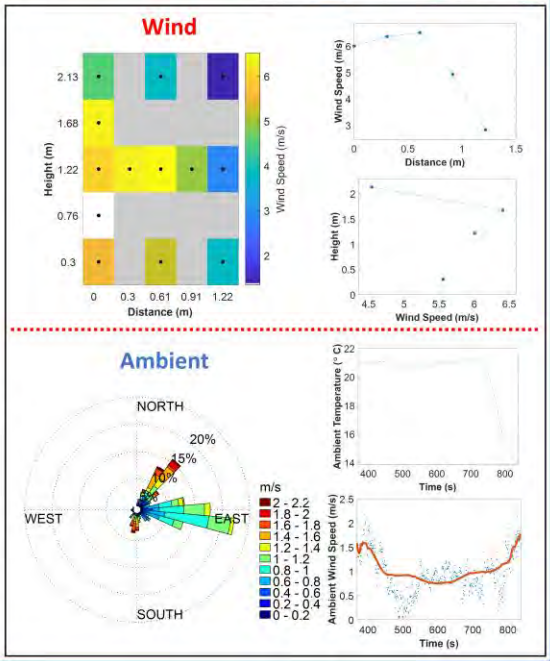

Variable	Value / Average	Expanded Uncertainty
Test duration (min:s)	7:53	0:02
Time to end of fence (min:s)	6:15	0:10
Time to first spot (min:s)	6:44	0:20
Time to spot reaching wall (min:s)	6:44	0:20
Time to flames on wall (min:s)	7:08	0:06
Mean wind sp. 4 ctr. probes (m/s)	6.0	0.5
Ambient wind speed (m/s)	0.95	0.20
Ambient wind direction (°)	88	11
Ambient temperature (°C)	20.1	4.4

Test # E-2

Fence only

Wood-Plastic Composite (WPC1) Fence
Wind speed: Low
Sep. distance: 1.8 m (6 ft)
9/25/2020

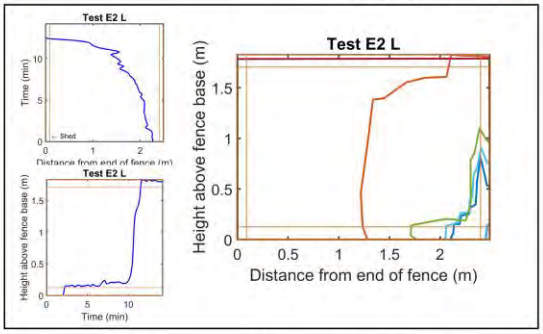

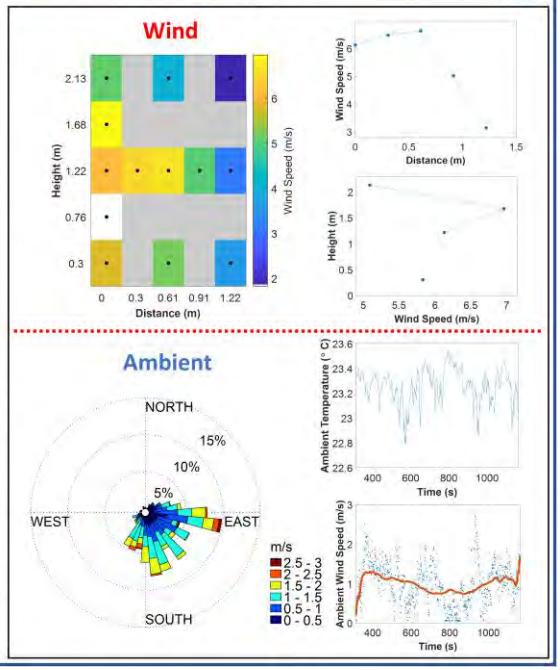

Variable	Value / Average	Expanded Uncertainty
Test duration (min:s)	14:16	0:02
Time to end of fence (min:s)	12:21	0:10
Time to first spot (min:s)	11:50	0:20
Time to spot reaching wall (min:s)	--	--
Time to flames on wall (min:s)	--	--
Mean wind sp. 4 ctr. probes (m/s)	6.3	0.5
Ambient wind speed (m/s)	1.00	0.20
Ambient wind direction (°)	140	11
Ambient temperature (°C)	23.3	4.4

Test # F-1

Fence + Mulch

Wood-Plastic Composite (WPC2) Fence + Shredded Hardwood Mulch
Wind speed: Low
Sep. distance: 1.8 m (6 ft)
Note: Horizontal boards slip down as they burn.

6/25/2021

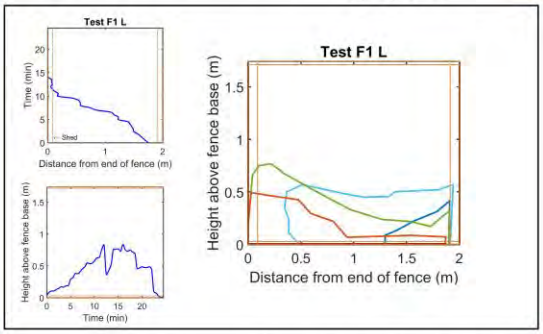

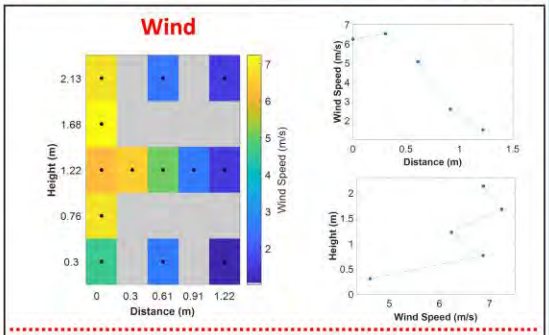

Variable	Value / Average	Expanded Uncertainty
Test duration (min:s)	24:37	0:02
Time to end of fence (min:s)	14:00	0:20
Time to first spot (min:s)	19:46	0:20
Time to spot reaching wall (min:s)	20:10	0:20
Time to flames on wall (min:s)	21:08	0:06
Mean wind sp. 4 ctr. probes (m/s)	6.2	0.4
Ambient wind speed (m/s)	1.74	0.21
Ambient wind direction (°)	182	10
Ambient temperature (°C)	27.4	4.5

Test # H-3

Fence only

Wood-Plastic Composite (WPC2) Fence
Wind speed: Low
Sep. distance: 1.8 m (6 ft)

9/22/2023

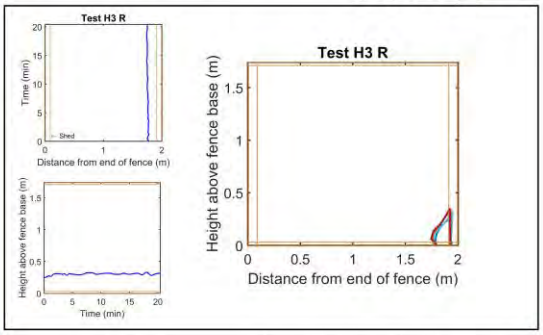

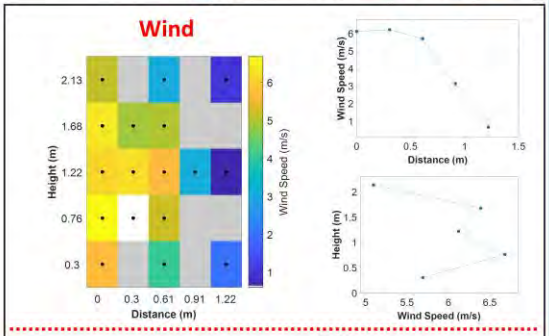

Variable	Value / Average	Expanded Uncertainty
Test duration (min:s)	20:50	0:02
Time to end of fence (min:s)	--	--
Time to first spot (min:s)	--	--
Time to spot reaching wall (min:s)	--	--
Time to flames on wall (min:s)	--	--
Mean wind sp. 4 ctr. probes (m/s)	6.2	0.4
Ambient wind speed (m/s)	0.77	0.20
Ambient wind direction (°)	286	11
Ambient temperature (°C)	25.5	4.5

Test # H-1

Fence + Mulch

Steel-Plastic Composite (SPC) Fence + Shredded Hardwood Mulch
Wind speed: Low
Sep. distance: 1.8 m (6 ft)

9/22/2023

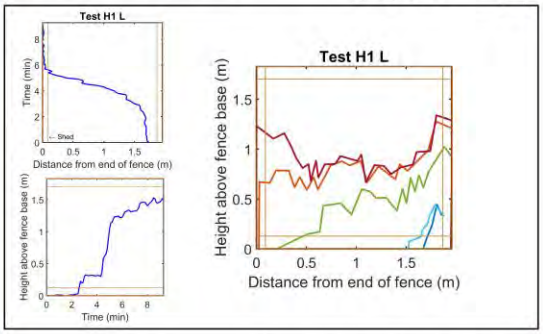

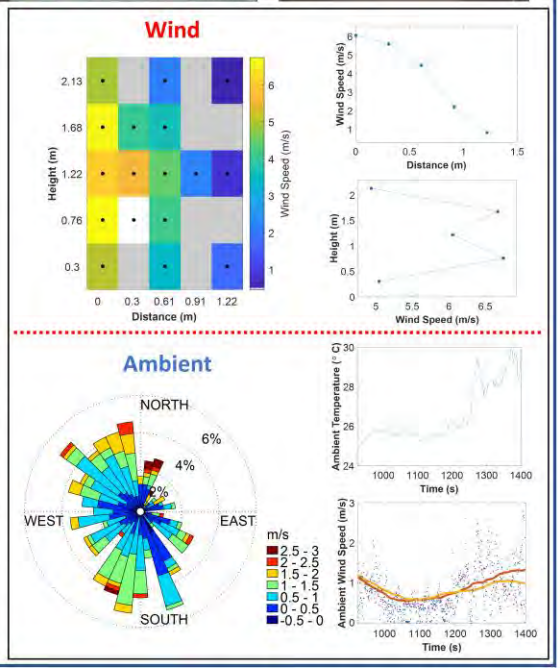

Variable	Value / Average	Expanded Uncertainty
Test duration (min:s)	9:29	0:02
Time to end of fence (min:s)	5:40	0:10
Time to first spot (min:s)	6:55	0:20
Time to spot reaching wall (min:s)	6:55	0:20
Time to flames on wall (min:s)	9:19	0:06
Mean wind sp. 4 ctr. probes (m/s)	6.1	0.4
Ambient wind speed (m/s)	0.99	0.21
Ambient wind direction (°)	269	12
Ambient temperature (°C)	25.9	4.5

Test # H-2

Fence only

Steel-Plastic Composite (SPC) Fence
Wind speed: Low
Sep. distance: 1.8 m (6 ft)

9/22/2023

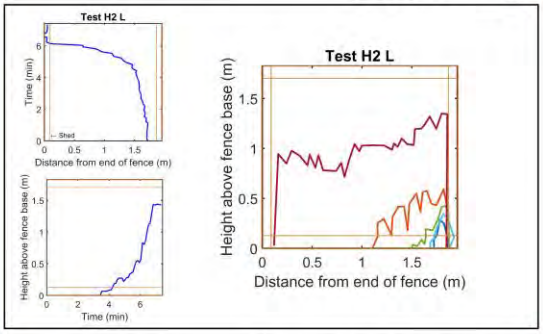

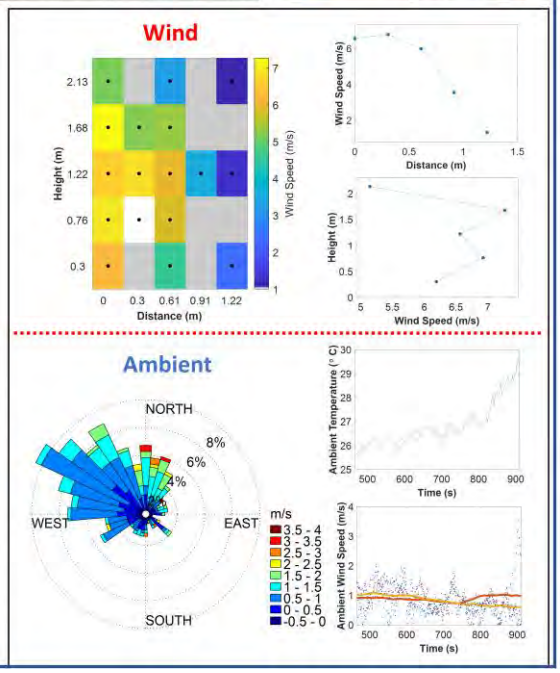

Variable	Value / Average	Expanded Uncertainty
Test duration (min:s)	7:40	0:02
Time to end of fence (min:s)	6:12	0:10
Time to first spot (min:s)	7:06	0:20
Time to spot reaching wall (min:s)	7:06	0:20
Time to flames on wall (min:s)	--	--
Mean wind sp. 4 ctr. probes (m/s)	6.7	0.5
Ambient wind speed (m/s)	1.02	0.21
Ambient wind direction (°)	1	11
Ambient temperature (°C)	26.6	4.5